

Contributions à l'étude des méthodes de production de masse des cellules endothéliales cornéennes humaines

Binh Minh Ha Thi

▶ **To cite this version:**

Binh Minh Ha Thi. Contributions à l'étude des méthodes de production de masse des cellules endothéliales cornéennes humaines. Ingénierie biomédicale. Université Jean Monnet - Saint-Etienne, 2014. Français. NNT : 2014STET001T . tel-01424105

HAL Id: tel-01424105
https://theses.hal.science/tel-01424105

Submitted on 2 Jan 2017

HAL is a multi-disciplinary open access archive for the deposit and dissemination of scientific research documents, whether they are published or not. The documents may come from teaching and research institutions in France or abroad, or from public or private research centers.

L'archive ouverte pluridisciplinaire **HAL**, est destinée au dépôt et à la diffusion de documents scientifiques de niveau recherche, publiés ou non, émanant des établissements d'enseignement et de recherche français ou étrangers, des laboratoires publics ou privés.

UNIVERSITE JEAN MONNET DE SAINT-ETIENNE

Année Universitaire 2013-2014

THESE

Présentée pour l'obtention du titre de

DOCTEUR DE L'UNIVERSITE JEAN MONNET

Discipline: Biologie, Médecine et Santé

Contributions à l'étude des méthodes de production de masse des cellules endothéliales cornéennes humaines

Présenté et soutenue publiquement par

Mademoiselle HA THI Binh Minh

Le 30 janvier 2014

Directeur de thèse: Pr. Philippe GAIN

Co-directeur de thèse: Pr. Gilles THURET

Membre du Jury:

Pr. Bernard DELBOSC (CHU de Besançon)	Rapporteur
Dr. Florent APTEL (CHU de Grenoble)	Rapporteur
Pr. Michel PEOC'H (CHU Saint-Etienne)	Membre du jury
Pr. Philippe GAIN (CHU Saint-Etienne)	Directeur de thèse
Pr. Gilles THURET (CHU Saint-Etienne)	Co-directeur de thèse

Remerciements

La chance de pouvoir faire une thèse m'est venue quand Pr. Gain a accepté de m'accueillir dans son laboratoire. Ces trois ans ont été pour moi un moment de vie particulier au long duquel j'ai pu me dévouer entièrement à ma passion pour la recherche.

Je voudrais remercier mes professeurs Philippe Gain et Gilles Thuret. Leur grande motivation et leur énergie inépuisable pour mettre en application la recherche fondamentale m'ont beaucoup guidé dans mes travaux de recherche. Je tiens à les remercier pour la confiance qu'ils m'ont accordée et leur grand soutien pour mon travail.

Je tiens à remercier les membres du jury, le Pr. Bernard DELBOSC, le Dr. Florent APTEL, et le Pr. Michel PEOC'H pour le temps précieux qu'ils ont bien voulu accorder à la relecture et à la correction de mon manuscrit. Leurs avis sont particulièrement importants pour aider un chercheur débutant à s'améliorer et à s'y inspirer pour les prochaines activités de recherche.

Je voudrais remercier tous les membres de l'équipe du BiiGC pour le quotidien à votre côté. Grand merci à Simone et Chantal d'avoir assumé la lourde responsabilité de l'encadrement du quotidien du BiiGC. Merci à mes "co-équipiers" Zhiguo, Aurélien, Clotilde, Giacomo, Nadine, Tanguy, Emmanuel, Chaker, Nelly, Nicolas, Anne-Sophie, Mari-Caroline, sans oublier également mes amis du LINA, GIMAP, LBTO et LPE. J'apprécie la précieuse présence de chacun d'entre vous. Merci pour de beaux moments de discussion, de rigolade, de partage, merci pour vos conseils, votre gentillesse, votre disponibilité et pleines d'autres belles choses que ces pages ne suffisent pas à tout dire.

Enfin, je voudrais remercier mes amis et ma famille qui étaient de près ou de loin, de très près ou de très loin. Leur confiance à mes décisions et leur encouragement à chaque reprise étaient indispensables à ma réussite.

La thèse n'étant que le début d'une aventure de la science et de la vie, je vous remercie pour votre participation à la réalisation de cette thèse et je souhaite pouvoir partager avec vous mes prochaines expériences

Sommaire

PARTIE BIBLIOGRAPHIQUE 12

CHAPITRE I - De l'endothélium primitif à l'endothélium adulte 13

1. Morphogénèse de la cornée 13
   1.1. Etapes de développement 13
      1.1.1. Rappels sur l'embryogénèse humaine 13
      1.1.2. Morphogénèse de l'œil et de la cornée 14
   1.2. Mécanismes moléculaires 17
      1.2.1. Facteurs de transcription 18
      1.2.2. Voie de signalisation Wnt 20
      1.2.3. Angiogenèse 23
      1.2.4. Neurogenèse, guidage d'axones, innervation 24

2. Endothélium cornéen adulte 26
   2.1. Anatomie 26
      2.1.1. La cornée 26
      2.1.2. Anatomie endothéliale 29
      2.1.3. Structures péri-cornéennes 32
   2.2. Régulation de la transparence de la cornée 34
      2.2.1. Balance pompe-fuite (« pump-leak » des anglo-saxons) 35
      2.2.2. Transport d'actifs par l'endothélium 36
      2.2.3. Mécanismes de la déturgescence 40
      2.2.4. Rôle de la structure cytosquelettique 43
   2.3. Interactions avec l'environnement 46
      2.3.1. Membrane Descemet 46
      2.3.2. Humeur aqueuse 50

3. Marqueurs endothéliaux 55

CHAPITRE II - Cycle cellulaire, Capacité proliférative et Sénescence 57

1. Rappel de mécanismes moléculaires de régulation du cycle cellulaire 57
   1.1. Généralités sur le cycle cellulaire 57
   1.2. Les phases du cycle cellulaire 59
      1.2.1. Phase G0 59
      1.2.2. Phase G1 59
      1.2.3. Transition G1/S 60
      1.2.4. Phase S 61
      1.2.5. Phase G2 61
      1.2.6. Transition G2/M 62
      1.2.7. Phase M 62
      1.2.8. Transition M/G1 64
   1.3. Points de contrôle 64
      1.3.1. Point de contrôle G1/S 64
      1.3.2. Point de contrôle G2/M 65
      1.3.3. Point de contrôle en métaphase 66

2. Arrêt du cycle cellulaire de l'endothélium cornéen à la phase G1 68
   2.1. Inhibition de contact 70

2.2. Régulation par des facteurs de croissance 71

3. Sénescence 75
3.1. Généralités sur la sénescence 76
3.1.1. Sénescence réplicative 76
3.1.2. Sénescence prématurée 77
3.1.3. Mécanismes d'arrêt du cycle cellulaire dans la sénescence 80
3.1.4. Marqueur de la sénescence 80
3.2. Etat de sénescence de l'endothélium cornéen 81
3.2.1. Hypothèse 1 : sénescence réplicative peu probable 82
3.2.2. Hypothèse 2 : Sénescence prématurée prouvée 82

4. Capacité proliférative résiduelle 84
4.1. Effet de l'âge et de la localisation centrale ou périphérique 84
4.2. Zone péricornéenne 88

CHAPITRE III - Cultures de l'endothélium cornéen 90

1. Culture primaire 90
1.1. Optimisation des conditions de culture 90
1.1.1. Milieu de culture 91
1.1.2. Coating 95
1.1.3. Densité d'ensemencement 98
1.1.4. Culture en hypoxie 100
1.2. Sélection du matériel cellulaire de départ 102
1.2.1. Âge de donneur 102
1.2.2. Localisation centrale versus périphérique des cellules endothéliales de départ 103
1.2.3. Culture en sphère (sphere-forming assay) 104
1.3. Choix des protocoles 106

2. Différenciation/Transdifférenciation 108

3. Thérapie ciblée 112
3.1. Transfection d'oncogènes 112
3.2. Déblocage de l'arrêt du cycle en phase G1 113
3.3. "Rajeunissement" par la télomérase 115
3.4. Introduction de facteurs anti-apoptotiques 117

4. Critères qualité des cellules obtenues 117
4.1. Indentité des cellules obtenues (CQA 1) 117
4.2. Fonctionalité des cellules obtenues (CQA 3) 118

REFERENCES BIBLIOGRAPHIQUES 122

PARTIE EXPERIMENTALE..... 131

Articles en premier auteur 132

ARTICLE I: Microarray analysis of cell cycle gene expression in adult human corneal endothelium cells 132

ARTICLE II: Corneal endothelial cells from old donors: differentiation, senescence, proliferative capacities and optimized culture conditions..... 180

ARTICLE III: Electric pulses trigger mitosis in human corneal endothelial cells 205

Article en temps que co-auteur 221

ARTICLE I: Revisited microanatomy of the corneal endothelial periphery: new evidence for continuous centripetal migration of endothelial cells in humans..... 221

ARTICLE II: Optimization of immunolocalization of cell cycle proteins in human corneal endothelial cells..... 234

ARTICLE III: Effects of fixatives temperature on immunolocalization in flat-mounted human corneal endothelial cells..... 253

CONCLUSION..... 271

Publications et communications scientifiques 274

Curriculum vitae..... 277

Abréviations

CE: cellule endothéliale

CDK: kinase cycline-dépendante

CKI: inhibiteur des kinases cycline-dépendantes

CN: crête neurale

CS: cellule souche

DCE: densité cellulaire endothéliale

OC: organoculture

OCT: tomographie à cohérence optique

MLC: chaînes légères de la myosin

SVF: sérum de veau foetal

Avant-propos

La cécité cornéenne peut être traitée par l'allogreffe d'une cornée prélevée sur un donneur décédé. Cette affirmation cache en pratique une situation bien plus complexe dont le principal élément limitant est, au niveau mondial, le nombre très insuffisant de dons de cornées. L'optimisation du don principalement dans de nombreux pays d'Europe et aux USA montre qu'il est possible de couvrir les besoins nationaux et même d'être exportateur, mais cette situation n'est pas extrapolable aux pays émergents, en premier lieu à ceux des continents Asiatiques et Africains où vivent les populations qui ont les plus grands besoins en greffe. Les multiples obstacles aux dons (religieux, sociétaux, éducationnels, logistiques…) font que, probablement, le nombre d'allogreffes de cornées actuellement pratiqué est proche de son maximum et que les solutions pour atteindre un équilibre offre/demande sont ailleurs.

La prévention des pathologies cornéennes cécitantes s'améliore constamment (trachome surtout, mais également herpès et réduction des dystrophies du pseudophaque post cataracte) mais d'autres pathologies cornéennes ont une incidence qui augmente: certaines sont liées au vieillissement comme la dystrophie endothéliale de Fuchs qui menace par exemple 4% des américains de plus de 40 ans et les regreffes cornéennes, d'autres sont iatrogènes et concernent les implants de chambre antérieure pour la correction de la myopie forte. Enfin, à l'échelle mondiale, les séquelles de kératites infectieuses restent nombreuses et leur incidence ne baissera probablement pas avant le développement des solutions alternatives à la greffe.

En parallèle, se sont développées récemment (ou re-développées de façon plus standardisée) les greffes lamellaires, qu'elle soit antérieure pout les pathologies du stroma à endothélium normal ou endothéliale pour les pathologies endothéliales à stroma encore normal. En apportant plus de sécurité chirurgicale et une réhabilitation visuelle souvent plus rapide que la greffe perforante centenaire, elles ont contribué à élargir les indications de la greffe cornéenne et donc nécessairement à augmenter les besoins en greffon. Il s'agit de plus de techniques « consommatrices » de greffons puisque la préparation des greffons lamellaires endothéliaux s'accompagne d'un pourcentage non négligeable d'échec qui n'est pas compensé par la possibilité (plus théorique que réelle) de greffer la partie antérieure d'une cornée à un patient et la partie postérieure à un second receveur.

Enfin, l'augmentation constante des niveaux d'exigence de contrôles de qualité et de sécurité imposés aux greffons cornéens limite toujours un peu plus le nombre de cornées utilisables.

L'ensemble de ces facteurs déséquilibre encore la balance offre/demande et le développement d'alternative à l'allogreffe à partir d'un donneur devient un impératif reconnu. **La principale alternative réaliste est la bioingénierie cornéenne endothéliale.** En effet, si la reconstruction au laboratoire d'une cornée entière est en échec depuis plus de 20 ans, celle de substituts aux greffes endothéliales est, quant-à elle, réaliste. Les indications de greffes endothéliales représentent globalement 1/3 de toutes les indications mondiales. Le développement de solutions alternatives à la greffe endothéliale permettrait donc de réserver les cornées des donneurs aux autres indications. Deux stratégies sont d'ores et déjà en cours de développement et ont fait récemment leurs preuves de concepts. La première est l'injection directement dans la chambre antérieure du patient de CEs en suspension, la seconde est la reconstruction in vitro d'un greffon constitué d'un support transparent, fin, manipulable par le chirurgien, recouvert d'une monocouche de CEs fonctionnelles (voir ci-après). Ces nouvelles thérapies cellulaires et tissulaires, véritable médecine régénérative, utiliseront des cellules ou tissus qui auront le statut de médicaments de thérapie innovante (MTI) dans la législation française. Dans les deux cas, **la première étape indispensable est l'obtention de façon reproductible, de culture de CEs cornéennes humaines en très grand nombre**, disponibles à tout moment pour réaliser l'une ou l'autre des thérapies.

Le travail de Thèse que nous présentons est le premier du laboratoire BiiGC à concerner la bioingénierie endothéliale cornéenne. Nous comprenons la bioingénierie comme un ensemble de procédés destinés à « produire du vivant » en respectant un enchainement contrôlé et raisonné d'étapes dérivées du monde industriel. A ce titre, la bioingénierie endothéliale cornéenne devra aboutir à une méthode efficace et acceptable sur un plan médico-économique pour être diffusée sur la planète comme cela a été possible dans d'autres domaines médicaux comme la greffe de cellules souches hématopoïétiques. Cette Thèse explore les différentes possibilités permettant d'obtenir une culture de masse de CEs. Une connaissance approfondie de la biologie fondamentale de l'endothélium cornéen humain est un prérequis nécessaire puisque l'absence de prolifération in vivo et les capacités très limitées in vitro constituent l'obstacle majeur. Deux aspects sont en particuliers incontournables car ils impactent

potentiellement les stratégies d'obtention de CEs fonctionnelles: l'embryologie et le cycle cellulaire de l'endothélium cornéen. Nous avons, dans le premier chapitre, repris les principes du développement embryonnaire de la cornée humaine en intégrant les travaux les plus récents sur les voies de signalisation (en particulier celle de Wnt/caténines) qui auront très probablement des applications directes dans l'induction en laboratoire de la différenciation de cellules souches (embryonnaires ou pluripotentes induites) en CEs adultes matures. Nous avons ensuite rappelé les caractéristiques des CEs adultes fonctionnelles en cataloguant les protéines supportant les fonctions de pompes ioniques et celles responsables de l'effet barrière. Cette connaissance est indispensable à la mise en place des critères qualités qui permettront de certifier l'identité et la fonctionnalité des cellules obtenues avant d'envisager leur utilisation thérapeutique. Notons qu'actuellement ces critères ne font l'objet d'aucun consensus formel et qu'une proposition est faite à la fin du chapitre 3.

Le second chapitre présente les limitations des capacités prolifératives des CEs en réalisant la synthèse des connaissances sur le cycle cellulaire endothélial, la sénescence induite par le stress et les capacités résiduelles de certaines CEs localisées en périphérie de l'endothélium (**Article en co-auteur dans Stem-Cells**). L'une des stratégies de production de masse des CEs étant l'optimisation des cultures primaires, il est indispensable de connaître quels sont les freins physiologiques à la division des CEs. L'arrêt en phase G1 est du en partie à l'expression des cyclin kinases inhibitors p16, p21 et P27 eux même respectivement liés à la sénescence prématurée induite par le stress et qui augmente avec l'âge, à la voie p53 activée en réponse à des dommages oxydatifs à l'ADN et à la voie TGF-β et l'inhibition de contact. Le premier travail expérimental présenté (**Article 1 soumis à Plos One**) explore avec une biopuce dédiée à l'analyse des transcripts des gènes contrôlant le cycle cellulaire, 6 type de CEs susceptibles d'avoir un statut prolifératif différent : cornées port mortem, cornées en organoculture, culture in vitro confluente, culture in vitro non confluente, lignée cellulaire immortalisée HCEC-12. Ces 5 conditions expérimentales sont comparées au profil transcriptomique de CEs analysées immédiatement après prélèvement au cours d'une greffe de cornée pour kératocône. Jamais le profil de CEs aussi proche des conditions in vivo n'avait été analysé. Nos résultats, cohérents avec la littérature, retrouvent en plus pour la première fois les ARNm de plusieurs protéines impliquées dans l'arrêt prolifératif après dommage à l'ADN.

Le dernier chapitre, plus pragmatique, propose d'établir l'état actuel des connaissances sur les méthodes de cultures de masse des CEs. Il découle naturellement des notions fondamentales énoncées lors des 2 chapitres fondamentaux précédents. Les cultures primaires, en échec pendant de nombreuses années depuis les descriptions initiales de nos amis J. Bednarz et K. Engelmann (Hambourg) ont récemment été largement optimisées par l'équipe du Singapore Eye Research Institute qui a défini une séquence de culture utilisant plusieurs milieux d'expansion et stabilisation et les densités optimales de repiquage. Nous avons, pour chacune des techniques envisagées, insisté plus particulièrement sur les « cellules de départ » tant la sélection des donneurs et la localisation centrale ou périphérique influence la quantité de cellules possible à la fin de chaque processus d'expansion. La quasi totalité des publications décrivant le succès de stratégies de culture à partir d'endothélium cornéen de donneurs utilisent des donneurs jeunes, dans tous les cas de moins de 50 ans et souvent de moins de 30 ans. Etant profondément inscrits dans une démarche pragmatique translationnelle, nous avons étudié le statut prolifératif, le niveau de différenciation, les capacités de migration et de différenciation en présence de sérum de veau fœtal de CEs prélevées chez des donneurs ayant l'âge habituel des donneurs en Europe (Moyenne d'âge = 70 ans) (**Article 2, prévu pour Aging Cell**). Le but était de définir les possibilités réalistes de bioingénierie endothéliale à partir des donneurs habituels en France afin de décider ou non de s'orienter vers d'autres alternatives, en particulier les cellules souches. Notons que cette étude permettra également de définir les bases d'un travail collaboratif avec le Service de Biologie intégrative du CEA sur la sénescence des CEs et les méthodes pour la contourner.

Nous présentons ensuite les autres stratégies d'expansion cellulaire déjà décrites : 1/sélection et expansion des progéniteurs endothéliaux périphériques décrites uniquement par l'équipe Japonaise de Mimura et Amano (Tokyo) et que le BiiGC souhaite développer en sélectionnant encore plus précisément la zone contenant des clusters de CEs à l'extrême périphérie cornéenne, 2/ différenciation de cellules souches (travail en cours à BiiGC uniquement abordé ici), 3/ thérapies ciblées comprenant la transfection par un perturbateur du cycle cellulaire susceptible de relancer la prolifération des CE. A ce titre nous présentons en troisième article la description d'un effet inattendu, original, pro-prolifératif, d'un train d'impulsions électriques initialement destinées à l'électroporation de gène dans les CEs (**Article 3, prévu pour**

Mol Vis). Nous avons mis en évidence que ce stimulus physique était capable de déclencher la progression du cycle cellulaire jusqu'à la mitose de CEs in situ sur des cornées entières (le plus grand nombre de mitoses jamais décrit dans la littérature !) mais uniquement dans des zones de faible densité cellulaire, probablement par rupture de l'inhibition de contact lors de la lésion aléatoire par le choc électrique de CEs de grandes tailles.

Nous terminons la partie bibliographique de notre Thèse par la synthèse des contrôles qualités actuellement proposés pour s'assurer de l'identité des cellules produites (sont-elles bien des CEs ?) et sur leur fonctionnalité (sont-elles capables d'assurer la déturgescence du stroma cornéen ?). La spécialisation du BiiGC dans l'imagerie endothéliale nous permet de développer des techniques d'immunomarquage (**Article en co-auteur**) indispensable à la vérification de l'expression en bonne position des principales protéines caractérisant les CEs (en l'absence de marqueur spécifique). La branche "ingénierie" du BiiGC permet, pour finir, de présenter le bioréacteur cornéen (breveté) qui permettra pour la première fois et de manière beaucoup plus précise que les chambres de perfusion d'autrefois de vérifier sur des cornées humaines ex vivo maintenues dans leur environnement pressionnel habituel, la bonne fonctionnalité des différentes types de MTI développés au BiiGC au ailleurs.

PARTIE BIBLIOGRAPHIQUE

CHAPITRE I - De l'endothélium primitif à l'endothélium adulte

1. Morphogénèse de la cornée

1.1. Etapes de développement

Afin de mieux comprendre l'origine de l'endothélium cornéen, cette partie a pour objectif de présenter une synthèse des processus de développement de la cornée au cours de l'embryogénèse. Comprendre comment le neuroectoderme se différencie en endothélium cornéen devrait permettre de développer plus rapidement des procédés adaptés de bioingénierie pour différencier des cellules souches (CS) en cellules endothéliales (CE).

1.1.1. Rappels sur l'embryogénèse humaine

L'embryogénèse humaine se résume en principales étapes schématisées en Figure 1 (NIH 2009).

Segmentation : durant la 1ère semaine après la fécondation, en migrant vers la cavité utérine, les cellules **totipotentes** se divisent pour former la morula, puis se différencient en blastocyste constitué d'une couche externe s'appelant trophoblaste (origine du placenta et du chorion) et une masse cellulaire interne, l'embryoblaste (cellules **pluripotentes**).

Prégastrulation : durant la 2ème semaine, le développement du trophoblaste permet à l'embryon de s'implanter dans la muqueuse utérine. L'embryoblaste se transforme en embryon didermique composé d'épiblaste (à l'origine des tissus embryonnaires) et d'hypoblaste (à l'origine des parties extra-embryonnaires). L'épiblaste se creuse et forme la cavité amniotique, ce qui sert de nutrition à l'embryon, de protection contre les chocs, d'isolation thermique, d'hydratation des tissus et facilite les mouvements. L'hypoblaste, ou l'endoderme extra-embryonnaire, forme le sac vitellin qui régresse pendant le développement.

Gastrulation : à partir de la 3ème semaine, l'invagination de l'épiblaste forme le sillon primitif. Les premières cellules épiblastiques migrent, envahissent l'hypoblaste, le déplacent pour le remplacer par l'entoblaste définitif. Une autre partie des cellules épiblastiques migrent entre l'épiblaste et l'entoblaste, forme le 3ème feuillet

intermédiaire, le mésoblaste (mésoderme). L'épiblaste forme ainsi 3 feuillets : l'**ectoderme** (cellules épiblastiques non migrants), l'**entoderme** et le **mésoderme**.

Neurulation : l'invagination de l'ectoderme forme le tube neural et génère les crêtes neurales (CN). Il s'agit de la première étape de formation du système nerveux, le début de l'organogénèse.

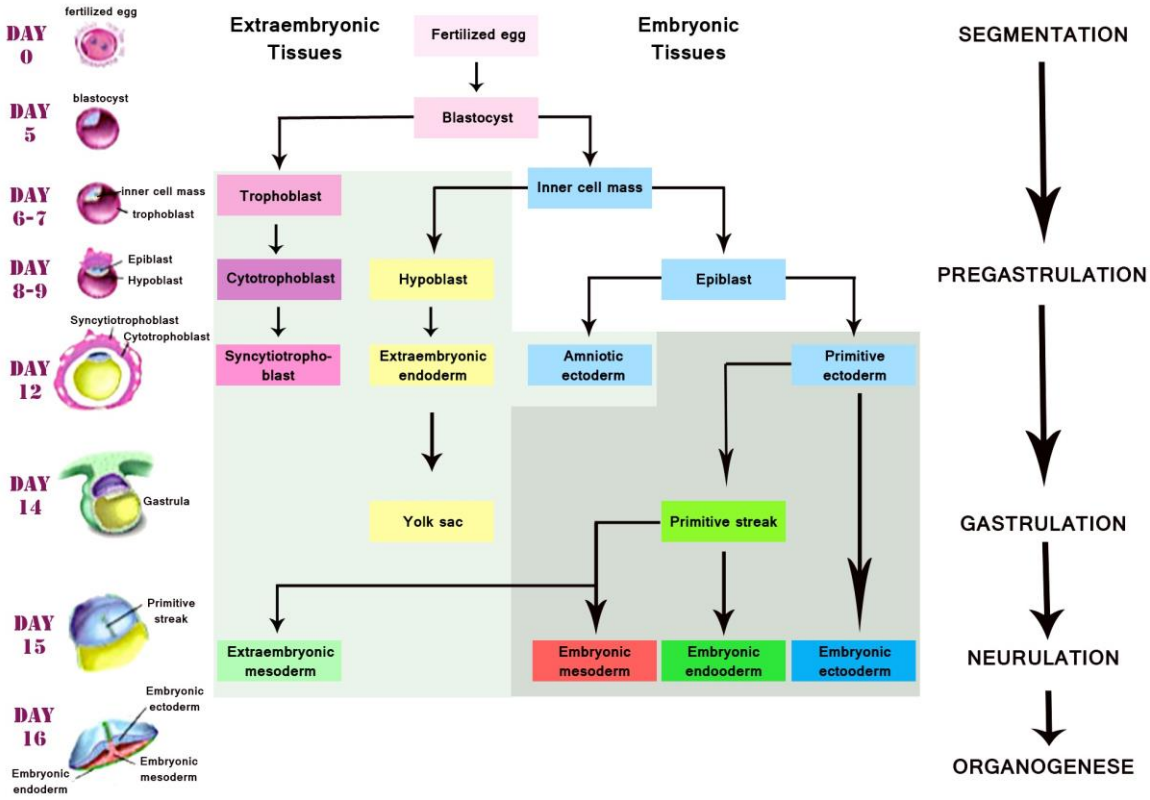


Figure 1. Principales étapes de l'embryogénèse humaine (d'après le site web National Institutes of Health, http://stemcells.nih.gov)

1.1.2. Morphogénèse de l'œil et de la cornée

Le développement de l'œil débute très tôt durant l'organogénèse humaine (Tripathi *et al.* 1991; Cook *et al.* 2006) (Figure 2).

Vers le 24ème jour du développement embryonnaire, après la fermeture du tube neural, la vésicule optique se forme à partir du neuroectoderme des 2 côtés de façon symétrique. Au 27ème jour, l'échange de signaux de l'ectoderme de surface avec la vésicule optique induit la formation la placode cristallinienne sur l'ectoderme de surface, puis son invagination pour former la vésicule cristallinienne. La vésicule optique se creuse en cupule optique qui sera la rétine. Au 33ème jour, la vésicule

cristallinienne se détache complètement de l'ectoderme pour se transformer en cristallin. La cupule optique se différencie en couche nerveuse et couche pigmentaire.

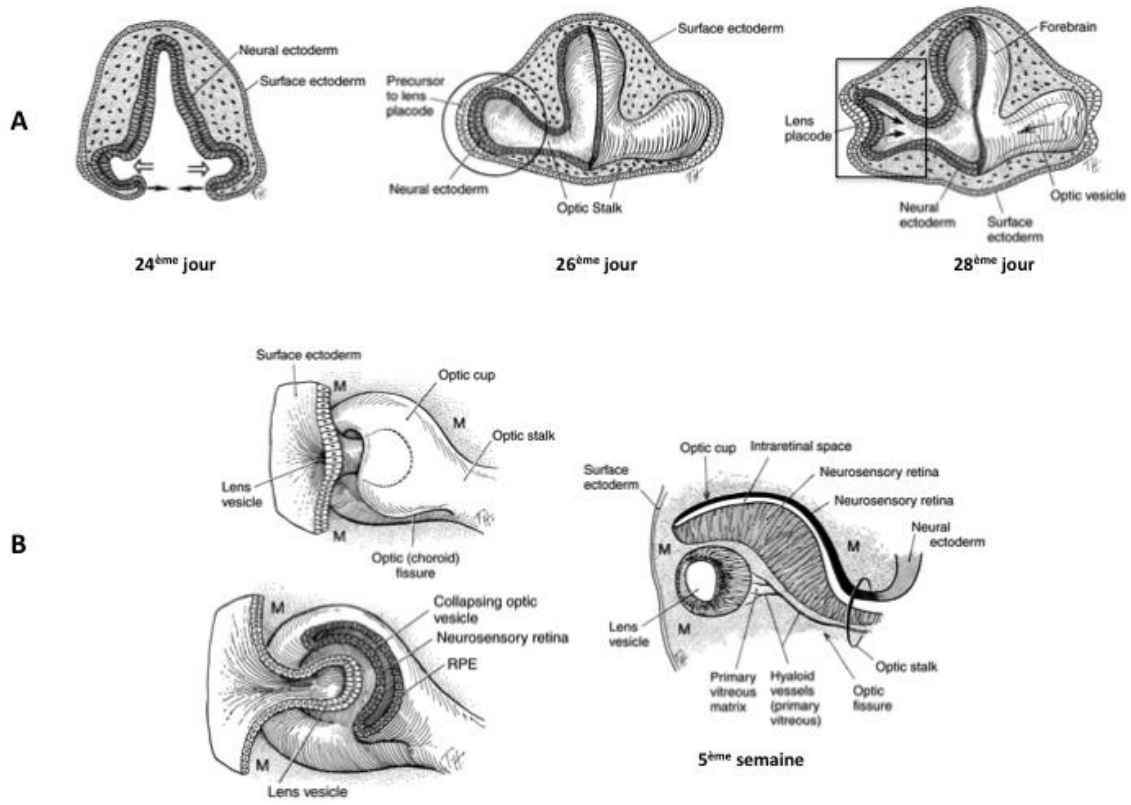


Figure 2. Morphogenèse de l'œil (D'après Cook CS et al. 2006). A: Après la fermeture de la tube neurale (24ème jour), l'échange de signaux avec la vésicule optique du neuroectoderme induit la formation de la placode cristallinienne au niveau de l'ectoderme de surface (26ème jour), puis l'invagination de la placode cristallinienne et la formation de la cupule optique (28ème jour). B: Durant la 5ème semaine, le développement de l'œil (A, zone cadré) continue par la formation de la vésicule cristallinienne qui se sépare de l'ectoderme de surface, futur l'épithélium cornéen. La cupule optique se transforme en couche pigmentaire et rétine. La migration des cellules mésenchymateuses dérivées de la crête neurale entre la vésicule cristallinienne et l'ectoderme de surface forme l'endothélium et le stroma cornéen.

Du 33ème au 57ème jour, l'ectoderme de surface forme l'épithélium cornéen (Figure 3). Ensuite, les cellules mésenchymateuses périoculaires dérivées de la CN migrent entre l'épithélium et la vésicule cristallinienne pour former la cornée ainsi que le segment antérieur de l'œil. Au 37ème jour, la 1ère vague de ces cellules forme l'endothélium cornéen en monocouche qui sécrète une lamelle basale appelée la membrane Descemet. La 2ème vague forme l'iris par migration à partir du contour de la cupule optique. Lors du 7ème semaine, le mésenchyme périoculaire d'origine de la CN continue de migrer entre l'épithélium et l'endothélium, puis se différencie en kératocytes du stroma qui sécrètent les fibres de collagène type I et la matrice

extracellulaire. Le mésenchyme périoculaire participe également au développement de la sclère et du trabéculum, formant l'angle iridocornéen.

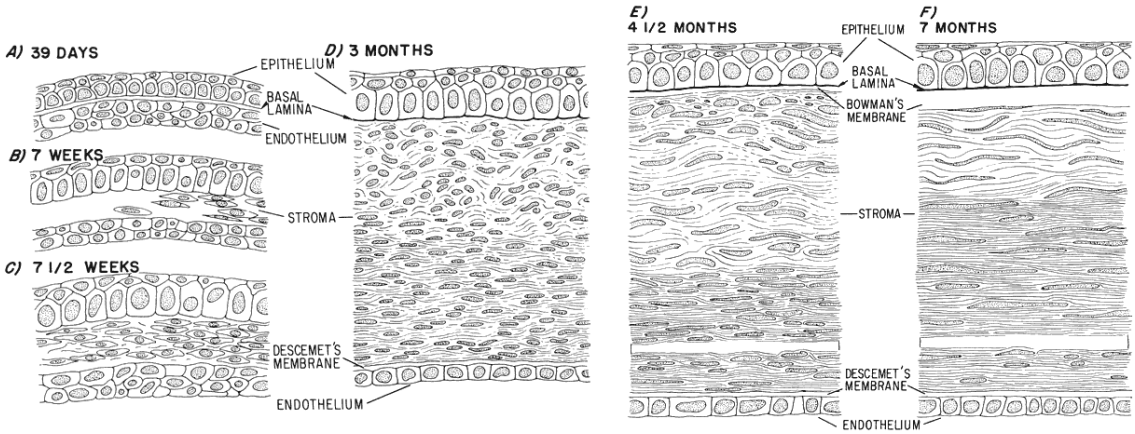


Figure 3. Formation et maturation de la cornée (D'après Cook CS et al. 2006). La première vague de migration (39ème jour) des cellules mésenchymateuses originaires des crêtes neurales forme l'endothélium cornéen. La deuxième vague de cellules se différencie en stroma cornéen.

Après l'organogénèse, les 3 couches de la cornée mâturent pour former une cornée fonctionnelle (Swamynathan 2013). L'ectoderme de surface forme l'épithélium qui passe de mono à bicouche à la naissance puis forme des cellules épithéliales squameuses de 5-6 couches après la naissance. La couche superficielle de l'épithélium se renouvelle à partir des cellules basales qui sont elles-mêmes régénérées à partir des niches limbiques de CS. Les cellules stromales secrètent de la matrice extracellulaire constituée de fibres de collagènes et de différents protéoglycanes, assurant la structure, la transparence et la résistance mécanique de la cornée. Le stroma se distingue en couche antérieure et postérieure ayant des propriétés différentes. L'endothélium est un nom trompeur car cette couche cellulaire dérive de la CN et non de l'endoderme. Il a été adopté par l'usage car il tapisse en fait une partie une cavité interne.

Entre les espèces, le développement de la cornée se déroule selon les mêmes séquences mais se distingue par la durée de gestation et de formation finale de la cornée (Cook *et al.* 2006). Plusieurs modèles animaux ont été utilisés pour se substituer au modèle humain : modèles murins, aviaire, poisson, etc. Chez le rat (Swamynathan 2013), la formation de la placode cristallinienne débute à partir du 10ème jour, puis l'invagination du placode cristallinienne formant la vésicule cristallinienne au 11ème jour et la migration de la CN entre la surface ectoderme et la vésicule cristallinienne, formant le stroma et l'endothélium à partir du 13ème jour. La cornée de rat est mature à partir de 6 semaines. Chez le xenopus laevis (Hu *et al.* 2013), la formation de

l'épithélium début à partir du 22ème jour, le stroma à partir du 37ème jour mais la membrane Descemet est formée seulement à partir du 55ème jour. Chez les oiseaux, il existe 3 vagues de migrations des cellules mésenchymateuses dérivées de la CN (Reneker *et al.* 2000) tandis que chez la souris, une seule vague de migration a été observée pour former l'endothélium et le stroma. D'autre part, différents modèles de souris transgéniques ont étés construits pour étudier l'impact de la sur/sous expression de certains gènes sur la formation de la cornée (Kao *et al.* 2013).

1.2. Mécanismes moléculaires

La morphogénèse de l'œil est un processus complexe impliquant plusieurs mécanismes moléculaires permettant d'induire la différenciation des cellules multipotentes en différents compartiments fonctionnels. Les stimuli externes activent des cascades de signalisation intracellulaires via différents facteurs de transcription, ainsi orientent la transformation vers un tissu spécifique.

L'échange de signaux entre la vésicule optique et l'ectoderme de surface induit la différenciation de l'ectoderme en placode cristallinienne qui se transforme en cristallin, et l'invagination de la vésicule optique en cupule optique qui devient la rétine (Fuhrmann 2010). En parallèle, l'induction de la migration et la différenciation du mésenchyme périoculaire originaire de la CN permet de former la cornée et la chambre antérieure. Une formation correcte de l'endothélium permet de dissocier l'iris et l'épithélium cristallinien de la cornée (Reneker *et al.* 2000). D'autre part, le développement du trabéculum dans la zone frontalière entre la cornée et l'iris, formant l'angle iridocornéen, est lié à la régularisation du flux de l'humeur aqueuse. La transparence de la cornée est également liée à l'absence de vascularisaton.

Le dysfonctionnement de ces processus provoque une malformation de la cornée et du segment antérieur. A titre d'exemple, dans le syndrome de Peters, les perturbations de la migration et de la différenciation du mésenchyme périoculaire ont été identifiées comme la cause des défauts de formation de l'endothélium et de la membrane de Descemet. Ces altérations entrainent l'opacité de la cornée centrale, l'adhésion entre la cornée et la surface antérieure du cristallin ou l'iris, et une malformation de l'angle iridocornéen à l'origine d'un glaucome congénital (Ohkawa *et al.* 2003).

En se focalisant sur la formation de la cornée et plus particulièrement de l'endothélium cornéen, cette partie a pour but de résumer la conception actuelle des mécanismes de différenciation de la CN en endothélium cornéen.

1.2.1. Facteurs de transcription

Le développement de modèles de souris transgéniques ou knock-out a permis d'identifier l'implication de certains facteurs de transcription dans la morphogénèse de la cornée, ainsi que son lien étroit avec les troubles oculaires chez l'homme (Swamynathan 2013) (Figure 4).

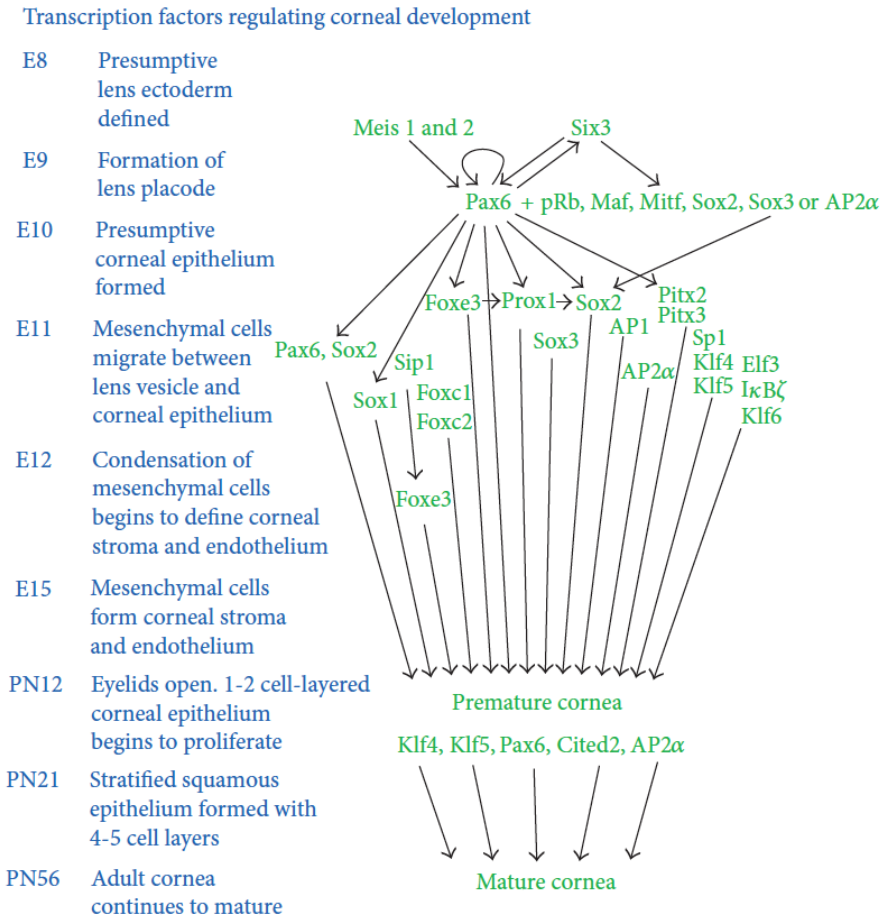


Figure 4. Implication des facteurs de transcription dans le développement de la cornée. Pax6 a été identifié comme le régulateur principal qui orchestre la formation de la cornée (Swamynathan 2013)

Pax6 est le facteur de transcription à homéodomaine principal[1] régulant la formation initiale de la cornée et de la chambre antérieure. Son expression a été détectée dès le début de la morphogénèse. Pax6 induit la formation de la placode cristallinienne, la formation de l'épithélium, du tissu conjonctif de la paupière et la distribution des cellules dérivées de la CN permettant de former le stroma et l'épithélium cornéen chez les souris. Durant la maturation de la cornée, Pax6 est impliqué dans la maintenance des CS limbiques et dans le mécanisme de réparation épithéliale après lésion. Le rôle exact de Pax6 dans la différenciation de la CN est encore peu connu.

Le deuxième facteur de transcription à homéodomaine est Pitx2 directement impliqué dans la migration et la différenciation des cellules dérivées de la CN en cornée. La mutation de Pitx2 chez les souris induit l'opacification de la cornée, la malformation de l'angle iridocornéen, ainsi qu'une hypertrophie de la cornée. La mutation du gène codant pour Pitx2 a été trouvée chez les patients atteints du syndrome d'Axenfeld-Rieger caractérisé par une malformation du segment antérieur. Le rôle de Pitx2 dans la différenciation du mésenchyme périoculaire en endothélium cornéen a été identifié comme passant par l'inhibition de la voie de signalisation Wnt canonique (voir 1.2.2).

A coté des facteurs de transcription à homéodomaine, d'autres facteurs ont été repérés comme ayant un lien dans la formation de la cornée, notamment Foxc1 exprimé par le mésenchyme périoculaire au 12ème jour de l'embryogénèse murine et impliqué dans la différenciation de endothélium. L'absence d'expression de Foxc1 génère la fusion cornée-cristallin et l'épaississement de l'épithélium cornéen. La mutation du gène codant Foxc1 a été également identifiée comme cause du syndrome d'Axenfeld-Rieger. D'autre part, Foxc1 a un effet dose dépendant pour la formation de néovaisseaux en contrôlant la balance entre les facteurs pro et anti angiogéniques.

Le rôle de plusieurs autres facteurs impliqués dans la formation de l'épithélium cornéen et du segment antérieur a été plus ou moins clarifié. En effet, les découvertes actuelles utilisant des modèles d'embryogénèse transgéniques, se limitent aux

[1] L'homéodomaine est la séquence d'acides aminés dont la conformation permet de reconnaître de façon spécifique des régions régulatrices d'autres gènes (UPMC - UFR des Sciences de la Vie (UFR 927), http://www.snv.jussieu.fr)

observations morphologiques mais développent peu d'explication à l'échelle moléculaire.

1.2.2. Voie de signalisation Wnt

Définition : Les protéines Wnt [1] sont impliquées dans les processus de développement, prolifération et différenciation des progéniteurs des différents organes. Il y a au moins 3 voies de signalisation Wnt (Figure 5): voie canonique, voie de polarité planaire des cellules (PCP, planar cell polarity) et voie dépendant du calcium. Pour la voie canonique, la fixation des ligands Wnt à leurs récepteurs stabilise la β-caténine cytoplasmique en empêchant sa dégradation. L'entrée de la β-caténine dans le noyau peut activer l'expression de certains gènes via son interaction avec les facteurs de transcription T-cell (TCF) et des coactivateurs. La voie PCP consiste en l'activation de RhoA (RAS homologue gene-family member A) et RAC1 (ras-related C3 botulinum toxin substrate 1), conduisant à l'activation de la kinase du stress JNK et de ROCK, déclenchant ainsi la remodélisation du cytosquelette et le changement dans l'adhérence et la motilité cellulaire. La voie dépendante du Ca^{2+} agit via des protéines G et des phospholipases, entrainant l'augmentation transitoire du Ca^{2+} cytoplasmique, ce qui active la protéine kinase C (PKC), CAMKII et la Phosphatase calcineurin (Kanehisa & Goto 2000; Kanehisa *et al.* 2012). La signalisation Wnt a le rôle important dans le développement des tissus durant l'embryogénèse et aussi le maintien de la CS à l'état indifférencié à l'âge adulte.

[1] Wnt est l'abbréviation de Wingless intégration site pour les drosophiles sans ailes

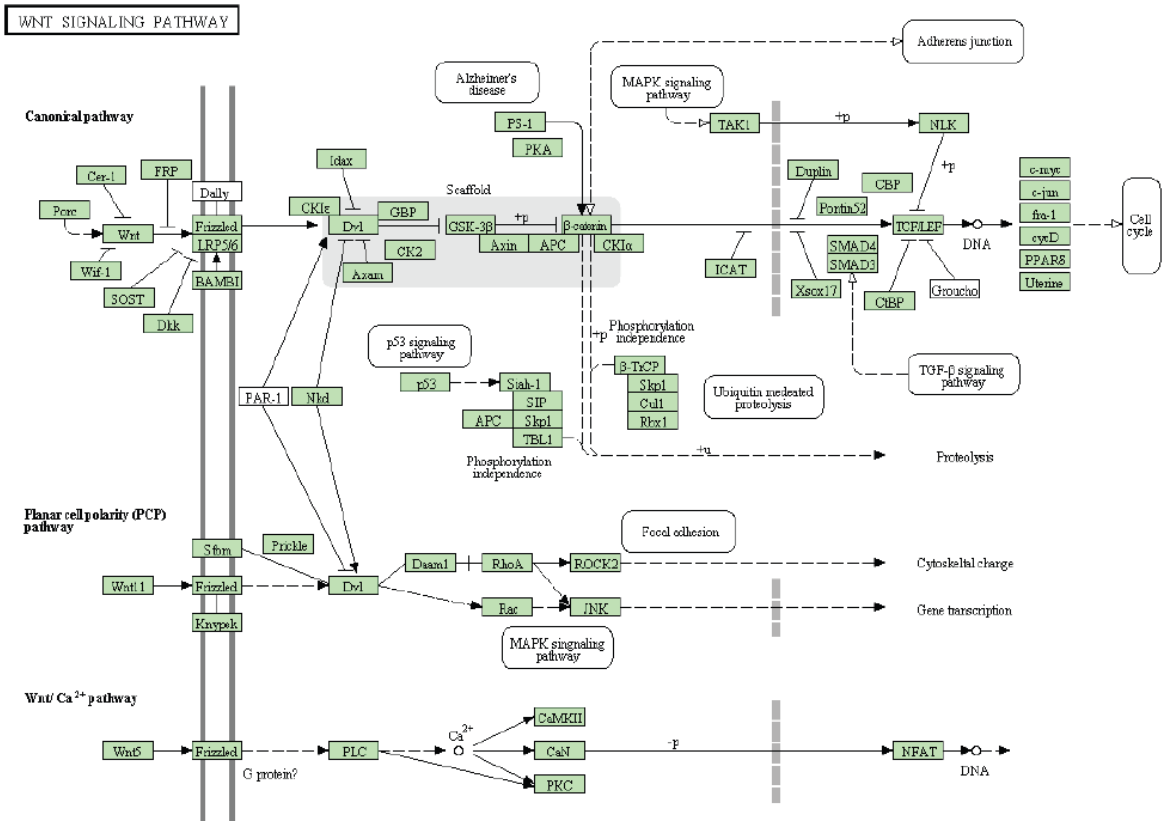


Figure 5. Voies de signalisation Wnt chez l'homme (Kanehisa & Goto 2000; Kanehisa et al. 2012). Schéma de synthèse obtenu à partir de Kyoto Encyclopedia of Genes and Genomes (KEGG, http://www.genome.jp/kegg/).

La voie Wnt/β-caténine (voie Wnt canonique) est détectée dès le début du développement de l'œil. L'activation de la β-caténine au niveau de l'ectoderme de surface bloque l'induction de la placode cristallinienne et de la glande lacrymale (Gage *et al.* 2008).

L'implication de la voie Wnt dans la formation de la cornée est confirmée par la variation d'expression de ses ligands durant les différents stades d'évolution. L'expression de Wnt1 liée à celle du Kératocan a été détectée durant la différenciation de la CN en stroma cornéen chez les souris (Kao *et al.* 2013). Chez les volailles, l'expression de Wnt-5a et Wnt-11 ont été observée lors de l'invasion du stroma cornéen (Jin *et al.* 2002), celle de Wnt9a est observée au niveau de l'endothélium (Fokina & Frolova 2006).

Plusieurs travaux récents ont montré la différenciation du mésenchyme périoculaire en endothélium via l'inhibition de la voie Wnt/β-caténine par Pitx2 et par la voie de signalisation de l'acide rétinoïque (Gage *et al.* 2008; Kumar & Duester 2010).

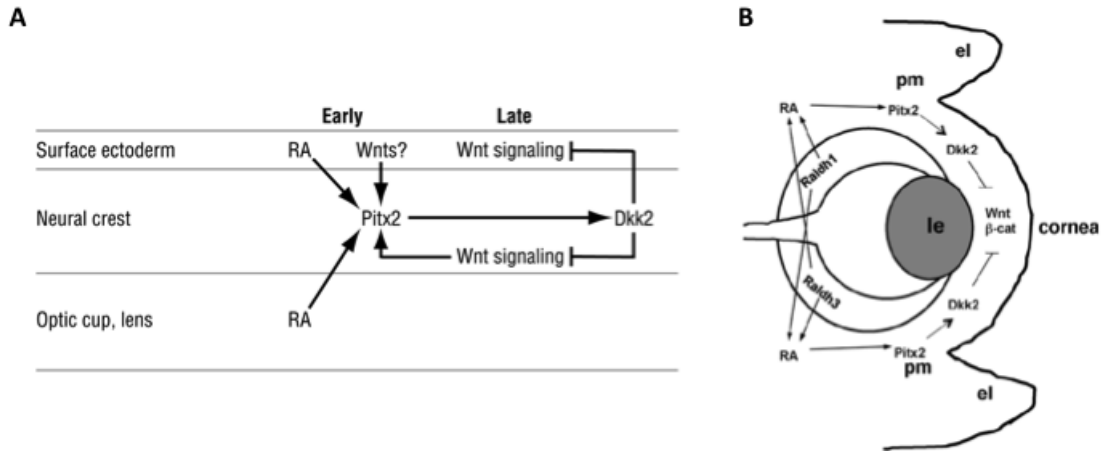


Figure 6. Modèle d'interférence de signal entre l'acide rétinoïque et la voie Wnt/β-caténine durant la morphogénèse de l'œil. A: Pitx2 inhibe la voie Wnt canonique via induction de Dkk2 et s'autorégule durant le développement du segment antérieur (Gage et al. 2008). B: L'acide rétinoïque synthétisé par la rétine induit l'expression de Pitx2, puis Dkk2 et inhibe la voie de signalisation Wnt/β-caténine au niveau du mésenchyme périoculaire, ce qui provoque sa migration entre l'épithélium et le cristallin pour former l'endothélium et le stroma cornéen (Kumar & Duester 2010). RA, acide rétinoïque; pm, mésenchyme périoculaire); el, eyelid =paupière; le,lens= cristallin

La voie de signalisation de l'acide rétinoïque implique directement la morphogénèse du segment antérieur à partir de la CN via l'induction du facteur de transcription Pitx2. L'effecteur direct de Pitx2 semble être Dkk2 qui est antagoniste extracellulaire de la voie canonique Wnt/β-caténine. L'inhibition de la voie Wnt canonique par Dkk2 au niveau du mésenchyme périoculaire permet sa différenciation en cellule de la cornée et non en tissu conjonctif. La formation de la surface oculaire nécessite la suppression de la voie Wnt canonique au centre et son augmentation vers la périphérie de la cornée. D'autre part, Pitx2 s'autorégule via Dkk2, la suppression de Dkk2 augmente l'expression de Pitx2.

Considérant que la CN se différencie en endothélium cornéen via l'inhibition de la voie Wnt canonique, il est possible que l'ingénierie tissulaire à partir des CS ou progénitrices nécessite la suppression transitoire de la voie Wnt canonique (Gage *et al.* 2008). Récemment, il a été d'ailleurs démontré la possibilité de transdifférencier les CS stromales humaines en cellules exprimant l'ARNm des marqueurs endothéliaux (*ATP1A1, SLC4A4, CA2, COL4A2, COL8A2, CDH2*) en utilisant de l'acide rétinoïque et l'inhibiteur de GSK-3β pour réguler la voie Wnt canonique (Hatou *et al.* 2013) . Pourtant, l'effet simultané de l'acide rétinoïque et de l'inhibiteur de GSK-3β est restraint à l'activation de l'expression de Pitx2 par les

précurseurs d'origine stromale de souris. La régulation de la voie Wnt canonique des cellules humaines sous ces éléments n'ont pas été clarifiée (voir Chapitre III - 2).

A côté de la voie Wnt canonique, la voie de polarité planaire des cellules est également impliquée dans la formation de l'endothélium cornéen et de l'angle iridocornéen (Yuan *et al.* 2013).

1.2.3. Angiogenèse

L'angiogenèse contribue indirectement à la transparence de la cornée en limitant son développement au niveau du limbe. Le rôle de certains facteurs de transcription au niveau du mésenchyme périoculaire a été rapporté dans la formation de la zone périphérique de la cornée. Selon les descriptions précédentes (voir 1.2.2), Dkk2 agit comme inhibiteur pour l'induction de la différenciation du mésenchyme périoculaire en cellules de la cornée. L'absence d'expression de Dkk2 chez la souris induit la formation anormale des vaisseaux sanguins qui dépassent la limite du limbe (Gage *et al.* 2008). D'autre part, Lmx1b (Liu & Johnson 2010) et FoxC1 (Koo & Kume 2013) ont également été identifiés comme facteurs régulateurs de l'angiogenèse au niveau du limbe. L'expression de Lmx1b au niveau du mésenchyme périoculaire antérieur est nécessaire pour le développement du trabéculum et le maintien de la transparence de la cornée en limitant l'invasion de vaisseaux sanguins au niveau de la cornée. L'expression de Foxc1 par le mésenchyme périoculaire maintient une balance entre les facteurs pro et anti-angiogéniques (Figure 7). Il a été constaté que Foxc1 est sous-exprimé par les CE cornéennes adultes par rapport à la naissance (Swamynathan 2013).

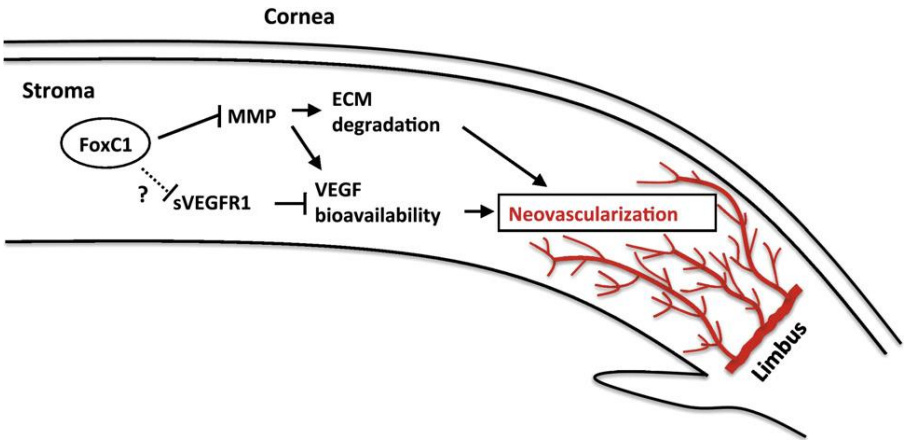


Figure 7. FoxC1 régule précisément la balance entre les voies pro et anti angiogéniques (Koo & Kume 2013).

1.2.4. Neurogenèse, guidage d'axones, innervation

Le développement du système nerveux aboutit à ce que la cornée soit le tissu le plus innervé du corps. Il a été reporté récemment que le guidage d'axone contribue également à l'orientation de la migration et la différenciation de la CN.

Les signalisations liées aux récepteurs Neuropilin (Npn) et aux Semaphorines (Sema) durant l'innervation du stroma (McKenna *et al.* 2012) influencent également la migration et différenciation des cellules de la CN durant l'organogénèse chez les volailles et les souris (Gammill *et al.* 2006), notamment la signalisation Sema3A/Npn-1 (Lwigale & Bronner-Fraser 2009) (Figure 8) de l'embryon de poulet. L'expression de Sema3A a été détectée au niveau de l'épithélium cristallinien et Npn-1 au niveau du mésenchyme périoculaire avant la migration entre l'épithélium et le cristallin. L'absence de cette signalisation favorise la migration prématurée des cellules de la CN. L'épithélium cristallinien secrète Sema3A dans la région périoculaire au 4ème jour du développement embryonnaire du poulet, ce qui inhibe la migration du mésenchyme périoculaire via les récepteurs membranaires Npn-1. Ensuite, une partie des cellules du mésenchyme périoculaire s'adapte en sous-exprimant Npn-1 et devient insensible à l'inhibition par Sema3A. Ces cellules changent de morphologie et migrent entre l'épithélium et le cristallin, formant l'endothélium, puis le stroma. Cela explique la pause de migration d'environ 2 jours du mésenchyme périoculaire entre l'ectoderme de surface et la cupule optique avant son invasion entre le cristallin et l'épithélium cornéen chez les volailles. D'autre part, une partie du mésenchyme périoculaire maintenant l'expression de Npn-1 continue d'être inhibée par Sema3A et reste dans la zone périoculaire pour former l'uvée antérieure et les vaisseaux sanguins.

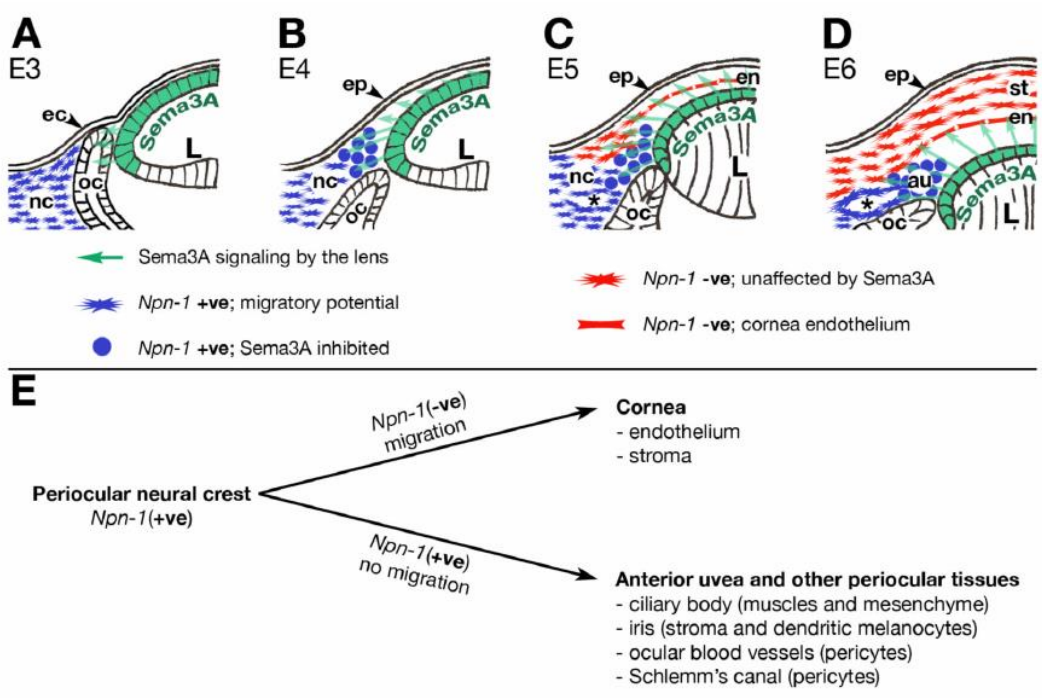


Figure 8. Modèle de régulation de la migration de la crête neurale (CN) par la signalisation Sema3A/Npn-1 durant le développement de l'œil (Lwigale & Bronner-Fraser 2009). A: la barrière physique entre l'ectoderme et la cupule optique empêche la migration des cellules de la CN. B: La cupule optique se sépare de l'épithélium cornéen, mais la migration des cellules exprimant Npn-1 est inhibée par Sema3A secrété par le cristallin. C-D: Les cellules sous-exprimant Npn-1 perdent leur sensibilité avec Sema3A et migrent entre l'épithélium et le cristallin, formant l'endothélium et le stroma cornéen. Les cellules maintenant l'expression de Npn-1 restent dans la région périoculaire et forment l'uvée antérieur et les vaisseaux sanguins. E: La signalisation Sema3A/Npn-1 sépare les cellules mésenchymateuses originaires de la CN en deux lignées: les cellules sous-exprimant Npn-1 pouvant migrer et former la cornée, et les cellules exprimant Npn-1 non migrant, formant l'uvée antérieur et d'autres tissus périoculaires.

Pour conclure, l'échange de signaux entre les cellules permet d'induire leurs différenciations via l'activation de cascades de signalisation intracellulaire qui modifient le comportement des cellules, donc leurs fonctionnalités. La compréhension de ces mécanismes est primordiale pour étudier le comportement des CE cornéennes adultes ainsi que leur processus de régénération et leurs états de différenciation. Plusieurs découvertes récentes sur l'implication des voies de signalisation Wnt canonique et Npn/Sema ont partiellement éclaircie ces processus et devraient servir à la bioengénierie cellulaire et tissulaire. D'autre part, la différenciation de l'endothélium cornéen doit être interprétée en parallèle du développement des autres composants du segment antérieur comme l'angle iridocornéen ou l'angiogenèse, la formation du cristallin et celle du stroma cornéen, pour avoir une vision complète de la fonctionnalité de la cornée.

2. Endothélium cornéen adulte

Après la naissance, la cornée continue sa maturation morphologique pour assurer ses fonctions dont les principaux mécanismes de maintien de la transparence sont régulés par l'endothélium cornéen. Cette partie consiste à décrire les changements anatomiques de l'endothélium au niveau de la cornée humaine, ainsi que le développement de ses fonctions en interaction avec son environnement.

2.1. Anatomie

2.1.1. La cornée

Constituée de trois couches cellulaires à la naissance, la cornée continue sa maturation et atteint en moyenne 11,5 mm de diamètre et 536±31 µm d'épaisseur centrale à l'âge adulte (Doughty & Zaman 2000) (Figure 9).

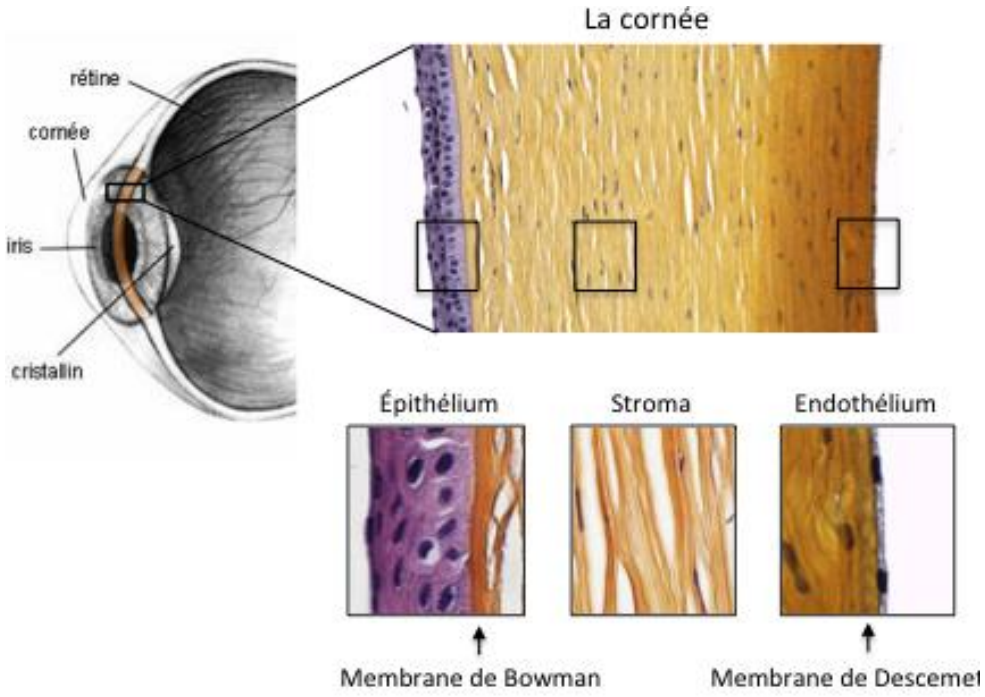


Figure 9. Coupe transversale de la cornée humaine adulte, colorée à l'Hématéine-Eosine-Safran (EA2521 BiiGC, Université Jean Monnet, Saint Etienne)

La couche externe de la cornée est l'**épithélium**. Composée de 4 à 7 couches cellulaires, ces cellules forment une barrière anti-inflammatoire et anti-angiogénique. Les cellules basales au contact de la **membrane de Bowman** sont la source du renouvellement vertical des cellules jusqu'à la couche superficielle.

En dessous de l'épithélium, le **stroma** cornéen représente 90% l'épaisseur de la cornée. Constitué principalement de protéoglycanes et de fibres de collagène de type I et V organisés de façon dense et régulier en lamelle, le stroma permet la transmission de la lumière à travers la cornée. A la naissance, les kératoblastes dérivés du mésenchyme périoculaire secrètent la couche de stroma antérieur puis se différencient en kératocytes secrétant le stroma postérieur plus dense en matrice extracellulaire à l'âge adulte (Hassell & Birk 2010).

En parallèle de la matrice extracellulaire permettant de contraindre l'organisation des fibres de collagène, la transparence du stroma cornéen est régulée principalement par la monocouche de CE à la face postérieure de la cornée. Occupant seulement 2% de l'épaisseur de la cornée, l'**endothélium** est séparé du stroma par la **membrane de Descemet** (MD) et fonctionne comme barrière sélective pour le transport d'ions et d'eau entre la chambre antérieure et le stroma.

Afin d'évaluer la qualité de la cornée chez les patients (*in vivo*) ou du greffon cornéen (*ex vivo*) avant greffe, plusieurs méthodes ont été développées pour quantifier la fonctionnalité du stroma et de l'endothélium (Figure 10). Brièvement et sans être exhaustif, la bonne organisation de l'ultrastructure du stroma évaluée en microscopie électronique en transmission reflet sa capacité à transmettre les contrastes d'une image. La **transparence** des greffons cornéens peut aussi être qualifiée par un dispositif original mis au point et validé au BiiGC basé sur la fonction de modulation de trasfert appelé "transparomètre" (Acquart *et al.* 2013). D'autre part, son **épaisseur** peut être mesurée par pachymétrie ultrasonore, pachymétrie laser ou par tomographie à cohérence optique (OCT). Pour l'endothélium, la **densité cellulaire endothéliale** (DCE) minimum *in vivo* capable d'assurer la déturgescence de la cornée est de 400-500 cellules/mm^2. Elle peut être mesurée par microscopie spéculaire sur les patients ou pour les greffons conservés en hypothermie à +4°C (méthode américaine), ou par microscopie après dilatation temporaire des jonctions intercellulaires pour les greffons conservés en organoculture (OC, méthode européenne).

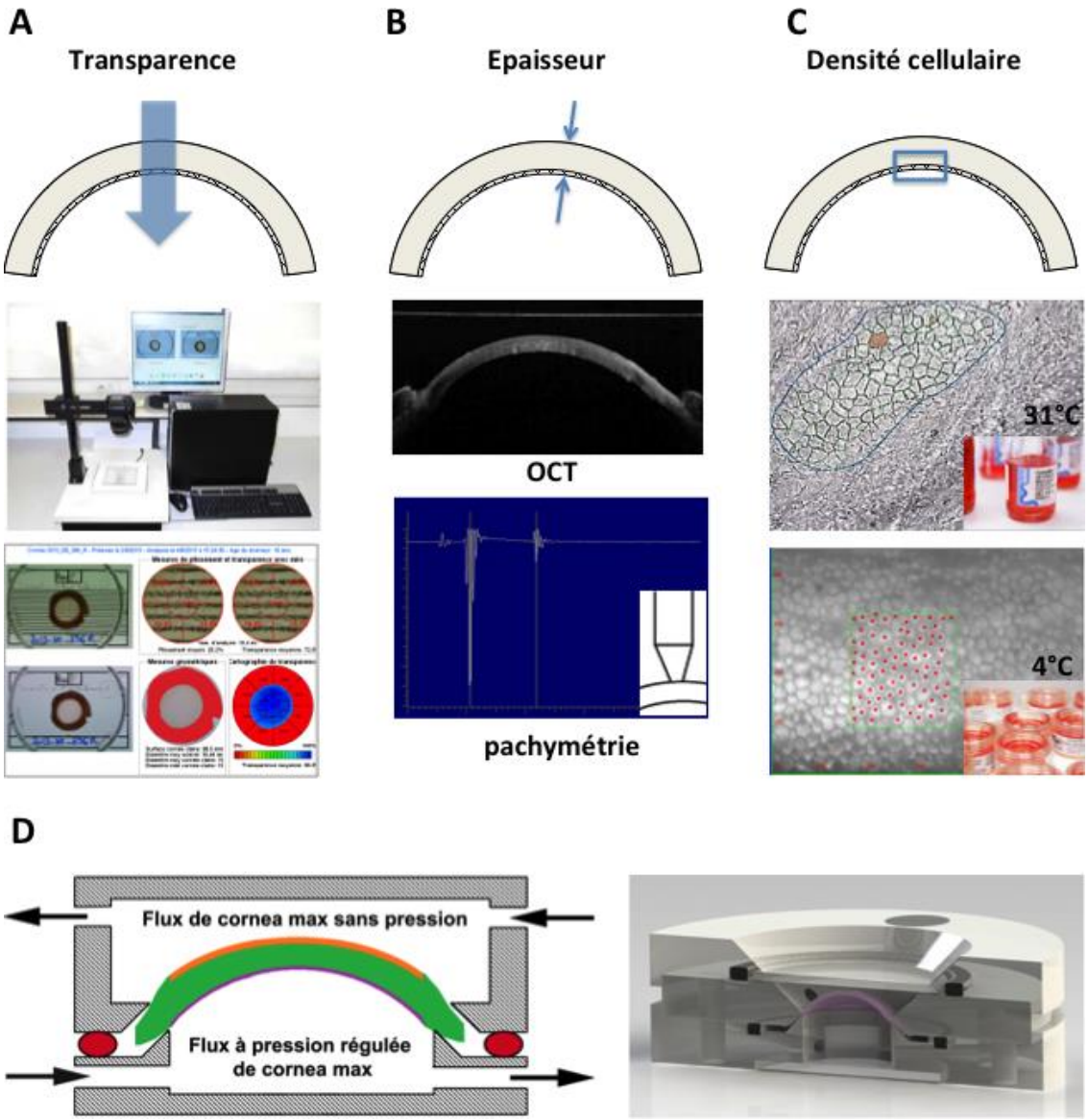


Figure 10. Evaluation fonctionnelle du greffon endothélial cornéen par trois critères de qualité (A-C) et conception de bioréacteur de cornée (D) (EA2521 BiiGC, Université Jean Monnet, Saint Etienne)

Enfin, plus récemment et de façon originale, notre laboratoire BiiGC a breveté un bioréacteur capable de reproduire un environnement de circulation de milieu et de pression, et qui permet aussi un analyse de la biofonctionalité de la cornée humaine ex vivo (Figure 10D).

Tout récemment, une collaboration avec l'institut optique de recherche vise à mettre en évidence, par une imagerie OCT de haute résolution, la microstructure de la périphérie cornéenne (Figure 11).

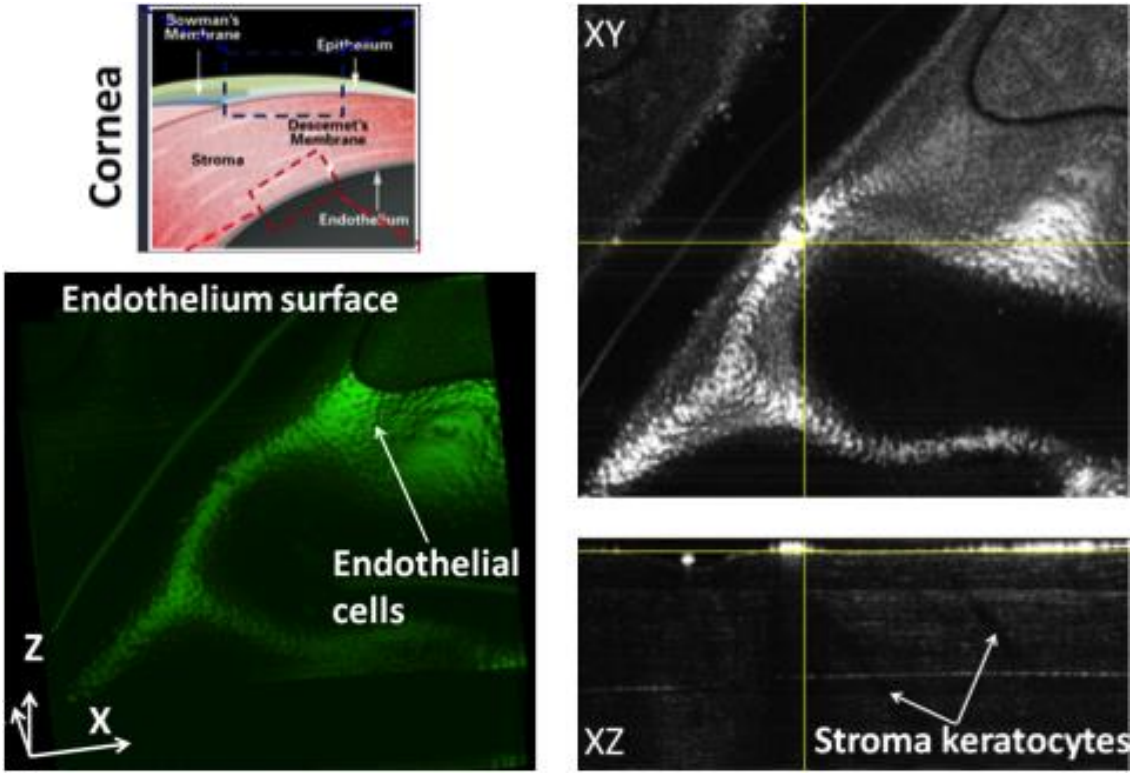


Figure 11. Analyse en 3D de la morphologie de l'endothélium cornéen humain in vivo par microscopie à cohérence optique à domaine Gabor (GD-OCM) (EA2521 BiiGC, Université Jean Monnet, Saint Etienne)

2.1.2. Anatomie endothéliale

L'endothélium constitue la barrière entre la chambre antérieure et le stroma cornéen. Formant une monocouche, les CE sont exposées à la pression intraoculaire variant de 10 à 21 mmHg à l'état normale. La DCE d'environ 6000 cellules/mm^2 à la naissance, chute rapidement dans les premières années de vie, puis diminue beaucoup moins vite (0,56% par an) à l'âge adulte (Murphy *et al.* 1984). La DCE peut chuter plus rapidement en cas de traumatismes mécaniques, ou au cours des pathologies endothéliales primitives (comme la dystrophie de Fuchs, dite cornea guttata, pathologie endothéliale primitive la plus fréquente), ou secondaires (implants cristalliniens rétrocornéens, implants myomiques rétrocornéens) (Figure 12). La réparation cellulaire se fait uniquement par élargissement et migration des cellules voisines.

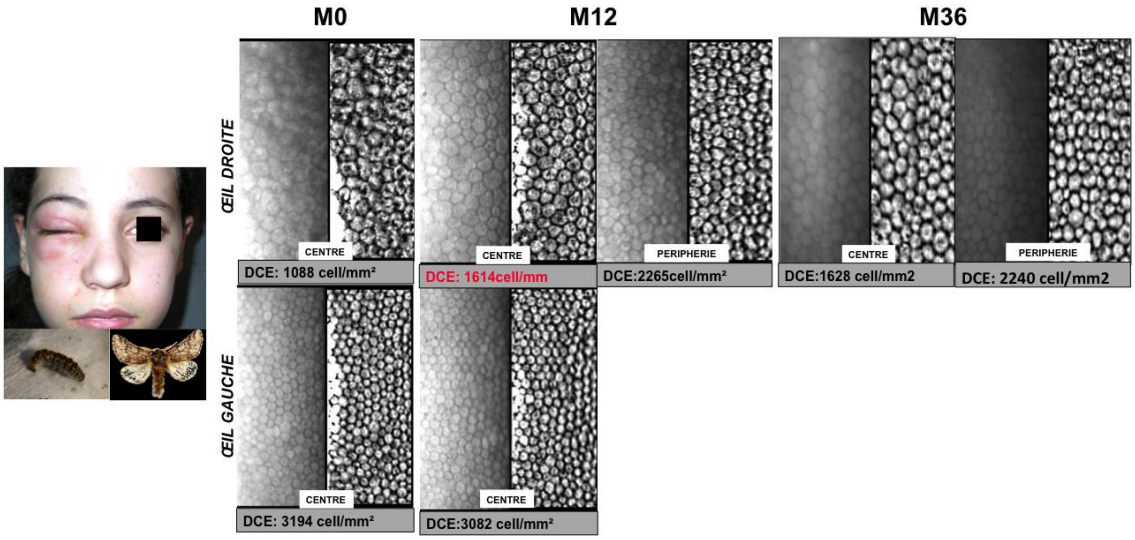


Figure 12. Exemple de chute rapide de la DCE du au traumatisme par poil de chenille chez l'enfant et redistribution par migration/élargissement de cellules endothéliales voisine après 12 et 36 mois (EA2521 BiiGC, Université Jean Monnet, Saint Etienne)

Au pôle apical, face à l'humeur aqueuse, les CE forment un réseau de cellules hexagonales dues aux jonctions serrées entre les cellules (Figure 13A,B). La présence d'un cil sur la membrane apicale suppose un rôle dans des échanges métaboliques ou la détection de la pression intra oculaire (Figure 13C). D'autre part, les cils peuvent aussi jouer un rôle important dans l'échange de signaux entre l'endothélium et l'épithélium cristallinien ou l'iris permettant la dissociation de la cornée, du cristallin et de l'iris. La formation des cils varie entre les CE présentes à la naissance, à l'état adulte sain et après lésions (Blitzer *et al.* 2011). Contrairement au pôle apical, la membrane basale est irrégulière et forme de nombreuses expansions et interdigitations, permettant l'accrochage des CE à la membrane Descemet.

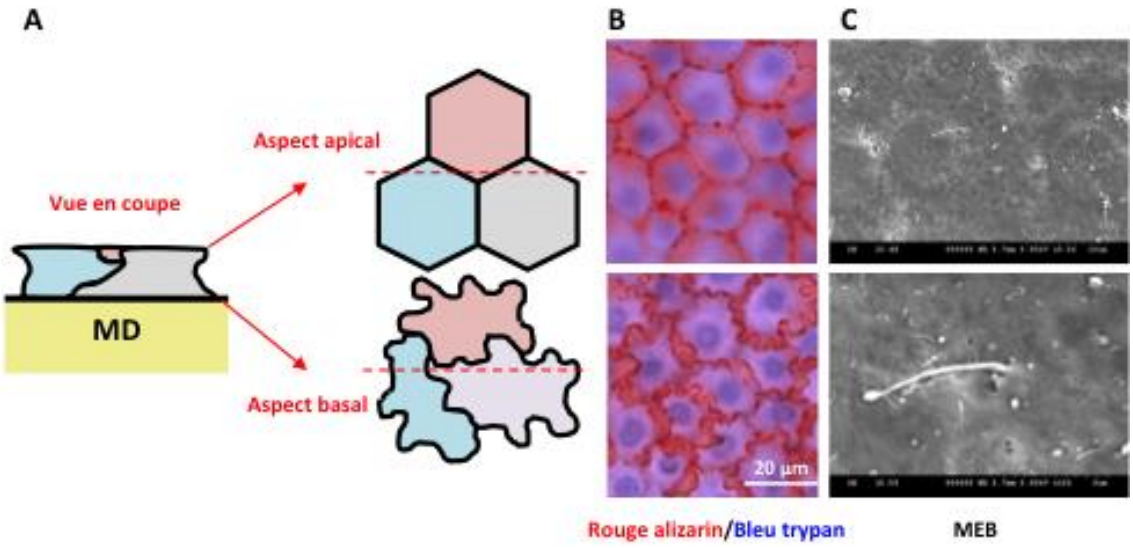


Figure 13. Morphologie de l'endothélium cornéen au pôle apical et basal par illustration (A) et mise en évidence par coloration au bleu trypan et au rouge alizarine (B). Formation des cils sur la membrane apicale observée par microscopie électronique à balayage (MEB, C) (EA 2521 BiiGC, Université Jean Monnet, Saint Etienne). MD: Membrane de Descemet

La distribution et la morphologie des CE sont hétérogènes entre le centre et la périphérie de la cornée (Figure 14). Au centre, les CE ont une forme hexagonale, lisse avec des noyaux ronds et sont distribuées de façon homogène. A la périphérie, la DCE est 45% plus dense qu'au centre. Les CE périphériques sont moins régulières, plus épaisses et s'alignent entre des structures Descemétiques disposées en sillon centripètes. A l'extrême périphérie, les CE forment des amas de cellules en multicouche, inclus entre les corps Hassal-Henlé.

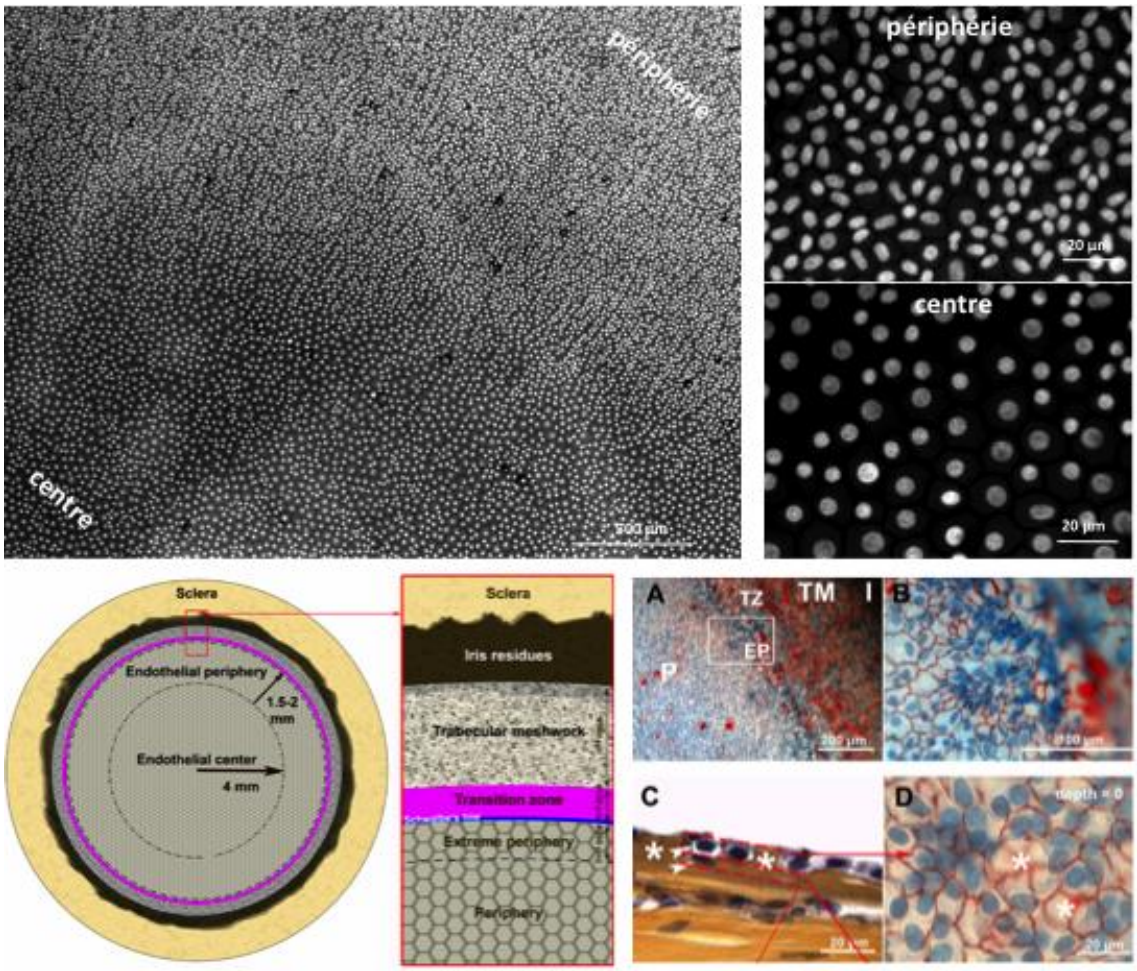


Figure 14. Analyse morphologique de l'endothélium cornéen, du centre à la périphérie et l'extrême périphérie. Les cellules endothéiales (CE) s'alignent à la périphérie et se répartissent de façon homogène au centre de la cornée. L'extrême périphérie est constituée des amas de CE en multicouche (He, Hathi et al. Stem Cell 2012, EA2521 BiiGC, Université Jean Monnet, Saint Etienne)

2.1.3. Structures péri-cornéennes

Les CE sont en interaction avec d'autres tissus à proximité. Focalisée sur le fonctionnement de l'endothélium, ce paragraphe décrit les structures péri-endothéliales de la face postérieure de la cornée (Figure 15).

La limite de l'extrême périphérie de l'endothélium cornéen est marquée par le bord de la MD s'appelant ligne de Schwalbe suivi d'une zone de transition avant d'atteindre le trabéculum. Actuellement peu de description morphologique de la zone de transition a été effectuée.

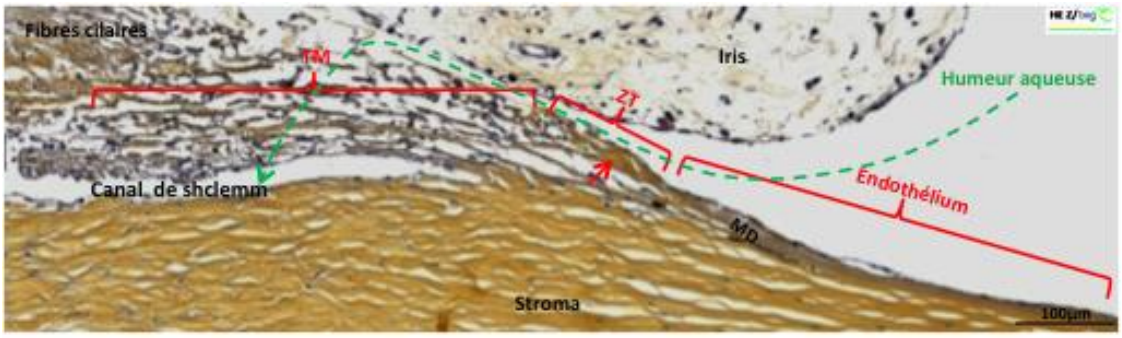


Figure 15. Histologie en coupe transversale de la structure périoculaire de la cornée. Coloration HES; TM, trabéculum; ZT, zone de transition; MD, membrane de Descemet (EA2521 BiiGC, Université Jean Monnet, Saint Etienne).

La zone de transition mesure environ 100µm et contient des populations cellulaires encore peu connues. Des études récentes supposent que les cellules de cette zone résultent de la migration du trabéculum à l'endothélium (McGowan *et al.* 2007), ou qu'il existe des niches de CS ou de progéniteurs (2012 JBB Yu) (voir Chapitre II - 4.2).

Développé à partir de la CN après la formation du stroma cornéen, le trabéculum constitue d'un maillage spongieux de filaments contractiles permettant l'humeur aqueuse d'accéder au canal de Schlemm. Les trabéculocytes synthétisent en continu de la matrice extracellulaire comme du collagène, des glycoprotéines ou des glycosaminoglycanes pour renouveler celle qui est altérée lors de la perfusion aqueuse. Ces cellules ont également la capacité de phagocyter les débris circulant dans l'humeur aqueuse. Cette zone avasculaire est particulièrement importante dans la régulation du flux d'humeur aqueuse. Ses anomalies sont impliquées dans les glaucomes. De façon notable les inhibiteurs de ROCK, capable d'induire des remaniements du cytosquelette, sont des molécules candidates pour le traitement du glaucome chronique à angle ouvert (Yu *et al.* 2011).

Le canal de Schlemm collecte l'humeur aqueuse afin de régulariser le flux intraoculaire. Entouré des CE d'origine mésodermique, ce canal se trouve à proximité du trabéculum, de la zone de transition et du stroma. Cette zone carrefour pourrait potentiellement abriter des CS dont celles de l'endothélium cornéen (McGowan *et al.* 2007).

Les modèles de régénération de l'endothélium ont été inspirés de celui de l'épithélium se trouvant à la face antérieure de la cornée. Le limbe est la zone

intermédiaire entre la cornéen postérieure et la sclère. Il a été démontré que cette zone contient des CS limbiques pour la régénération de l'épithélium cornéen, et aussi les CS stromales qui régénèrent les kératocytes (Pinnamaneni & Funderburgh 2012) (Figure 16).

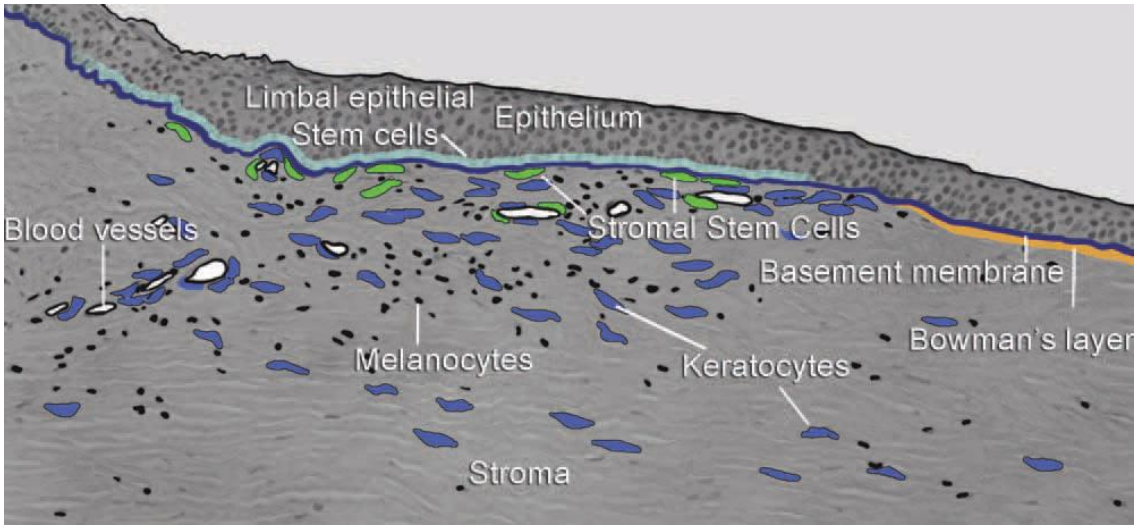


Figure 16. Coupe transversale de la région antérieure de la zone de transition entre la cornée et la sclère, appelée limbe (Pinnamaneni & Funderburgh 2012). L'épithélium s'épaissit vers la périphérie, dans la zone ondulée de la membrane de Bowman (palissade de Vogt). Les cellules souches (CS) limbiques se trouvent dans l'épithélium basal limbique. Le stroma limbique est vascularisé, contient des mélanocytes (noir) et des kératocytes mésenchymateux (bleu). Les CS stromales cornéennes (vert) sont sous la membrane basale à côté de l'épithélium limbique.

La compréhension de l'environnement cellulaire permet d'interpréter le rôle de l'endothélium cornéen, de sa formation à la naissance jusqu'à sa différenciation en interaction avec les structures péri-endothéliales.

2.2. Régulation de la transparence de la cornée

Etant la barrière entre le stroma cornéen et la chambre antérieure, l'endothélium régularise l'apport de nutriments pour l'ensemble des cellules stromales et épithéliales et le maintien de la transparence du stroma cornéen. Cette fonction est assurée par plusieurs mécanismes intracellulaires, mais aussi par l'interaction entre les cellules. La clarification de ces mécanismes est nécessaire pour envisager des actions préventives lors de la conservation de la cornée et ainsi limiter les perturbations de la transparence cornéenne.

2.2.1. Balance pompe-fuite (« pump-leak » des anglo-saxons)

La théorie des réseaux (lattice theory) proposée par Maurice dans les années 1950, fait reposer la transparence stromale sur la parfaite organisation des fibres de collagène pratiquement toutes de même diamètre (275-350 Å) et très régulièrement espacées (Mergler & Pleyer 2007) (Figure 17), à la différence de la sclère de même composition mais dépourvue de la cette organisation.

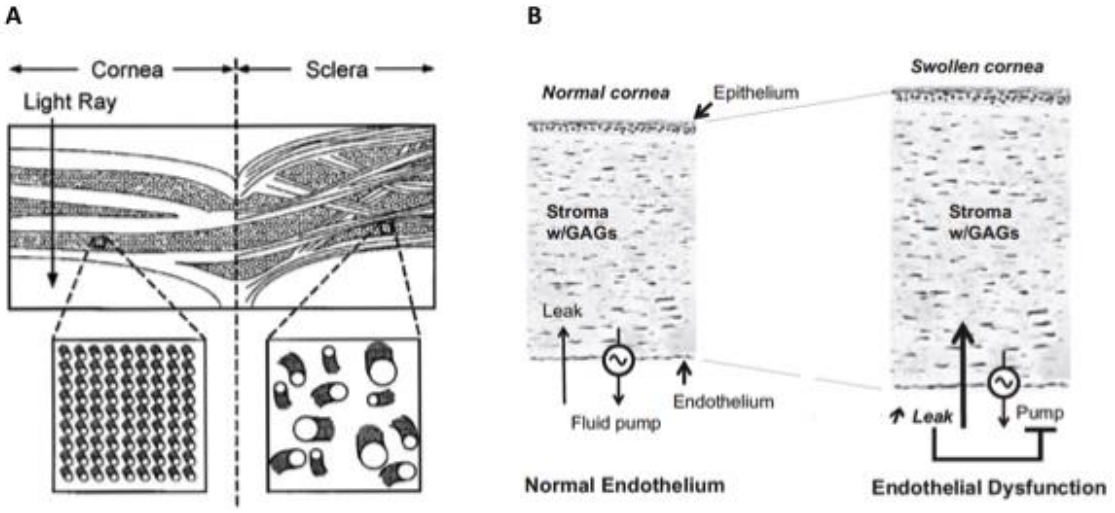


Figure 17. Maintien de la transparence de la cornée par la théorie « pompe-fuite » (Srinivas 2012). A: L'organisation parfaite des fibres de collagène du stroma rend la cornée transparente. B: L'entrée de fluide dans le stroma due à la pression de gonflement du stroma d'environ 50 mmHg est contrebalancée par la pompe endothéliale.

Le maintien de cette organisation stromale dépend de son niveau d'hydratation régulé par le mécanisme pompe-fuite (Figure 17) (Srinivas 2012). La pression de gonflement du stroma d'environ 50 mmHg due aux charges négatives des glycosaminoglycanes (GAGs) du stroma, induit le passage en continu de liquide de la chambre antérieure à l'intérieur du stroma à travers l'endothélium. L'entrée passive d'humeur aqueuse (« la fuite ») est la source majeure des nutriments pour les cellules stromales et épithéliales puisque la cornée est avasculaire. Cependant, une trop grande quantité d'eau entraine également des espaces non uniformes entre les fibres de collagènes, et perturbe le passage de la lumière. Le gonflement du stroma provoque donc inévitablement une perte de sa transparence. La fuite est contrebalancée par des mécanismes de transports ioniques actifs par les CE. Cette « pompe » implique

l'activité des protéines membranaires et cytosoliques et une structure cytosquelettique particulière des CE. La perturbation de ces fonctions entraine un oedème stromal.

2.2.2. Transport d'actifs par l'endothélium

Plusieurs protéines membranaires potentiellement impliquées dans l'activité de transport ont été localisées sur les membranes basolatérale et apicale. Il s'agit de canaux ioniques, de transporteurs ou co-transporteurs ou d'enzymes régulatrices intermédiaires (Figure 18).

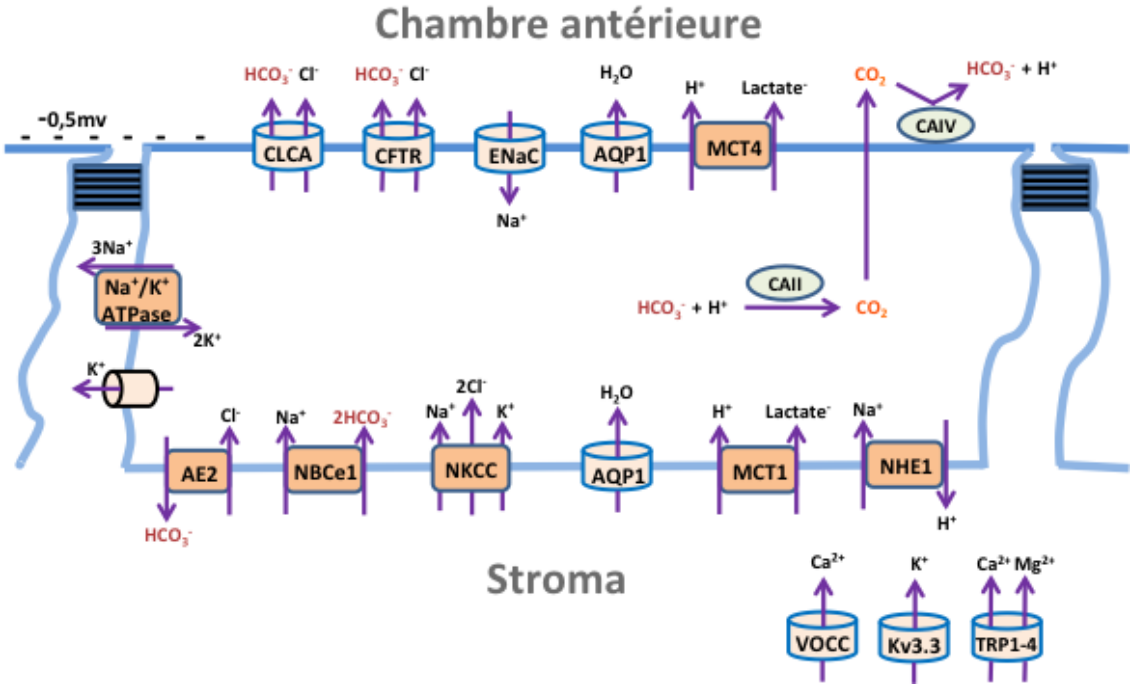


Figure 18. Transport transmembranaire de l'endothélium cornéen (2011 Bonanno, 2007 Mergler) AE2: anion exchange protein 2, AQP1: aquaporine 1, CA: carbonic anhydrase, CFTR: cystic fibrosis transmembrane conductance regulatro, CLCA: calcium-activated chloride channel, ENaC: epithelial Na^+ channel, MCT: monocarboxylate transporter, NBCe1: Na^+ bicarbonate cotransporter electrogenic 1, NKCC: Na^+:K^+:2Cl^- cotransporteur, NHE1: Na^+ H^+ exchanger 1, TRP: transient receptor potentiel channel, VOCC: voltage dependent calcium channel (EA2521 BiiGC, Université Jean Monnet, Saint Etienne).

Canaux ioniques :

Les canaux ioniques sont des pores transmembranaires perméables aux ions en fonction des gradients électrochimiques. Ils sont stimulés par différents paramètres comme la tension, les neurotransmetteurs, le stress mécanique, etc. L'ouverture des pores est sélective de certains ions (Mergler & Pleyer 2007).

Les canaux chloriques ont été décrits. CFTR (cystic fibrosis transmembrane conductance regulator, gène codant *CFTR*) est situé dans la membrane apicale. Sa stimulation par l'AMPc augmente la perméabilité apicale des anions HCO_3^- et Cl^- dans les CE bovines (Sun & Bonanno 2002; Li *et al.* 2008; Bonanno 2012). CLCA1 (calcium-activated Cl^- channel-1, gène codant *CLCA1*) est situé dans la membrane apicale des CE. Son activation par l'ion Ca^{2+} intracellulaire augmente la perméabilité apicale de HCO_3^- (Zhang *et al.* 2006; Bonanno 2012).

Les canaux potassiques sont souvent impliqués dans le potentiel de repos. Détecté par patch-clamp sur la membrane apicale des CE de lapin, Kv3.3 a été suggéré comme responsable du potentiel membranaire de repos de -50 à -60 mV de l'endothélium (Mergler & Pleyer 2007).

Parmi les canaux de sodium, ENaC (epithelial Na^+ channel) détecté dans la membrane apicale est impliqué dans le transport de Na^+ par les CEs. La densité de ces canaux augmente sous l'activité du SGK1 (serum glucocorticoid kinase) qui favorise également l'activité des pompes Na^+/K^+ATPase. Un autre canal de sodium a été détecté chez les CE bovines comme voltage-dépendant sensible au tetrodotoxin (TTX-VOCC) dont le rôle n'est pas encore bien clarifié (Mergler & Pleyer 2007).

Parmi les canaux calciques, les canaux VOCC type L (voltage operated calcium channel) ont été détectés comme voltage-dépendants par patch-clamp pour le transport de Ca^{2+}. Ils sont partiellement activés au potentiel membranaire de repos, et sont sensibles aux facteurs de croissance EGF & endothelin-1 (ET-1). Il semble exister par ailleurs d'autres canaux calciques non voltage-dépendants.

D'autre part, la modulation des paramètres physiologiques de l'endothélium cornéen due aux changements de température est réduite par différents mécanismes de régulation des canaux et des transporteurs échangeurs permettant le maintien du niveau physiologique de Ca^{2+} intracellulaire. Les canaux TRP1-4 (transient receptor potentiel channel) activés par la variation de la température peuvent participer à la régularisation de l'homéostasie des cellules via le transport des ions Ca^{2+} et Mg^{2+} (Mergler *et al.* 2011).

Canal hydrique : la diffusion d'eau à travers la membrane est facilitée par des protéines transmembranaires de la famille des aquaporines. Seule l'AQP1 a été détectée

à la membrane apicale et basolatérale de CE bovine (Wen *et al.* 2001). AQP1 n'étant pas impliquée dans la sécrétion active d'eau, son rôle reste très controversé.

Transporteurs membranaires :

Les transporteurs sont des protéines transmembranaires possédant des sites de fixation de substrat. Le couplage avec son substrat spécifique induit le changement de sa conformation et le déplace dans le sens de son gradient. Les transporteurs peuvent être uniport, antiport (échangeur) ou symport (cotransporteur). L'expression de plusieurs transporteurs a été décrits dans les CEs.

NKCC1 & NKCC2 (Na^+:K^+:2Cl^- cotransporteur, gènes codant *SLC12A2*, *SLC12A1*) (Diecke *et al.* 2005) sont situés sur la membrane basolatérale des CEs. Ils contribuent à l'afflux de Na^+, K^+ et Cl^-. Ils sont responsables de l'afflux de Cl^- jusqu'à 40 mM dans les CE bovines et sont impliqués dans la régulation du volume cellulaire.

NBCe1 (Na^+ bicarbonate cotransporter electrogenic, gène codant *SLC4A4*) (Bonanno *et al.* 1999; Li *et al.* 2005) existe sous deux variants, pNBCe1 et kNBCe1, mais seul pNBCe1 a été détecté sur la membrane basolatérale des CEs. Il est responsable de l'afflux de Na^+ et de la perméabilité basolatérale de HCO_3^-.

AE2 (anion exchanger, gène codant *SLC4A2*) est exprimé sur la membrane basolatérale desCEet est responsable de l'afflux de Cl^- et de l'efflux de HCO_3^- (Bonanno 2003).

NHE1 (Na^+ H^+ exchanger, gène codant *SLC9A1*) (Jentsch *et al.* 1985) est exprimé sur la membrane basolatérale desCEet est responsable de l'afflux de Na^+ et de l'efflux de H^+.

Les transporteurs MCTs (monocarboxylate transporter) (Nguyen & Bonanno 2011) sont responsables du flux de $Lactate^-$ et d'H^+ du stroma cornéen vers la chambre antérieure. MCT1 (gène codant *SLC16A1*) exprimé sur la membrane basolatérale est responsable de l'afflux et MCT4 (gène codant *SLC16A4*) sur la membrane apicale est responsable de l'efflux de $Lactate^-$ et H^+

Pompe ionique : Il s'agit des complexes protéiques transmembranaires qui nécessitent l'énergie de l'hydrolyse de l'ATP pour le transport d'ions contre le gradient électrochimique. Dans les CEs, Na^+/K^+ATPase (Sodium-Potassium Adenosine

Triphosphatase, gènes codant *ATP1A*, *ATP1B*) (Geroski & Edelhauser 1984; Geroski *et al.* 1985) est localisée sur la membrane basolatérale. Elle est responsable de l'afflux de 2 ions K^+ pour l'export de 3 ions Na^+.

Diffusion passive : Les gaz et les molécules hydrophobes ont une perméabilité élevée à travers la membrane bilipidique. Impliqués dans la conversion de $HCO_3^- + H^+ <=> CO_2$, les enzymes catalyseurs anhydrase carbonique (CA) ont été identifiés dans les CEs. CAII facilite la formation de CO_2 intracellulaire et CAIV joue un rôle tampon à la membrane apicale du côté chambre antérieure.

A partir de ces protéines transmembranaires, plusieurs modèles de couplages d'activité ont été suggérés pour la régulation du transport membranaire. Cette liste incomplète de canaux, de pompes et de transporteurs contribue à la compréhension du maintien de la transparence de la cornée.

Pour mettre en évidence la fonctionalité de ces protéines membranaires ainsi que la déturgescence de l'endothélium sur les greffons cornéens, certains outils d'évaluation ont été conçus comme la chambre de perfusion, la chambre d'Ussing ou récemment le bioréacteur breveté par le laboratoire BiiGC. La chambre de perfusion est constituée de deux compartiments séparés par l'épaisseur de cornée, ce qui permet d'observer l'activité de transport à travers la cornée et aussi le changement de la morphologie de la cornée (épaisseur, viabilité, etc.) durant cet activité (Maurice 1972). Basant sur le même principe, la chambre d'Ussing permet d'analyser l'activité de transport des monocouches de cellules en culture in vitro. L'isolation du pôle apical du pôle basal permet la formation d'une différence en voltage entre les 2 compartiments suite aux transports d'ions. Cette différence est détectable et quantifiable grâce à un système d'électrodes reliant les 2 compartiments (http://www.ussingchamber.com/). Le bioréacteur conçu au laboratoire BiiGC permet non seulement de polariser les cellules endothéliales par deux compartiments, mais aussi de maintenir la pression physiologique du côté endothélial, ce qui peut avoir un grand impact sur la fonctionalité de CE et d'autres tissus de la cornée.

2.2.3. Mécanismes de la déturgescence

La déturgescence est l'ensemble des activités permettant l'extraction d'eau du stroma cornéen qui rééquilibre son niveau d'hydratation par rapport à la fuite passive d'entrée d'humeur aqueuse.

La déturgescence par l'endothélium cornéen a été mise en évidence sur cornée de lapin utilisant une chambre de Ussing modifiée. Une cornée désépithélialisée a été perfusée par la solution Ringer à partir du côté épithélial pour provoquer son gonflement, puis la face épithéliale couverte par de l'huile de silicone pour bloquer l'entrée d'eau. La déturgescence observée correspondant à la diminution exponentielle de l'épaisseur du stroma a donc été rattachée à la pompe endothéliale (Bonanno 2012). En enlevant HCO_3^- ou en ajoutant de l'ouabaïne (inhibiteur de l'ATPase) de la solution de perfusion, le gonflement de la cornée, ou plutôt l'absence de déturgescence a été observée. Ces expérimentations initiales ont démontrées l'implication des transports ioniques dans le processus de déturgescence.

Les CEs maintiennent un potentiel membranaire de -55 mV entre les membranes basolatérale et apicale. Afin d'expliquer le flux d'eau sortant du stroma cornéen, plusieurs modèles de couplage de transports ont été suggérés via la voie transcellulaire ou paracellulaire (Figure 19).

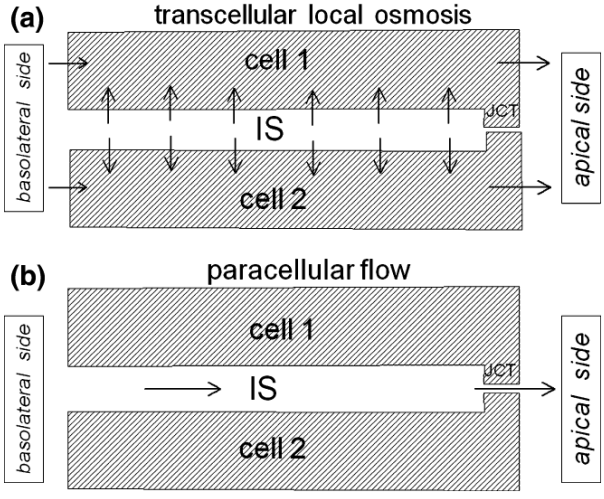


Figure 19. Modèle de sécrétion de fluide par deux voies, la voie transcellulaire via la membrane basolatérale et apicale, et la voie paracellulaire via l'espace intercellulaire et les jonctions serrées (2006 JMB Fischbarg).

Couplage soluté-solvant

La théorie de couplage soluté-solvant consiste en l'induction d'un gradient osmotique local à travers la membrane apicale par le mouvement net de Na^+ et HCO_3^- /Cl^- du stroma vers l'humeur aqueuse. Le gradient ainsi créé déclenche un mouvement de fluide vers la chambre antérieure. (Srinivas 2012).

Les gradients ioniques sont mis en place par nombreuses protéines membranaires. Sur la membrane basolatérale, l'afflux d'anions HCO_3^- et Cl^- provient de différents canaux ioniques et transporteurs membranaires. NBCe1 importe directement HCO_3^- du stroma. NHE1 exporte H^+ des CEs, donc maintient indirectement la concentration intracellulaire de HCO_3^- en défavorisant la formation de CO_2 à partir de HCO_3^- catalysée par l'anhydrase carbonique type II. AE2 diminue le gradient de HCO_3^- en l'exportant par le côté basolatéral mais importe Cl^-. Le cotransporteur NKCC1 importe Cl^- à l'intérieur des cellules jusqu'à environ 40mM. Sur la membrane apicale, deux canaux anioniques CFTR et CLCA exportent HCO_3^- et Cl^-, mais la perméabilité pour Cl^- est 4 fois plus élevée que pour HCO_3^-. **Cependant, aucun échangeur de Cl^- et HCO_3^- n'a été détecté**. L'accumulation de HCO3- intracellulaire suggère soit l'existence d'autres canaux ioniques apicaux, soit un autre mécanisme de diffusion passive de CO_2. En effet, HCO_3^- importé à l'intérieur des CE peut être converti en CO_2 par le catalyseur CAII. CO_2 hautement diffusible à travers la membrane bilipidique peut être reconverti en HCO_3^- sous l'activité tampon du catalyseur CAIV du côté apical.

Par conséquence, ce gradient d'anions pourrait induire le mouvement d'eau transendothélial. Cela peut être facilité par les canaux hydriques AQP1 détectés sur la membrane apicale et basolatérale de l'endothélium cornéen.

Ce premier modèle reste actuellement très controversé (Figure 20). La preuve sur l'existence d'un flux net transendothélial d'anions est absente. D'autre part, contrairement à l'hypothèse sur l'implication d'AQP1 dans la diffusion apicale d'eau, il a été montré que l'absence d'expression d'AQP1 dans un modèle animal n'affecte pas la déturgescence de la cornée. Cela suppose que AQP1 représente une voie de diffusion passive d'eau durant la fluctuation de la pression osmotique, mais le transport d'eau implique d'autres mécanismes que le couplage soluté-solvant.

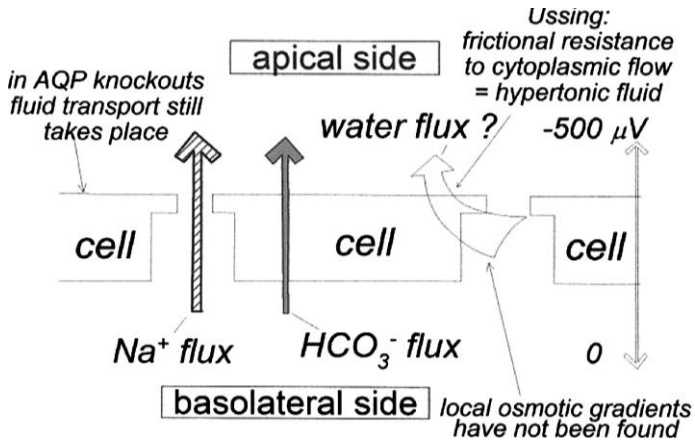


Figure 20. Controverse sur le couplage soluté-solvant dans le transport d'eau du stroma (basolateral side) à la chambre antérieure (apical side) (Fischbarg et al. 2006).

Couplage électro-osmotique

Afin de trouver une explication plus satisfaisante à la déturgescence à travers l'endothélium, Fischbarg a proposé un modèle de couplage électro-osmotique (Srinivas 2010).

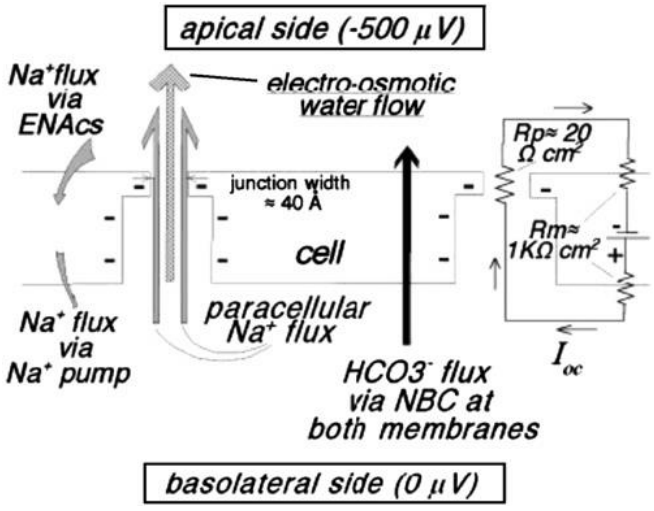


Figure 21. Modèle de déturgescence par couplage électro-osmotique (Mergler & Pleyer 2007). La diffusion paracellulaire de Na^+ couplé au flux d'anions transmembranaire induit un flux d'eau par la voie paracellulaire.

En effet, le flux d'anions HCO_3^- et Cl^- décrit précédemment induit un potentiel transendothélial de -0,5 V et également un flux de contre-ion Na^+ paracellulaire. Le mouvement de Na^+ est couplé avec le mouvement d'eau paracellulaire, c'est à dire à travers les jonctions serrées intercellulaires.

La résistance électrique transendothéliale reste faible, d'environ 30 Ω (Srinivas 2012), comprenant la résistance membranaire (membrane apicale & basolatérale) et la résistance paracellulaire (jonctions inter-cellulaires) (Fischbarg *et al.* 2006). Le flux de Na^+ du stroma vers la chambre antérieure via l'espace latérale entre les cellules et les jonctions serrées provient de l'activité des pompes basolatérales Na^+/K^+ATPase. Activés en même temps que Na^+/K^+ATPase par l'activité de SGK1, les canaux apicaux ENaC sont supposés de réduire l'hyperpolarisation due à l'activité des ATPases pour maintenir un stable potentiel membranaire (Bonanno 2012).

A part ces modèles de couplages, le transport d'anions lactate$^-$ a été également identifié comme impliqué dans la déturgescence de la cornée. En effet, 85% de glucose consommé par la cornée est transformé en acide lactique. [Lactate$^-$] est 2 fois plus élevée dans la cornée (13mM) que dans la chambre antérieure (7mM). L'hypoxie augmente [Lactate$^-$] et entraîne le gonflement de la cornée. Le transport de Lactate$^-$ et de H^- est assuré par les transporteurs MCT1 et MCT4 détectés sur la membrane basolatérale et apicale de l'endothélium cornéen.

La découverte de ces mécanismes permet d'avoir une bonne méthode d'évaluation de l'état fonctionnel de l'endothélium cornéen, ainsi d'adapter les manipulations de l'endothélium, notamment le renforcement de ses fonctions par des agonistes. En se basant sur ces mécanismes de transport, certains agonistes de la déturgescence ont été identifiés. AMPc active les canaux apicaux CFTR, favorise donc le flux Cl^- et HCO_3^-. ATP active les récepteurs purinergiques et augmente la perméabilité des canaux d'anions. Ce processus est probablement lié à la réponse physiologique qui semble faire suite à l'inflammation, le stress oxydatif ou le stress traumatique.

2.2.4. Rôle de la structure cytosquelettique

Le transport de matière entre le stroma et la chambre antérieure est maintenu par une structure endothéliale spécifique. A côté de l'expression des protéines membranaires rendant perméable la membrane apicale et basolatérale, les CEs maintiennent une structure polarisée apicale-basal grâce aux jonctions inter-cellulaires, et aussi une plasticité grâce à la contraction/relaxation du cytosquelette. L'intégrité de la barrière endothéliale a des impacts directs sur sa fonctionnalité.

Jonctions intercellulaires

Les CEs se lient par des jonctions serrées (JS) et adhérentes, formant une barrière étanche (Figure 22). Les JS se forment par l'attachement des protéines de liaisons transmembranaires comme ocludines, et claudines, quand les cellules sont à proximité. Pour avoir des mouvements de fluide efficaces, l'intégrité des JS empêche la dissipation des gradients ioniques en bloquant le flux rétrograde à travers l'espace paracellulaire (gate fonction). D'autre part, ces jonctions maintiennent la polarité apical-basal en limitant la diffusion latérale de protéines membranaires apicales (fence fonction). (Srinivas 2012).

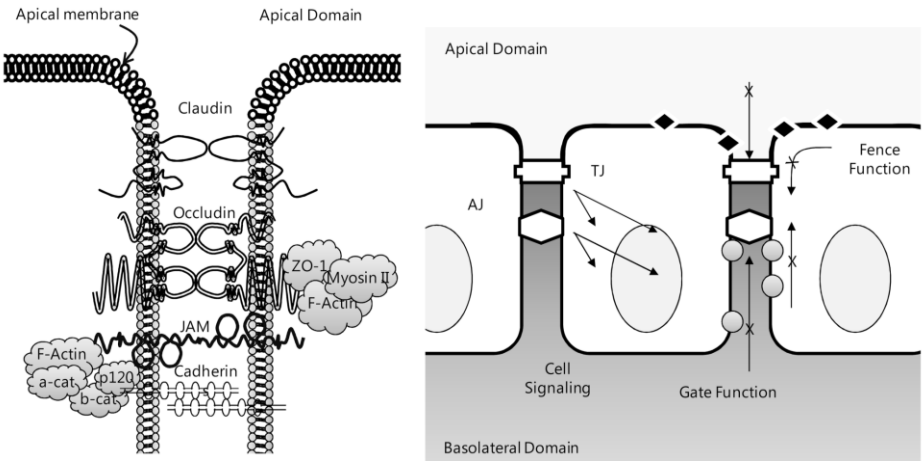


Figure 22. Schéma du complexe de jonctions apicales de l'endothélium cornéen (Srinivas 2010). Les JS bloquent la voie paracellulaire (gate function) via les interactions des protéines transmembranaires liées à l'actine cytosquelettique via les protéines adaptatrices comme ZO-1. Les jonctions adhérentes sont formées via les cadherines couplées aux composants du cytoplasme comme caténines. Elles aident à maintenir l'intégrité de la barrière endothéliale en préservant la polarité des cellules (fence function) et l'espace latéral entre les cellules.

Participant au maintien fonctionnel de l'endothélium, l'intégrité de ces jonctions peut être interrompue par la contraction du cytosquelette (actine-myosin) en exerçant des forces centripètes opposant à ces forces d'attachement au niveau de JS (Srinivas 2012). Malgré cela, cette barrière garde une certaine plasticité en fonction de son milieu physiologique. L'absence de Ca^{2+} désassemble les jonctions adhérentes (N-cadherine), induit la contraction de l'actomyosine, ce qui rompt les JS (ZO-1). L'inhibition de ces voies par ROCK-inhibitor retarde l'effet de la déplétion en Ca^{2+}. Ce processus est réversible en réajoutant du Ca^{2+}. L'intégrité de la barrière peut être évaluée par la mesure de la résistance électrique transendothéliale (TER).

Contraction de l'actomyosine

La contraction de l'actomyosine est directement liée à l'intégrité de la barrière endothéliale. Ce mécanisme est constitué de deux voies (Figure 23), celle induisant la contraction et celle induisant la relaxation du cytoplasme. La contraction de l'actomyosine a lieu suite à la phosphorylation des chaînes légères de la myosine MLC (myosin light chain) induit par la MLC kinase (MLCK) activée par la fixation du complexe cadmodulin-Ca^{2+}. La relaxation de l'actomyosine correspond à la déphosphorylation de MLC par la forme active de MLC phosphatase (MLCP). Cet état actif de MLCP peut être désactivé par phosphorylation par Rho kinase de MYPT1, une des 3 sous-unités de MLCP, ce qui provoque la contraction du cytosquelette.

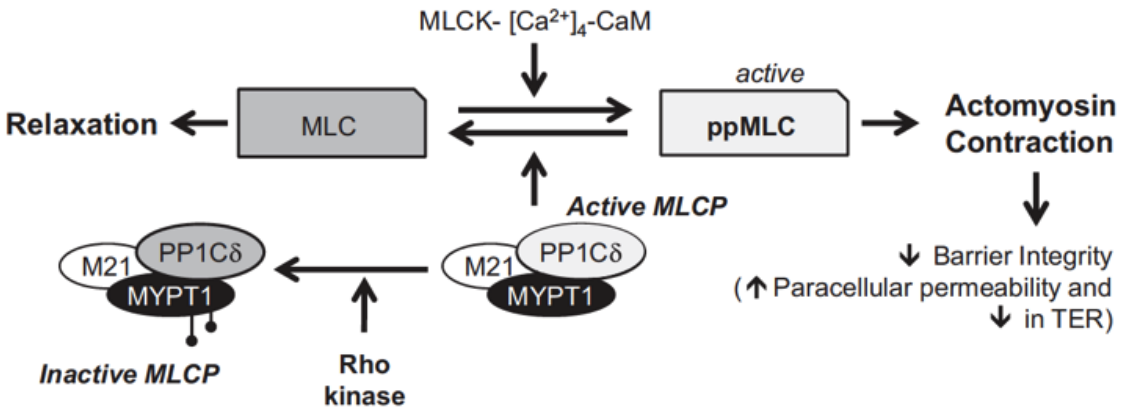


Figure 23. Voies de signalisation de la contraction de l'actomyosine (Srinivas 2012). La contraction de l'actomyosine est liée à la phosphorylation de MLC (ppMLC) activé par la forme active du MLCK. La relaxation du cytosquelette est liée à la déphosphorylation de ppMLC par la forme active de MLCP. Rho kinase peut inhiber la voie de relaxation via la désactivation d'une sous-unité de MLCP.

Etant en contact avec la chambre antérieure, l'endothélium reçoit différents stimuli de l'humeur aqueuse, ce qui induit le changement de la structure du cytosquelette et fragilise la barrière d'intégrité formée par les CE. Parmi les agents pharmacologiques, il a été montré que la thrombine active la voie RhoA-Rho kinase et rompt ainsi l'intégrité de la barrière. L'ajout d'AMPc désactive RhoA, inhibe sa signalisation et neutralise l'effet de la thrombine. D'autre part, parmi les cytokines impliquées dans le rejet des allogreffes de cornée, TNF-α induit la perte de l'intégrité de la barrière endothéliale vasculaire via le processus de désassemblage de microtubules. Il a été démontré que le désassemblage de microtubules induit par le nocodazole active RhoA, la contraction de l'actomyosine et la dispersion de ZO-1 dans

l'endothélium cornéen. Ainsi, le traitement par le paclitaxel, agent stabilisateur des microtubules, neutralise l'effet induit par le TNF-α. La perte de l'intégrité de la barrière endothéliale par TNF-α implique l'activation de p38 MAP kinase et la réorganisation du cytosquelette.

Ces découvertes ont partiellement clarifié les mécanismes d'activation intracellulaire en réponse à différents stimuli, et qui déclenchent des changements d'interaction entre les CE et leur fonctionnalité. La compréhension de ces caractéristiques est primordiale dans la recherche des solutions thérapeutiques pour les pathologies endothéliales.

2.3. Interactions avec l'environnement

2.3.1. Membrane Descemet

Situées à la face postérieure de la cornée, l'endothélium n'est pas en contact direct du stroma cornéen mais repose sur une couche intermédiaire appelée membrane de Descemet (MD). Il s'agit de la matrice extracellulaire secrétée par l'endothélium dès l'organogénèse, après la première vague de migration du mésenchyme périoculaire originaire de la CN.

Morphologie

L'épaisseur de la MD augmente du stade foetal à l'âge adulte (Kabosova *et al.* 2007). A la naissance, la membrane de Descemet mesure environ 3 µm d'épaisseur et à 6-8 µm chez les âgés 60-80 ans (Murphy *et al.* 1984). Sur une cornée, la partie centrale est fine et lisse mais devient épaisse et irrégulier vers la périphérie (Figure 24) (He *et al.* 2012). Cette épaisseur peut augmenter jusqu'à 20 µm en cas de pathologie comme la dystrophie endothéliale de Fuchs ou cornea guttata.

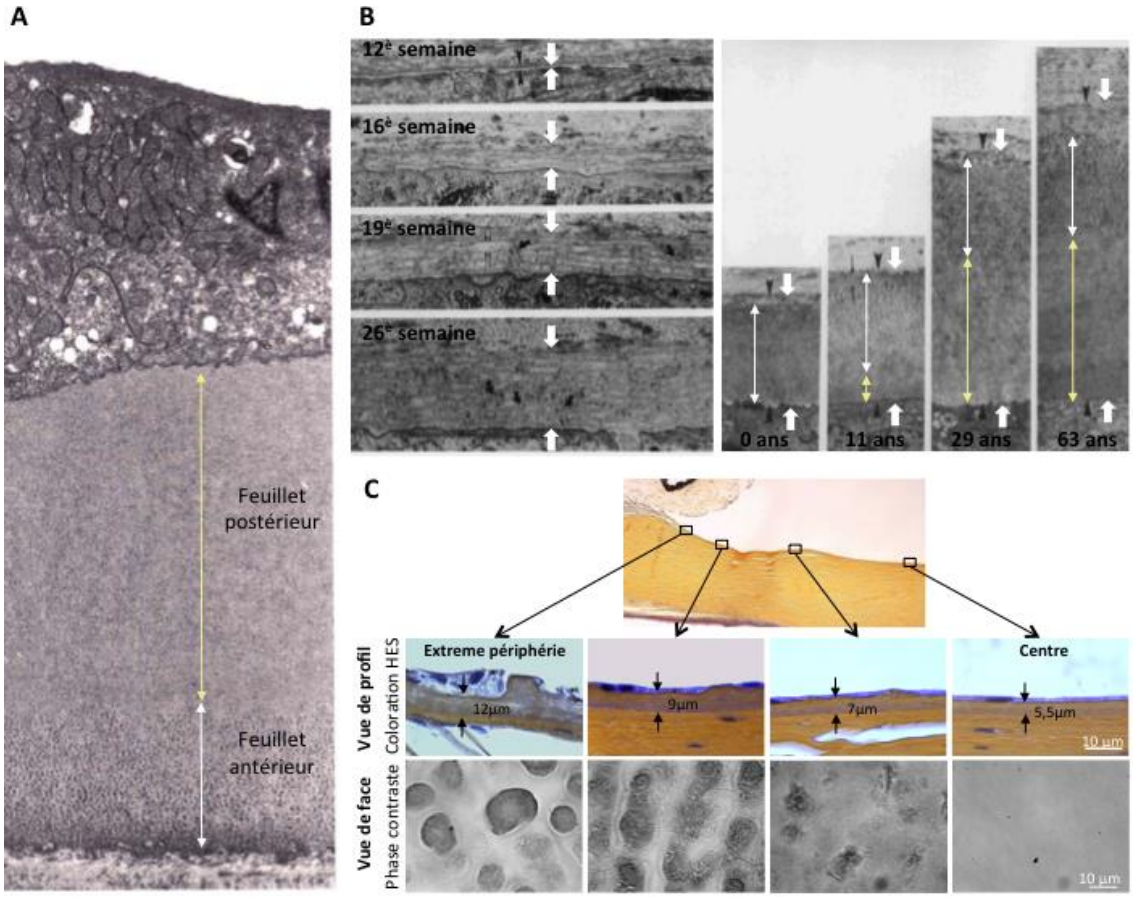


Figure 24. Membrane de Descemet. A. Composition en feuillet postérieur non strié et feuillet antérieur strié, image MET x 8300 (Levy et al. 1995). B. Formation du feuillet antérieur durant la gestation (gauche, image MET x 20750) et formation postnatal du feuillet postérieur (droite, image MET x16500) (Murphy et al. 1984). C. Variation de la régularité et de l'épaisseur de la membrane de Descemet du centre à l'extrême périphérie de la cornée (EA2521 BiiGC, Université Jean Monnet, Saint Etienne).

Au niveau microscopique, la MD se compose de deux feuillets (Murphy *et al.* 1984; Kabosova *et al.* 2007). Le feuillet antérieur, partie striée (anterior banded zone), secrété durant l'embryogénèse a un rôle dans l'adhésion avec le stroma. Ce feuillet est constitué de la matrice extracellulaire appelée "wide-spaced collagen" (Sawada *et al.* 1990; Levy *et al.* 1995). Le feuillet postérieur, partie non striée (posterior non-banded zone), est généré durant la maturation de la cornée après la naissance. Cette morphologie en 2 feuillets facilite son clivage lors du pelage de la MD durant la kératoplastie endothéliale de la MD (DMEK).

Il a été reporté récemment par Dua l'existence d'une couche intermédiaire entre la MD et le stroma (Dua *et al.* 2013) (Figure 25). Cette couche acellulaire mesure environ 10µm d'épaisseur, se compose de 5 à 8 couches de collagènes. Elle s'étend jusqu'à 8,5 mm de diamètre vers la périphérie tandis que la MD jusqu'à 10,5 mm de

diamètre. Par rapport à la MD, celle-ci est plus résistante à la pression et imperméable à l'air.

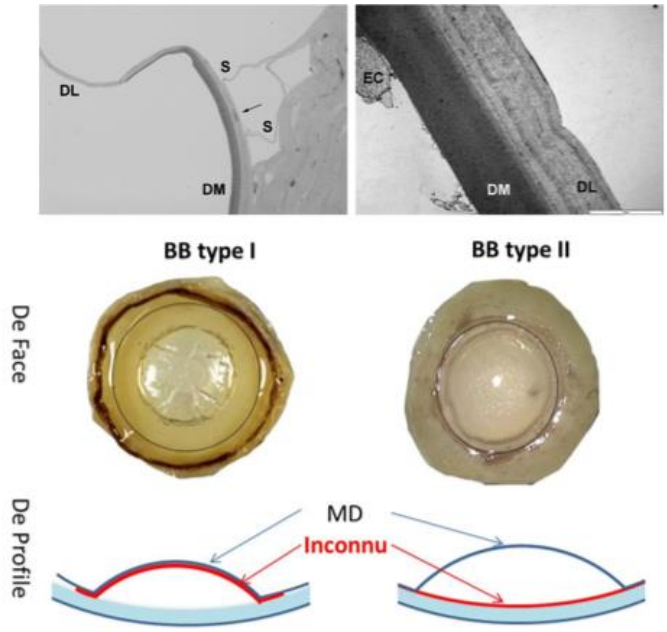


Figure 25. Couche pré-Descemetique (DL, Dua's layer) se trouvant entre la membrane de Descemet (DM) et le stroma cornéen (S). L'expansion et la résistance de la couche pré-Descemetique est mise en évidence par la technique de la "big bubble" (BB) type I (entre DL et le stroma) et type II (entre la membrane de Descemet et DL) (Dua et al. 2013)

Composition

L'endothélium synthétise différents composants basals et non-basals de la matrice extracellulaire qui sont soit intérés à la MD, soit détruits à l'intérieur des cellules (chez le lapin), (Leung *et al.* 2000). Ainsi, la composition de la MD varie en fonction de l'état de différenciation de l'endothélium cornéen.

Tout d'abord, cette composition varie avec l'âge (Kabosova *et al.* 2007) (Figure 26). Collagène IV α1-α6, perlecan, nidogen-1, nidogen-2, et netrin-4 sont présents aux 2 faces de la MD chez l'enfant mais seulement à la face endothéliale chez l'adulte. Chez l'adulte les chaînes α1-α2 de collagène IV sont présents sur la face stromale et α3-α6 sur la face endothéliale. Tenascin-C, fibrillin-1, SPARC, and laminin-332 sont positifs sur la face stromale chez l'enfant mais disparaissent chez l'adulte. L'expression de tenascin-C et fibrillin-1 a également été détectée au centre des cornées foetales ou d'enfants et diminuent avec l'âge après la naissance. Du collagène de type VIII est présent sur la face endothéliale chez l'enfant et se localise à la face stromale chez l'adulte. Ces modifications de distribution durant le développement postnatal reflètent

la différenciation et/ou les changements prolifératifs des cellules. Les composants secrétés par les cellules stromales et les CE sur les 2 faces chez l'enfant peuvent être synthétisés seulement par les kératocytes du stroma chez l'adulte. Le matrilin-4 présent chez l'enfant disparaît à partir de 3 ans (Kabosova *et al.* 2007). La composition de la MD en collagène IV, laminin et fibronectin est aussi hétérogène dans le sens vertical.

	Adult DM		Infant DM	
Component	**Stromal Face**	**Endo. Face**	**Stromal Face**	**Endo. Face**
Type IV collagen chains	α1,α2	α3–α6	α1–α6	α-1–α6
Laminin chains	None	α4,α5,β1,γ1	α3–α5,β1,β3,γ1,γ2	α4, α5,β1,γ1
Possible laminin isoforms	None	411,511	311,332,411,511	411,511
Nidogen-1/entactin-1	−	+	+	+
Nidogen-2/entactin-2	−	+	+	+
Perlecan	−	+	+	+
Netrin-4/β-netrin	−	+	+	+
Matrilin-4	−	±†	+	+
Tenascin-C	−	−	+	−
Fibrillin-1	−	−	+	−
Type VIII collagen	+	−	−	+
Type XII collagen	−	+ (Short form)	−	+ (Both forms)
SPARC/BM-40/osteonectin*	±	−	+	−
Type XVIII collagen	−	±	−	±
Thrombospondin-1	−	+	−	+
Fibronectin	+	−	+	−
Vitronectin	+	−	+	−

Figure 26. Distribution de composants de la membrane de Descemet chez l'enfant (12 jours - 3 ans) et chez l'adulte (13-75 ans) sur la face en contact avec l'endothélium et celle avec le stroma (Kabosova et al. 2007).

En cas de pathologies, les CEs anormales peuvent former des couches de matrice extracellulaire anormale perturbant la transparence de la cornée. Il s'agit des couches postérieures de collagènes dans le syndrome irido-cornéo-endothélial (ICE syndrome) (Levy *et al.* 1995), ou des membranes fibreuses rétrocornéennes dans de nombreuses autres pathologies (Leung *et al.* 2000). Ces structures anormales sont constituées de collagène I, III normalement synthétisés et détruits à l'intérieur des cellules. D'autres composants absents chez les adultes sains comme la tenascine et la fibrilline peuvent réapparaître dans la kératopathie bulleuse ou la dystrophie de Fuchs (Kabosova *et al.* 2007). De plus, la formation de membranes fibreuses rétrocornéennes est identifiée comme de la fibrose due à la transformation mésenchymateuse des CE en fibroblastes (Leung *et al.* 2000).

En résumé, la composition de la MD reflète l'état de différenciation des CE. Une différenciation cellulaire anormale peut induire des matrices extracellulaires non physiologiques et perturber la transparence. Ces observations justifient l'importance du statut de différenciation des CE aussi bien dans la bioingénierie de l'endothélium cornéen que dans le diagnostic des pathologies de la cornée.

2.3.2. Humeur aqueuse

Etant la barrière entre la cornée et la chambre antérieure, l'endothélium communique avec la chambre antérieure via l'humeur aqueuse (HA). L'HA est secrétée par le corps ciliaire dans la chambre postérieure, qui circule ensuite entre le cristallin et l'iris vers la chambre antérieure et s'extériorise par 2 voies de drainage : la voie conventionnelle par le canal de Schlemm puis les veines épisclérales, et la voie uvéosclérale via les faisseaux du muscle ciliare et les espaces suprachoroïdaux (Figure 27) (Chowdhury *et al.* 2010; Goel *et al.* 2010).

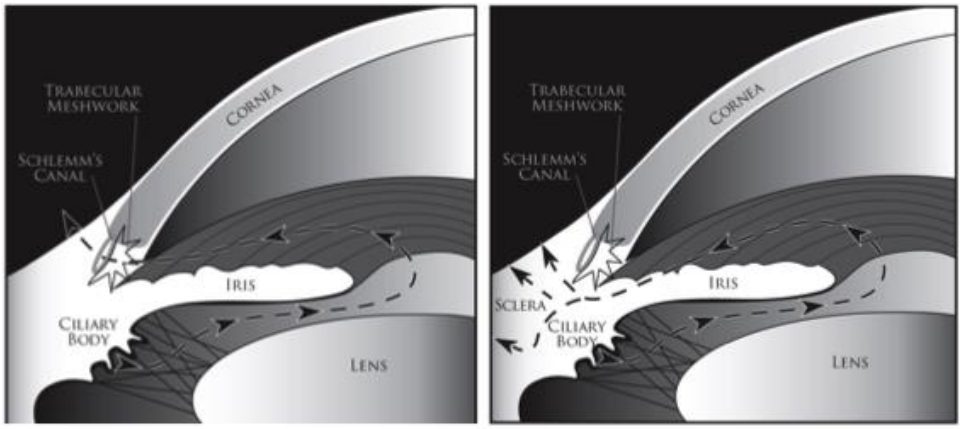


Figure 27. Flux de circulation de l'humeur aqueuse via les deux voies de drainage, la voie conventionnelle (gauche) et la voie uveosclérale (droite) (Goel et al. 2010)

Occupant la chambre antérieure et postérieure de l'oeil, l'HA maintient les propriétés optiques et réfractives de l'oeil (Chowdhury *et al.* 2010) par une pression intraoculaire stable d'environ 13-21 mmHg. Malgré un rythme circadien du flux d'HA, allant de 2,48 µl/min à midi à 1,27 µl/min à minuit (Nau *et al.* 2013), la pression intraoculaire reste stable chez les sujets sains grâce à la compensation de la production d'HA par les 2 voies de drainage. En contact avec les tissus avasculaires du segment antérieur (cornée, angle iridocornéen, cristallin), l'HA est leur seul apport nutritionnel et contribue donc à la régulation de l'homéostasie des tissus oculaires (Chowdhury *et al.* 2010; Goel *et al.* 2010).

Mécanisme de sécrétion

L'HA est secrété principalement par l'épithélium ciliaire non pigmentaire (Figure 28). Faisant partie de l'angle iridocornéen, le corps ciliaire est en continuité avec la choroïde. Les procès ciliaires sur la surface postérieure des corps ciliaires sont

revêtus par une double couche d'épithéliums cubiques (Chowdhury *et al.* 2010). Il s'agit d'une couche superficielle de cellules épithéliales ciliaires non pigmentées en continuité avec la rétine, et d'une couche profonde très pigmentée en continuité avec l'épithélium pigmentaire rétinien (Goel *et al.* 2010).

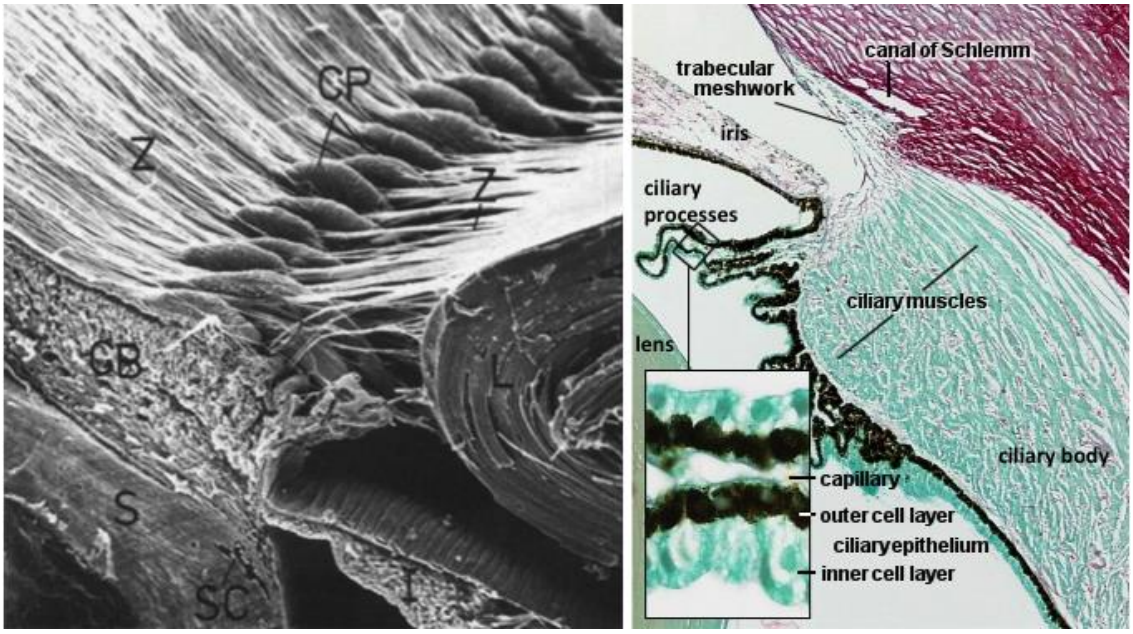


Figure 28. Structure tissulaire de l'angle iridocornéen en microscopie électronique à balayage (gauche) (Kiel et al. 2011) et en coupe histologie (droite) selon University of Western Australia http://www.lab.anhb.uwa.edu.au). Situés à la face postérieure du corps ciliaire, les procès ciliaires sont revêtus d'une double couche épithéliale pigmentaire et non pigmentaire. CB: corps ciliaires, CP: procès ciliaires, L: cristallin, I: iris, S: sclère, SC: canal de Schlemm, Z: zonules

Les procès ciliaires sont abondamment vascularisés et sécrètent l'HA grâce aux mécanismes de sécrétion active, d'ultrafiltration et de diffusion (Goel *et al.* 2010; Kiel *et al.* 2011), en 3 étapes (Figure 29). 1- Apport d'eau, d'ions, de protéines et de composés métaboliques par la circulation sanguine. 2- Ultrafiltration et diffusion des composés des capillaires sanguines vers le stroma ciliaire induit par la pression oncotique, la pression hydrostatique et les gradients de concentration. La diffusion est le transport de solutés et de substances liposolubles entre les capillaires et la chambre postérieure proportionnel au gradient de concentration à travers la membrane. L'ultrafiltration est le flux d'eau et des substances hydrosolubles, limité par leurs tailles et leurs charges, à travers l'endothélium capillaire fenêtré vers le stroma ciliaire. 3- Transport actif vers les espaces basolatéraux entre les cellules épithéliales non pigmentaires, suivi par un flux d'eau vers la chambre postérieure. Plusieurs canaux et pompes ont été détectés comme AQP1, AQP4, Na^+/K^+ATPase, anhydrase carbonique,

etc. Le mouvement d'électrolytes à travers l'épithélium ciliaire est conduit par différents gradients électrochimiques. Cl^- est l'anion majeur transporté via différents canaux chloriques. Le transport actif crée un gradient osmotique à travers l'épithélium ciliaire, ce qui favorise le mouvement des constituants du plasma par ultrafiltration et diffusion. En présence de récepteurs variables et de seconds messagers au sein de l'épithélium ciliaire, il est possible d'inhiber la production d'HA par différents médicaments

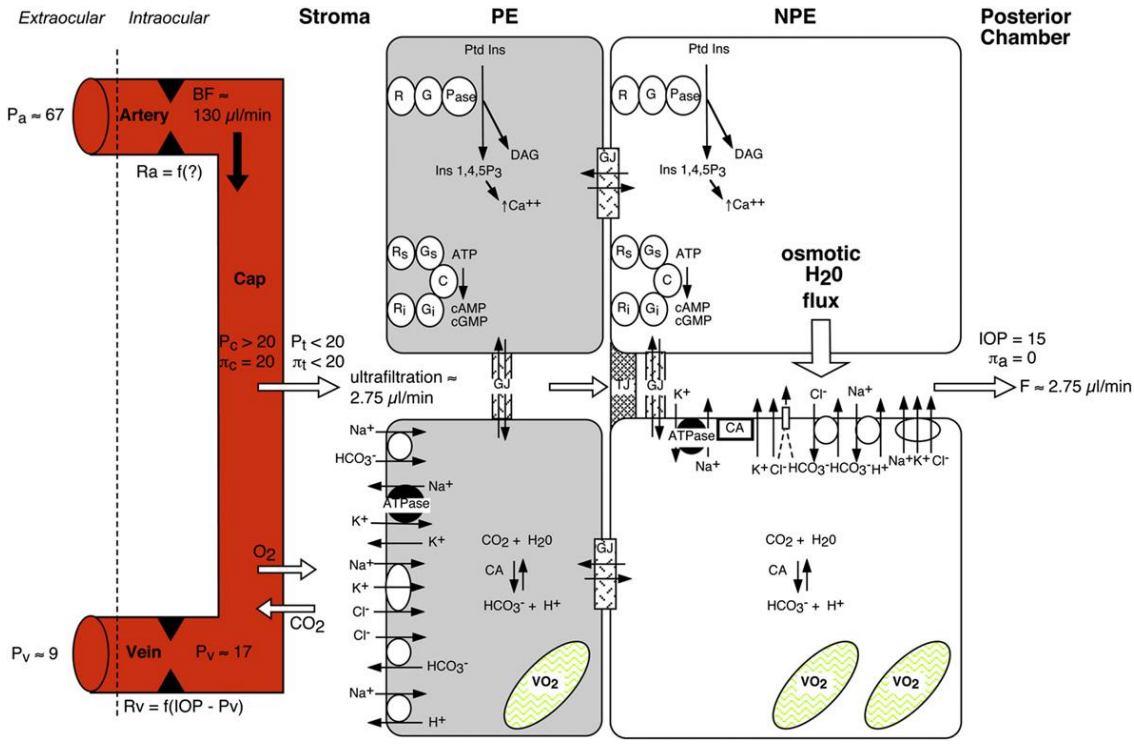


Figure 29. Formation de l'humeur aqueuse via les transports transcellulaires (Kiel et al. 2011)

Composition

L'HA est caractérisée par un pH de 7,2 (Crooke *et al.* 2008) et une faible concentration en protéines, 0,2-0,5 mg/ml, environ 200 fois moins que le plasma (Grus *et al.* 2007; Goel *et al.* 2010). La composition de l'HA est différente de celle du plasma au niveau quantitatif et qualitatif. Elle contient certains composants du plasma comme l'albumine, les globulines, la transferrine et une haute concentration en sels inorganiques (Grus *et al.* 2007) mais également d'autres secrétés par des tissus du segment antérieur.

Concernant la signalisation intercellulaire, l'HA contient peu de facteurs de croissance, cytokines et récepteurs (Chowdhury *et al.* 2010). TGFβ, TNF, FGF, interleukines, facteurs de croissance et de différenciation (GDF), et récepteurs de

cytokine (notamment des récepteurs solubles) ont néanmoins été détectés. Les récepteurs solubles modulent l'activité des facteurs de croissances des cytokines (Chowdhury *et al.* 2010).

L'HA contient des substances anti-oxydantes ayant probablement un rôle de protection contre les dommages oxydatifs induits par les différents stress (lumière/température) comme le glutathion, et l'acide ascorbique (concentration 15-20 fois plus élevée que dans le plasma) (Crooke *et al.* 2008; Goel *et al.* 2010; Sacca & Izzotti 2013). Elle contient également des vitamines, des protéines protectrices comme l'albumine (Sacca & Izzotti 2013), plusieurs protéines catalytiques comme la lactate dehydrogenase impliquée dans la régulation de l'évacuation de l'HA, l'aldolase, la ketolase secrétés par les cellules en contact avec l'HA (Chowdhury *et al.* 2010). L'HA contient également des concentrations élevées en lactate et bicarbonate (Sacca & Izzotti 2013), 2 anions impliquées dans le mécanisme fondamental de la pompe endothéliale.

L'HA contient 23 protéines du système du complément, les régulateurs comme CD59 et les inhibiteurs. La balance du système du complément et les molécules régulatrices aide à maintenir l'absence de réactions auto-immunes dans le segment antérieur de sujet sain (Chowdhury *et al.* 2010).

L'HA contient également des molécules pro-et anti-angiogeniques dont le déséquilibre est impliqué dans la pathogénèse des maladies du segment antérieur (Chowdhury *et al.* 2010).

Interaction avec l'endothélium cornéen

Malgré les découvertes sur l'activité de transport actif de l'endothélium cornéen, l'interaction des voies de transduction de signal avec les médiateurs de HA reste peu étudiée (Crooke *et al.* 2008) (Figure 30).

L'expression de récepteurs à P2Y[1] par les CE bovines, suppose leur stimulation par leurs agonistes à partir de L'HA. L'HA contient en effet des mononucléotides (les plus abondants sont l'AMP, l'ADP et l'ATP) et des dinucléotides (diadénosine polyphosphates, à concentration moins élevée que l'ATP) impliqués dans le transport d'ions et la régulation de la pression intraoculaire. Les CE peuvent également, relarguer

[1] Les récepteurs P2Y appartiennent à la famille des récepteurs P2 couplés aux protéines G activés par les nucléotides extracellulaires (www.ncbi.nlm.nih.gov/)

de l'ATP en cas de lésion endothéliale ou d'oedème du stroma. Ces ATP peuvent activer non seulement des pompes Na^+/K^+ATPase mais aussi des récepteurs purinergiques qui stimulent le relarguage de Ca^{2+} par le réticulum endoplasmique dans le cytoplasme. L'ion Ca^{2+} active les canaux chloriques CaCC qui augmente le flux d'HCO_3^-. Des composés puriniques peuvent également favoriser la déphosphorylation des MLC, et ainsi la relaxation de l'actine du cytosquelette des CEs, avec pour conséquence de renforcer l'intégrité de ses jonctions serrées, ce qui limite la fuite de fluide vers le stroma.

D'autre part, les CE contiennent des ecto-adénosine triphosphatases qui hydrolysent l'ATP en adénosine, et expriment le récepteur à l'adénosine A2B. La fixation de l'adénosine sur les récepteurs A2B active la voie AMPc qui active le régulateur CFTR et augmente la perméabilité apicale des anions Cl^- et HCO_3^-. D'autre part, l'augmentation de la concentration d'AMPc par traitement par la forskoline (activateur de l'adényl cyclase, utilisée il y a logtemps dans le traitement du glaucome), ou le blocage de la dégradation de l'AMPc par rolipram (inhibiteur sélectif de la phosphodiesterase 4) peuvent aussi stimuler le transport de fluide par les CEs.

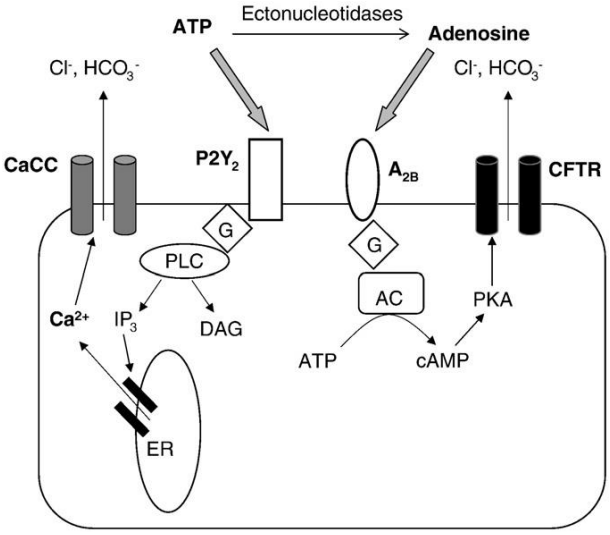


Figure 30. Modèle de l'implication de l'ATP et de l'adénosine dans la régulation des canaux ioniques sur la membrane apicale de l'endothélium cornéen (Crooke et al. 2008)

A coté de ces cascades d'activation, durant l'organogénèse l'HA est le support de différents échanges de signaux entre les tissus, notamment l'induction de la différenciation du mésenchyme périoculaire en CE (voir Chapitre I - 1.2.4). L'HA est fortement impliquée dans le maintien de l'homéostasie des tissus avec lesquels elle est

en contact. Le changement de sa composition dans des cas de pathologie (glaucome, diabète, etc.) est en cours d'étude pour trouver des marqueurs diagnostiques précoces et des solutions thérapeutiques ciblées.

3. Marqueurs endothéliaux

Possédant des spécificités structurelles et fonctionnelles, l'endothélium cornéen peut être distingué des tissus voisins par différents marqueurs (Figure 31).

Tout d'abord, il s'agit des spécificités structurelles. En condition physiologique, l'endothélium cornéen forme une monocouche de cellules. La formation des jonctions serrées peut être détectée par l'immunomarquage de protéines adaptatrice ZO-1. Les jonctions adhérentes sont marquées avec N-cadherin et JAM-1. D'autres protéines d'adhésion cellulaire sont NCAM-1 (Foets *et al.* 1992).

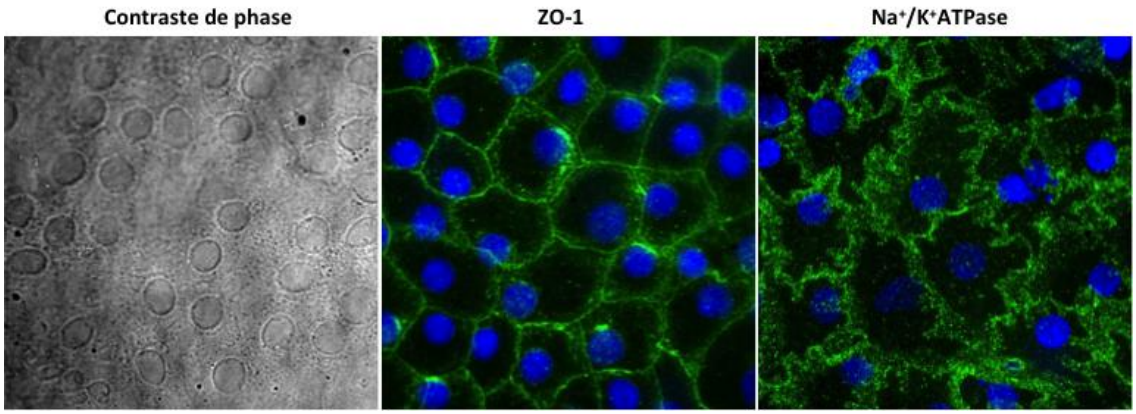


Figure 31. Immunomarquage de deux marqueurs les plus fréquemment utilisés pour l'endothélium cornéen, ZO-1 et Na^+/K^+ATPase, sur cornée ex vivo (EA2521 BiiGC, Université Jean Monnet, Saint Etienne).

L'endothélium est également caractérisé par sa fonctionnalité de transport de solutés. Les expressions d'ARNm et/ou de protéines des pompes membranaires ont été révélées comme Na^+/K^+ATPase, VDAC2, VDAC3, SLC4A4, SLC4A11, CLCN2, CLCN3, ou encore le canal hydrique aquaporine-1 (AQP1) (Shima *et al.* 2011; Chng *et al.* 2013).

D'autre part, par séquençage d'ARN, SLC4A11, Col8A2, CYYR1, Wnt5a, S100A4, S100A6, IER3 ont été identifiés comme marqueurs spécifiques exprimés par l'endothélium des cornées humaines fraîches (ARN extrait postmortem) (Chen *et al.* 2013; Chng *et al.* 2013). L'expression des protéiques de Wnt5a, S100A4, S100A6 et IER3 a été confirmée par immunomarquage (Chen *et al.* 2013). Récemment, par

immunomarquage suivi du cytométrie en flux, l'identification de deux protéines membranaires supplémentaires, glypican (GPC4) et CD200 (une glycoprotéine de la superfamille des immunoglobulines), a permis de distinguer les CE en culture in vitro des fibroblastes du stroma (Cheong *et al.* 2013). De façon notable, de nombreux marqueurs potentiels de CE n'ont été décrits que par la présence de leurs ARNm sans que l'expression de la protéine ne soit confirmée.

	Target proteins	End	S	Epi	RPE
Cell structure	ZO-1	+	+/-	+	+
	Actin	+	+	+	+
	Vimentin	+	+	-	+
	JAM-1	+/-	-	+	?
	CK3/12	-	-	+	?
Pump function	Na+/K+ ATPase	+	+	+	+
	AQP1	+	+	-	+
	VDAC2	+	+	?	?
	VDAC3	+	+	?	?
	SLC4A4	+	+	?	?
	SLC4A11	+	-	+	?
	CLCN2	+	+	?	?
	CLCN3	+	+	?	?
FACS	GPC4	+	-	?	?
	CD200	+	-	?	?

	Target proteins	End	S	Epi	RPE
Others	COL8A2	+	-	?	?
	CYYR1	+	-	?	?
	MYO5A	+	-	?	?
	Keratan sulfate	-	+	-	?
	NSE	+	+/-	+	?
	S100A4	+	+	+	?
	S100A6	+	+	+	?
	Wnt5a	+	?	-	?
	IER3	+	+	-	?

End: Corneal endothelial cells
S: Corneal stromal cells
Epi: Corneal epithelial cells
RPE: retinal pigmented endothelial cells
+/-: contradictory bibliographies
?: no reference
Expression mRNA
Expression protein

Figure 32. Bilan d'expression des marqueurs endothéliaux cornéens humains comparés aux kératocytes et cellules épithéliales cornéennes, ainsi que cellules de l'épithlium pigmentaire rétinien (EA2521 BiiGC, Université Jean Monnet, Saint Etienne).

En combinant plusieurs critères morphologiques, structurels et fonctionnels, il semble possible d'identifier les CE parmi d'autres, de les trier ou d'analyser leurs comportements sous différentes conditions. Cette combinaison de marqueurs devrait être utile en particulier lors des étapes de contrôle qualité des CE-like produites par bioingénierie cellulaire.

CHAPITRE II - Cycle cellulaire, Capacité prolifération et Sénescence

Prenant en compte de l'origine et la fonctionnalité de l'endothélium en interaction avec son environnement, cette partie a pour but de caractériser son cycle cellulaire et son éventuelle capacité d'auto-renouvellement. Dans le cadre de la bioingénierie, l'identification des mécanismes de régulation du cycle cellulaire spécifiques à l'endothélium devrait permettre d'adapter les interventions afin de prolonger sa durée de vie sur la cornée.

1. Rappel de mécanismes moléculaires de régulation du cycle cellulaire

Cette partie a pour but de rappeler les mécanismes moléculaires de régulation permettant d'activer ou d'inhiber la division cellulaire. Ces rappels proviennent de la base de données **Reactome** (Joshi-Tope *et al.* 2005; Vastrik *et al.* 2007; Matthews *et al.* 2009) qui synthétise les travaux effectués jusqu'à présent sur le cycle cellulaire .

1.1. Généralités sur le cycle cellulaire

Le cycle cellulaire se compose de phases principales dont l'enchaînement (Figure 33) est régulé par différents acteurs moléculaires.

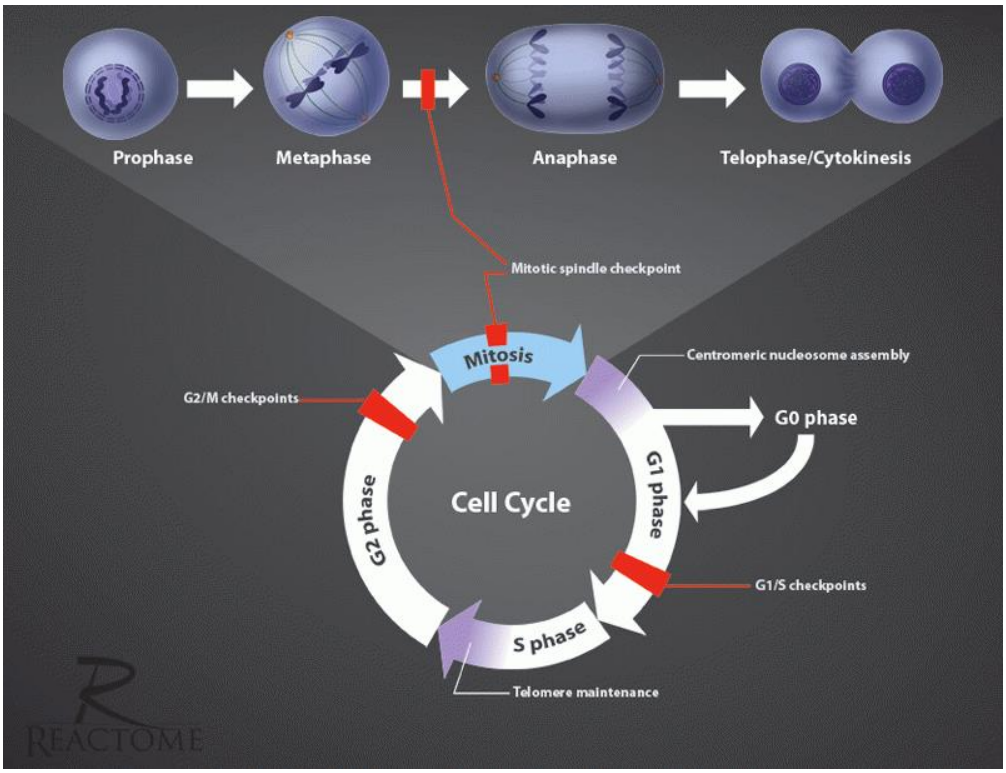


Figure 33. Evolution générale du cycle cellulaire (Joshi-Tope et al. 2005; Vastrik et al. 2007; Matthews et al. 2009)

Définition: il s'agit d'une série d'interactions permettant la réplication du génome et la ségrégation des chromosomes en 2 cellules filles. La réplication de l'ADN est appelée phase S (synthèse). La condensation de chromosome durant la réorganisation de l'architecture cellulaire est appelée mitose ou phase M. Entre ces 2 phases, il existe 2 intervalles (gap), la phase G1 de la mitose à la phase S, et la phase G2 de la phase S à la mitose.

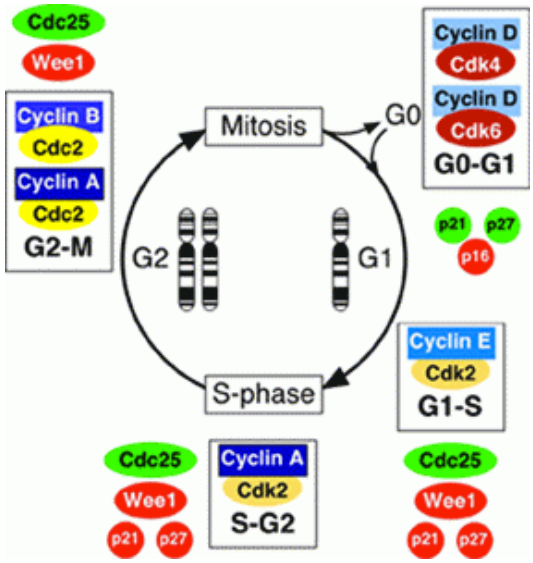


Figure 34. Régulation de la progression du cycle cellulaire par les complexes Cyclin-Cdks

Parmi les acteurs moléculaires, les Cyclines et les Cdks (cyclin-dependent kinases) orchestrent la progression du cycle cellulaire (Figure 34). Les Cdks appartiennent à la famille des protéines sérine/thréonine kinases. Formant des complexes avec les Cyclines partenaires, les Cdks contrôlent la progression du cycle cellulaire via leurs activités catalytiques. La variation du niveau des cyclines combinée à leur activation par des CDKs au bon moment et au bon endroit favorise l'évolution du cycle cellulaire. Ainsi l'expression des Cyclines et des CDKs est utilisée pour identifier le stade prolifératif des cellules. L'activité des Cdks est régularisée par d'autres protéines qui modifient leurs structures post-traductionnelles.

Lors de la transition entre les phases, il existe trois points de contrôle (checkpoints) où certains mécanismes moléculaires particuliers permettent de vérifier soit l'absence des anomalies, soit en cas de présence, de les réparer ou les éliminer.

L'interaction avec l'environnement peut induire des mécanismes favorisant ou inhibant le cycle cellulaire. Ainsi, une cellule peut soit aboutir à sa division en 2

cellules filles, soit se retirer du cycle cellulaire pour un moment (quiescence), soit se différencier en un type cellulaire qui ne se divise plus et change de morphologie pour devenir fonctionnelle (sénescence), soit finalement programmée pour être éliminée (apoptose).

1.2. Les phases du cycle cellulaire

1.2.1. Phase G0

La phase G0 caractérise l'état de quiescence, donc l'absence de la division cellulaire. La transition entre G0 vers le début de la phase G1 marque l'entrée du cycle cellulaire.

La surexpression des protéines RB1 (retinoblastoma-like 1, ou p130) et RBL2 (p107) entraîne l'arrêt du cycle cellulaire. Durant G0 et au début de G1, RBL2 forme un complexe DREAM avec E2F4/E2F5, DP1/DP2 et le complexe MuvB. Ce complexe bien conservé réprime la transcription des gènes du cycle cellulaire. D'autre part, au début de G1, RBL1 s'attache à E2F4 et DP1/DP2 formant un complexe réprimant la transcription des gènes cibles des facteurs de transcription E2F.

1.2.2. Phase G1

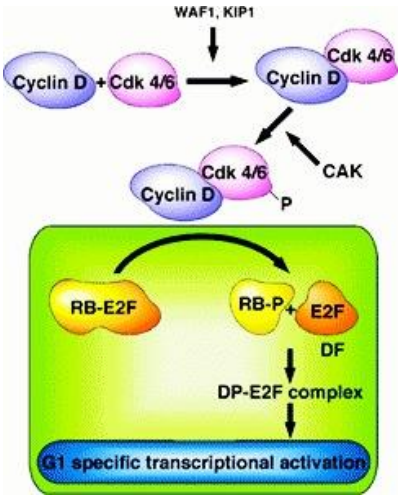


Figure 35. Mécanisme d'activation de la phase G1

La progression vers la phase G1 est contrôlée par les Cyclines D, Cdk4 et Cdk6 (Figure 35). Il existe 3 types de Cycline D. La formation du complexe Cycline D-Cdk4/6 est favorisée par 2 protéines, p21Cip1/Waf1 (p21) et p27Kip1 (p27), ou inhibée

par fixation aux protéines inhibitrices (cyclin-dependent kinase inhibitor, Cki) p15INK4B (p15), p16INK4A (p16), p18INK4C (p18), p19INK4D (p19). Attaché à Cycline D, Cdk4/6 est ensuite activé par sa phosphorylation par CAK (Cdk-activating kinases).

Le complexe Cycline D-phospho Cdk4/6 phosphoryle les protéines RB1, RBL1 et RBL2 qui se détachent de leurs complexes et libèrent les facteurs de transcription E2F (E2F1, E2F2, E2F3, E2F4, E2F5) qui activent la transcription des gènes du cycle cellulaire, menant à la transition G1/S.

1.2.3. Transition G1/S

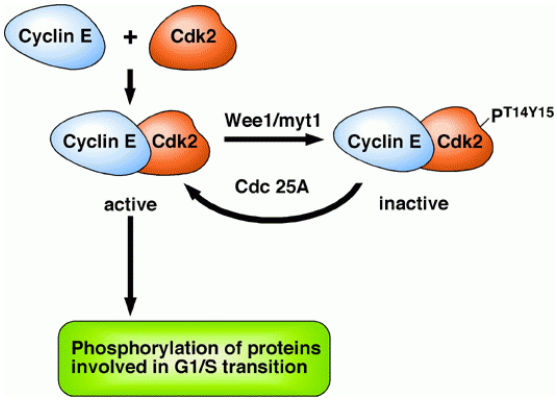


Figure 36. Mécanisme d'activation de la transition G1/S

Cette transition est contrôlée par les complexes CyclinE-Cdk2 qui phosphorylent les protéines spécifiques de la transition G1/S (Figure 36), incluant les éléments nécessaires à l'initiation de la réplication d'ADN. La formation des complexes Cycline E-Cdk2 et Cycline A-Cdk2 résulte de la séquestration de p21Cip/Waf1 ou p27Kip1 qui ont plutôt un effet inhibiteur.

Dans sa forme complexée, Cdk2 peut être désactivé par phosphorylation (Threonine-14 et Tyrosine-15) par Wee1 et Myt1 kinases. Ce processus est réversible par la déphosphorylation de Cdk2 par les phosphatases Cdc25 (Cdc25A, B et C).

Ensuite, les 2 protéines sont soumises à la protéolyse par le complexe des ubiquitines.

1.2.4. Phase S

Le complexe Cycline A-Cdk2 favorise la phosphorylation des protéines impliquées dans la transition G1/S, permettant ainsi de déclencher la phase S. Formé dans le cytoplasme durant la phase G1, ce complexe se translocalise dans le noyau durant cette phase. Son activité est inhibée par la phosphorylation Tyr15 du Cdk2 et par l'association des 2 Ckis p27 et p21 dans le noyau.

L'entrée en phase S est marquée par la levée de cette inhibition, c'est à dire la dégradation de p27/p21 via SCF (Skp2) suivie de la déphosphorylation de Cdk2 par les phosphatases Cdc25. La synthèse de l'ADN, l'initiation de la réplication par l'ADN polymérase à son élongation, est régulée par les protéines Orc (origin recognition complex) à différents niveaux. Les 6 sous-unités d'Orc contrôlent le site d'initiation de la réplication de l'ADN et la formation du complexe pré-réplicatif.

Ensuite, la dégradation de la Cycline D débute par sa phosphorylation, sa relocalisation du noyau vers le cytoplasme, puis sa dégradation par ubiquitination et sa dégradation dans le protéasome.

Finalement, les complexes cohésine s'attachent aux deux chromatides soeurs associés après la réplication pour établir leurs cohésions. Cette fixation transitoire est nécessaire pour assurer l'identification des chromatides soeurs comme paire.

1.2.5. Phase G2

Cette phase d'intervalle entre la synthèse de l'ADN et le début de la mitose correspond à la synthèse protéique pour se préparer à la mitose. Durant cette phase, le complexe Cycline A-phosphoCdk2 s'associe à E2F1 et E2F3, puis les phosphoryle, menant à leur dégradation.

1.2.6. Transition G2/M

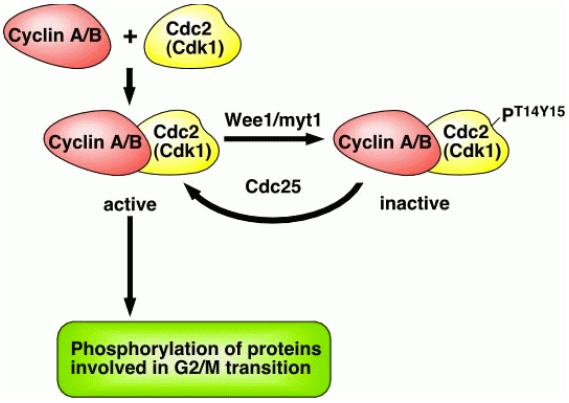


Figure 37. Mécanisme de l'activation de la transition G2/M

La transition G2/M nécessite la formation des complexes Cycline A/B-Cdk1 (ou Cdc2) qui phosphorylent d'autres protéines impliquées dans la structure et la fonction du fuseaux mitotiques, la dégradation de l'enveloppe nucléaire, les changements topologiques des chromosomes permettant leur condensation lors de la mitose.

Cette transition est négativement régulée par Wee1 et Myt1 qui désactivent ce complexe en phosphorylant (T14 et Y15) Cdk1 (Figure 37). Cette inhibition est réversible via sa déphosphorylation par Cdc25.

1.2.7. Phase M

La phase M, appelée également mitose, implique la division des noyaux et la cytokinèse donnant deux cellules filles. Cette phase se compose principalement de la prophase, prométaphase, métaphase, anaphase, télophase (Figure 38). La cytokinèse finalise la division cellulaire.

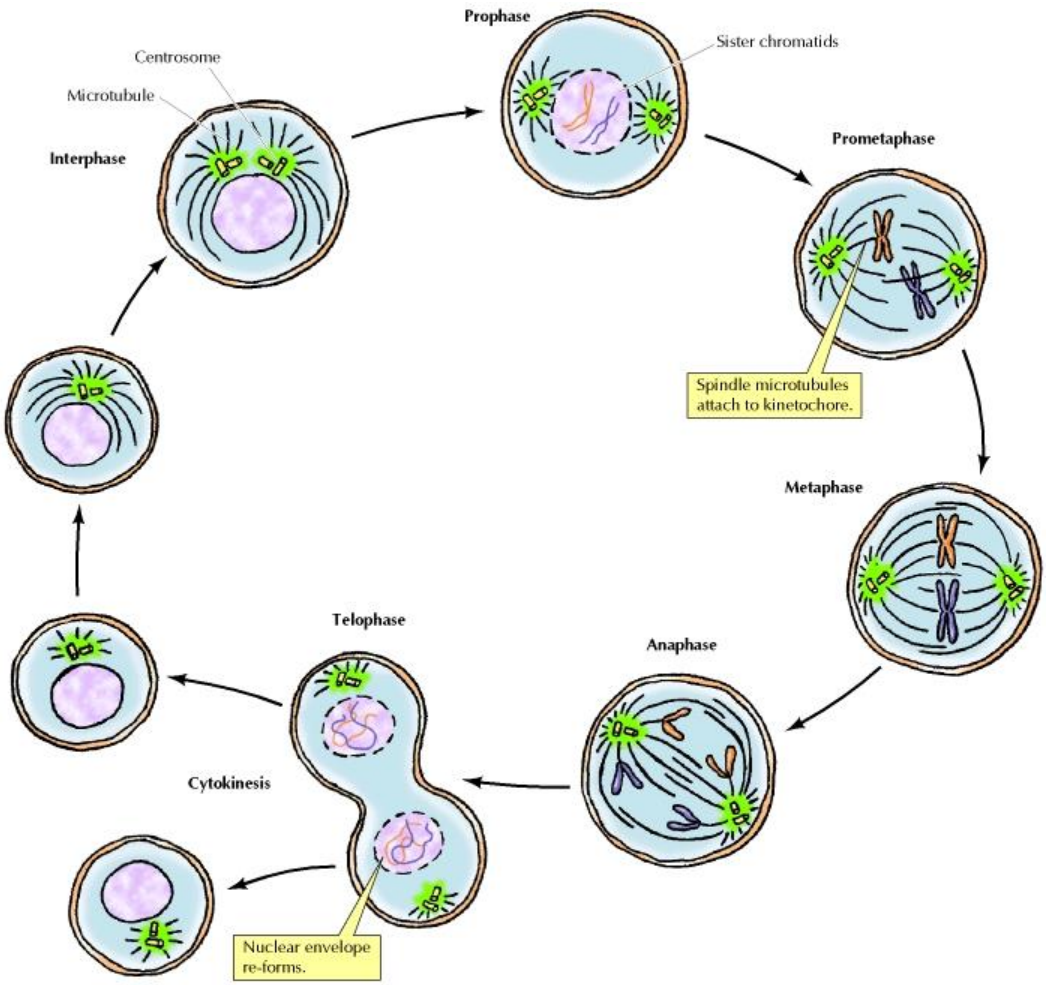


Figure 38. Evolution de la mitose (D'après The cell: A molecular Approach, 2nd edition, 2000)

Prophase : cette étape est caractérisée par la condensation de la chromatine dans le noyau et la disparition des nucléoles. Les centrioles se forment dans les 2 pôles de la cellule. Certaines fibres s'étendent des centromères à travers la cellule pour former le fuseau mitotique.

Prométaphase : la dissolution de la membrane nucléaire marque le début de la prométaphase. Les kinétochores sont formés par l'attachement des protéines aux centromères. Ensuite, les microtubules s'attachent aux kinétochores et les chromosomes commencent à se déplacer vers la plaque métaphasique.

Métaphase: cette étape est marquée par la formation de plaque métaphasique quand les fuseaux alignent les chromosomes le long du centre de la cellule. Cette organisation permet de distribuer de façon égale les copies des chromosomes quand ils se séparent de chaque côté des nouveaux noyaux.

Transition Métaphase/Anaphase: cette transition est déclenchée par la destruction des Cyclines mitotiques.

Anaphase : les paires de chromosomes se séparent au niveau des centromères et se dirigent vers 2 côtés opposés de la cellule. Ce mouvement de chromosomes est conditionné par la combinaison des mouvements des kinétochores au long des fuseaux de microtubules et par interaction physique des microtubules polaires.

Telophase/Cytokinèse : cette étape est caractérisée par la formation de nouvelles membranes autour de deux parties des chromatides. Les chromosomes et les fuseaux se dispersent et l'anneau d'actine au centre des 2 cellules ce contracte pour dissocier les 2 cellules filles.

1.2.8. Transition M/G1

Cette transition est caractérisée par l'inactivation du complexe Cycline B-Cdc2 par protéolyse ubiquitine-dépendante des Cyclines A et B. Ce processus est régulé par le complexe APC (anaphase promoting complex).

1.3. Points de contrôle

Les points de contrôle ont le rôle d'assurer la complémentarité et l'interdépendance entre la phase S et M, l'intégrité du génome et la ségrégation de chromosome. Lors de la détection d'anomalies, ce processus consiste à retarder l'activation des Cdks par différents mécanismes correspondant à chaque étape du cycle cellulaire.

1.3.1. Point de contrôle G1/S

Ce point de contrôle a pour but de contrôler l'intégrité de l'ADN avant la transition G1/S. En absence d'anomalie, la réplication est mise en route par l'activation de ses facteurs inducteurs. A l'opposé, les dommages à l'ADN détectés à ce stade peuvent induire 2 types de réponses dépendante ou indépendante de p53 (Figure 39). L'échec de ce point de contrôle conduit à des mutations et d'autres défauts de réplication.

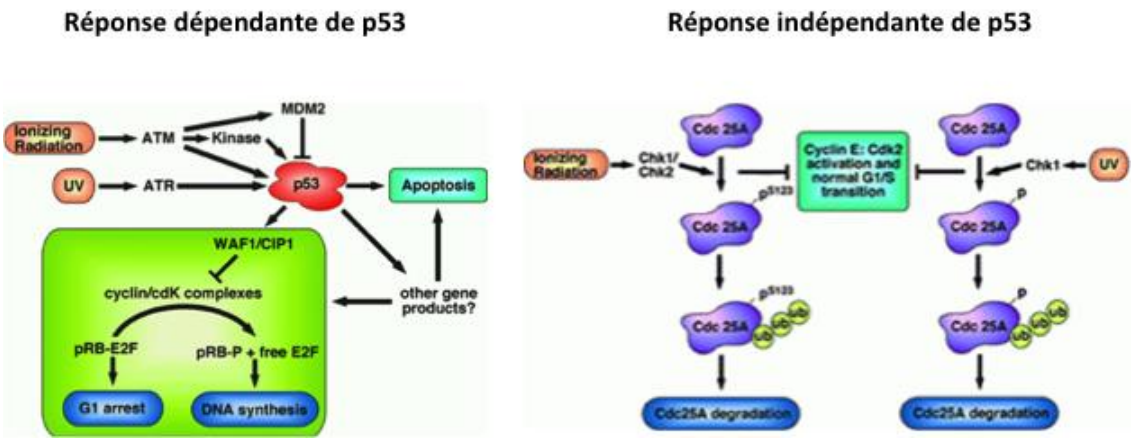


Figure 39. Induction de l'arrêt du cycle cellulaire à la phase G1 via 2 voies au point de contrôle G1/S.

La réponse dépendante de p53 consiste à l'inhibition des Cdks via la sur-expression de Ckis via la protéine p53. En conditions normales, la protéine MDM2 inhibe l'activité de p53 en facilitant sa dégradation par ubiquitination dans le cytoplasme. Après la détection d'une lésion de l'ADN, l'activation de l'ATM kinases et d'autres kinases bloque MDM2 en le phosphorylant tout en activant p53 en le phosphorylant. p53 phosphorylé active la transcription de p21 qui inactive Cdk2 sur les complexes CyclinE-Cdk2 (voir Chapitre II - 1.2.2) et arrête le cycle cellulaire à la phase G1.

La réponse indépendante de p53 consiste à l'inhibition des Cdks via leur phosphorylation sur T14Y15. Suite à des lésions de l'ADN après exposition aux UV ou aux radiations ionisantes, Cdc25A est phosphorylé par Chk1 ou Chk2, ce qui signalant sa dégradation par ubiquitination. L'absence de Cdc25A ne permet pas de déphosphoryler Cdk2 dans son complexe avec la Cycline E, donc induit l'arrêt à la phase G1 (voir Chapitre II - 1.2.2).

1.3.2. Point de contrôle G2/M

Avant la transition G2/M, ce point de contrôle a pour rôle de vérifier l'absence de lésion de l'ADN, l'absence d'erreur de réplication, ou encore l'unique réplication du génome par le cycle celulaire (Figure 40). En absence d'anomalie, la mitose est mise en route par l'activation des facteurs mitotiques. Par contre, l'absence de réplication ou l'endommagement de l'ADN entraîne l'inactivation de Cdk1, ce qui empêche l'entrée

dans la mitose. Un niveau important d'endommagement d'ADN peut conduire la cellule en apoptose.

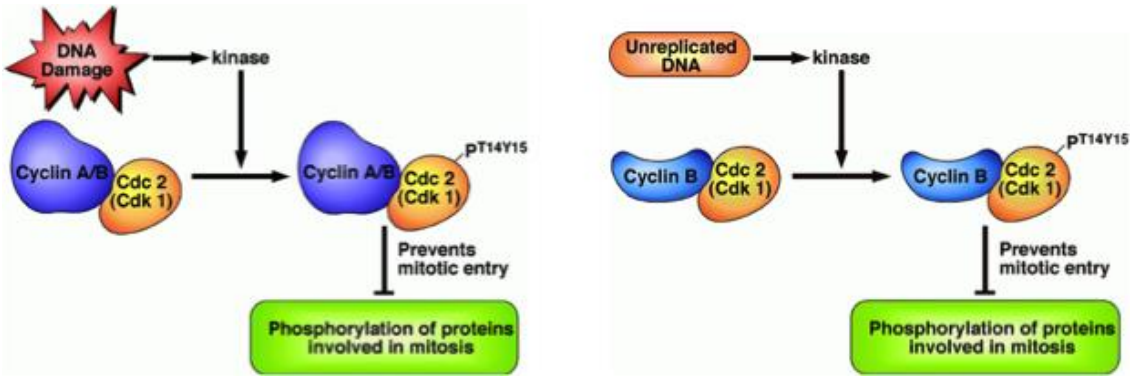


Figure 40. Inhibition de l'entrée de la mitose en cas d'endommagement de l'ADN (gauche) ou de réplication incomplète (droite) au point de contrôle G2/M.

L'endommagement de l'ADN à la phase G2 déclenche l'activation des Chk1 et Chk2 par ATM. Chk1 ou Chk2 activé phosphorylent Wee1 kinase et Cdc25C, ce qui maintient la phosphorylation de Cdk1 dans son complexe avec Cycline A/B, donc inhibe l'entrée dans la mitose (voir Chapitre II - 1.2.5).

En cas de réplication incomplète, ce point de contrôle empêche l'entrée dans la mitose en inactivant le complexe Cycline B-Cdk1 par la phosphorylation de Cdk1 par Myt-1 (voir Chapitre II - 1.2.5).

D'autre part, le stress génotoxique, dû à l'endommagement de l'ADN ou au défaut de réplication, peut causer l'instabilité du génome. Ce contrôle fait appel à ces mécanismes pour arrêter ou ralentir la progression du cycle cellulaire.

1.3.3. Point de contrôle en métaphase

Ce point de contrôle a pour rôle d'assurer l'alignement de tous les chromosomes sur l'équateur des fuseaux avant le passage à l'anaphase. En effet, tous les chromosomes ne s'alignent pas sur l'équateur en même temps. Ce processus permet le début de l'anaphase si et seulement si tous les chromosomes sont alignés.

Cette fonction est assurée grâce aux protéines de contrôle associées aux kinétochores (Figure 41). Les défauts mécaniques liés à l'absence d'alignement activent ces protéines de contrôle qui envoient un signal dans le cytoplasme. Ce signal est

amplifié pour empêcher l'activation des processus protéolytiques nécessaires à l'anaphase.

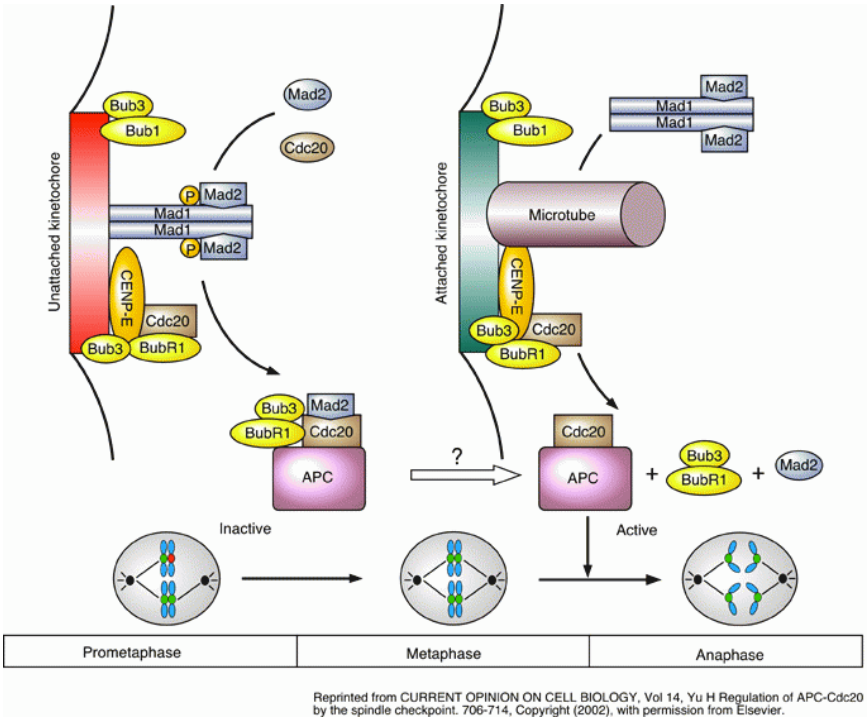


Figure 41. Modèle d'inhibition de l'anaphase par libération de Mad2 en cas d'absence d'alignement des chromosomes.

Les kinétochores non alignés sont caractérisés par l'insaturation des microtubules associés et l'absence de tension exercée sur eux. Il existe deux modèles de signalisation. En cas de non alignement, le premier modèle consiste à la libération de Mad2 dans la cellule qui inhibe l'action d'APC pour l'entrée de l'anaphase. Le deuxième modèle suppose la transmission de signal via des cascades de kinases comprenant hBUBR1, hBUB1, hMPS1 qui sont encore peu clarifiés.

Conclusion : le cycle cellulaire comprend plusieurs mécanismes de régulation très conservés au cours du temps entre les espèces et entre les différents tissus. L'identification des acteurs moléculaires de ces processus et de leurs modes d'interaction permet d'avoir une référence pour explorer le cycle cellulaire de l'endothélium cornéen.

2. Arrêt du cycle cellulaire de l'endothélium cornéen à la phase G1

En se basant sur les divers mécanismes de régularisation pré-établis, cette partie a pour but d'identifier le statut prolifératif de l'endothélium cornéen et ses mécanismes régulateurs.

La baisse de DCE au fil de la vie de l'homme a été décrite il a plus de 30 ans (Murphy *et al.* 1984). Le développement de la surface postérieure cornéenne explique la baisse de la DCE durant l'embryogénèse et juste après la naissance. Après ces périodes, la DCE baisse très progressivement, de 0,56% par an (Bourne *et al.* 1997; Moller-Pedersen 1997), signifiant que, les mécanismes de renouvellement endothéliaux, s'ils existent, ne sont pas efficaces pour empêcher la dégénérescence progressive avec l'âge. Heureusement, la durée de vie de l'humain, de 77,4 ans chez l'homme et 83,2 ans chez la femme dans les pays à haut niveau de vie selon les données de l'année 2011 (Institut national d'études démographiques, www.ined.fr/) fait que cette perte de DCE ne s'accompagne pas d'une instauration d'un oedème cornéen (qui survient par une DCE de l'ordre de 400-500 cellules/mm^2). Une cornée survivait ainsi près de 2 siècles.

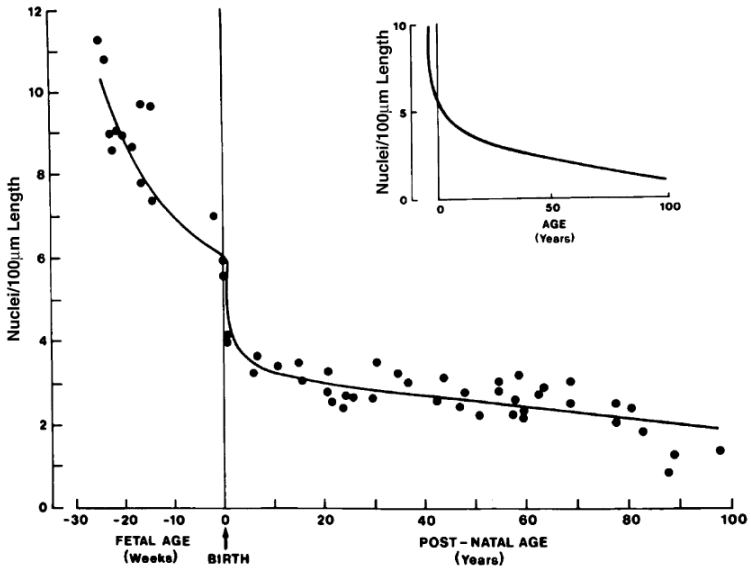


Figure 42. Baisse de la densité de cellules endothéliales (DCE) cornéennes humaines avec l'âge. La DCE est exprimée par le nombre de noyau compté sur 100 µm de longueur sur l'endothélium (Murphy et al. 1984)

Plusieurs observations concordantes ont montrer l'arrêt du cycle cellulaire des CE humaines à la phase G1 (Figure 43. Illustration des mécanismes de régulation positive (A) et négative (B) du cycle cellulaire (Joyce 2012).. L'entrée à la phase S

demande le déblocage des facteurs de transcription E2F par la phosphorylation de RB. Une des premières preuves consiste en l'absence de l'activation de la transcription des gènes du cycle cellulaire par les facteurs de transcription E2F à la phase G1. A l'opposé, l'introduction de E2F2 par transfection par vecteur adenoviral dans les CE humaines ex vivo stimule l'entrée en phase S (BrdU) et une augmentation significative de la DCE (McAlister *et al.* 2005). D'autre part, l'intensification de ce bloquage avec l'âge est démontrée par la plus faible hyper-phosphorylation de Rb des CE in vitro provenant de donneurs âgés par rapport aux donneurs jeunes (Joyce 2012).

L'inhibition de l'entrée en phase S provient de plusieurs facteurs environnementaux qui enchaînent des cascades de signalisation intracellulaire menant à la désactivation des complexes Cycline-Cdk par des Ckis (voir Chapitre II - 1.2.2). Parmi les Ckis, la famille INK notamment p16 se fixe spécialement sur CDK4 et le désactive. En présence de p16, les protéines Cip/Kip comme p21 et p27 se fixent principalement sur le complexe Cycline E/Cdk2 (Joyce 2012). L'expression de p16, p21 et p27 a été détectée dans les CE humaines. Leurs effets sur le cycle cellulaire impliquent des **mécanismes dépendants et d'autres indépendants de l'âge**. En effet, p27 est exprimé par les CE aussi bien chez les donneurs jeunes (< 30 ans) que âgés (> 50 ans). Par contre l'expression de p16 et de p21 augmente de façon significative chez les donneurs âgés par rapport aux donneurs jeunes (Joyce & Harris 2010).

Au niveau du point de contrôle G1/S, le blocage du cycle cellulaire est lié à p53 (voir Chapitre II - 1.3.1). L'expression protéique de p53 a été détectée dans les CE humaines, environ 2 fois plus forte au centre qu'en périphérie cornéenne (Paull & Whikehart 2005). Il n'y a pas de différence significative entre les donneurs jeunes et âgés.

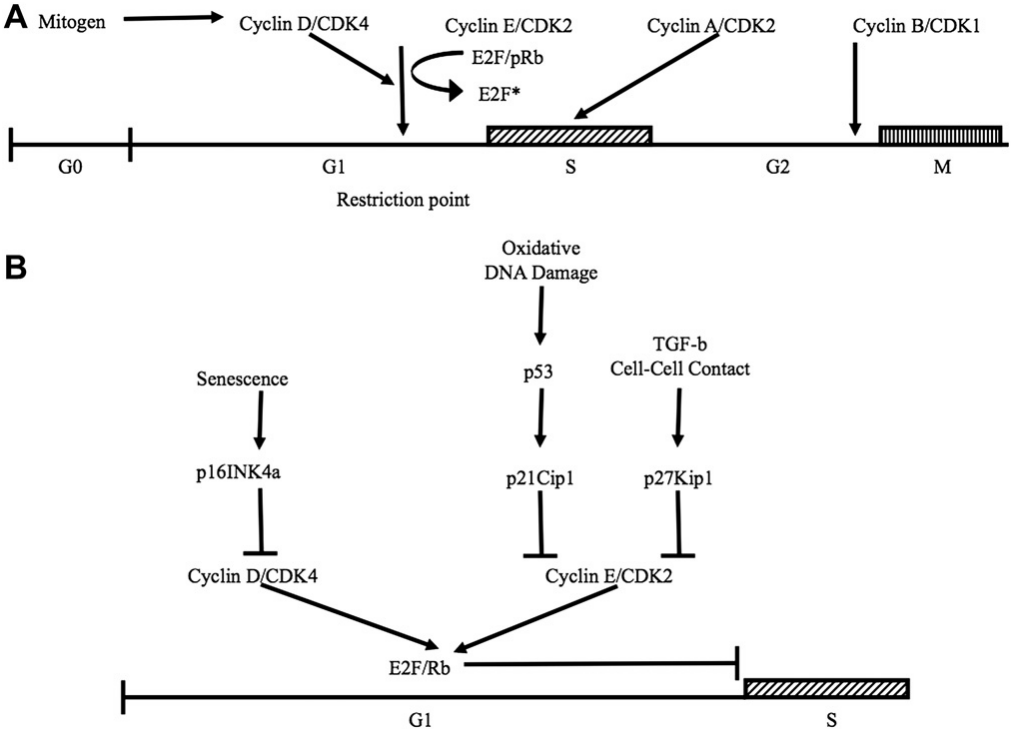


Figure 43. Illustration des mécanismes de régulation positive (A) et négative (B) du cycle cellulaire (Joyce 2012).

Le maintien de cet arrêt du cycle cellulaire provient des interactions entre CE et entre CE et l'HA qui génèrent plusieurs mécanismes simultanés.

2.1. Inhibition de contact

La maturation des CE débute par la formation d'une monocouche en se liant par des jonctions serrées durant l'embryogénèse (voir Chapitre I - 1.1.2). Ce mécanisme rend l'endothélium fonctionnel (voir Chapitre I - 2.2.4) mais inhibe également la division cellulaire. Cette inhibition indépendante de l'âge implique le CKI p27. Cela a été démontré sur les modèle d'animaux in vivo (rat et souris) dont la maturation des CE survient après la naissance. L'arrêt des divsions cellulaires en postnatal est corrélé à l'augmentation d'expression de p27 (Joyce 2012). Chez l'homme, la libération des jonctions cellulaire par l'EDTA ou en cas de lésion (ex vivo) ou sur des cultures non-confluentes (in vitro) active la division cellulaire marquée par expression de Ki67 (Figure 44).

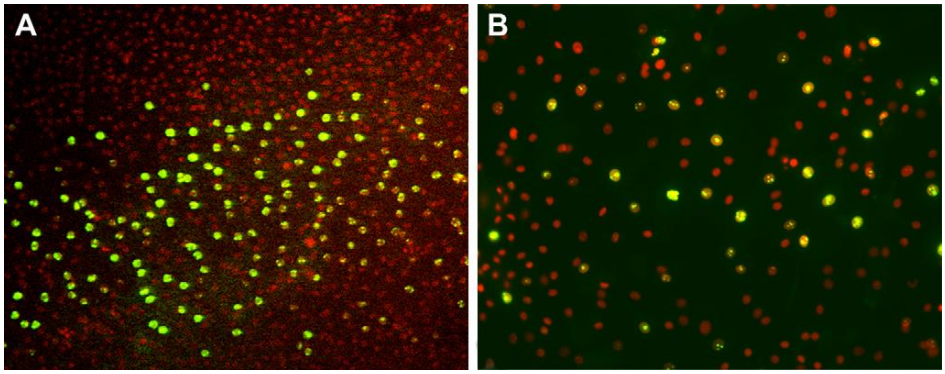


Figure 44. Activation de la division cellulaire (immunomarquage de Ki67, vert) ex vivo en cas de lésion (A) ou in vitro sur culture primaire non confluente (B). Contre-coloration du noyau par DAPI (rouge) (Joyce 2012).

2.2. Régulation par des facteurs de croissance

Etant en contact avec l'HA, la CE régule son cycle cellulaire sous la stimulation des composants de l'HA. Analysant l'activation des voies de signalisation intracellulaires sous l'effet de différents facteurs de croissance, les découvertes ont identifié leurs impacts sur la division cellulaire et les mécanismes de réparation de lésion endothéliale.

L'HA est peu riche en facteurs de croissance (Chowdhury *et al.* 2010; Joyce 2012). Elle contient 0.27-2.24 ng/ml de TGF-β dont 20-830 pg/ml sous forme active (Joko *et al.* 2013). Ce facteur de croissance et ses récepteurs sont également secrétés par les CE humaines. La forme latente de TGF-β peut être activée par la thrombospondine-1 exprimée par les CE humaines (Joyce 2012).

Les voies de signalisation TGF-β et MAPK [1] ont été reportées comme mécanismes inducteurs de l'arrêt du cycle cellulaire.

Chez le lapin, TGF-β2 réprime l'expression de CDK4 et limite l'export de p27 hors du noyau, ce qui empêche sa dégradation dans le cytoplasme et maintient son effet d'inhibiteur par l'arrêt à la phase G1 (Joyce 2012). Une autre hypothèse suppose

[1] MAPK est l'abréviation de mitogen-activated protein kinase, indiquant les cascades d'activation intracellulaire impliqué dans la régulation de la prolifération, de la différenciation et de la migration cellulaire Kanehisa M , Goto S (2000). KEGG: kyoto encyclopedia of genes and genomes. *Nucleic acids research*. **28**, 27-30, Kanehisa M, Goto S, Sato Y, Furumichi M , Tanabe M (2012). KEGG for integration and interpretation of large-scale molecular data sets. Ibid. **40**, D109-114.

l'inhibition de prolifération chez le lapin par la prostaglandine E2 dont la synthèse et secrétion sont stimulées par TGF-β2 (Joyce 2012).

Chez l'homme, TGF-β2 a un effet inhibiteur dose-dépendant sur la prolifération des CE mais stimule aussi leur migration (Joko *et al.* 2013). En se fixant sur son récepteur TGF-β type I, TGF-β2 active MKK3/6 et active la phosphorylation de p38 MAPK (1,9 fois) qui induit l'inhibition du cycle cellulaire. D'autres voies MAPK liées à Erk1/2 ou JNK ne sont pas activées. D'autre part, la signalisation via les récepteurs TGF-β est inhibée par Smad7 chez le lapin.

FGF-2 a été également rapporté comme facteur régulateur de la prolifération et de la migration des CE (Figure 45). La concentration de FGF-2 est de 0.48-1.44 ng/ml dans l'HA humaine normale (Joko *et al.* 2013). FGF-2 a un effet synergique avec TGF-β dans l'activation de la phosphorylation de p38 MAPK et de la migration cellulaire (Joko *et al.* 2013). Concernant la signalisation MAPK, FGF-2 stimule la prolifération via phosphatidylinositol-kinase de type 3 (PI3K) qui phosphoryle Erk1/2 et active cette voie. La voie PI3K-Erk1/2 favorise la phosphorylation de p27, et ainsi l'inactive.

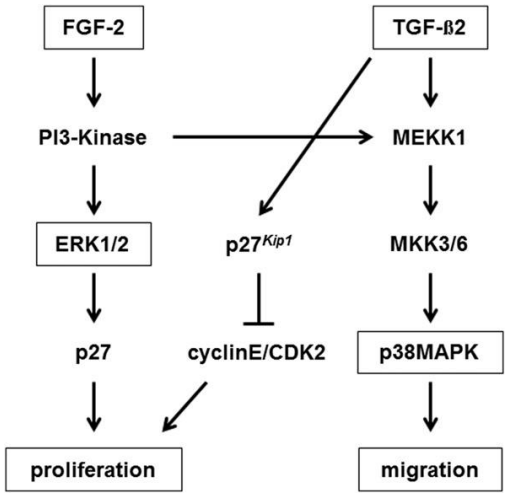


Figure 45. Activation des cascades de signalisations intracellulaires par TGF-β2 et FGF-2 et leurs effets sur la prolifération et la migration de cellules endothéliales humaines (Joko et al. 2013)

D'autre part, via ce mécanisme, les CE peuvent suivre une transition suite à une inflammation ou une lésion sévère (Lee & Heur 2013). En effet, chez le lapin, FGF-2 dégrade p27 via l'activation de PI3K, facilite la synthèse et la secrétion de Collagène I par les CE dans la matrice extracellulaire, et induit les changements morphologiques et la migration cellulaire via la régulation des GTPases de la famille Rho.

L'expression de FGF-2 peut être stimulée par l'interleukin 1β (Figure 46). En effet, il a été démontré sur une lignée CE humaines immortalisées (B4G12) que sa fixation sur son récepteur forme des complexes IRAK2, IRAK4, TRAF6 qui activent PI3K qui active NF-κB et AP-1 qui stimulent l'expression de FGF-2 (Lee & Heur 2013).

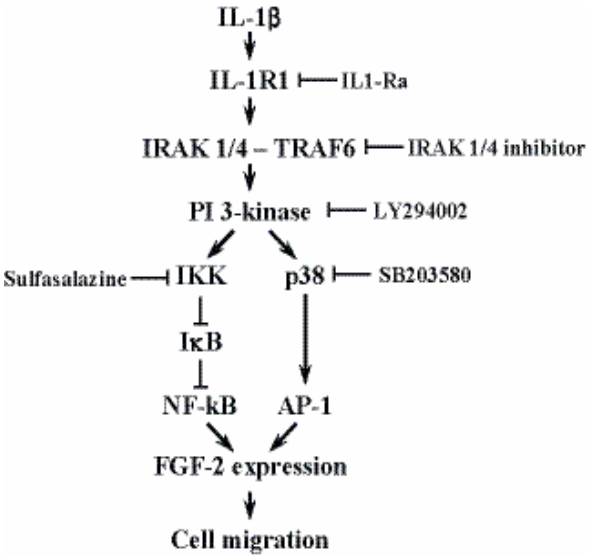


Figure 46. Cascade d'activation des signaux intracellulaires par IL-1β menant à la migration cellulaire (Lee & Heur 2013).

Les précédentes descriptions sur l'effet de TGF-β et FGF-2 ont été repérées dans l'ensemble des voies de signalisations de TGF-β et MAPK représentées par KEG (*Figure 47*, *Figure 48*).

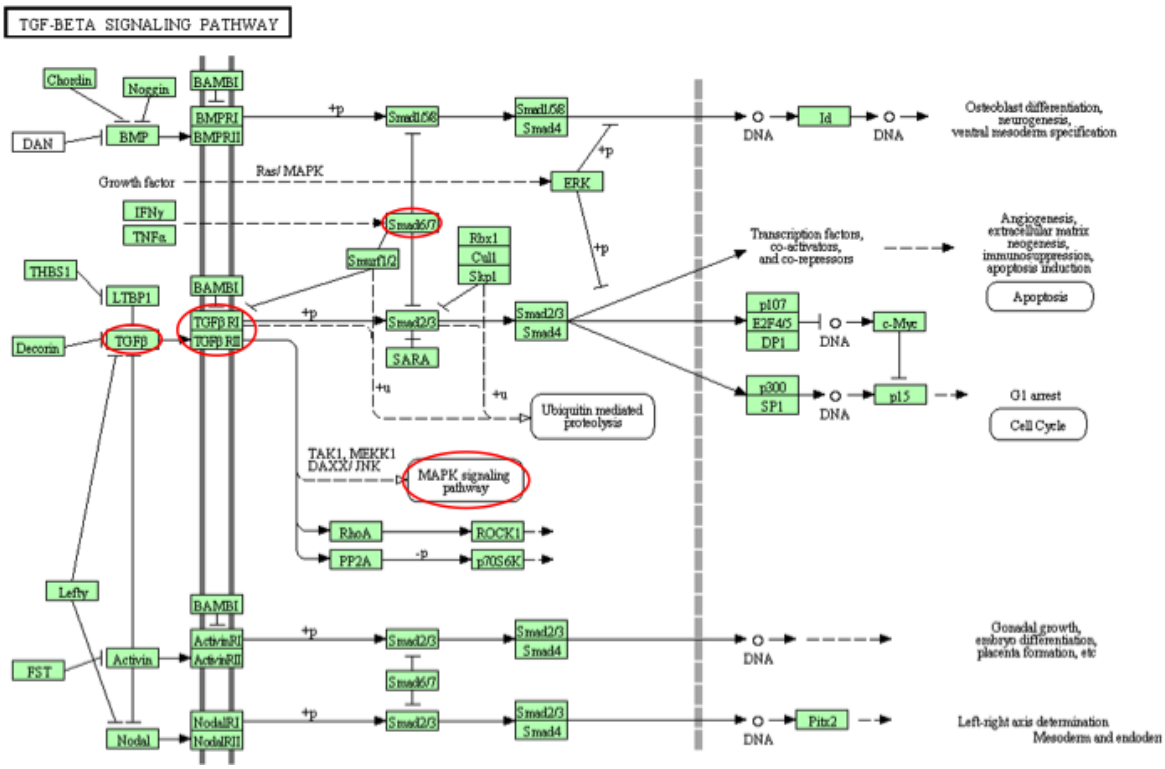


Figure 47. Voies de signalisation TGF-β chez l'homme (Kanehisa & Goto 2000; Kanehisa et al. 2012). Schéma de synthèse obtenu à partir de Kyoto Encyclopedia of Genes and Genomes (KEGG, http://www.genome.jp/kegg/). Les éléments impliqués dans la régulation de l'endothélium humain sont entourés en rouge.

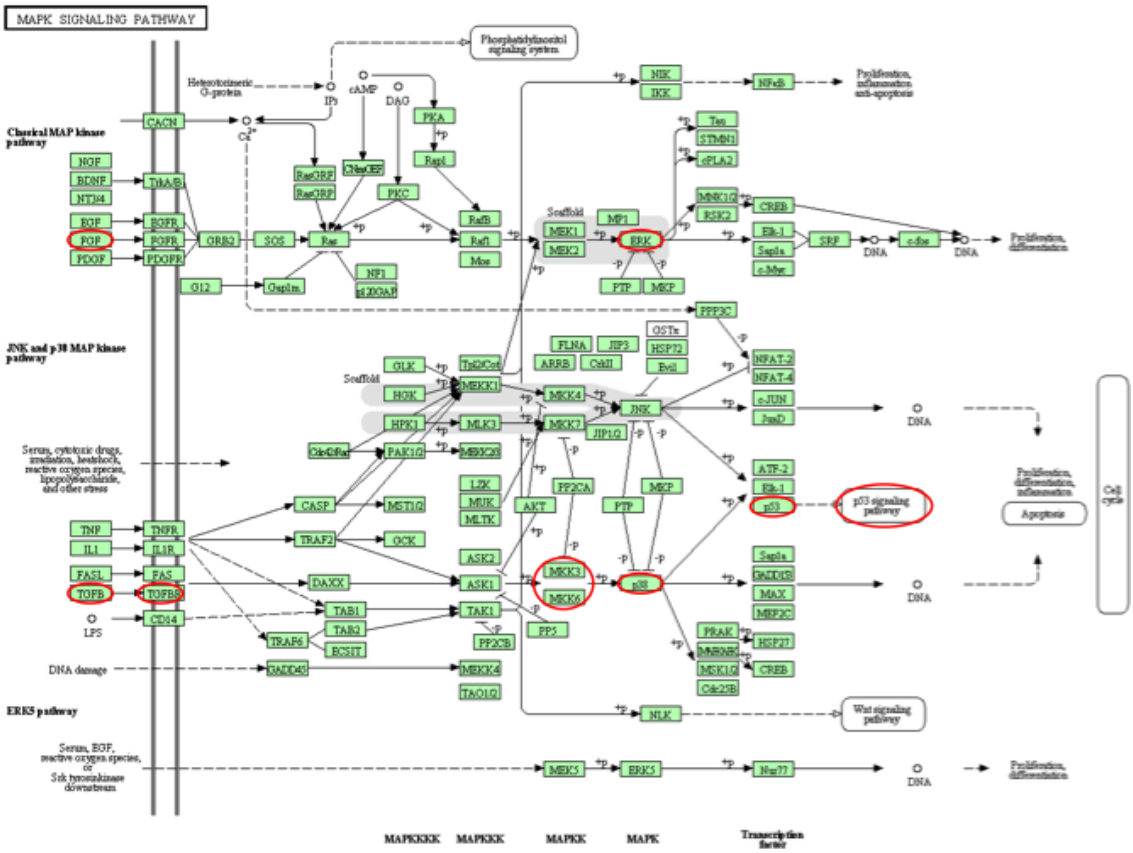


Figure 48. Voies de signalisation MAPK chez l'homme (Kanehisa & Goto 2000; Kanehisa et al. 2012). Schéma de synthèse obtenu à partir de Kyoto Encyclopedia of Genes and Genomes (KEGG, http://www.genome.jp/kegg/). Les éléments impliqués dans la régulation de l'endothélium humain sont entourés en rouge.

La prise en compte des facteurs environnementaux aide partiellement à expliquer l'absence de prolifération cliniquement significative de l'endothélium cornéen humain. Ces travaux font partie des nombreux mécanismes moléculaires qui ont des impacts directs sur la capacité d'auto-renouvellement ou d'auto-réparation de l'endothélium.

3. Sénescence

Les mécanismes de bloquage à la phase G1 liés aux Ckis expliquent partiellement l'absence de la division des CE humaines. Cette partie analyse le statut prolifératif de l'endothélium sous l'angle de la sénescence et sa capacité à progresser dans le cycle cellulaire.

3.1. Généralités sur la sénescence

La sénescence est l'état d'arrêt quasi irréversible du cycle cellulaire. Deux causes principales déterminent 2 types de sénescence : sénescence réplicative et sénescence prématurée.

3.1.1. Sénescence réplicative

La sénescence réplicative est la perte de capacité de division due à l'épuisement des télomères durant les précédents cycles de division.

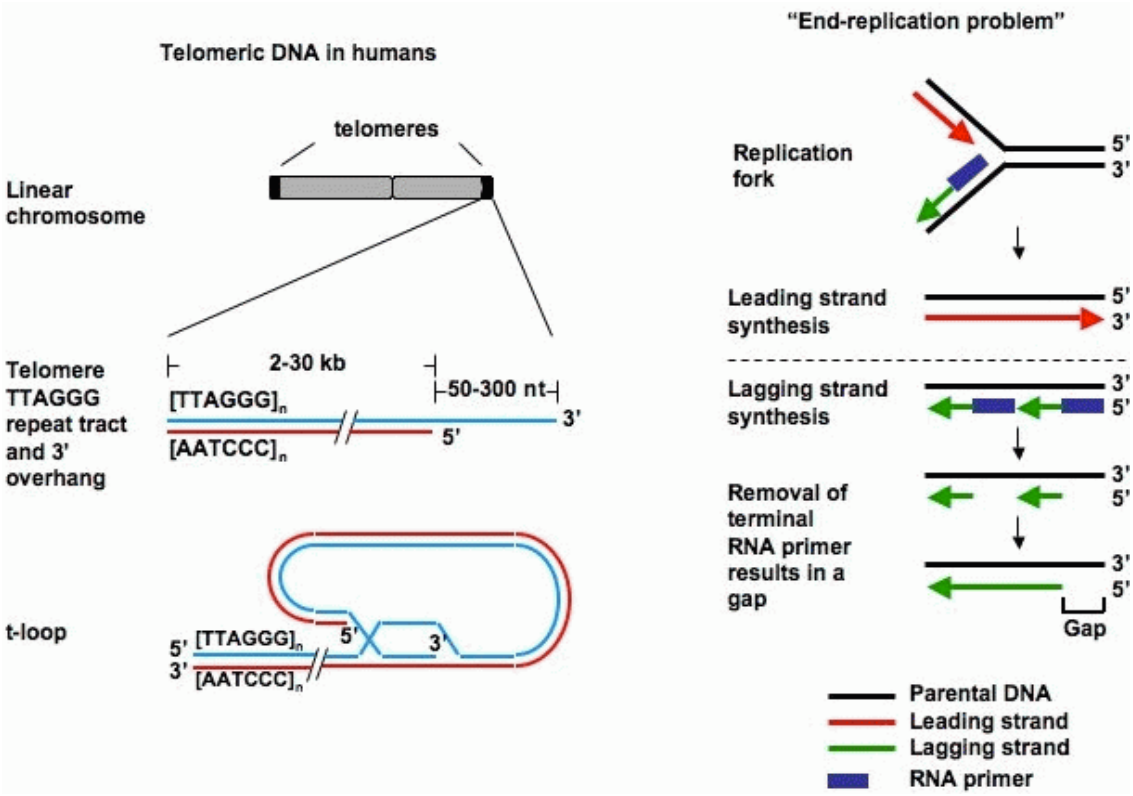


Figure 49. Structure de l'ADN télomérique humain (gauche) et raccourcissement de télomères en fin de réplication (droite) (d'après Réactome book)

Les télomères sont des complexes protéines-ADN situés à l'extrémité des chromosomes linéaires et qui ont pour rôle de maintenir la stabilité du génôme (Figure 49). Chez l'homme, le télomère se compose des séquences riches en guanine TTAGGG de 2 à 30 kb. La formation d'une structure en lassot (T loop) à l'extrémité 3' des simples brins d'ADN, empêche son extension en double brin.

L'ADN télomérique est fixé par plusieurs facteurs protéiques qui régulent la longueur des télomères et protègent le chromosome contre la recombinaison non

homologue, contre le déclenchement des signaux de dommage de l'ADN et contre l'attaque nucléolytique.

L'attrition de l'ADN au niveau des télomères a lieu à la fin de la réplication de l'ADN ou quand la réplication est incomplète. Le raccourcissement des télomères à un stade critique déclenche un mécanisme de synthèse et de maintenance des répétitions télomériques par la télomérase (Figure 50). Cette enzyme est un complexe ribonucléoprotéique contenant un domaine transcriptase réverse, appelé télomerase réverse transcriptase (TERT) et un ARN modèle pour la génération des séquences 3' riche en G.

En absence de l'action de la télomérase, un « signal de détresse » est envoyé et la cellule sort du cycle cellulaire, correspondant à la sénescence réplicative.

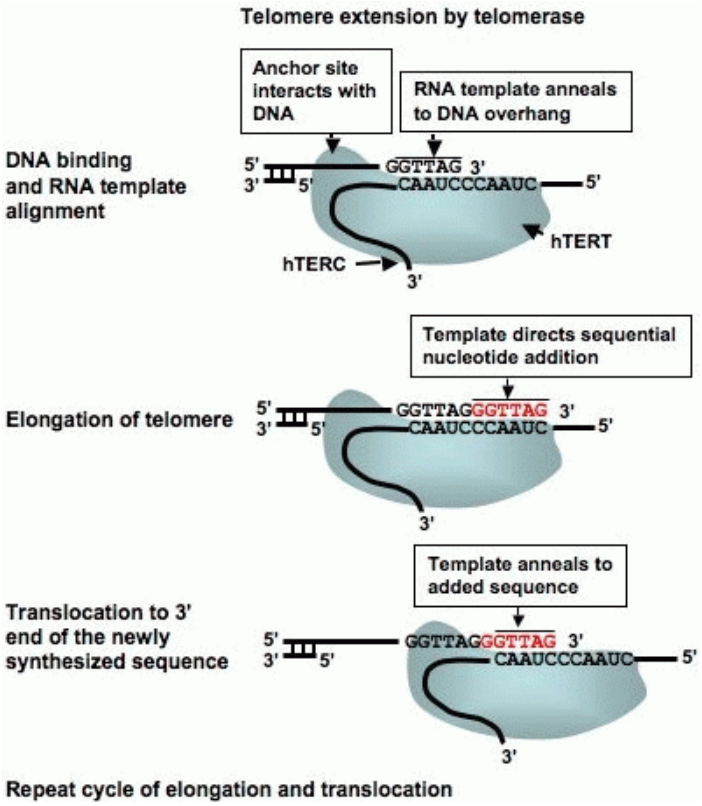


Figure 50. Extension du télomère par la télomérase (d'après Réactome book)

3.1.2. Sénescence prématurée

Ce type de sénescence est appelé "prématurée" ou "accélérée" car la cellule perd la capacité de proliférer avant le raccourcissement des télomères (Joyce 2012). Elle est

souvent induite par le stress oxydatif provenant de multiples facteurs environnementaux.

La notion de stress oxydatif implique des dérivés réactifs de l'oxygène (ou espèces radicalaires de l'oxygène (ERO), reactive oxygen species, ROS, en anglais). Il s'agit des dérivés de l'O_2 apparaissant sous l'effet d'agents physiques comme les rayonnements, des réactions chimiques et surtout enzymatiques.

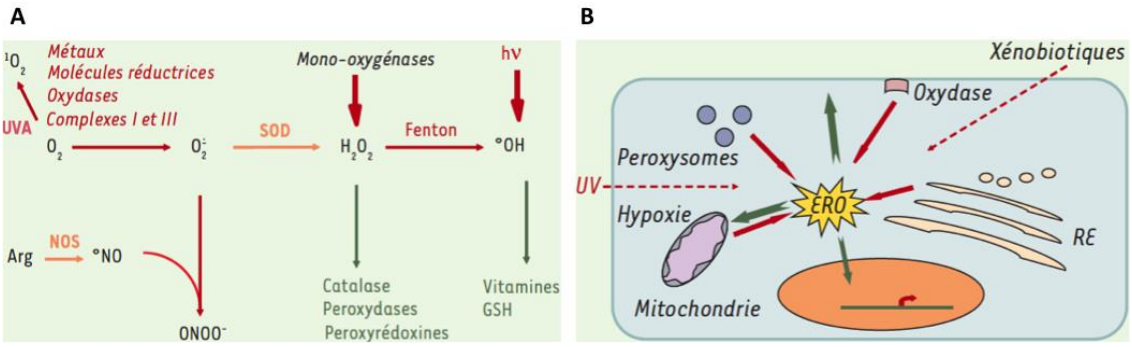


Figure 51. Voie métabolique de l'oxygène et des espèces radicalaires de l'oxygène (ERO)(A) et origines (B, flèches rouges) et actions (B, flèches verts) des ERO sur différents compartiments cellulaires (Barouki 2006)

Origine : toute réaction impliquant l'O_2 et un système réducteur de transfert d'électrons est susceptible de libérer des ERO, notamment la chaîne respiratoire, les activités enzymatiques comme NADPH oxydases au cours de l'inflammation et les cytochromes P450 au cours de la détoxication des xénobiotiques (Figure 51). Ainsi, dans une cellule, la mitochondrie, la membrane plasmique et le réticulum endoplasmique sont les sièges principaux de libération d'ERO.

Fonctionalité : en participant aux réactions d'oxydo-réduction qui induisent des cascades de signalisation, les ERO jouent un rôle physiologique important dans l'inflammation et l'équilibre entre la croissance, l'apoptose et la sénescence. D'autre part, la réactivité particulière des ERO peut mener à des propriétés toxiques importantes sur toutes les macromolécules cellulaires. Notamment, la génotoxicité des ERO consiste en l'oxydation des bases nucléiques, conduisant à la formation de 8-oxo-guanine qui est à l'origine des mutations géniques. L'ADN mitochondrial qui se situe à proximité de la chaîne respiratoire et n'est pas organisé en chromatine est donc particulièrement exposé à l'oxydation. Les ERO sont impliqués dans la maturation des protéines, surtout au niveau des acides aminés cystéines, méthionine et tyrosine, mais

peuvent aussi provoquer la carbonylation ou la dénaturation des protéines. Avec les acides gras insaturés, les ERO peuvent former de l'hydroperoxyde.

Le stress oxydant est défini comme le déséquilibre entre les systèmes oxydants et les capacités anti-oxydantes d'un organisme, d'une cellule ou d'un compartiment cellulaire (Figure 52).

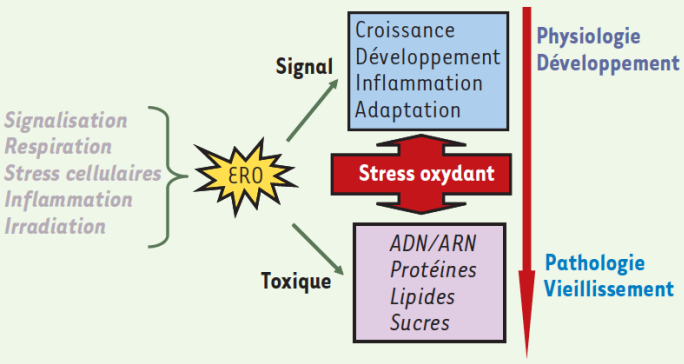


Figure 52. Réponse adaptative cellulaire par stress oxydant lié au déséquilibre entre les effets physiologiqes et délétères des espèces radicalaires de l'oxygène (Barouki 2006)

En effet, sous l'effet oxydant des ERO, les cellules sont capables de déclencher les mécanismes anti-oxydants. Tout d'abord, les ERO peuvent être neutralisés par les molécules de défense anti-oxydantes comme le Glutathion, les vitamines E et C, bilirubine, l'acide lipoïque, des enzymes comme la catalase, la superoxyde dismutase, la glutathion peroxydase, les peroxyrédoxines, etc. Si l'accumulation des ERO persiste, les cellules s'adaptent par l'induction des gènes codant des enzymes anti-oxydantes, des protéines chaperonnes, des enzymes impliqués dans la réparation de l'ADN etc., ou/et la répression des systèmes susceptibles de libérer des ERO (chaîne respiratoire, cytochromes P450, NADPH oxydase). Au stade ultime, les cellules peuvent être dirigées vers l'apoptose ou l'arrêt du cycle cellulaire **déclenchant ainsi la sénescence prématurée**.

D'autre part, le niveau de stress oxydant augmente avec l'âge. Cela est du à l'accumulation de stress chronique et l'échec des mécanismes de réparation et de maintien, induisant un taux croissant de cellules sénescentes (Thorin-Trescases *et al.* 2010).

3.1.3. Mécanismes d'arrêt du cycle cellulaire dans la sénescence

Au cours de la sénescence réplicative, l'érosion progressive des télomères jusqu'à un seuil critique où les télomères deviennent dysfonctionnels, active des protéines telles qu'ATM qui induit la phosphorylation de H2AX, un marqueur d'endommagement de l'ADN (Figure 53). De nombreuses protéines sont alors activées pour propager ce signal de dommage, dont p53 qui active p21, empêche la phosphorylation de Rb et bloque ainsi la prolifération cellulaire.

Au cours de la sénescence prématurée, l'activation de p38 MAPK induit aussi l'activation de la voie p53-pRb. L'inhibition du cycle cellulaire par p53 et p21 est suggérée comme transitoire, induisant la sur-expression de p16 qui maintien l'arrêt de croissance des cellules (Thorin-Trescases *et al.* 2010).

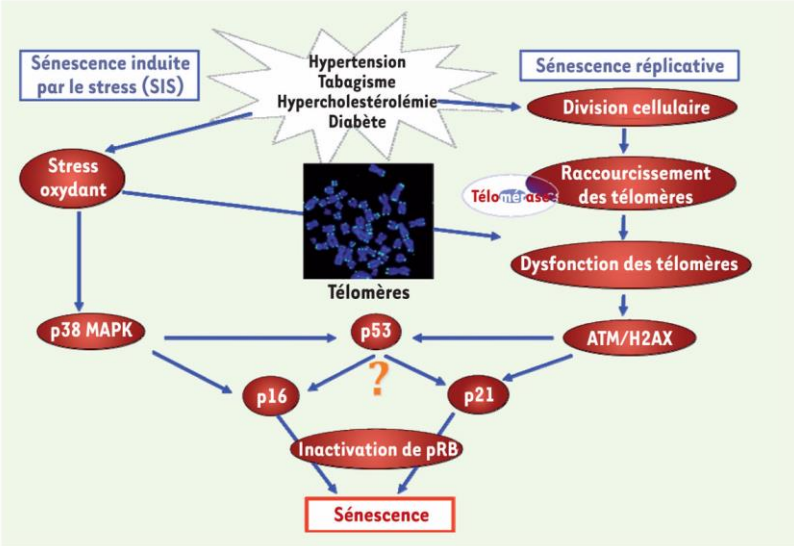


Figure 53. Activation des cascades de signalisation de la sénescence par différents stimulus (Thorin-Trescases et al. 2010), MAPK : mitogen activated protein kinase ; ATM : ataxia telangiectasia muté ; H2AX : histone de type H2AX ; pRb : protéine rétinoblastome phosphorylée

3.1.4. Marqueur de la sénescence

Les cellules sénescentes sont caractérisées non seulement par l'absence de division cellulaire, mais aussi par leur morphologie et par des changements de structures biochimiques et moléculaires spécifiques (Schmitt 2007). En culture in vitro, une cellule sénescente a habituellement une morphologie aplatie, vacuolisée avec un contour irrégulier. Concernant les changements biochimiques et moléculaires, la sénescence est marquée par une augmentation de l'activité SA-β-galactosidase (SA-β-

Gal), une sur-expression des inhibiteurs comme p21, p53, p16, PML (promyelocytic leukemia protein), p15, l'expression de γH2AX (marqueur de dommage à l'ADN). Au niveau de la chromatine, il s'agit de la formation de SAHFs (senescence associated heterochromatin foci), de la méthylation locale de la lysine 9 de l'histone H3 et du recrutement local de la protéine HP1.

En cas de sénescence prématurée, la présence du stress oxydatif peut être détecté par différents marqueurs de l'oxydation par les ERO, notamment les dialdéhydes, la 8-oxo-guanine (8-oxodG) appelé également 8- hydroxy-2'-deoxyguanosine (8-OHdG), les AGE (advanced glycation endproducts), la carbonylation des protéines, ou par l'induction des enzymes anti-oxydantes (Barouki 2006; Valavanidis *et al.* 2009).

Récemment, le laboratoire BiiGC a initié un travail avec le Service de Biologie Intégrative et de Génétique Moléculaire de l'Institut de biologie et de technologies de Saclay (iBiTec-S, CEA) portant sur un nouveau marqueur de sénescence. Il s'agit d'un anticorps dirigé contre le variant H2AJ des histones H2A, un variant très peu étudié mais pour lequel il existe une accumulation (justifié par la spectrométrie de masse, par le Western-blot et par l'immunomarquage) dans les cas de sénescence cellulaire avec dommage persistants à l'ADN (Figure 56).

En résumé, le rappel des mécanismes fondamentaux de la sénescence aide à caractériser l'état prolifératif de l'endothélium cornéen, et également à choisir les outils pour l'étudier.

3.2. Etat de sénescence de l'endothélium cornéen

Bloqué en phase G1, l'endothélium cornéen exprime des caractéristiques typiques des cellules sénescentes comme un arrêt stable du cycle cellulaire, l'augmentation de l'expression protéique de p53 de p21 et de p16 (Joyce 2012).

Par marquage de l'activité SA-β-Gal à pH 6.0, la sénescence des CE révèle une forte dépendence à l'âge et à la localisation centrale ou périphérique (Figure 54). Chez les donneurs jeunes, il n'y a pas ou peu de marquage à SA-β-Gal au centre et à la périphérie. Par contre, l'endothélium des donneurs âgés montre un marquage intense au centre et intermédiaire à la périphérie.

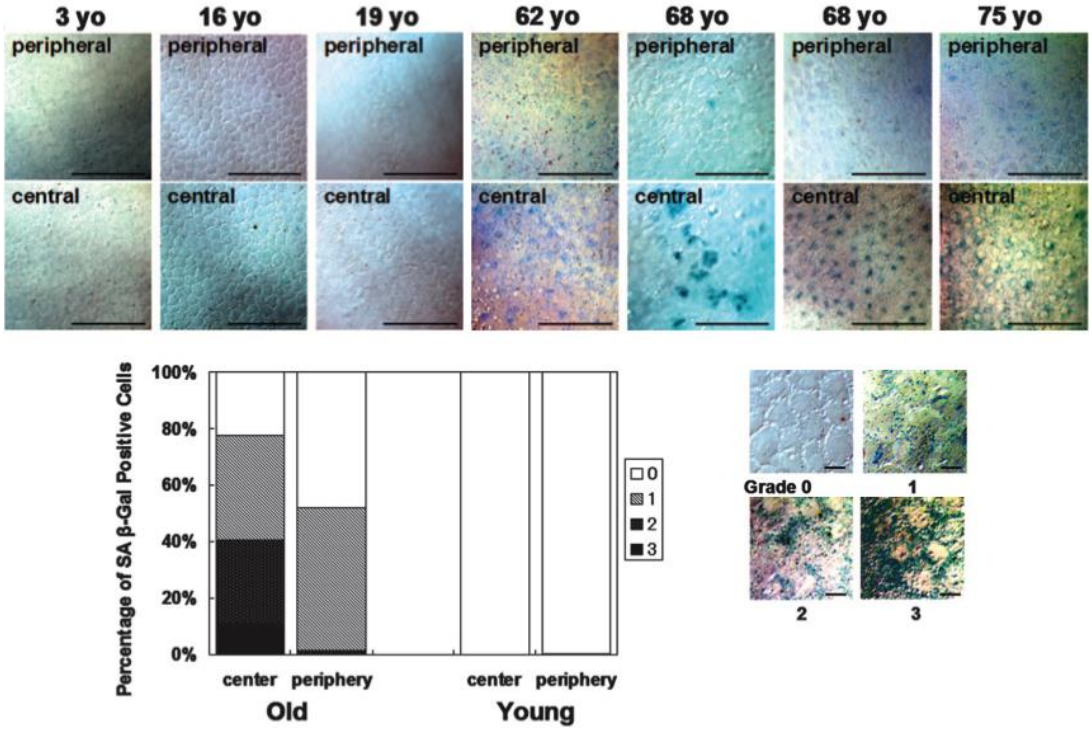


Figure 54. Evaluation semi-quantitative de la sénescence par marquage à SA-β-Gal sur cornée ex vivo des donneurs de 3 à 75 ans (yo, years old) (Mimura & Joyce 2006). Le degrée de marquage est scoré en absent (O), faible (1), intermédiaire (2) et intense (3).

Plusieurs études ont été menées pour trouver l'origine de la sénescence des CEs.

3.2.1. Hypothèse 1 : sénescence réplicative peu probable

L'hypothèse de la sénescence réplicative a été évaluée par mesure de la longueur de télomère de l'endothélium cornéen humain. Le résultat montre une longueur de 11 à 12.5 kb indépendant l'âge (donneurs de 5 semaines à 84 ans) et de la localisation centre versus périphérie (Mimura *et al.* 2013). Les CE humaines disposent donc de séquence de télomères suffisamment longues pour la division cellulaire. L'hypothèse de la sénescence réplicative de l'endothélium cornéen est par conséquent peu probable.

3.2.2. Hypothèse 2 : Sénescence prématurée prouvée

L'hypothèse de la sénescence prématurée a été directement évaluée par immunomarquage et dosage (ELISA) de 8-OHdG, un des ERO libérés à l'issu de l'endommagement de l'ADN, utilisé comme marqueur du stress oxydant (Joyce 2012; Mimura *et al.* 2013).

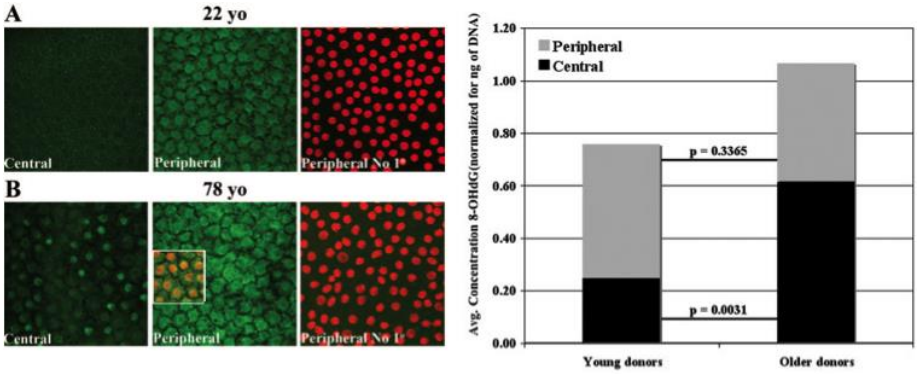


Figure 55. Evaluation du stress oxydatif de l'endothélium cornéen humain par immunomarquage de 8-OHdG (gauche) et quantification par ELISA (droite) à partir des donneurs jeunes (<30 ans) et âgés (>50 ans) (Joyce et al. 2009)

Le marquage positif pour le 8-OHdG confirme la présence du stress oxydatif qui entraine l'endommagement de l'ADN et l'état de sénescence prématurée des CE humaine (Figure 55). Sa distribution se trouve à 2 niveaux, mitochondrial et nucléaire. L'endommagement de l'ADN mitochondrial est indépendant de l'âge et se localise principalement à la périphérie. Par contre, l'effet sur l'ADN nucléaire est plus intense au centre qu'à la périphérie, et plus intense chez les donneurs âgés que chez les donneurs jeunes.

D'autre part, la sénescence prématurée est confirmée par la présence des mécanismes de réparation de l'ADN. La formation de sites focaux de réparation de l'ADN a été détectée dans le noyau de CE de donneurs âgés par immunomarquage de Histone phosphorylé H2AX-Ser139 (Joyce 2012) et récemment de H2AJ (Figure 56) au centre et à la périphérie de l'endothélium cornéen (EA2521 BiiGC, Université Jean Monnet, Saint Etienne). Cependant cela ne suffit pas pour limiter le stress oxydatif et la baisse de la capacité proliférative des CE avec l'âge (Joyce 2012), puisque les CE humaines exposées au stress oxydatif par traitement à H_2O_2 présente également une baisse de la prolifération.

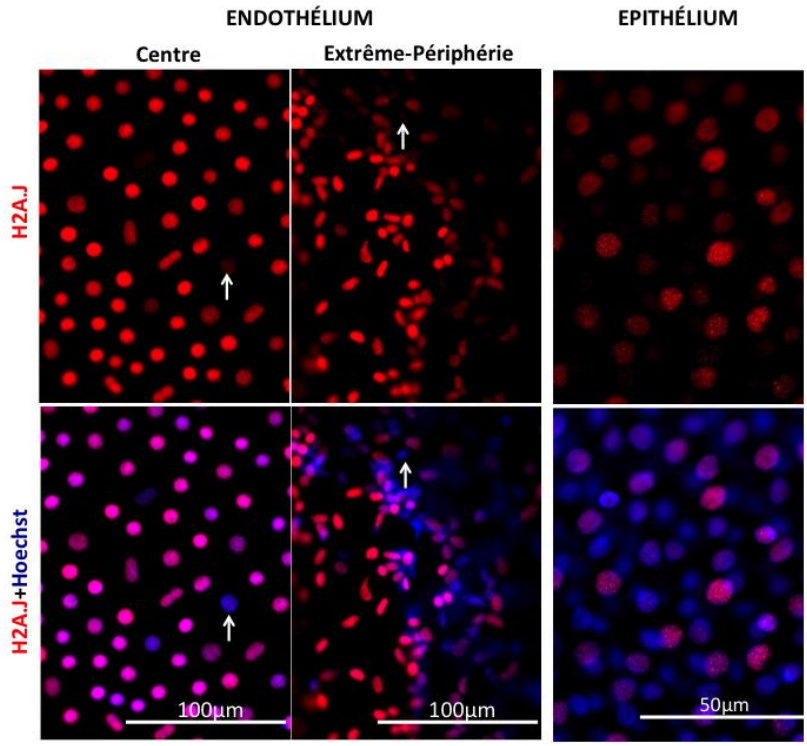


Figure 56. Expression de H2AJ (rouge) par l'endothélium et l'épithélium sur une cornée humaine postmortem par immunomarquage. L'endothélium contient des cellules marquées et non marquées à H2AJ (flèche blanche). Contre-coloration du noyau par Hoechst 33342 (bleu) (EA2521 BiiGC, Université Jean Monnet, Saint Etienne).

4. Capacité proliférative résiduelle

Malgré ce blocage du cycle cellulaire, certaines études ont démontré l'existence de mécanismes de régénération (lente et cliniquement peu efficace) de l'endothélium. Cette partie aide à synthétiser ces résultats, évaluer leurs impacts sur l'homéostasie de l'endothélium et sur les possibilités de les exploiter dans un but thérapeutique.

4.1. Effet de l'âge et de la localisation centrale ou périphérique

A partir de l'étude des différents mécanismes de régulation du cycle cellulaire cités ci-dessus, il a été démontré que la capacité proliférative des CE ex vivo après lésion mécanique était **meilleure chez les donneurs jeunes et à la périphérie de la cornée**.

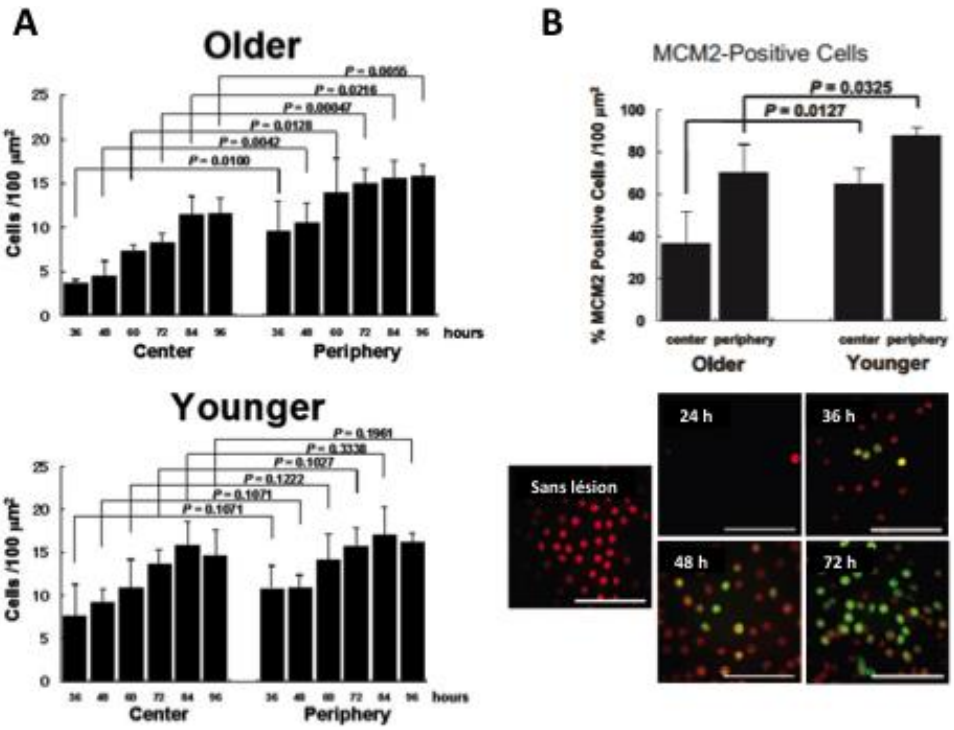


Figure 57. Différence de densité cellulaire (A) et évaluation de la compétence réplicative par immunomarquage à MCM2 (vert) après lésion (24h, 36h, 48h et 72h) de l'endothélium sur cornée ex vivo (Joyce et al. 2009). Contre coloration du noyau par propidium iodure (rouge).

A l'état physiologique, la DCE est plus élevée chez les sujets jeunes, et à la périphérie cornéenne (Mimura *et al.* 2013). En cas de lésion mécanique expérimentale ex vivo, les CE périphériques ont une meilleure compétence réplicative par rapport au centre, et meilleure chez les donneurs jeunes que chez les donneurs âgés. Dans ce travail, la compétence réplicative a été évaluée par immunomarquage de minichromosome maintenance-2 (MCM2) qui constitue le complexe reconnaissant l'origine de la réplication indispensable à la phase S (Figure 57) (Joyce *et al.* 2012).

In vitro, les CE mises en culture à partir des donneurs jeunes prolifèrent plus que celles établies à partir de donneurs âgés avec des temps de doublement respectivement de 46,25 heures versus 90,25 heures (Joyce *et al.* 2012).

Ces observations suggèrent l'existence de **progéniteurs à la périphérie** de la cornée humaine, non sénescents et gardant une certaine capacité de division. Une des hypothèses actuelles est que la perte de CE au centre conduit à des réarrangements de l'ensemble de la mosaïque endothéliale comportant des mouvements centripètes lents à partir de CEs périphériques plus nombreuses et moins différenciées. Ce mouvement reproduit, à une vitesse infiniment plus lente, le processus de développement

embryonnaire de la cornée par migration centripète des cellules mésenchymateuses originaires de la CN et qui se différencient en CEs matures (Mimura *et al.* 2013).

L'expression de marqueurs de pluripotence comme la télomérase, nestin et ABCG2, ont en effet été détectées par immunomarquage à la périphérie de lendothélium mais pas au centre (Whikehart *et al.* 2005; He *et al.* 2012). Une étude récente a également détecté l'expression de LGR5, un marqueur de cellules progénitrices, dans les CE périphériques chez l'homme et suggéré son rôle dans le maintien du caractère endothélial en inhibant la voie Wnt/β-caténine (Hirata-Tominaga *et al.* 2013).

D'autre part, l'existence des progéniteurs de CE a été démontrée chez l'homme par une équipe japonaise en utilisant la technique de la culture en sphère en milieu semi-solide (Yokoo *et al.* 2005; Yamagami *et al.* 2007) (Figure 58). Dans ces conditions de culture très particulières en 3D sans laisser la possibilité aux cellules d'adhérer à un support, seules les cellules ayant un caractère prolifératif survivent et forment des microsphères grossissant au fil des divisions cellulaires successives. La prolifération des CE dans les microsphères a été confirmée par incorporation de BrdU. Les CE sont capables de générer des sphères à partir de cellules isolées, mais cette capacité diminue avec les repiquages successifs. Par rapport au centre, les sphères sont 4 fois plus nombreuses à partir de CE isolées en périphérie de l'endothélium (Yokoo *et al.* 2005; Yamagami *et al.* 2007).

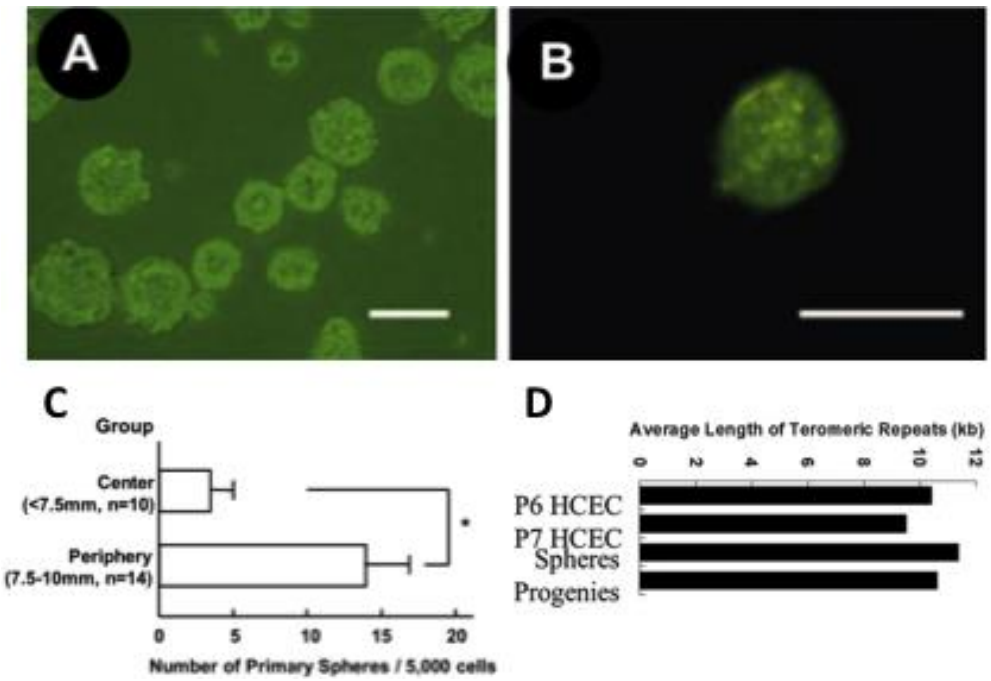


Figure 58. Culture en sphère de cellules endothéliales (CE) humaines (Mimura et al. 2013). Formation de sphère après 10 jours de culture (A). Marquage de la division cellulaire par incorporation de BrdU (B). La formation de sphère est environ 4 fois plus importante pour les CE périphériques que pour les CE centrales (C). L'isolement en sphère permet d'isoler les cellules "jeunes" ayant les télomères les plus longs par rapport aux cultures adhérentes au 6ème et 7ème passage (D).

Concernant le profil d'expression protéique, les sphères dérivés de CE expriment la Nestin (marqueur de cellule immature), αSMA (marqueur de myofibroblaste mésenchymateux), β3-tubulin (marqueur de cellule neurale immature), et GFAP (marqueur de cellule astrogliale) (Mimura *et al.* 2013).

La capacité proliférative des sphères a été également évaluée via la longueur des télomères. Les séquences des télomères des CE en sphère (11,4 kb) sont plus longues que des ceux provenant de cultures adhérentes conventionnelles au 7ème passage (9,5 kb). D'autre part, l'activité télomérase des sphères est plus forte que celle de la culture adhérente à P7 (Mimura *et al.* 2013).

Ces résultats sont les premières descriptions de progéniteurs endothéliaux à la périphérie de la cornée humaine. Cette présence semble cohérente avec l'expérience clinique des cas de greffes de cornées réalisées chez des receveurs ayant une DCE élevée en périphérie et donc probablement des progéniteurs sains (kératocône, dystrophie stromales à endothélium normal) et qui ont une excellente survie à long terme par rapport aux receveurs sans aucune réserve endothéliale périphérique.

4.2. Zone péricornéenne

En plus de la périphérie endothéliale, les progéniteurs de CE pourraient être localisés dans différentes régions anatomiques de la périphérie cornéenne : la zone de transition, le trabéculum et au niveau de l'endothélium trabéculaire à proximité du canal de Schlemm (McGowan *et al.* 2007; Yu *et al.* 2011). Cette région complexe sur le plan embryologique et anatomique pourrait ainsi abriter la niche de la CS endothéliale, si elle existe.

Provenant de la CN, l'endothélium cornéen est obtenu après la migration des cellules multipotentes de la zone périoculaire vers le centre durant l'embryogénèse. A l'âge adulte, la zone de transition exprime certains marqueurs de progéniteur comme télomérase, nestin, alkaline phosphatase ou la prolifération cellulaire détectée par l'incorporation de BrdU (Whikehart *et al.* 2005; McGowan *et al.* 2007). En cas de lésion, l'activation des expressions de marqueurs de cellules souche (Oct3/4, Wnt1) ou de différenciation (Pax6, Sox2) a été également observée dans la zone de transition et au niveau du trabéculum en contact avec le canal de Schlemm.

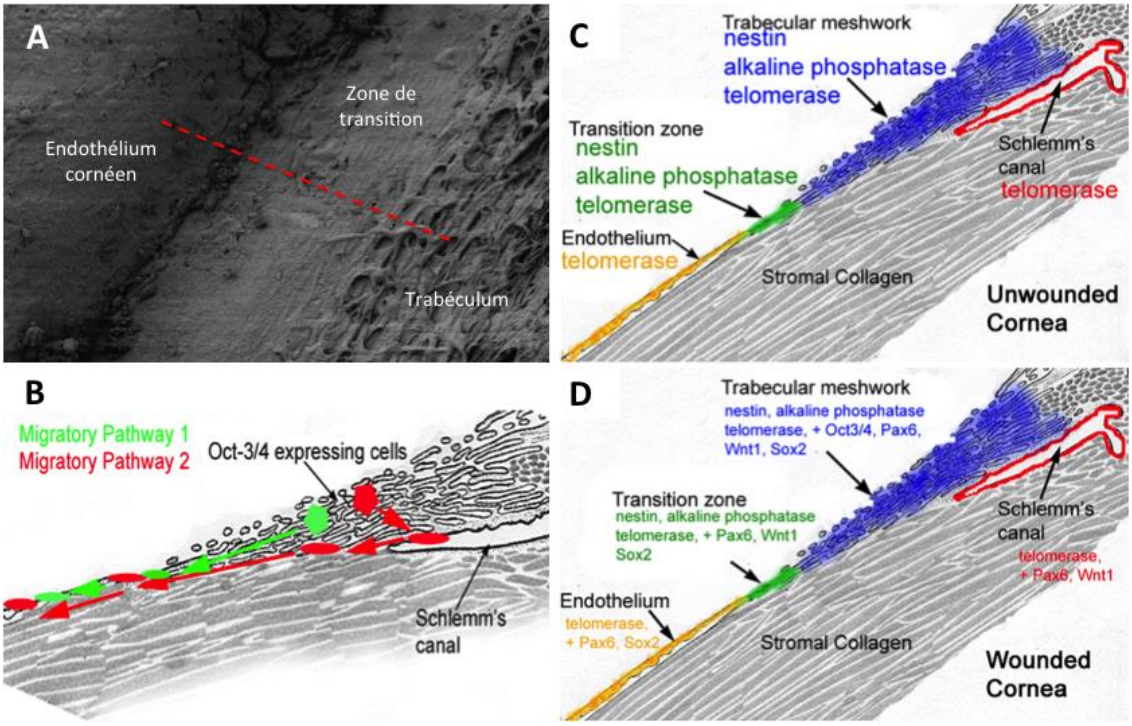


Figure 59. Schémas synthétiques de l'expression des marqueurs de progéniteurs dans la zone péricornéenne. Morphologie de la zone péricornéenne observée par MEB de la surface postérieure (A) (Yu et al. 2011) et illustration sur coupe transversale (B, C, D) (McGowan et al. 2007). Deux voies de migration (B) sont proposées basant sur l'expression des marqueurs en cas normal (C) et en cas de lésion (D).

A partir de ces observations, McGowan et al. supposent 2 voies de migrations possibles de cellules progénitrices exprimant Oct3/4 pour régénérer l'endothélium cornéen, soit par migration directe à partir du trabéculum à travers la zone de transition, soit à travers les CE trabéculaires, puis la zone de transition avant d'atteindre l'endothélium (Figure 59).

La migration centripète des CEs de l'extrême périphérique est récapitulée dans le schéma suivant :

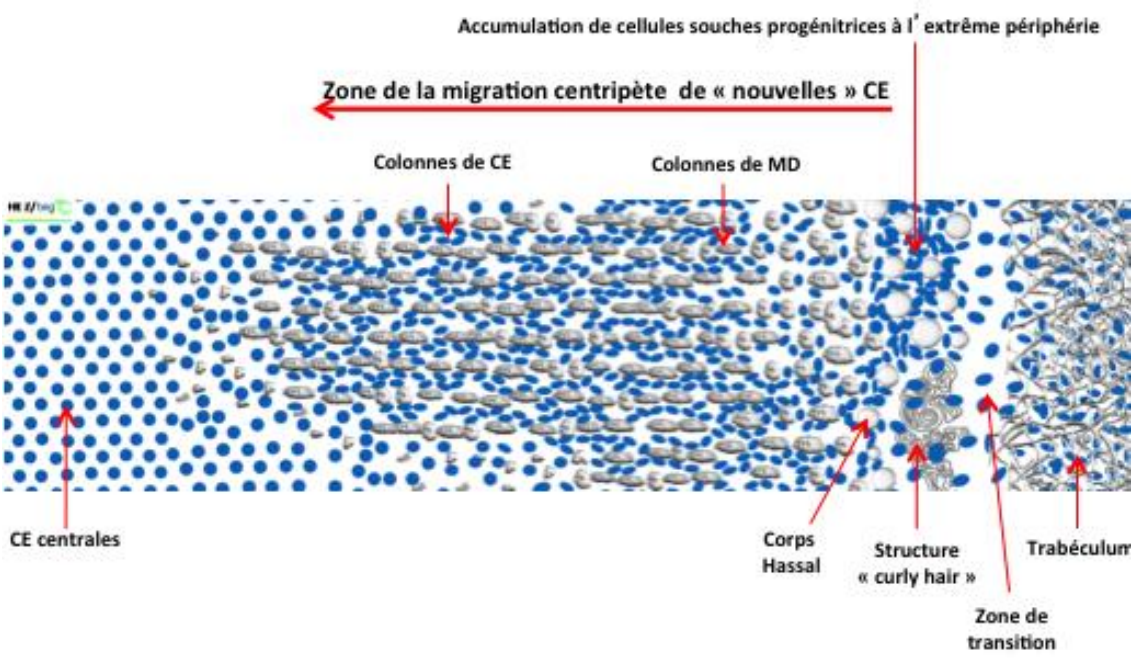


Figure 60. Modèle de migration centripète de cellules endothéliales de l'extrême périphérie vers le centre de la cornée (EA2521 BiiGC, Université Jean Monnet, Saint Etienne).

Pour conclure, ces travaux démontrent que, même à l'âge adulte, certaines CE conservent une capacité proliférative, très probablement à l'extrême périphérie de l'endothélium et dans la zone de transition. Ces cellules pourraient être les meilleures candidates pour les applications de bioingénierie où des étapes de sélection et d'expansion cellulaire sont indispensables pour obtenir une très grande quantité de cellules CEs-like.

CHAPITRE III - Cultures de l'endothélium cornéen

Afin de surmonter les déficiences de l'endothélium dont les mécanismes de réparation naturels ne sont pas suffisants, la bioingénierie endothéliale a pour but de produire in vitro des cellules capables d'assumer les mêmes fonctions de contrôle de l'hydratation stromale, avec un niveau de sécurité maximale (absence de prolifération incontrôlée, absence de migration hors de l'endothélium, absence de transformation et de potentielle oncogénèse). Deux stratégies thérapeutiques sont envisagées : 1/l'injection de CE dans la chambre antérieure des patients associés à des moyens garantissant leur adhérence à la face postérieure de la cornée ; 2/ le reconstruction d'un greffon lamellaire en recouvrant un fin support transparent par les CEs en culture puis en greffant ce greffons bioingénierié avec les techniques actuelles de greffe endothéliale. Ces 2 stratégies complémentaires nécessitent un procédé robuste de culture en masse de CEs capables de s'intégrer au tissu cornéen d'origine et d'y fonctionner normalement.

Focalisé sur l'expansion de CEs in vitro, ce chapitre synthétise les méthodes actuelles permettant d'obtenir une forte prolifération, de prolonger leur durée de vie tout en maintenant la complexité de leur fonctionalité. Il existe trois approches principales : 1/ expansion à partir de cultures primaires non modifiées, 2/ différenciation ou transidfférenciation de CS, 3/ thérapie génique sur cultures primaires. Les optimisations de chaque approche et leurs combinaisons seront détaillées.

1. Culture primaire

La mise en culture primaire consiste à isoler les CEs de la cornée et les maintenir dans un environnement adapté in vitro. Afin d'obtenir une meilleure qualité de culture cellulaire finale, cette technique nécessite non seulement l'optimisation de tout l'environnement des CEs, résumé sous les termes « conditions de culture », mais également des méthodes de choix et de recueil des CEs initiales.

1.1. Optimisation des conditions de culture

La mise en culture primaire consiste à isoler les cellules de leur environnement physiologique pour les maintenir sur un support, dans un milieu de culture et une

pression environnementale adaptée. L'objectif est de limiter des facteurs défavorables à la survie cellulaire et ajouter des facteurs de soutien.

1.1.1. Milieu de culture

In vitro, les CEs survivent au mieux dans un environnement semblable à l'HA. Peu concentrée en facteurs de croissance, l'HA contient néanmoins du FGF, EGF, NGF et PDGF-B qui ont démontré leurs effets bénéfiques sur la viabilité et la prolifération des CEs in vitro (Mimura *et al.* 2013). FGF-2 et TGF-β aident notamment à maintenir la morphologie endothéliale et favorise la migration en cas de lésion (voir Chapitre II - 2.2).

L'ajout d'autres composants de l'HA est également bénéfique :

- La **L-ascorbic acid 2-phosphate** (Asc-2P) favorise la prolifération de CE en limitant le stress oxydatif au niveau de l'ADN mitochondrial (Shima *et al.* 2011) via la récupération d'ERO et la régulation de la synthèse des protéines du cycle cellulaire (Mimura *et al.* 2013) (Figure 61). Les CEs mises en culture à partir des donneurs de 12 à 74 ans forment une monocouche et expriment les marqueurs protéiques des CEs comme ZO-1, Na^+/K^+ATPase, N-cadhérine et Connexin43. D'autre part, la combinaison de l'Asc-2P avec FGF-2 et le coating par atelocollagène optimise encore les conditions de culture et le maintien des CEs à long terme.

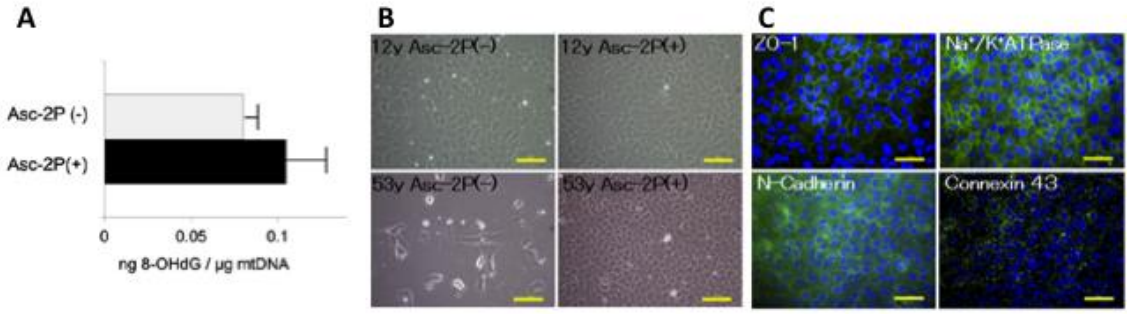


Figure 61. Effet de l'acide ascorbique 2-phosphate (Asc-2P) sur la culture in vitro de l'endothélium cornéen humain (Shima et al. 2011): réduction du stress oxydatif révélé par le marqueur 8-OHdG (A), augmentation de la viabilité, surtout pour les CEs des donneurs âgés (B), maintien de l'expression des protéines utilisées habituellement comme marqueurs de CEs (C).

- La **laminin soluble**, notamment la laminin-5 améliore les capacités de réparation de la mosaïque endothéliale in vitro (Mimura *et al.* 2013). Les CEs expriment des récepteurs à la laminin-5 comme l'intégrine α3β1. Cet effet bénéfique de la laminin-5 soluble

montre que les interactions ligand-récepteur sont impliquées dans l'adhésion, la migration et la prolifération des CEs.

Certains agents pharmacologiques peuvent avoir des effets bénéfiques

-L'équipe de S. Kinoshita et N. Koizumi (Tokyo, Japon) a très largement raporté que l'inhibiteur des Rho kinases (Rock-inhibitor) Y-27632 à 10µM favorisait l'adhésion, l'inhibition de l'apoptose et la prolifération des CEs de primate (Okumura *et al.* 2009). Malgré les nombreuses applications développées par cette équipe japonaise sur différents modèles in vivo, la seule voie de signalisation de Y-27632 identifiée jusque là est l'inhibition de la contraction de l'actine cytosquelettique qui retarde l'assemblage ou le désassemblage des jonctions serrées des CEs bovines in vitro (Srinivas 2010 IOVS) (Figure 63A). Ce résutlat a été confirmé sur le modèle ex vivo des CEs humaine par notre laboratoire (Figure 63B), ou seulement confirmé sur l'effet de ROCK inhibiteur à la migration cellulaire (Figure 62) (Pipparelli *et al.* 2013).

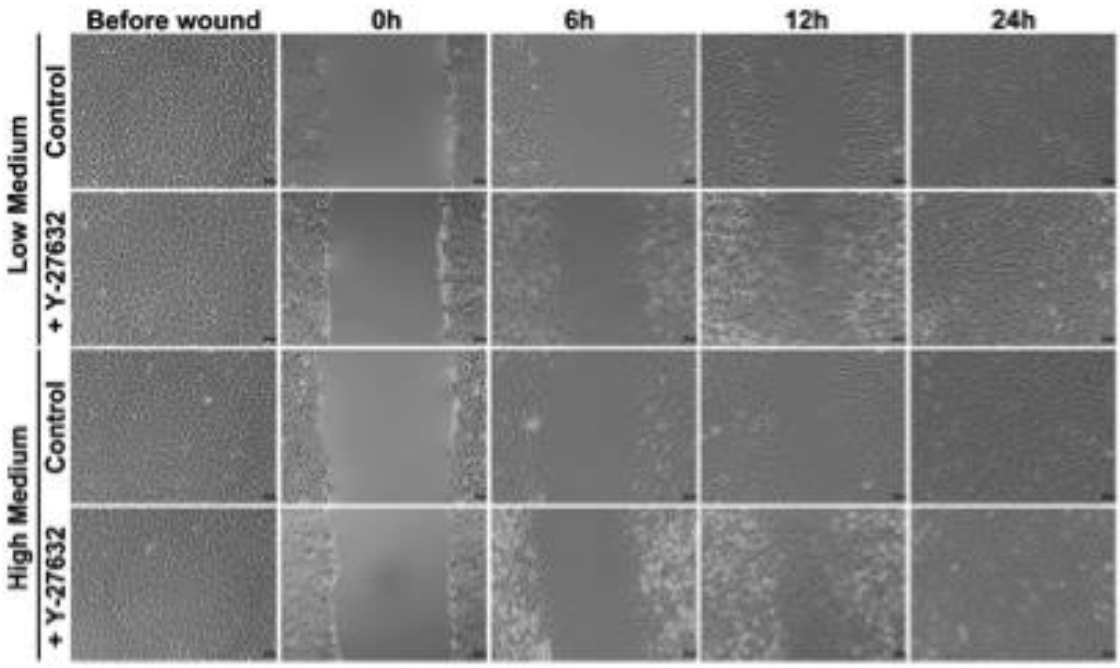


Figure 62. Effet de Y-27632 (10µM) sur la migration cellulaire en milieu OptiMEM-I conventionnel (High medium) ou en milieu OptiMEM-I 4%SVF (Pipparelli et al. 2013)

-D'autres molécules comme la rapamycine et la cystéamine améliore la viabilité in vitro en réduisant le taux d'ERO des CEs (Shin *et al.* 2011a; Shin *et al.* 2011b) via l'augmentation du taux de GSH.

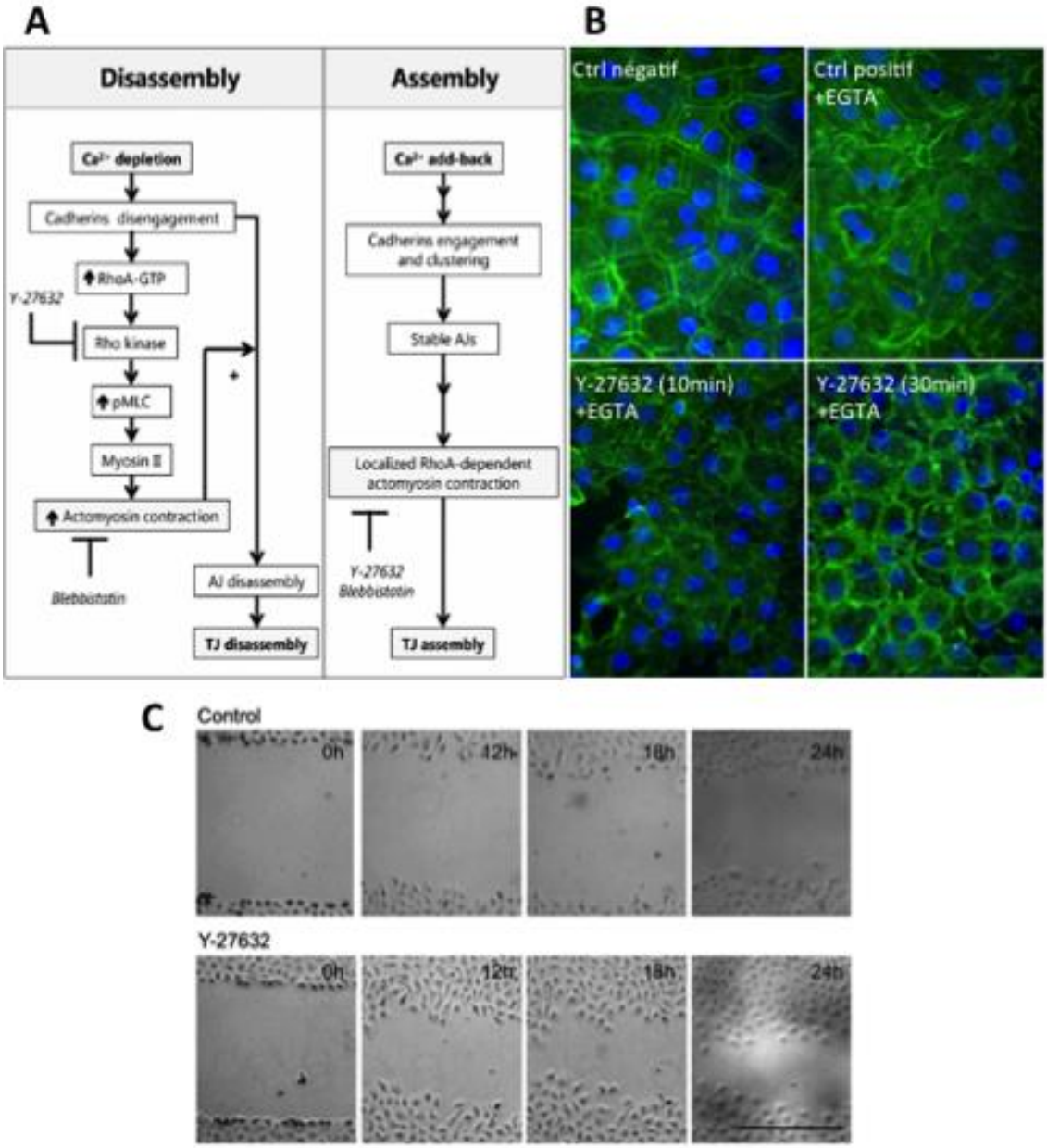


Figure 63. Effet du Rock-inhibitor Y-27632 sur l'endothélium cornéen in vitro et ex vivo. Y-27632 retarde la contraction de l'actine cytosquettique sur un modèle de CEs bovines in vitro (A) (Srinivas 2010) et de CEs humaines ex vivo (B, EA2521 BiiGC, Université Jean Monnet, Saint Etienne), mais favorise la migration et la survie des CEs de primate in vitro (C) (Okumura et al. 2011). Marquage de l'actine des CEs humaines par phalloidine (vert) et contre-coloration du noyau par Hoechst 33342 (bleu).

En combinant différents éléments additifs, certaines « recettes » ont été proposées pour favoriser la survie et la prolifération des CEs in vitro. Récemment, une comparaison de l'effet de ces compositions sur les CE humaines in vitro (Peh *et al.* 2011) a permis de sélectionner OptiMEM-I et F99 comme les deux meilleurs milieux pour limiter l'apoptose et favoriser la prolifération (Mimura *et al.* 2013) (Figure 64). Ces expériences sur les collerettes des **donneurs de 10 à 42 ans** ont permis d'obtenir

une DCE maximale de 952 cellules/mm^2. Ces milieux permettent aux CEs de garder une forte expression de ZO-1 et Na^+/K^+ATPase à court terme mais à partir du 3ème passage, la morphologie des CEs est alternée.

Author	Basal medium	Serum	Supplements	Journal (year)
Engelmann et al.	F99 Ham's F12 & M199 (1:1 ratio)	5%	20 mg/ml ascorbic acid 20 mg/ml bovine insulin 2.5 mg/ml transferrin 0.6 ng/ml sodium selenite 10 ng/ml bFGF	In Vitro Cell Dev Biol (1989) Cornea (1995)
Miyata et al. Mimura et al.	Low-glucose DMEM	15%	2.5 mg/L amphotericin B 2.5 mg/L doxycycline 2 ng/mL bFGF	Cornea (2001) Exp Eye Res (2004a) Invest Ophthalmol Vis Sci (2004b)
Zhu and Joyce	Opti-MEM-I	8%	20 ng/ml NGF 5 ng/ml EGF 20 µg/ml ascorbic acid 200 mg/L calcium chloride 100 µg/ml pituitary extract 50 µg/ml gentamicin 1 × antibiotic/antimycotic 0.08% chondroitin sulfate	Invest Ophthalmol Vis Sci (2004)
Ishino et al.	DMEM	10%	2 ng/ml bFGF 50 U/ml penicillin 50 mg/ml streptomycin	Invest Ophthalmol Vis Sci (2004)
Li et al.	SHEM Ham's F12 & DMEM (1:1 ratio)	5%	0.5% DMSO 2 ng/ml EGF 5 mg/ml insulin 5 mg/ml transferrin 5 ng/ml selenium 0.5 mg/ml hydrocortisone 1 nM cholera toxin 50 mg/ml gentamicin 1.25 mg/ml amphotericin B	Invest Ophthalmol Vis Sci (2007)

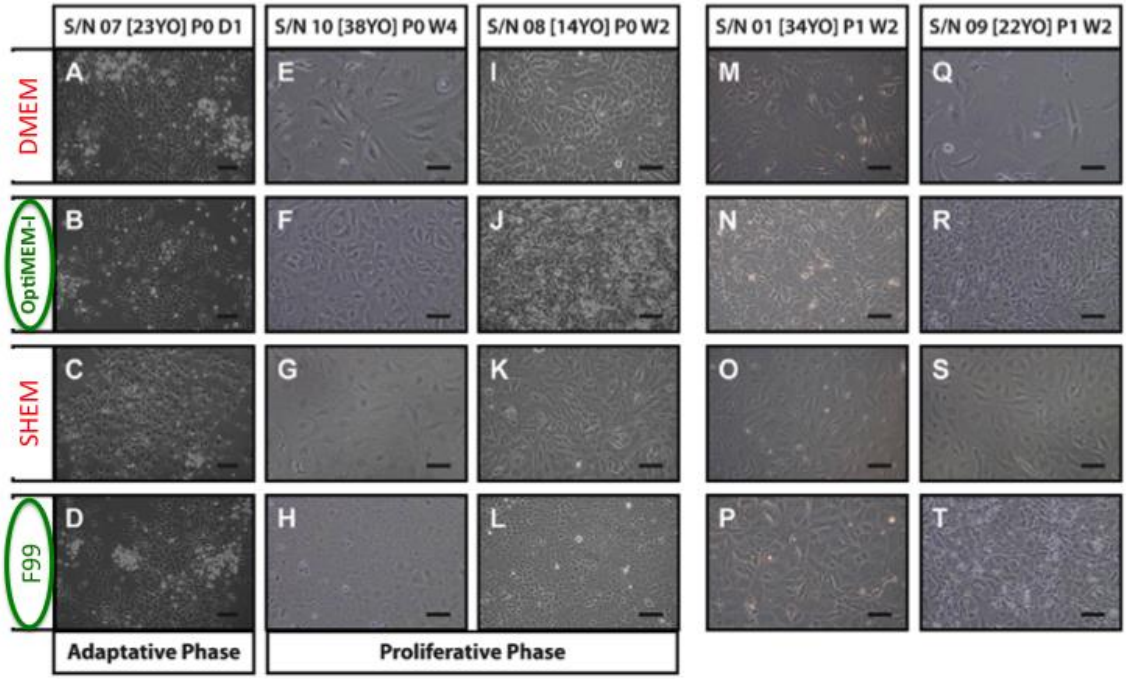


Figure 64. Synthèse des formules de milieu les plus courants (en haut) (Mimura et al. 2013) et comparaison de l'efficacité des milieux sur la culture in vitro de CEs humaines (en bas) (Peh et al. 2011). F99 et OptiMEM-I sont les meilleurs candidats pour limiter la mort cellulaire et favoriser la prolifération des CEs.

En prenant en compte ces inconvénients majeurs, un autre protocole récent propose deux phases de culture (Peh *et al.* 2013), une phase de prolifération dans du milieu F99 dès l'ensemmencement des CEs in vitro, et avant d'atteindre la confluence, une stabilisation de la morphologie endothéliale dans le milieu Human Endothelial-

SFM (Jackel *et al.* 2011) supplémenté de SVF à 5% (Figure 65). Ces expériences **sur les donneurs très jeunes, (19-35 ans), ont permis d'obtenir une DCE maximale de 2941 cellules/mm^2**. Le milieu de stabilisation permet de maintenir la morphologie endothéliale typique et l'expression des protéines « marqueurs » de fonction au delà du 3ème passage.

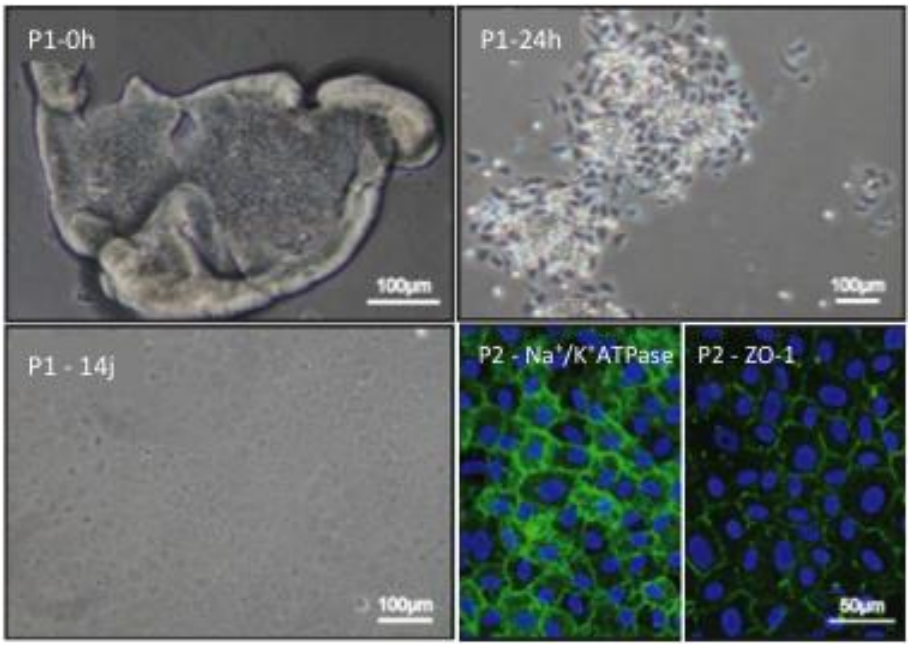


Figure 65. Mise en culture in vitro de CEs humaines selon le protocole en 2 phases prolifération-stabilisation (Peh et al. 2013). La culture de CEs à partir des donneurs de 19 à 35 ans exprime des marqueurs endothéliales (Na^+/K^+ATPase et ZO-1 en vert par immunomarquage) et atteint des DCE élevées, de 2591 à 2941 cellules/mm^2.

Le milieu de culture est l'élément principal pour préserver les CEs en culture in vitro, stimuler la division cellulaire ou/et la différenciation/dédifférenciation. Malgré l'effet bénéfique de certains éléments comme le sérum de veau foetal sur la survie cellulaire, ils peuvent également induire de façon prématurée la sénescence ou la différenciation des CEs vers d'autres types cellulaires. **Cette approche est détaillée dans la Partie expérimentale - Article 1.**

1.1.2. Coating

A côté du milieu de culture, le coating joue un rôle important dans la protection des cellules contre les stress de la mise en culture. L'ensemmencement des CEs sur un support leur permettant d'adhérer rapidement juste après leur isolation de la cornée augmente leur survie. Pour cela, les éléments de la matrice extracellulaire peuvent être utilisés pour revêtir la surface de culture ("coating" en anglais). Plusieurs molécules ont

démontré leurs effets bénéfiques sur l'adhésion des CEs comme les collagènes type I, et IV, la laminine et la fibronectine. Leur interactions avec les CEs humaines ont été récemment étudiées (Choi *et al.* 2013). La conclusion est que plusieurs composés favorisent l'adhésion in vitro des CEs et qu'ils peuvent avoir un effet synergique sur le maintien de la culture à long terme. Actuellement certaines formules de coating ont été proposés comme le mélange laminine + chondroïtine sulfate, le mélange fibronectine + collagene type I + albumine (FNC coating Mix®), ou même la matrice extracellulaire secrétée par les CEs bovines (Mimura *et al.* 2013) (Figure 66).

Author	Extracellular matrices	Journal (year)
Engelmann et al.	Laminin and chondroitin sulfate	Invest Ophthalmol Vis Sci (1988)
Miyata et al.	Extracellular matrix secreted	Cornea (2001)
Mimura et al.	by bovine corneal endothelial cells	Exp Eye Res (2004a)
		Invest Ophthalmol Vis Sci (2004b)
Joyce and Zhu	Fibronectin plus type I collagen (FNC Coating Mix®)	Cornea (2004)
Yamaguchi, Yamagami, et al.	Laminin-5	Invest Ophthalmol Vis Sci (2011)

Author	Species of cultured CEC	Cell carrier	Host animal	Transplantation technique	Journal (year)
Mimura	Human	Collagen	Rabbit	DSAEK	Invest Ophthalmol Vis Sci (2004)
Ishino	Human	Amniotic membrane	Rabbit	PKP	Invest Ophthalmol Vis Sci (2004)
Sumide	Human	PNIPAAm	Rabbit	PKP	FASEB J (2006)
Lai	Human	PNIPAAm and gelatin	Rabbit	DSAEK	Transplantation (2007)
Koizumi	Monkey	Collagen	Monkey	DSAEK	Invest Ophthalmol Vis Sci (2007)
Honda	Human	Thin human corneal stromal disc	Rabbit	DSAEK	Arch Ophthalmol (2009)

Figure 66. Tableau synthetique des formules de coating (gauche) ou des biomatériaux utilisés pour la fabrication des lamelles endothéliales (droite) (Mimura et al. 2013)

En plus de la composition biochimique du support de culture, sa structure de surface peut avoir un impact sur la qualité des cultures de CEs. Une étude récente a démontré que sa micro et nanostructuration peut favoriser l'adhérence, la diffusion, ainsi que la fonctionalité des CEs (Teo *et al.* 2012). En effet, parmi plusieurs géométries de surface à l'échelle micro et nanométrique, une surface revêtu de micro-plots d'1µm produit une meilleure morphologie des CEs. Ces structures ont été fabriquées par impression par microcontact (Figure 67). La surface de ces structures est revêtue en poly(methylmethacrylate) (PMMA), puis recouverte de laminin-1.

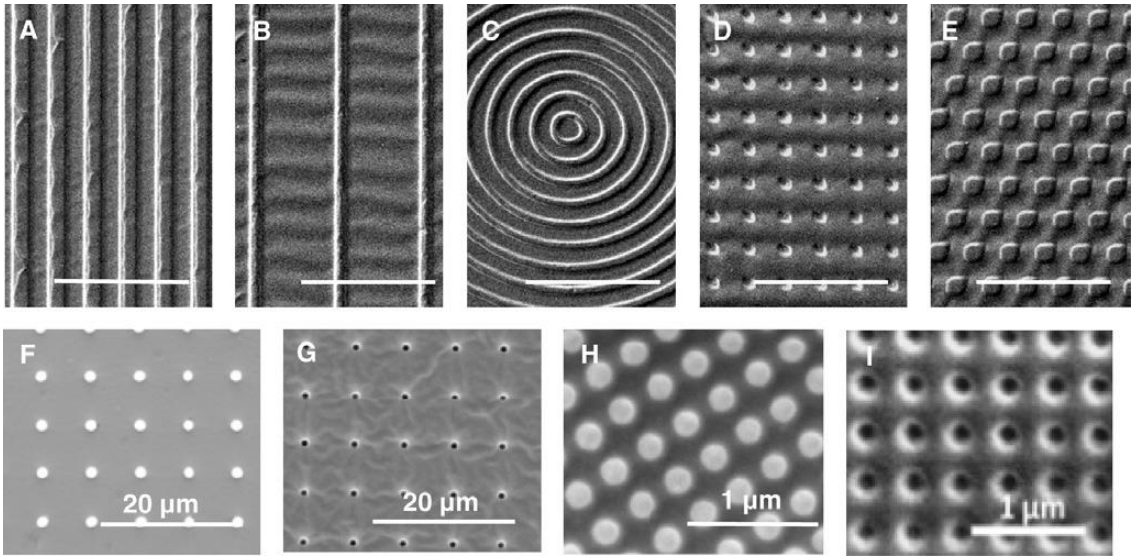


Figure 67. Traitement de surfaces de culture par nanotopographie (Teo et al. 2012). A: canaux, B: grilles, C: cercles concentriques, D: puits ronds, E: plots ronds, F: plots de 1µm de diamètre, G: puits de 1µm de diamètre, H: plots de 250nm de diamètre, I: puits de 250nm de diamètre.

Même s'il ne s'agit pas à proprement parlé de supports destinés à améliorer le rendement des cultures primaires, nous citons également les biomatériaux raportés jusqu'à présent pour la reconstruction in vitro de greffons endothéliaux puisqu'ils doivent par définition favoriser l'adhérence et le maintien de la différenciation des CEs ensemencées (Table 1). Il s'agit de lamelles en collagène type I compressé (collagène type I extrait de queues de rat), de feuilles de chitosan (protéine de la carapace des insectes) polycaprolactone, d'hydrogel de gélatine et enfin de lamelle de stroma cornéen décellularisée (Table 1).

Table 1. Synthèse des matériaux biocompatibles en cours d'étude pour la greffe lamellaire de l'endothélium (EA2521 BiiGC, Université Jean Monnet, Saint Etienne)

	Matériaux	Auteurs
Support synthétique	Collagène type I compressé	(Mimura *et al.* 2004; Levis *et al.* 2012)
	Disque de gélatine	(Hsiue *et al.* 2006; Lai *et al.* 2006; Watanabe *et al.* 2011; Lai *et al.* 2013)
	Chitosan et polycaprolactone	(Wang *et al.* 2012)

Support biologique	Membrane amniotique		(Ishino *et al.* 2004)
	Capsule cristallinien antérieur		(Yoeruek *et al.* 2009)
	Lamelle de stroma décellularisée	porc	(Ju *et al.* 2012)
		bovin	(Bayyoud *et al.* 2012)
		humain	(Choi *et al.* 2010)

1.1.3. Densité d'ensemencement

L'objectif final chez le patient ou sur le greffon bioingénieré est d'atteindre une DCE élevée, idéalement largement > 2000 cellules/mm^2 afin d'assurer une bonne fonctionalité de la monocouche, et une survie durable. Une DCE élevée assurera la reconstitution d'une réserve endothéliale capable de résister aux stress de la transplantation et des évènements post opératoires probables (réactions immunitaires, lésions chirurgicales, etc.). Il a par ailleurs été démontré qu'une faible DCE altère les jonctions intercellulaires (Singh *et al.* 2013) et diminue l'efficacité du transport actif par les pompes membranaires (voir Chapitre I - 2.2.4). Il est donc important de déterminer la quantité initiale de CEs à ensemmencer sur le support pour obtenir une DCE finale ≥ 2000 cellules/mm^2 à la fin du procédé de bioingénierie. Cette connaissance pourrait également aider à déterminer la quantité de CEs à injecter dans la chambre antérieure des patients.

La résolution de cette problématique revient à connaître la dynamique de division cellulaire de la CE. La division des CEs est normalement inhibée par la formation des contacts intercellulaires (Chapitre II - 2.1). Ex vivo, en cas de lésion mécanique, la mosaïque perd son intégrité et les CEs voisines du défect endothélial peuvent se diviser en présence de certains facteurs de croissance rajoutés au milieu (dont FGF et EGF) (Mimura & Joyce 2006). Lors de la mise en culture in vitro, la dissociation des CEs et la perte de leur environnement physiologique déclenchent ce mécanisme de réparation et peuvent donc initier la division cellulaire. Une fois ensemmencées, les CEs non confluentes continuent théoriquement à se diviser jusqu'à ce que des jonctions intercellulaires mâtures soient formées.

Dans une publication récente, l'équipe de D. Tan du Singapore Eye Research Institute Peh *et al.* propose une densité d'ensemencement de 10 000 cellules/cm^2 pour favoriser la morphologie hexagonale régulière durant la première phase d'amplification par la culture in vitro (Peh *et al.* 2013) (Figure 68). Les CEs amplifiées au 3ème passage paraissent fiables pour envisager **une injection in vivo à 3150 cellules/mm^2 sur une surface circulaire de 9 mm** de diamètre pour prévenir 20% de perte cellulaire durant les manipulations (Peh *et al.* 2013) et obtenir une DCE finale d'environ 2000 cellules/mm^2.

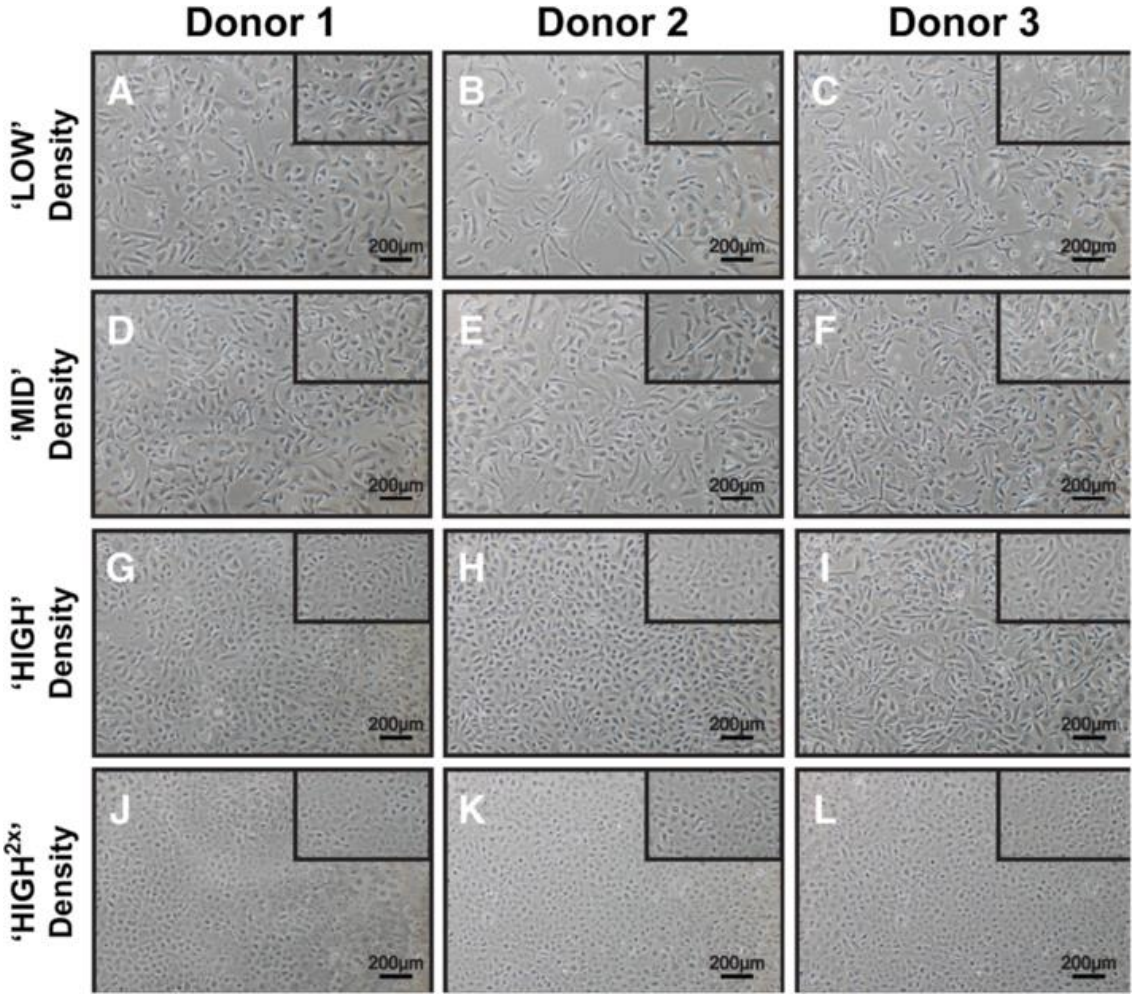


Figure 68. Effet de la densité d'ensemmencement sur la morphologie des CEs des donneurs jeunes (19-35 ans) à J5 et J10 (insert) (Peh et al. 2013). La faible densité d'ensemmencement favorise la morphologie fibroblastique des CEs. LOW: 2500 cellules/cm^2, MID: 5000 cellules/cm^2, HIGH: 10000 cellules/cm^2, HIGH^{2x}: 20000 cellules/cm^2.

Une faible DCE in vitro favorise en effet la morphologie fibroblastique des CEs. A haute DCE initiale, 10000 cellules/cm^2 (100 cellules/mm^2 << 2000 cellules/mm^2), les CEs provenant des donneurs jeunes (**19, 31 et 35 ans**) sont capables

de proliférer plus rapidement qu'à faible DCE. Pour l'application finale destinée à l'injection in vivo e CEs, l'équipe de Gary conseille une haute DCE à confluente pour favoriser une formation rapide de jonctions intercellulaires, ainsi préserver les CEs de l'épuisement de leurs capacités prolifératives. **Interrogé à l'oral en congrès (EUCORNEA 2013, Amsterdam), le Dr JS Mehta a confirmé que l'âge du donneur supérieur à 50 ans pouvait être un obstacle à cette stratégie de culture.**

Pour résumer, l'efficacité de l'étape d'expansion in vitro des cultures primaires dépend donc principalement des capacités prolifératives intrinsèques (et donc principalement de l'âge du donneur) et du profil de différenciation des CEs (et donc principalement des interactions cellules-cellules). Sur ce même principe, l'utilisation des cornées des donneurs âgés (moyenne d'âge de nos donneurs français = 72 ans) ayant par définition des capacités prolifératives moindres limite les possibilités d'expansion in vitro de CEs restant bien différenciées (voir Partie expérimentale - Article I).

1.1.4. Culture en hypoxie

Un autre paramètre implique dans le métabolisme des CE est le taux d'oxygène. Contrairement à l'environnement des niches préservant les cellules souches/progénitrices qui contient de 2 à 9% d'O_2, la culture in vitro en normoxie à 20% d'O_2 entraîne la faible prolifération, la sénescence prématurée et l'instabilité génétique des cellules souches (Haque *et al.* 2013). La culture en hypoxie consiste à maintenir un faible taux d'O_2 à 2-9% en culture in vitro, ce qui peut activer la régulation induite au facteur de transcription HIF-1 permettant de mieux préserver les CS. Il a été rapporté que l'hypoxie limite la dégradation de HIF-1 dans le cytoplasme, donc le permet à activer la transcription des protéines impliqué dans le métabolisme, la migation et l'angiogénèse (Figure 69A). Un des effets de ces protéines est de réduire le taux d'ERO via la suppression de l'activité de la chaîne respiratoire mitochondriale (Figure 69B).

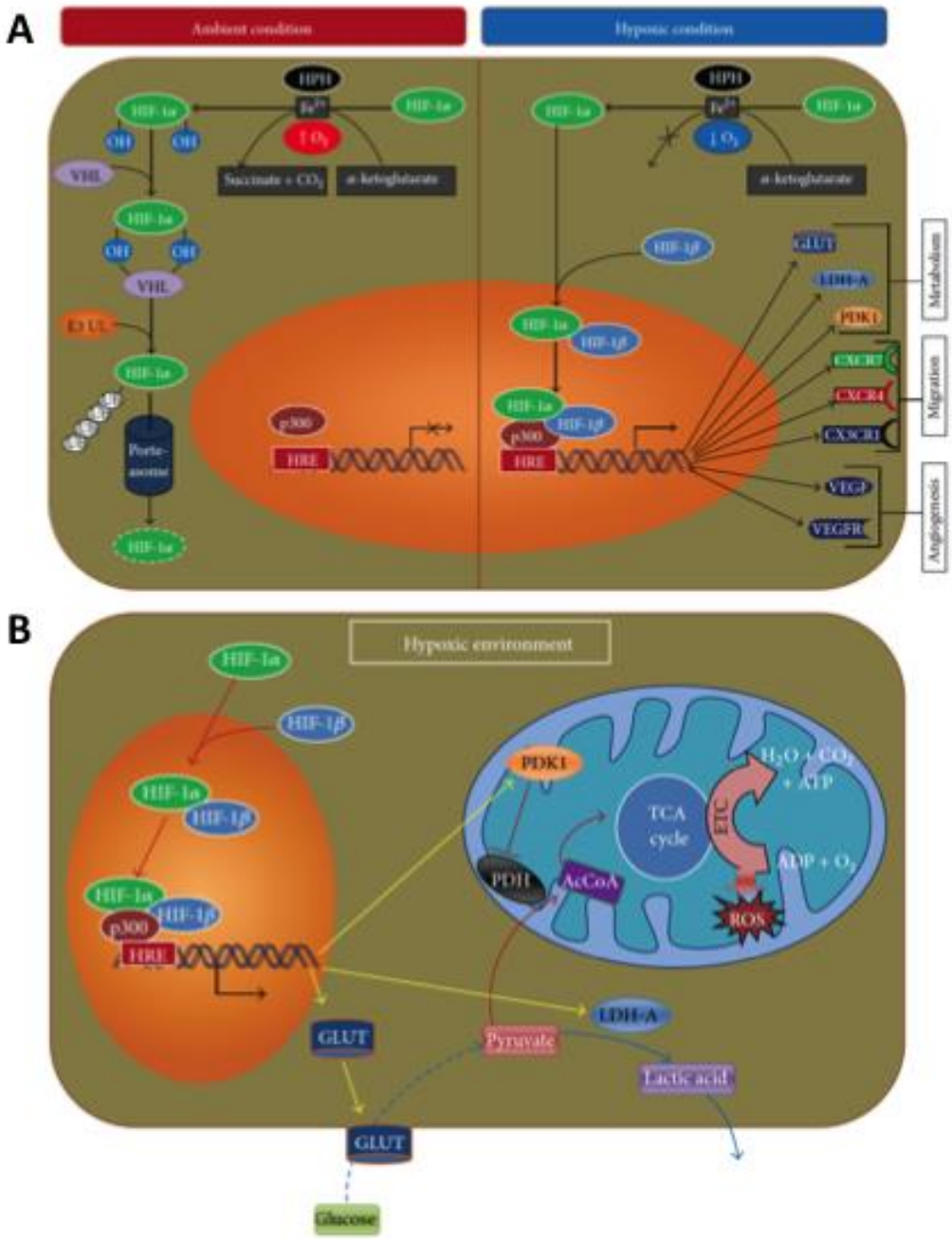


Figure 69. Effet de la culture en hypoxie sur l'activation de la transcription des gènes du métabolisme par HIF-1α (A), notamment HIF-1α limite l'activité de la chaîne respiratoire mitochondriale, ainsi réduit le taux d'espèce réactive oxygénique (ROS) cytoplasmique (B) (Haque et al. 2013)

Cette méthodologie encore très peu utilisée dans notre domaine mais dont les avantages ont été largement discutés en recherche sur les cellules tumorales pour reproduire l'environnement naturel de ces cellules et réduire le stress oxydant impose par les 21% d'O2 de l'atmosphère (Wion *et al.* 2008).

Conclusion: l'optimisation des conditions de culture permet de préserver au mieux les CEs des stress dûs aux changements d'environnement, mais il ne s'agit pas des paramètres uniques déterminant la réussite d'une culture de CEs. Le choix du matériel cellulaire de départ est un facteur décisif dans le maintien de la culture à long terme.

1.2. Sélection du matériel cellulaire de départ

Le but est de sélectionner les populations cellulaires présentant de fortes capacités prolifératives résidelles afin d'optimiser le rendement et de limiter les variations possibles. Il a été régulièrement rapporté que les capacités prolifératives de l'endothélium cornéen étaient plus importantes à la périphérie plus qu'au centre et chez les donneurs jeunes plus que chez les donneurs âgés.

1.2.1. Âge de donneur

La plupart des études sont **réalisées à partir des donneurs jeunes de moins de 30 ans** (Wilson *et al.* 1995; Peh *et al.* 2011; Liu *et al.* 2012; Schmedt *et al.* 2012; Yokoi *et al.* 2012; Peh *et al.* 2013). Les CEs provenant des donneurs âgés ont une morphologie plus élargie que celles de donneurs jeunes, lorsqu'elles sont en culture in vitro dans un milieu contenant 10% de SVF (Liu *et al.* 2012) (Figure 70).

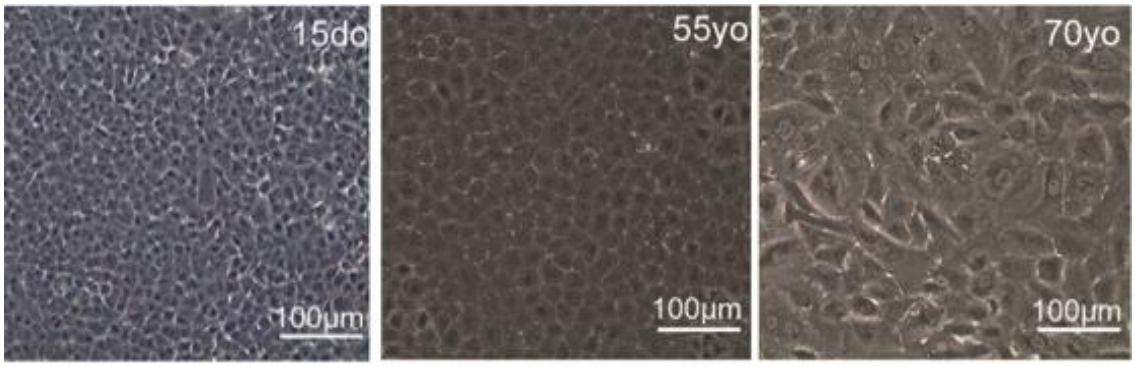


Figure 70. Culture in vitro de cellules endothéliales des donneurs de 15 jours, 55 ans et 70 ans en milieu DMEM 10% SVF (Liu et al. 2012)

Actuellement, selon les rapports annuels des banques de cornée (European Eye Bank Association, Eye Banks Association of America) , la moyenne d'âge des donneurs de cornée est de 61 ans (en 2011) en Europe et 59 ans (en 2012) aux Etats Unis. Aux Etats Unis, 83% des greffons proviennent des donneurs de 41-80 ans en 2012. **Avec le**

vieillissement de la population mondiale, le développement de la thérapie cellulaire à partir des cornées de donneurs âgés (> 50 ans) semble plus proche de la réalité. L'adaptation de la méthode de mise en culture de CEs à partir des donneurs âgés est détaillée dans l'article I de la Partie expérimentale.

1.2.2. Localisation centrale versus périphérique des cellules endothéliales de départ

La plus grande capacité proliférative des CEs périphériques par rapport aux CEs centrales, est un avantage pour la culture à long terme mais cette culture nécessite des conditions particulières. Nous avons en effet démontré récemment (Partie expérimentale - Article I) que, en milieu OptiMEM-I, les CEs périphériques sont moins différenciées et sont plus facilement soumises à la transition mésenchymateuse par rapport aux CEs du centre. En culture sans sérum, les CEs périphériques maintiennent une morphologie endothéliale typique et le taux de sénescence est moins important que les CE centrales (Figure 71).

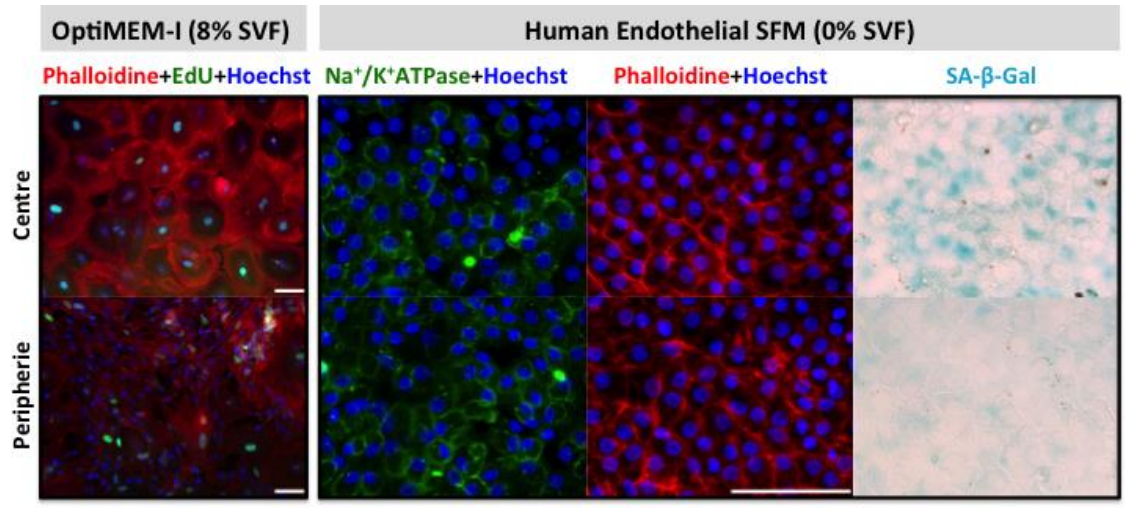


Figure 71. Culture de cellules endothéliales (CE) centrales et périphériques en milieu contenant 8% de sérum de veau fœtal (SVF) et 0% de SVF. Les CE périphériques deviennent fibroblastiques après 14 jours de culture en milieu OptiMEM-I contenant 8% SVF (cornée entière provenant de donneur de 50 ans). En milieu sans sérum, les CE centrales et périphériques maintiennent leur morphologie endothéliale et leur expression protéique de Na^+/K^+ATPase (immunomarquage, cornées entières provenant de donneurs de 70 et 75 ans). Les CE périphériques expriment moins de marqueur de sénescence, SA-β-Gal, que les CE centrales. Barre d'échelle de 100µm (EA2521 BiiGC, Université Jean Monnet, Saint Etienne).

Cette étude suggère que les CEs périphériques provenant des cornées entières ou des collerettes résiduelles après trépanation chirurgicale peuvent être utilisée pour la thérapie cellulaire. L'utilisation de ces CEs nécessite de limiter le pourcentage de SVF

dans le milieu de culture pour ne pas induire les signaux de dédifférenciation. D'autre part, la conservation en OC dans du milieu commercial CorneaMax contient 2% de SVF pourrait être à l'origine de l'altération des CEs périphériques. Par conséquence, une courte durée d'OC pourrait mieux préserver les CEs périphériques. La durée maximale d'OC reste à évaluer.

Récemment, la ressemblance entre les CEs cornéennes et les cellules endothéliales trabéculaires a été analysé (Yu *et al.* 2011). L'existence des phénotypes de CS dans la zone de transition et dans le trabéculum suppose l'existence d'une source potentielle de renouvellement de l'endothélium cornéen. Ainsi, l'isolement des précurseurs est leur différenciation ou transdifférenciation en CE cornéennes est une voie potentielle.

1.2.3. Culture en sphère (sphere-forming assay)

A côté la sélection par l'âge du donneur et par la localisation, la culture en sphère est un autre moyen pour isoler les cellules "jeunes" via leurs capacités à générer des sphères de cellules en milieu de culture semi-solide. Cette méthode a été découverte par la formation de neursphère des cellules de la zone sous ventriculaire. Dans les années 1960, cette zone a été identifiée comme source de la neurogénèse en continue, dans laquelle se trouvent des cellules capables de se renouveler et de se différencier en 3 types cellulaires (neurone, astrocyte, oligodendrocyte) durant une longue période. En même temps, une autre équipe a découvert le comportement particulier de ces cellules in vitro. En effet, après leur mise en culture en milieu sans sérum contenant le facteur EGF, certaines cellules se divisent, adhèrent au support, puis se détachent pour former des sphères de cellules proliférantes. Une fois mises en culture induite à l'adhésion, ces cellules en sphères sont capables de se différencier en cellules neuronales et cellules gliales (Pastrana *et al.* 2011).

Par ce moyen, certaines études récentes ont tenté d'isoler les CE de la cornée en culture en sphère qui sont censées être des progéniteurs endothéliaux (Yokoo *et al.* 2005; Mimura *et al.* 2010; Bi *et al.* 2013) (Figure 72). Le milieu proposé est le DMEM/F12 contenant 20 ng/ml d'EGF et 40 ng/ml de bFGF. Ce milieu peut être supplémenté des cocktail comme B-27 ou N2. Il est rendu semi-solide par 1,5% de matrice de méthylcellulose pour favoriser la formation de sphère en suspension.

L'adhésion des cellules est limitée par le coating des surfaces de culture par la poly-2-hydroxyethyl methacrylate (poly-HEMA).

Formée à partir des cellules isolées seules, les sphères de CEs sont capables de reformer des monocouches en culture adhérente (Mimura *et al.* 2010). D'autre part, le traitement des sphères par 30µM de Rock-inhibitor Y-27632 pendant 1h avant la recolonisation en culture adhérente augmente l'expression d'ARNm des pompes Na^+/K^+ATPase des CE (Bi *et al.* 2013).

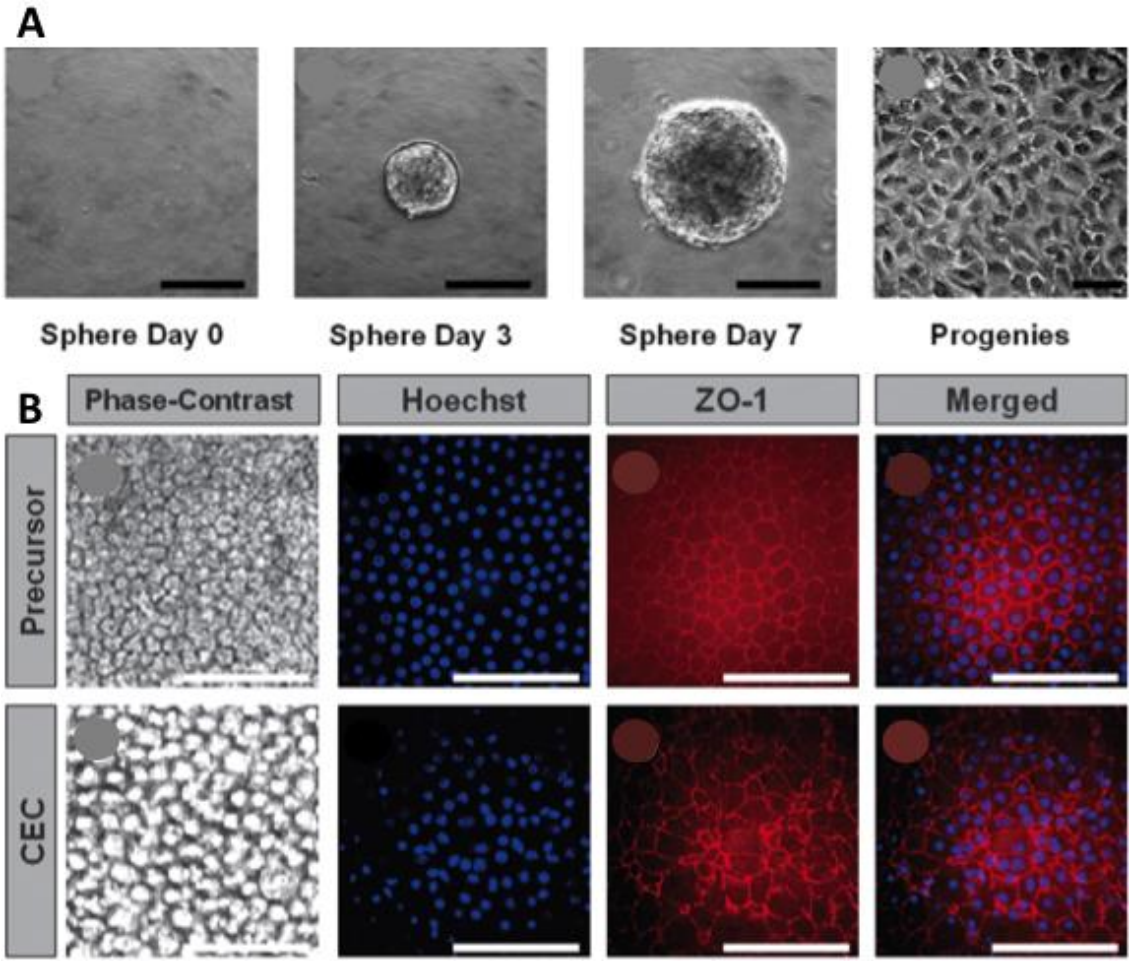


Figure 72. Formation de sphère de cellules endothéliale et recolonisation en culture adhérente (Mimura et al. 2010). (A) Formation de sphère à partir du 6ème passage d'une culture de CEs, donneur âgé de 43 ans, et recolonisation sur culture adhérente (progenies). (B) Culture d'un 5ème passage de culture en sphère sur membrane amniotique, donneur âgé de 39 ans. Immunomarquage de ZO-1 (rouge) et contre-coloration du noyau par Hoechst (bleu).

Par rapport à la culture adhérente, la culture en sphère permet de sélectioner les CEs directement par leur capacité proliférative. L'inconvénient de cette méthode est que la formation des sphères ne facilite pas l'évaluation morphologique des cellules

(fibroblastique ou en monocouche), et augmente ainsi le risque de contamination par d'autres types cellulaires.

1.3. Choix des protocoles

La thérapie cellulaire de l'endothélium cornéen se compose de deux étapes principales, l'amplification in vitro de cellule et l'enrichissement de l'endothélium par l'injection directe dans la chambre antérieure ou par une greffe de lamelle enrichie en CE. Pour l'étape d'amplification de cellules, le protocole de mise en culture de CE peut être adapté aux échantillions biologiques disponibles (Figure 73).

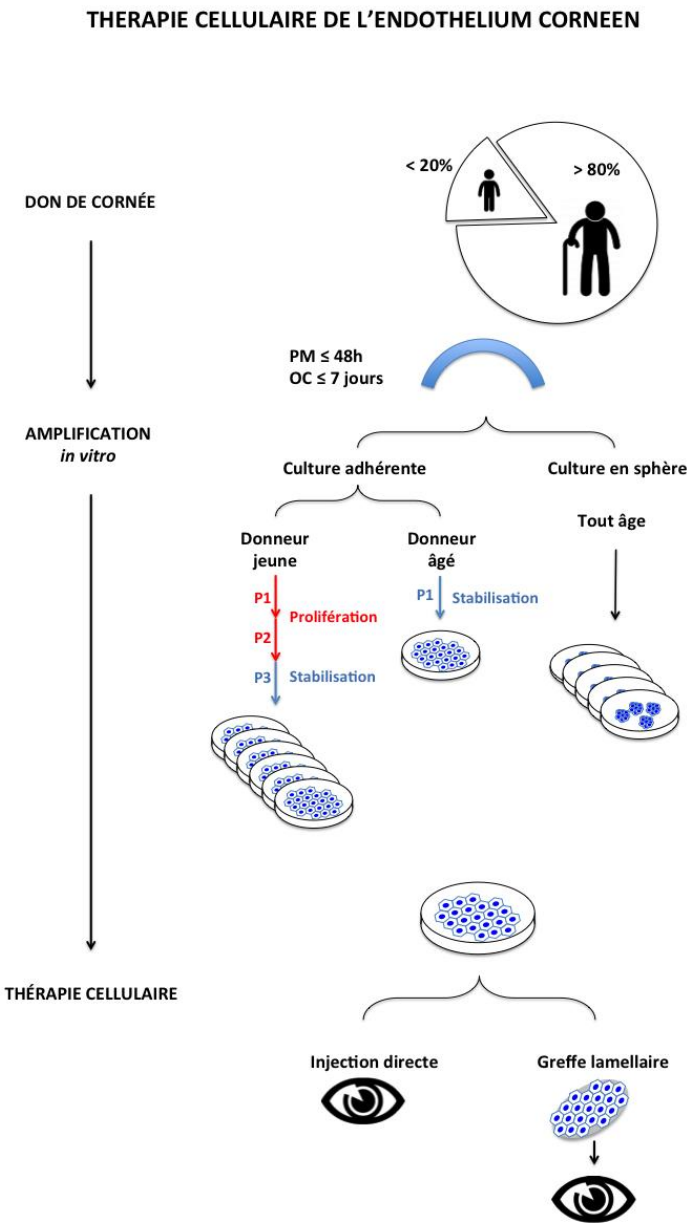


Figure 73. Evaluation des protocoles de culture cellulaire pour l'application à la thérapie cellulaire de l'endothélium cornéen (EA2521 BiiGC, Université Jean Monnet, Saint Etienne).

La culture adhérente est actuellement la méthode la plus répandue. L'endothélium provenant des donneurs jeunes semble pouvoir être soumis à une phase d'amplification en plusieurs passages en milieu Human Endothelial SFM 5%SVF avant d'être stabilisé dans le même milieu sans sérum complété de FGF-2 à 10ng/ml. Par contre, les CEs provenant des donneurs âgés disposent d'une capacité proliférative limitée et il semble qu'il faille limiter à un seul passage en culture in vitro dans du milieu de stabilisation pour purifier les cellules des débris tout en évitant d'épuiser leur potentiel de division. La relation entre l'âge et la qualité finale de CEs nécessite d'être clarifiée pour donner des critères de choix chiffrés. L'évaluation de la qualité des cellules peut se baser sur différentes analyses concernant l'état de sénescence, l'état du stress oxydatif ou le temps de doublement des cellules.

A côté de la culture adhérente, la culture en sphère permet de sélectionner de façon plus efficace les progéniteurs des CEs mais l'amplification in vitro par repiquage des cultures en sphère peut également épuiser leurs ressoures prolifératives. Cette méthode est essentiellement promue par une seule équipe japonaise (Amano S, Tokyo) Actuellement, la relation entre l'âge et la formation de sphère n'est pas encore bien établie. Afin d'évaluer la contamination par d'autres types cellulaire, cette méthode peut être combinée peut être suivie d'une étape de culture adhérente.

A ce stade, la faisabilité des différentes méthodes a été démontrée, mais avant de les transférer en pratique de thérapie cellulaire, il est nécessaire d'établir précisément des critères de sélection à chaque étape. D'autre part, il n'existe aucune étude médico-économique établissant le bilan entre le rendement (quelle quantité finale de CEs pour une cornée de donneur ?) et le coût engagé pour chaque protocole permettant d'orienter le choix.

Récemment, Peh et al. ont néanmoins proposé un bilan de rendement (Peh *et al.* 2013): une paire de cornée est capable de produire de $4{,}5x10^6$ à $7{,}5x10^6$ cellules au 2nd passage. Estimant qu'une injection nécessite $2x10^5$ cellules, il est théoriquement possible de traiter de 22 à 37 yeux avec une paire de cornée. Ces hypothèses ont été déterminées pour des cornées de 3 donneurs jeunes (19 - 35 ans) et en considérant que l'injection de 200 000 CEs suffira, ce qui reste très hypothétique.

2. Différenciation/Transdifférenciation

L'amplification in vitro de CEs primaires est limitée par leur capacité proliférative et par l'âge des donneurs. La recherche d'une solution alternative oriente vers une source de CS permettant de regénérer de façon plus efficace l'endothélium cornéen. Plusieurs sources de CS ont été étudiées : CS adultes de stroma cornéen, CS mésenchymateuses (CSM) et cellules souches pluripotentes induites (CSPi ou Human induced pluripotent stem cells hiPSC des anglo-saxons)).

CS adultes cornéennes : le stroma et l'endothélium cornéen se différencient à partir du même mésenchyme périoculaire originaire de la CN (voir Chapitre I - 1.1.2). Une première méthode consiste à transdifférencier les précurseurs d'origine stromale (Hatou *et al.* 2013) en altérant la voie Wnt/β-caténine par l'acide rétinoïque et l'inhibiteur de GSK-3β, et la voie Wnt/RhoA par ROCK inhibiteur (voir Chapitre I - 1.2.2)**.** A partir des donneurs de 66-69 ans, les précurseurs du stroma sont isolés de la cornée : après digestion enzymatique, le stroma cornéen est mis en culture en sphère en milieu DMEM/F12 supplémenté par 20ng/ml EGF, 20ng/ml FGF-2, B27 et N2, 2nM L-Glutamine, 5ng/ml Heparin. Une fois les sphères formées, la transdifférenciation en CEs est induite par un milieu dit « SEIM » (specific endothelium-inducing medium). Il s'agit du milieu MEM complété de 1% SVF, acide retinoique all-trans 1µM, 6-bromoindirubin-3'-oxime (BIO, GSK-3β inhibiteur) 1µM, TGF-β2 5ng/ml, Y-27632 10µM, insulin 1µM, $CaCl_2$ 1 mM, sodium pyruvate 1mM, MEM amino acid à 1X, MEM essencial vitamin mixture à 1X. Après 1 semaine d'induction, les cellules sont maintenues dans du milieu MEM supplémenté de $CaCl_2$ 1mM, sodium pyruvate 1mM, MEM amino acid 1X et MEM essential vitamin mixture 1X (Figure 74).

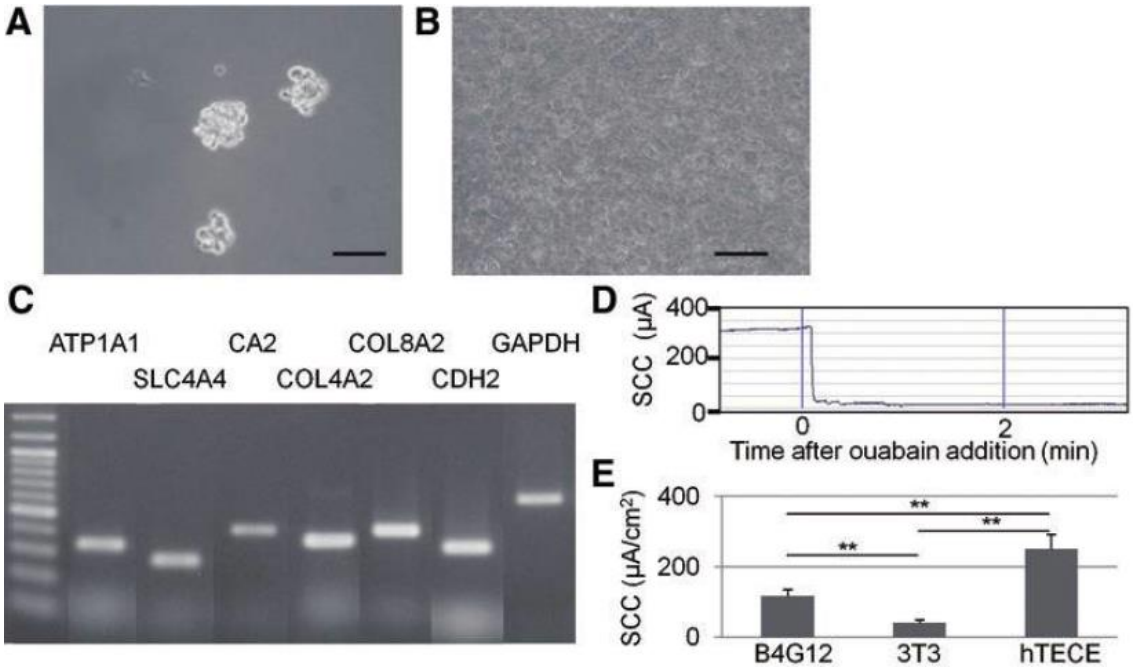


Figure 74. Transdifférenciation de précurseurs stromaux en cellules endothéliales (CEs) (Hatou et al. 2013). A: isolation des précurseurs du stroma par culture en sphère. B: induction de la morphologie endothéliale en milieu contenant de l'acide rétinoïque, de l'inhibiteur de GSK-3β et du Rock-inhibitor Y-27632. C : expression d'ARNm des marqueurs endothéliaux. D, E : évaluation de l'activité de pompe Na^+/K^+ATPase mesurée par la chambre de Ussing. hTECE : human tissue-engineered corneal endothelium, 3T3: lignée contrôle, B4G12: cellules endothéliales immortalisées.

Les cellules finales expriment les ARNm des marqueurs endothéliaux (Atp1a1, Slc4a4, Ca2, Col4a2, Col8a2 et Cdh2) et ont une activité de pompe Na^+/K^+ATPase détectée par la chambre de Ussing. Cependant, la formation d'une monocouche cellulaire n'est pas clairement démontrée. Le statut endothélial des cellules est à confirmer par l'expression protéique des principaux marqueurs usuels. Sur un plan plus fondamental, l'effet de l'acide rétinoïque et de l'inhibiteur du GSK-3β sur la voie Wnt canonique, est confirmé seulement pour l'activation de l'expression du facteur de transcription régulateur Pitx2 chez la souris (Hatou *et al.* 2013). Pitx2 peut réguler négativement la voie Wnt canonique (voir Chapitre I - 1.2.2), mais l'inhibiteur du GSK-3β a plutôt un effet activateur de la voie Wnt canonique. L'impact de ces 2 traitements combinés sur la voie Wnt canonique des progéniteurs stromaux reste donc à étudier.

CS mésenchymateuses : une autre stratégie consiste à différencier les CSM de cordon ombilical humain en CEs. Un seul travail expérimental a été conduit jusqu'à présent sur des cornées entières ex vivo et sur les CEs en culture in vitro. L'induction à la différenciation des CSM consiste à 3 milieux de culture: le milieu basal de CSM, le

milieu basal de cellules épithéliales de cristallin et un milieu conditionné aux cellules épithéliales de cristallin. Le seul résultat obtenu jusqu'à présent est l'adhérence des CSM à des lésions expérimentales de l'endothélium sur des cornées entières conservées en OC (Figure 75). Leur expression de ZO-1 et de N-cadhérine est cytoplasmique en milieu basal pour les CSM, mais plutôt au niveau des jonctions intercellulaires dans les deux milieux dédiés à l'épithélium cristallinien. Malgré ces changements, leur morphologie est beaucoup plus fibroblastique qu'endothéliale (Joyce 2012).

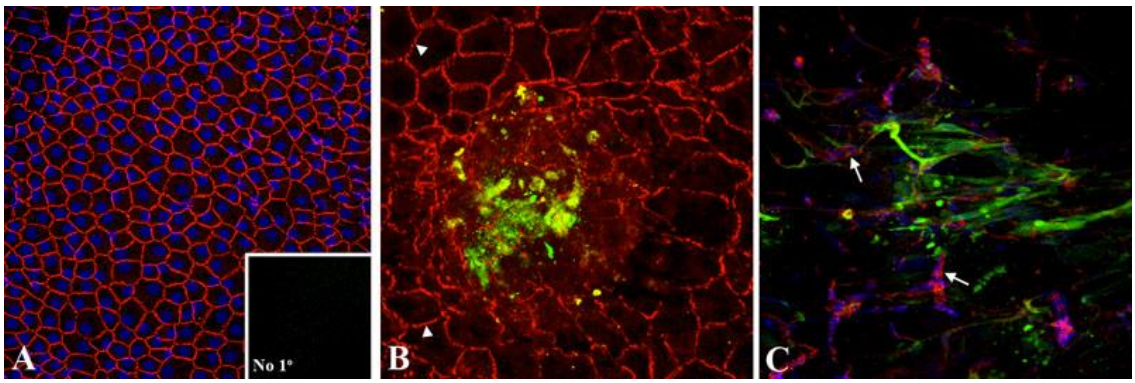


Figure 75. Attachement des cellules souches mésenchymateuses (CSM) exprimant la GFP (vert) aux lésions de l'endothélium cornéen humain ex vivo (Joyce et al. 2012). A : contrôle négatif, sans lésion. B et C: adhérence des CSM aux sites d'endommagement. L'intégrité de l'endothélium est représentée par l'immunomarquage de ZO-1 (rouge). Contre coloration du noyau par TO-PRO-3 (bleu).

CS pluripotentes induites (CSPi) ou human induced pluripotent stem cells (hIPSC) : les CSPi sont capables de s'auto-renouveller à l'infini tout en conservant leur capacité à se différencier en cellules somatiques (Takahashi & Yamanaka 2006). Ces cellules représentent donc une source inépuisable de cellules endothéliales (CE) potentiellement utilisables pour de nouvelles approches de thérapie cellulaire et tissulaire. Il n'existe actuellement aucune publication sur la différenciation de hIPSC en CEs. Il s'agit d'une des thématiques prioritaires du laboratoire BiiGC dont les premiers résulats seront présentés aux congrès de l'EEBA 2014 (Poster) et de la SFO 2014 (Communication orale). Des CSPi reprogrammées à partir d'adipocytes humaines par transfection rétrovirale (SBI, Mountain View, CA) ont été maintenues à l'état indifférencié et multipliées en milieu mTesr (Stem cell technologies, Grenoble, France). La différenciation en CE a ensuite été induite par un traitement séquentiel consistant à augmenter par pallier la concentration de différents facteurs de croissance pendant 2 semaines (co-culture, milieu conditionné, données non présentées car demande de brevet en cours). Les cellules différenciées ont été triées par billes

magnétiques avec une sélection positive pour le CD200R, marqueur de CE récemment décrit. La culture des cellules CD200R+ a été maintenue pendant 3 à 4 semaines. La différenciation spécifique en CE a été étudiée par immunomarquage de protéines caractéristiques des CE (ZO-1, Glypican-4, CD200R, Na^+/K^+ATPase, VDAC3, CLCN3), des cellules épithéliales pigmentées rétiniennes (MiTF), épithéliales cornéennes (K3/K12) et du marqueur de pluripotence Oct-4. Après 1 mois de traitement, les CSPi ont été différenciées de manière stable en une monocouche de cellules hexagonale. Les cellules jointives exprimaient les principaux marqueurs des CE et n'exprimaient pas les marqueurs des cellules épithéliales cornéennes ni pigmentaires rétiniennes. De plus, les cellules CD200R+ perdaient le marqueur de pluripotence Oct-4. La biofonctionnalité des CE dérivées des CSPi sera étudiée par deux méthodes complémentaire : (1) chambre de Ussing pour déterminer la différence de potentiel électrique de part et d'autre de l'endothélium reconstruit témoignant de la capacité à avoir une activité de pompe anionique et (2) bioréacteur innovant breveté par notre laboratoire pour déterminer leur capacité à déturger ex vivo une cornée humaine oédémateuse. En parallèle, nous développons des méthodes de reprogrammation de CSPi plus sécuritaires (virus non intégratifs, mini plasmides, méthodes physiques, protéines recombinantes seules) pour faciliter la translation à la clinique.

CS embryonnaires : Il n'existe aucune publication sur ce sujet. Le laboratoire BiiGC est en train d'efefctuer les démarches pour obtenir auprès de l'Agence de la Biomédecine (ABM), l'autorisation de travailler sur une lignée de CSE de grade thérapeutique (GMP). Cette voie pourrait à l'évidence permettre de s'affranchir des risques potentiels liés à la reprogrammation des hIPSC. Les mêmes protocoles de différencientionmis au point sur les hIPSC seront testés sur les CSE dès que nous auront les autorisations de l'ABM.

Actuellement, la faisabilité de générer des CEs à partir de CS n'est pas confirmée. Aucun modèle cellulaire ou protocole n'a été validé. Cette voie potentielle demande d'une connaissance profonde du microenvironnement des CEs et de ses processus de différenciation embryonnaire.

3. Thérapie ciblée

Une autre alternative consiste à « rajeunir » les CEs primaires ou prolonger leur durée de vie par la thérapie génique. Plusieurs voies d'activation de la prolifération ont été envisagées.

3.1. Transfection d'oncogènes

Cette voie consiste à immortaliser les CEs par l'induction de l'expression des oncogènes.

La transduction par rétrovirus de l'oncogène codant pour **human papilloma virus type 16 E6/E7** (HPV16 E6/E7) a immortalisé les CEs humaines avec succès (Wilson *et al.* 1995; Yokoi *et al.* 2012). La lignée finale forme une monocouche mais les cellules sont peu hexagonales. L'énorme capacité proliférative se traduit par plus de 50 doublements de population (Wilson *et al.* 1995).

Les CEs ont également été immortalisées après avoir été transfectées avec le gène codant pour le **virus simien 40 large T-antigen** (SV40 LT) par électroporation (Bednarz *et al.* 2000). Provenant d'un donneur de 91 ans, les CEs en culture dans du milieu F99 avaient une morphologie fibroblastique avant la transfection. Après transfection, les CEs ont récupéré leur morphologie endothéliale et leur capacité proliférative avec 300 doublements de population (Figure 76). Il reste étonnant qu'une transfection stable supposant une intégration génonique ait pu être obtenue par électroporation. Toujours est-il que cette lignée, désormais commercialisée est la seule disponible au monde.

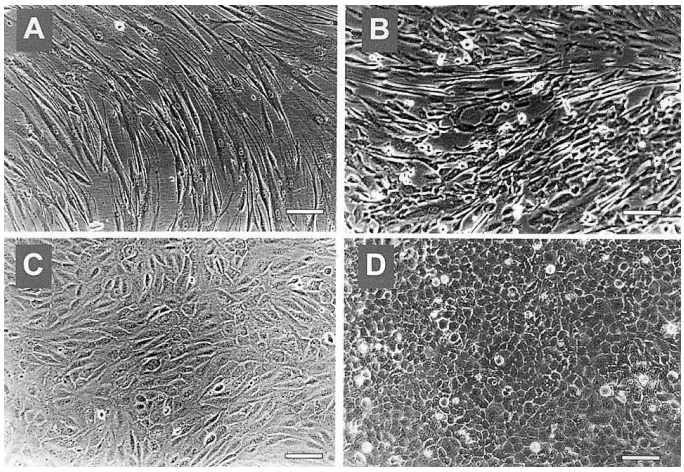


Figure 76. Immortalisation de CE par transfection de l'oncogène SV40 LT (Bednarz et al. 2000). Observation à contraste de phase de la culture in vitro avant la transfection (A), 6

doublements de population (DP) après la transfection (B), 35 DP (C) et 130 DP (D). Barre d'échelle 100µm.

Restant hétérogène, cette lignée a été divisée en deux lignées filles ayant des morphologies plus homogènes: B4G12 et H9C1 (Valtink *et al.* 2008). Les CE de la lignée B4G12 adhèrent fortement et forment une monocouche stricte des cellules hexagonales. Leur temps de doublement de 62 ± 14 heures. Les CE de la lignée H9C1 sont moins adhérentes et peuvent former des sphères flottantes. Leur temps de doublement est estimé à 44 ± 5 heures. Les deux lignées expriment ZO-1, occludin, mais peu de connexin-43. B4G12 exprime moins de Na^+/K^+ATPase que H9C1.

La lignée B4G12 est fréquemment utilisée par de nombreuses équipes comme outil d'étude in vitro de CEs en raison de sa morphologie homogène et sa grande capacité de division. Par contre, aucune utilisation clinique n'est évidemment envisageable puisqu'il existe un fort risque de prolifération incontrôlable liée à l'introduction d'oncogène viraux.

3.2. Déblocage de l'arrêt du cycle en phase G1

Cette stratégie consiste à débloquer l'arrêt du cycle cellulaire à la phase G1 à plusieurs niveaux :

-**Réduction de l'expression des inhibiteurs de complexes Cyclin-CDK** (CKI) impliqués dans ce blocage. La réduction de l'expression de **p27** des CEs en culture in vitro est obtenue par la transfection par lipide non-liposomale de siARN anti p27 (Kikuchi *et al.* 2006) (Figure 77). Après 144 heures d'incubation avec le siARN, une augmentation de la DCE a été mise en évidence uniquement sur des cultures provenant des donneurs jeunes (< 30 ans). La baisse d'expression de p27 n'altère pas la morphologie des CEs en culture.

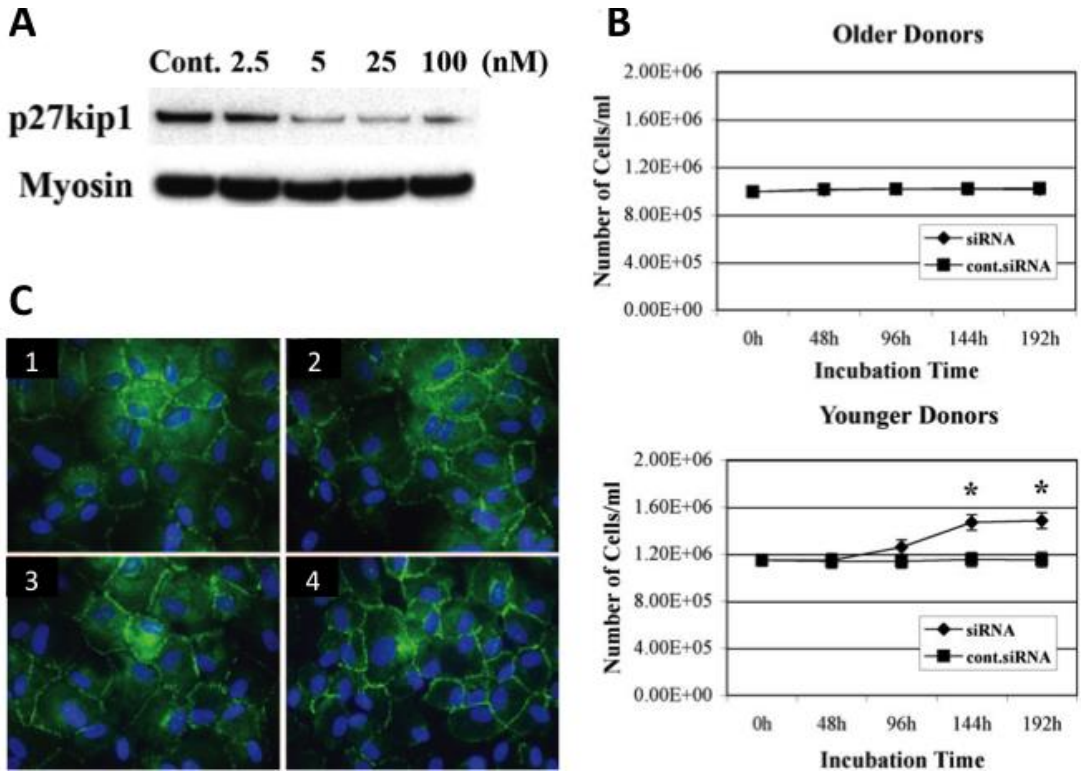


Figure 77. Effet de l'inhibition de l'expression de p27 par transfection de siARN sur des CEs in vitro (Kikuchi et al. 2006). La baisse d'expression de p27 observée par Western-blot en fonction de la concentration de siARN incubée (A) favorise la division cellulaire des CEs provenant des donneurs jeunes (B) tout en préservant la morphologie endothéliale. Expression de ZO-1 (vert) observée par immunomarquage en cas de non transfection (C1), de transfection sans siARN (C2), de transfection avec le siARN contrôle (3) et avec siARN contre p27 (C4). Contre coloration du noyau par Hoechst 33342 (bleu).

L'expression de **p21** et **p16** par les CEs in vitro a également été réduite par l'électroporation des siARN anti p21 et p16 dans des CE in vitro (Joyce & Harris 2010). Cela a favorisé la division cellulaire (expression de Ki67) et la DCE des cultures de CEs des donneurs jeunes (< 30 ans) et âgés (> 50 ans). Malgré cela, cet effet reste transitoire et donc peu efficace car le taux de mortalité après l'électroporation restait élevé.

-Surexpression forcée des complexes CDK4/Cyclins D. L'arrêt du cycle cellulaire à la phase G1 peut être débloqué en augmentant l'expression de **Cycline D1** et **CDK4** sous forme active (Figure 78). La transduction rétrovirale de Cdk4R24C/CyclinD1 dans les CEs d'un donneur très jeune (2 ans) a permet d'obtenir une lignée de haute potentialité proliférative (21 doublements de population) (Yokoi *et al.* 2012). Les CEs de cette lignée forment une monocouche, gardent l'expression protéique de ZO-1, N-cadherin, et l'expression d'ARNm de Na^+/K^+ATPase, CLCN3, VDAC3.

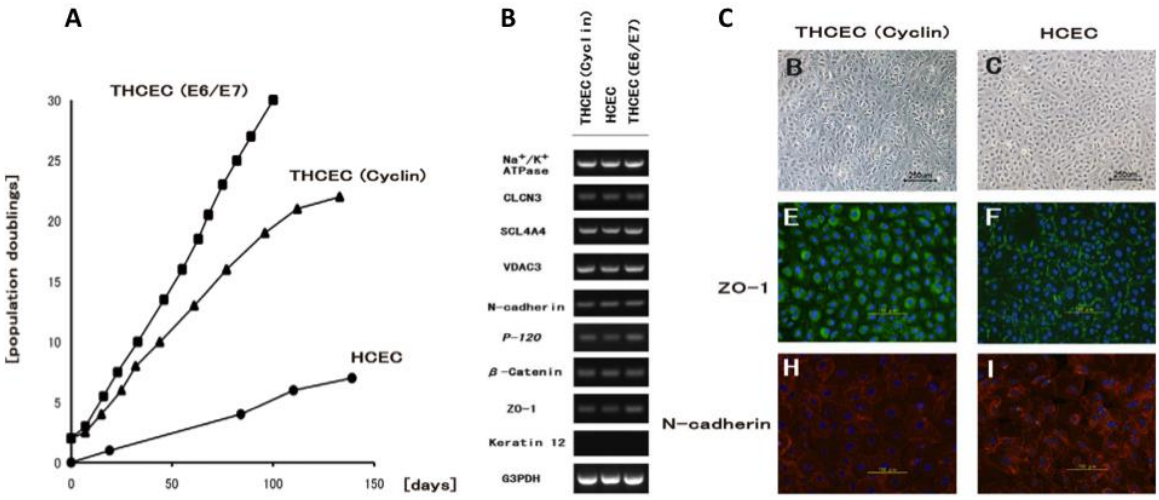


Figure 78. Prolongation de durée de vie de CEs humaines in vitro par transduction rétrovirale de Cdk4R24C/CyclinD1 (Yokoi et al. 2012). Par rapport aux CEs non traitées (HCEC), les cellules infectées (THCEC(Cyclin)) augmente de façon considérable leur capacité proliférative in vitro (A) tout en maintenant l'expression d'ARN (B) et l'expression protéique (C) des marqueurs endothéliaux cornéens.

Le déblocage de la phase G1 peut se faire au niveau des facteurs de transcription E2F qui sont sequestrés par RB et ne peuvent pas déclencher la transcription des gènes du cycle cellulaire (voir Chapitre II - 1.2.3). La transduction par vecteur adenovirus de l'expression d'**E2F2** de endothélium permet l'entrée dans la phase S et provoque l'augmentation transitoire de la DCE (McAlister *et al.* 2005). Cette expérience a été réalisé sur des CEs ex vivo. L'application sur la culture in vitro de CEs reste à explorer.

Le déblocage du point de contrôle G1/S aide à déclencher la division cellulaire de façon transitoire ou permanente. Cette méthode paraît moins risquée que l'introduction de l'expression des oncogènes mais il reste à étudier si la prolifération reste contrôlable par une inhibition de contact se produisant à une DCE suffisamment élevé.

3.3. "Rajeunissement" par la télomérase

Cette voie consiste à "rajeunir" les CE en déclenchant une surexpression de la télomérase. Malgré le fait que les CE disposent de télomères de longueur suffisante n'expliquant pas un arrêt de prolifération par sénescence réplicative, il a été démontré que l'augmentation de l'expression de cette enzyme parvient à améliorer leur capacité proliférative en culture in vitro.

La transfection par la lipofectamine de gène codant pour hTERT (human telomerase reverse transcriptase) prolonge la durée de vie des CE provenant de donneurs jeunes (< 30 ans) (Liu *et al.* 2012; Schmedt *et al.* 2012) (Figure 79). Après transfection, les CE se maintiennent en culture jusqu'à 36 passages (Liu *et al.* 2012). Elles forment une monocouche, expriment les marqueurs protéiques ZO-1, N-cadhérine, et les ARNm des pompes membranaires VDAC3, SLC4A4, CLCN3, Na^+/K^+ATPase.

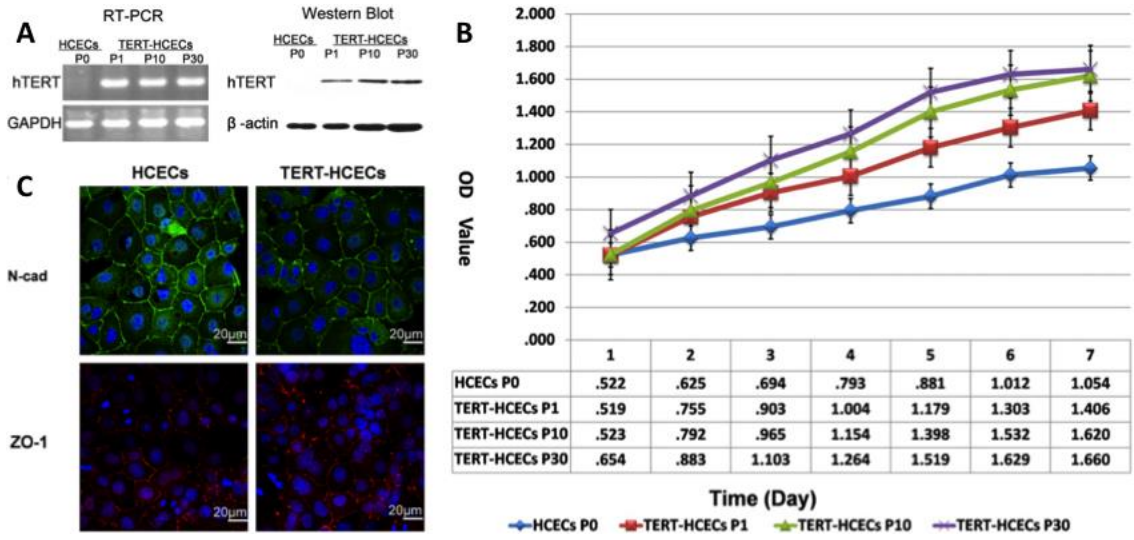


Figure 79. Effet de la transfection de la human telomerase reverse transcriptase (hTERT) sur les CEs en culture in vitro (Liu 2012 EER). La sur-expression de hTERT (A) induite par transfection améliore la capacité proliférative des CEs observée par test de prolifération MTT (B), tout en gardant l'expression protéique des marqueurs endothéliaux ZO-1 (rouge) et N-cadhérine (vert) observée par immunomarquage (C).

De plus, Sheerin et al supposent que la combinaison d'une sur-expression de hTERT et de CDK4 et d'une sous-expression de p53 parvient à immortaliser les CE. Par transduction rétrovirale des gènes codant hTERT et CDK4 et le shARN anti p53, des CE en culture in vitro ont été immortalisées et ont permis plus de 200 passages (Sheerin *et al.* 2012). Néanmoins, l'évaluation des phénotypes endothéliaux de cette lignée n'a pas été rapportée.

Cette voie représente peu de risque et semble prolonger la durée de vie des CEs de façon efficace. **Ainsi, le mécanisme d'action de la télomérase ne serait pas restreint à l'élongation des télomères et reste à explorer.**

3.4. Introduction de facteurs anti-apoptotiques

Cette stratégie consiste à limiter le déclenchement de l'apoptose des CEs. La transduction lentivirale de p35 ou Bcl-xL a des effets anti-apoptotiques sur les CEs in vitro et ex vivo (Fuchsluger *et al.* 2011b; Fuchsluger *et al.* 2011a). Notamment pour les suspensions de CEs primaires, Bcl-xL augmente leur résistance face à l'induction de l'apoptose par les deux voies intrinsèques et extrinsèques. p35 est plus protecteur contre l'activation de la voie intrinsèque.

Cette méthode peut aider à prolonger la survie des CEs en culture in vitro mais aussi à améliorer les conditions de conservation des greffon endothéliaux ou cornéens. Il paraît toutefois nécessaire de remplacer la transfecton rétrovirale par des méthodes plus sécurisantes comme l'introduction directe des protéines d'intérêt. Parmi les outils de thérapie génique, la transduction par infection virale est la plus souvent utilisée en raison de son efficacité. Néanmoins, cette utilisation est restreinte à la recherche préclinique et nécessite d'être remplacée par d'autres méthodes pour supprimer le risque de mutagénèse insertionnelle existant avec les virus intégratifs. D'autre part, la thérapie génique de l'endothélium a été la plus souvent réussie (à l'exception de la lignée allemande SV40LT) avec les CEs provenant des donneurs jeunes.

4. Critères qualité des cellules obtenues

Le développement de procédé de production en masse de CE-like impose le développement en parallèle des méthodes de caractérisation qui permettront de valider ou non ces medicaments de thérapie innovante (MTI). Nous avons défini 4 niveaux de critères qualité (Critical quality Attributes CQA in English) : identité, pureté, fonctionalité, sécurité. Nous détaillons ci-après les CQA1 et 3 qui sont finalement les plus importants au stade de la mise au point des procédés d'obtention des CEs. Les 2 autres CQA peuvent être mis en place ultérieurement lors de du passage à une production semi-industrielle et avant les experimentations précliniques animales.

4.1. Indentité des cellules obtenues (CQA 1)

Les cellules peuvent être considérées comme identiques aux CEs cornéennes humaines si elles remplissent des critères suivantes :

Sur un plan morphologique elles doivent former une monocouche de cellules hexagonales. D'autre part, la formation de l'inhibition de contact est primordiale pour

limiter une expansion non contrôlable. Les mécanismes d'inhibition de l'expansion des CEs vers la zone péricornéenne et l'absence d'adhérence entre la cornée, l'iris et l'épithélium cristallinien sont encore inconnus. Le non respect de ces propriétés pourrait provoquer l'envahissement de l'angle iridocornéen par les neo-CEs et entraîner un glaucome secondaire catastrophique puis l'envahissement du reste du segment antérieur.

En terme d'expression de marqueurs protéiques, le choix de la batterie de marqueurs positifs et négatifs (voir Chapitre I - 3) les plus pertinents ne fait l'objet d'aucun consensus. En reprenant les articles les plus récents, les cellules doivent exprimer au moins ZO-1 et N-cadhérine marquant la formation de jonctions adhérentes et jonctions serrées entre les cellules. La présence des pompes membranaires peut être validée par l'immunomarquage de Na^+/K^+ATPase et AQP1 et par détection d'ARNm de VDAC2, VDAC3, SCL4A4, SLC4A11, CLCN2, CLCN3. D'autres marqueurs protéiques de CEs cornéennes sont de plus en plus utilisés : GPC4, CD200, COL8A2, NSE, S100A4, S100A5, Wnt5a et IER3.

4.2. Fonctionalité des cellules obtenues (CQA 3)

Le gold standard théorique pour la mise en évidence de la fonctionalité des CE produites par différents moyens est l'étude de leur capacité à déturger une cornée humaine oedémateuse et à maitenir la transparence restaurée. Seule l'équipe allemande de Bednarz a effectivement mis en oeuvre cette technique pour prouver que la lignée transformée par SV40LT était fonctionnelle (Aboalchamat *et al.* 1999). En utilisant une chambre antérieure artificielle sur laquelle était montée une cornée humaine ensemencée avec les CEs de leur lignée immortalisée, ils ont mesuré périodiquement l'épaisseur centro cornéenne pour metter en evidence la déturgescence stromale puis inhibier de façon irreversible les ATPase membranaire par ouabaine pour constater la récidive oedémateuse.

L'expérience est effectuée sur quatres conditions : des cornées sans endothélium (contrôle négatif de la déturgescence), cornées avec endothélium natif (contrôle positif de la déturgescence), cornées ensemmencées de 50 000 ou 200 000 cellules immortalisées (effet dose-dépendant sur la déturgescence). Avant chaque expérience, la cornée est déturgée pendant une nuit dans du milieu MEM contenant 6% de Dextran

T500. Après le montage de la cornée sur la chambre de perfusion, la face endothéliale est perfusée par un flux de milieu MEM 10% SVF à 37°C à 50 µl/min. L'épaisseur de la cornée durant la perfusion est mesuré tous les heures jusqu'à 12 heures par pachymètre à ultrasonds. Le gonflement rapide de la cornée reflète l'absence de la déturgescence par l'endothélium. Une variation très progressive ou quasi nulle de l'épaisseur de la cornée reflète une activité de déturgescence optimale. C'est de cette façon que l'activité de la lignée immortalisée a été détectée. Ainsi, l'activité de Na^+/K^+ATPase est mesurée par la différence de la vitesse de gonflement en présence et absence de son inhibiteur ouabain à 100 mg/l dans la solution de perfusion (Figure 80). En présence des CEs immortalisées, l'augmentation de l'épaisseur commence dès le début de la perfusion, par rapport à une vitesse beaucoup plus progressive en absence de ouabain. Cela a mis en évidence la fonctionalité des pompes Na^+/K^+ATPase des CEs immortalisées.

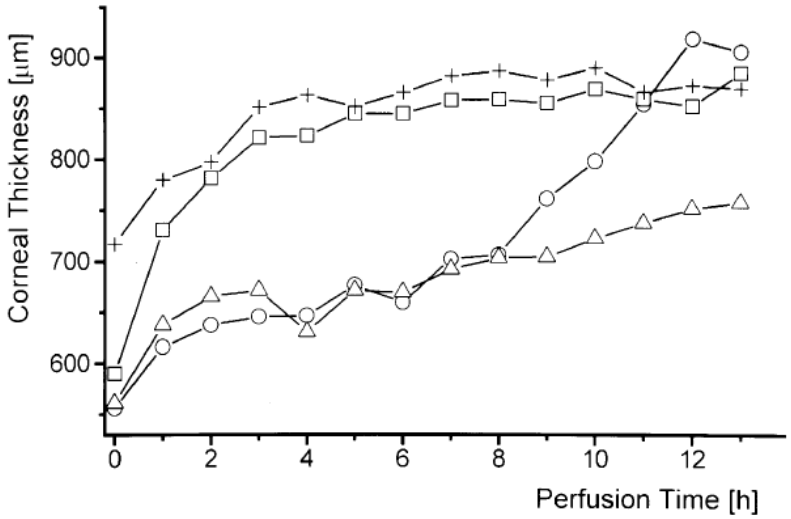


Figure 80. Mise en évidence de l'activité de pompe Na^+/K^+ATPase dans la déturgescence par les cellules immortalisées (Aboalchamat et al. 1999). En absence de l'endothélium (+), la cornée gonfle dès le début de la perfusion. Pour les cornées ensemmencées avec des cellules immortalisées: en présence de ouabain durant la déturgescence initiale (carré), la cornée gonfle également très rapidement. En absence de ouabain (triangle), la cornée gonfle légèrement. En introduisant de l'ouabain dans le milieu durant la perfusion (rond), l'épaisseur de la cornée augmente progressivement

En dehors de cette exception déjà ancienne, aucune autre équipe n'a reproduit ce montage experimental. Les travaux les plus récents (Liu *et al.* 2012; Yokoi *et al.* 2012; Bi *et al.* 2013; Hatou *et al.* 2013) utilisent un critère de substitution (surrogate criterion) qui est la mesure de la tension transcellulaire générée par le transport actif d'une monocouche de CE intacte. Cette mesure se fait dans une chamber de Ussing

(Figure 81). Il s'agit d'un montage de deux compartiments communiquant uniquement via une monocouche cellulaire. Le transport actif des cations et anion par les cellules entraîne une différence de potentiel entre les deux compartiments. Ce système dispose d'électrodes sensibles au voltage et qui sont au contact avec les 2 compartiments pour mesurer cette différence de potentiel en mV. Cette tension transmembranaire peut être égalisée par la formation d'un court-circuit à partir des 2 autres électrodes reliants ces 2 compartiments. Un microampèremètre permet de chiffrer le courant compensateur pour remettre la différence de potentiel à 0 mV. Ainsi, le transport actif par les cellules est estimé par deux paramètres : la différence de potentiel en mV et l'intensité du courant de court-circuit compensateur en µA.

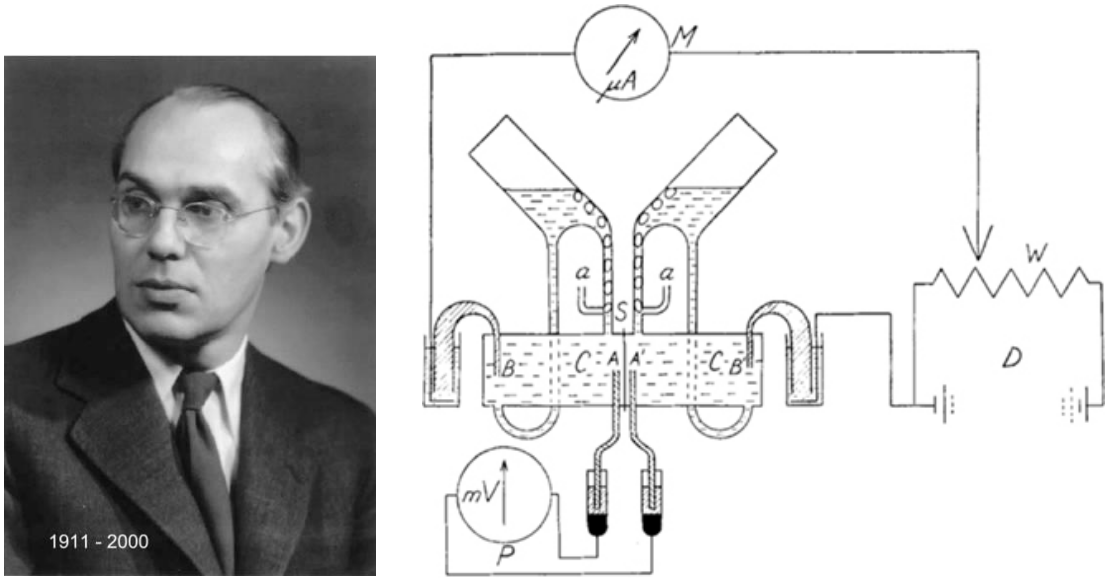


Figure 81. Diagramme de la chambre d'Ussing. A, A': électrodes sensibles au voltage. a : ligne d'air pour aérer le flux. B, B': electrodes générant un courant. C: deux compartiments. S: interface entre les deux compartiments, à laquelle se positionnent des cellules en monocouche. D: batterie, W: potentiel d'ajustement du voltage à 0 mV entre les deux compartiments (court circuit). P: potentiomètre. Tout courant compensant le potentiel des deux compartiements est mesuré par le microampèremètre M n µA reflète le transport actif à travers S. La chambre d'Ussing a été inventée par Ussing (photo de gauche) et Zerahn en 1951 (Hamilton 2011).

Récemment, notre laboratoire BiiGC a breveté un bioréacteur cornéen (Figure 82) qui permettra de réaliser l'étude de la fonctionalité des CE obtenues sur cornée humaine en combinant l'étude de la déturgescence par mapping OCT de l'épaisseur de l'ensemble de la cornée recellularisée, l'étude de sa transparence, l'étude de sa DCE (comptage par microscopie spéculaire ou microsopie en lumière transmise classique) et l'étude de la résistance trans-cornéenne (équivalent à la chambre de Ussing). Des ports d'entrée stériles permettront d'injecter au contact de l'endothélium de la ouabaine pour

vérifier l'arrêt de la pompe et conformer aisni le rôle du néo-endothélium dans la déturgescence observée.

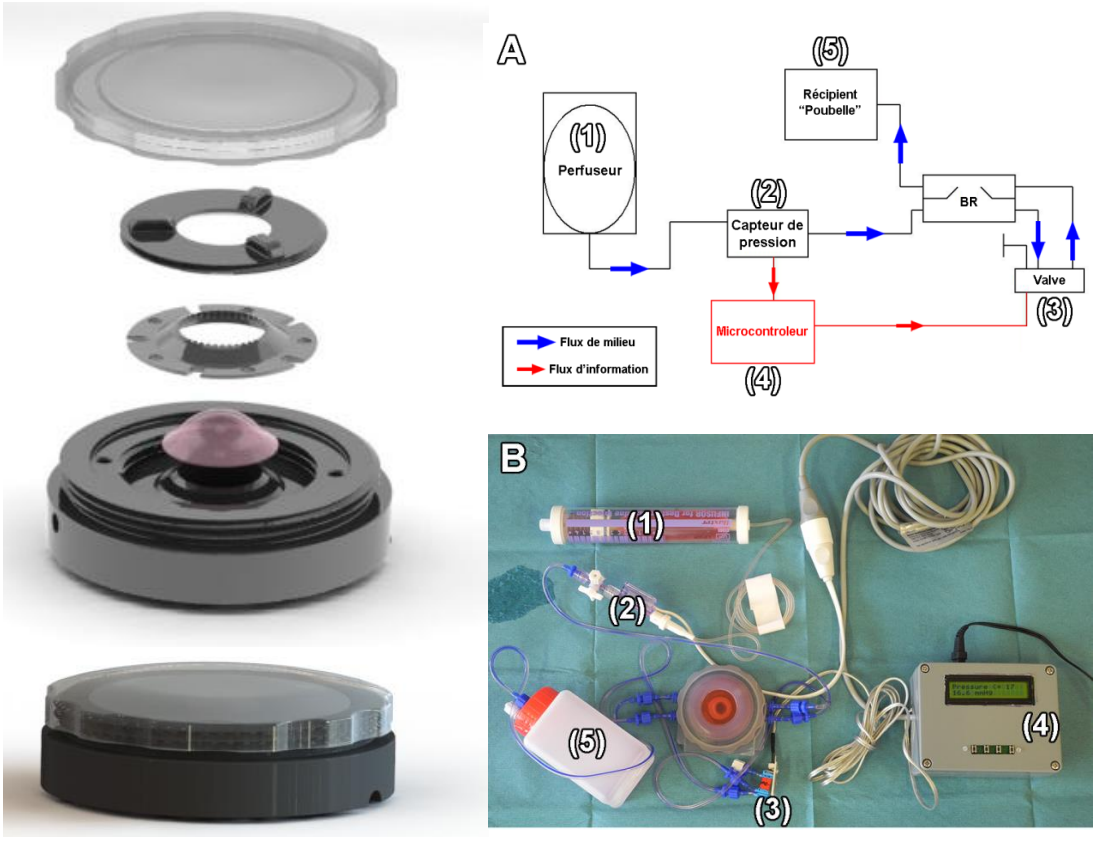


Figure 82. Conception du bioréacteur dédié au greffon cornéen (gauche) et la station de contrôle (droite) permettant de mimer la pression et le flux exercés sur l'endothélium cornéen à partir de la chambre antérieure (EA2521 BiiGC, Université Jean Monnet, Saint Etienne).

Enfin d'autres equipes valident leur production cellulaire par des expérimentations animales essentiellement sur le lapin et le primate. Ces modèles considérés de façon abstraite comme non proliférants ont subit des lésions endothéliales artificielles par cryocongélation transcornéennne ou par grattage. Les cellules en suspension ou cultivées sur des supports biocompatibles (voir Table 1) sont introduites via la chambre antérieure afin d'évaluer leur capacité de déturger la cornée comparant à l'oeil contrôle dont la cornée sera oedémateuse en absence de mécanisme de déturgescence (Okumura *et al.* 2011).

REFERENCES BIBLIOGRAPHIQUES

Aboalchamat B, Engelmann K, Bohnke M, Eggli P , Bednarz J (1999). Morphological and functional analysis of immortalized human corneal endothelial cells after transplantation. *Experimental eye research*. 69, 547-553.

Acquart S, Campolmi N, He Z, Pataia G, Jullienne R, Garraud O, Nguyen F, Peoc'h M, Lepine T, Thuret G , Gain P (2013). Non-invasive measurement of transparency, arcus senilis, and scleral rim diameter of corneas during eye banking. *Cell and tissue banking*.

Barouki R (2006). [Ageing free radicals and cellular stress]. *Medecine sciences : M/S*. 22, 266-272.

Bayyoud T, Thaler S, Hofmann J, Maurus C, Spitzer MS, Bartz-Schmidt KU, Szurman P , Yoeruek E (2012). Decellularized bovine corneal posterior lamellae as carrier matrix for cultivated human corneal endothelial cells. *Current eye research*. 37, 179-186.

Bednarz J, Teifel M, Friedl P , Engelmann K (2000). Immortalization of human corneal endothelial cells using electroporation protocol optimized for human corneal endothelial and human retinal pigment epithelial cells. *Acta ophthalmologica Scandinavica*. 78, 130-136.

Bi YL, Zhou Q, Du F, Wu MF, Xu GT , Sui GQ (2013). Regulation of functional corneal endothelial cells isolated from sphere colonies by Rho-associated protein kinase inhibitor. *Experimental and therapeutic medicine*. 5, 433-437.

Blitzer AL, Panagis L, Gusella GL, Danias J, Mlodzik M , Iomini C (2011). Primary cilia dynamics instruct tissue patterning and repair of corneal endothelium. *Proceedings of the National Academy of Sciences of the United States of America*. 108, 2819-2824.

Bonanno JA (2003). Identity and regulation of ion transport mechanisms in the corneal endothelium. *Progress in retinal and eye research*. 22, 69-94.

Bonanno JA (2012). Molecular mechanisms underlying the corneal endothelial pump. *Experimental eye research*. 95, 2-7.

Bonanno JA, Guan Y, Jelamskii S , Kang XJ (1999). Apical and basolateral CO2-HCO3- permeability in cultured bovine corneal endothelial cells. *The American journal of physiology*. 277, C545-553.

Bourne WM, Nelson LR , Hodge DO (1997). Central corneal endothelial cell changes over a ten-year period. *Investigative ophthalmology & visual science*. 38, 779-782.

Chen Y, Huang K, Nakatsu MN, Xue Z, Deng SX , Fan G (2013). Identification of novel molecular markers through transcriptomic analysis in human fetal and adult corneal endothelial cells. *Human molecular genetics*. 22, 1271-1279.

Cheong YK, Ngoh ZX, Peh GS, Ang HP, Seah XY, Chng Z, Colman A, Mehta JS , Sun W (2013). Identification of cell surface markers glypican-4 and CD200 that differentiate human corneal endothelium from stromal fibroblasts. *Investigative ophthalmology & visual science*. 54, 4538-4547.

Chng Z, Peh GS, Herath WB, Cheng TY, Ang HP, Toh KP, Robson P, Mehta JS , Colman A (2013). High throughput gene expression analysis identifies reliable expression markers of human corneal endothelial cells. *PloS one*. 8, e67546.

Choi JS, Kim EY, Kim MJ, Giegengack M, Khan FA, Khang G , Soker S (2013). In vitro evaluation of the interactions between human corneal endothelial cells and extracellular matrix proteins. *Biomed Mater*. 8, 014108.

Choi JS, Williams JK, Greven M, Walter KA, Laber PW, Khang G , Soker S (2010). Bioengineering endothelialized neo-corneas using donor-derived corneal endothelial cells and decellularized corneal stroma. *Biomaterials*. 31, 6738-6745.

Chowdhury UR, Madden BJ, Charlesworth MC , Fautsch MP (2010). Proteome analysis of human aqueous humor. *Investigative ophthalmology & visual science*. 51, 4921-4931.

Cook CS, Victoria O , Jakobiec FA (2006). Ocular Anatomy, Embryology, and Teratology - Chapter 2: Prenatal development of the eye and its adnexa. *Duane's Ophthalmology*. 1.

Crooke A, Guzman-Aranguez A, Peral A, Abdurrahman MK , Pintor J (2008). Nucleotides in ocular secretions: their role in ocular physiology. *Pharmacology & therapeutics*. 119, 55-73.

Diecke FP, Wen Q, Iserovich P, Li J, Kuang K , Fischbarg J (2005). Regulation of Na-K-2Cl cotransport in cultured bovine corneal endothelial cells. *Experimental eye research*. 80, 777-785.

Doughty MJ , Zaman ML (2000). Human corneal thickness and its impact on intraocular pressure measures: a review and meta-analysis approach. *Survey of ophthalmology*. 44, 367-408.

Dua HS, Faraj LA, Said DG, Gray T , Lowe J (2013). Human corneal anatomy redefined: a novel pre-Descemet's layer (Dua's layer). *Ophthalmology*. 120, 1778-1785.

Fischbarg J, Diecke FP, Iserovich P , Rubashkin A (2006). The Role of the Tight Junction in Paracellular Fluid Transport across Corneal Endothelium. Electro-osmosis as a Driving Force. *The Journal of membrane biology*. 210, 117-130.

Foets BJ, van den Oord JJ, Volpes R , Missotten L (1992). In situ immunohistochemical analysis of cell adhesion molecules on human corneal endothelial cells. *The British journal of ophthalmology*. 76, 205-209.

Fokina VM , Frolova EI (2006). Expression patterns of Wnt genes during development of an anterior part of the chicken eye. *Developmental dynamics : an official publication of the American Association of Anatomists*. 235, 496-505.

Fuchsluger TA, Jurkunas U, Kazlauskas A , Dana R (2011a). Anti-apoptotic gene therapy prolongs survival of corneal endothelial cells during storage. *Gene therapy*. 18, 778-787.

Fuchsluger TA, Jurkunas U, Kazlauskas A , Dana R (2011b). Corneal endothelial cells are protected from apoptosis by gene therapy. *Human gene therapy*. 22, 549-558.

Fuhrmann S (2010). Eye morphogenesis and patterning of the optic vesicle. *Current topics in developmental biology*. 93, 61-84.

Gage PJ, Qian M, Wu D , Rosenberg KI (2008). The canonical Wnt signaling antagonist DKK2 is an essential effector of PITX2 function during normal eye development. *Developmental biology*. 317, 310-324.

Gammill LS, Gonzalez C, Gu C , Bronner-Fraser M (2006). Guidance of trunk neural crest migration requires neuropilin 2/semaphorin 3F signaling. *Development*. 133, 99-106.

Geroski DH , Edelhauser HF (1984). Quantitation of Na/K ATPase pump sites in the rabbit corneal endothelium. *Investigative ophthalmology & visual science*. 25, 1056-1060.

Geroski DH, Matsuda M, Yee RW , Edelhauser HF (1985). Pump function of the human corneal endothelium. Effects of age and cornea guttata. *Ophthalmology*. 92, 759-763.

Goel M, Picciani RG, Lee RK , Bhattacharya SK (2010). Aqueous humor dynamics: a review. *The open ophthalmology journal*. 4, 52-59.

Grus FH, Joachim SC , Pfeiffer N (2007). Proteomics in ocular fluids. *Proteomics. Clinical applications*. 1, 876-888.

Hamilton KL (2011). Ussing's "Little Chamber": 60 Years+ Old and Counting. *Frontiers in physiology*. 2, 6.

Haque N, Rahman MT, Abu Kasim NH , Alabsi AM (2013). Hypoxic culture conditions as a solution for mesenchymal stem cell based regenerative therapy. *TheScientificWorldJournal*. 2013, 632972.

Hassell JR , Birk DE (2010). The molecular basis of corneal transparency. *Experimental eye research*. 91, 326-335.

Hatou S, Yoshida S, Higa K, Miyashita H, Inagaki E, Okano H, Tsubota K , Shimmura S (2013). Functional corneal endothelium derived from corneal stroma stem cells of neural crest origin by retinoic acid and Wnt/beta-catenin signaling. *Stem cells and development*. 22, 828-839.

He Z, Campolmi N, Gain P, Ha Thi BM, Dumollard JM, Duband S, Peoc'h M, Piselli S, Garraud O , Thuret G (2012). Revisited microanatomy of the corneal endothelial periphery: new evidence for continuous centripetal migration of endothelial cells in humans. *Stem Cells*. 30, 2523-2534.

Hirata-Tominaga K, Nakamura T, Okumura N, Kawasaki S, Kay EP, Barrandon Y, Koizumi N , Kinoshita S (2013). Corneal endothelial cell fate is maintained by LGR5 through the regulation of hedgehog and Wnt pathway. *Stem Cells*. 31, 1396-1407.

Hsiue GH, Lai JY, Chen KH , Hsu WM (2006). A novel strategy for corneal endothelial reconstruction with a bioengineered cell sheet. *Transplantation*. 81, 473-476.

Hu W, Haamedi N, Lee J, Kinoshita T , Ohnuma SI (2013). The structure and development of Xenopus laevis cornea. *Experimental eye research*. 116C, 109-128.

Ishino Y, Sano Y, Nakamura T, Connon CJ, Rigby H, Fullwood NJ , Kinoshita S (2004). Amniotic membrane as a carrier for cultivated human corneal endothelial cell transplantation. *Investigative ophthalmology & visual science*. 45, 800-806.

Jackel T, Knels L, Valtink M, Funk RH , Engelmann K (2011). Serum-free corneal organ culture medium (SFM) but not conventional minimal essential organ culture medium (MEM) protects human corneal endothelial cells from apoptotic and necrotic cell death. *The British journal of ophthalmology*. 95, 123-130.

Jentsch TJ, Stahlknecht TR, Hollwede H, Fischer DG, Keller SK , Wiederholt M (1985). A bicarbonate-dependent process inhibitable by disulfonic stilbenes and a Na+/H+ exchange mediate 22Na+ uptake into cultured bovine corneal endothelium. *The Journal of biological chemistry*. 260, 795-801.

Jin EJ, Burrus LW , Erickson CA (2002). The expression patterns of Wnts and their antagonists during avian eye development. *Mechanisms of development*. 116, 173-176.

Joko T, Shiraishi A, Akune Y, Tokumaru S, Kobayashi T, Miyata K , Ohashi Y (2013). Involvement of P38MAPK in human corneal endothelial cell migration induced by TGF-beta(2). *Experimental eye research*. 108, 23-32.

Joshi-Tope G, Gillespie M, Vastrik I, D'Eustachio P, Schmidt E, de Bono B, Jassal B, Gopinath GR, Wu GR, Matthews L, Lewis S, Birney E , Stein L (2005). Reactome: a knowledgebase of biological pathways. *Nucleic acids research*. 33, D428-432.

Joyce NC (2012). Proliferative capacity of corneal endothelial cells. *Experimental eye research*. 95, 16-23.

Joyce NC , Harris DL (2010). Decreasing expression of the G1-phase inhibitors, p21Cip1 and p16INK4a, promotes division of corneal endothelial cells from older donors. *Molecular vision*. 16, 897-906.

Joyce NC, Harris DL, Markov V, Zhang Z , Saitta B (2012). Potential of human umbilical cord blood mesenchymal stem cells to heal damaged corneal endothelium. *Molecular vision*. 18, 547-564.

Joyce NC, Zhu CC , Harris DL (2009). Relationship among oxidative stress, DNA damage, and proliferative capacity in human corneal endothelium. *Investigative ophthalmology & visual science*. 50, 2116-2122.

Ju C, Gao L, Wu X , Pang K (2012). A human corneal endothelium equivalent constructed with acellular porcine corneal matrix. *The Indian journal of medical research*. 135, 887-894.

Kabosova A, Azar DT, Bannikov GA, Campbell KP, Durbeej M, Ghohestani RF, Jones JC, Kenney MC, Koch M, Ninomiya Y, Patton BL, Paulsson M, Sado Y, Sage EH, Sasaki T, Sorokin LM, Steiner-Champliaud MF, Sun TT, Sundarraj N, Timpl R, Virtanen I , Ljubimov AV (2007). Compositional differences between infant and adult human corneal basement membranes. *Investigative ophthalmology & visual science*. 48, 4989-4999.

Kanehisa M , Goto S (2000). KEGG: kyoto encyclopedia of genes and genomes. *Nucleic acids research*. 28, 27-30.

Kanehisa M, Goto S, Sato Y, Furumichi M , Tanabe M (2012). KEGG for integration and interpretation of large-scale molecular data sets. *Nucleic acids research*. 40, D109-114.

Kao WW, Liu H , Zhang J (2013). Wakayama symposium: challenges of future research in ocular surface cell biology. *The ocular surface*. 11, 19-24.

Kiel JW, Hollingsworth M, Rao R, Chen M , Reitsamer HA (2011). Ciliary blood flow and aqueous humor production. *Progress in retinal and eye research*. 30, 1-17.

Kikuchi M, Zhu C, Senoo T, Obara Y , Joyce NC (2006). p27kip1 siRNA induces proliferation in corneal endothelial cells from young but not older donors. *Investigative ophthalmology & visual science*. 47, 4803-4809.

Koo HY , Kume T (2013). FoxC1-dependent regulation of vascular endothelial growth factor signaling in corneal avascularity. *Trends in cardiovascular medicine*. 23, 1-4.

Kumar S , Duester G (2010). Retinoic acid signaling in perioptic mesenchyme represses Wnt signaling via induction of Pitx2 and Dkk2. *Developmental biology*. 340, 67-74.

Lai JY, Lu PL, Chen KH, Tabata Y , Hsiue GH (2006). Effect of charge and molecular weight on the functionality of gelatin carriers for corneal endothelial cell therapy. *Biomacromolecules*. 7, 1836-1844.

Lai JY, Ma DH, Lai MH, Li YT, Chang RJ , Chen LM (2013). Characterization of cross-linked porous gelatin carriers and their interaction with corneal endothelium: biopolymer concentration effect. *PloS one*. 8, e54058.

Lee JG , Heur M (2013). Interleukin-1beta enhances cell migration through AP-1 and NF-kappaB pathway-dependent FGF2 expression in human corneal endothelial cells. *Biology of the cell / under the auspices of the European Cell Biology Organization*. 105, 175-189.

Leung EW, Rife L, Smith RE , Kay EP (2000). Extracellular matrix components in retrocorneal fibrous membrane in comparison to corneal endothelium and Descemet's membrane. *Molecular vision*. 6, 15-23.

Levis HJ, Peh GS, Toh KP, Poh R, Shortt AJ, Drake RA, Mehta JS , Daniels JT (2012). Plastic compressed collagen as a novel carrier for expanded human corneal endothelial cells for transplantation. *PloS one*. 7, e50993.

Levy SG, McCartney AC, Sawada H, Dopping-Hepenstal PJ, Alexander RA , Moss J (1995). Descemet's membrane in the iridocorneal-endothelial syndrome: morphology and composition. *Experimental eye research*. 61, 323-333.

Li J, Allen KT, Sun XC, Cui M , Bonanno JA (2008). Dependence of cAMP meditated increases in Cl- and HCO(3)- permeability on CFTR in bovine corneal endothelial cells. *Experimental eye research*. 86, 684-690.

Li J, Sun XC , Bonanno JA (2005). Role of NBC1 in apical and basolateral HCO3- permeabilities and transendothelial HCO3- fluxes in bovine corneal endothelium. *American journal of physiology. Cell physiology*. 288, C739-746.

Liu P , Johnson RL (2010). Lmx1b is required for murine trabecular meshwork formation and for maintenance of corneal transparency. *Developmental dynamics : an official publication of the American Association of Anatomists*. 239, 2161-2171.

Liu Z, Zhuang J, Li C, Wan P, Li N, Zhou Q, Zhou C, Huang Z , Wang Z (2012). Long-term cultivation of human corneal endothelial cells by telomerase expression. *Experimental eye research*. 100, 40-51.

Lwigale PY , Bronner-Fraser M (2009). Semaphorin3A/neuropilin-1 signaling acts as a molecular switch regulating neural crest migration during cornea development. *Developmental biology*. 336, 257-265.

Matthews L, Gopinath G, Gillespie M, Caudy M, Croft D, de Bono B, Garapati P, Hemish J, Hermjakob H, Jassal B, Kanapin A, Lewis S, Mahajan S, May B, Schmidt E, Vastrik I, Wu G, Birney E, Stein L , D'Eustachio P (2009). Reactome knowledgebase of human biological pathways and processes. *Nucleic acids research*. 37, D619-622.

Maurice DM (1972). The location of the fluid pump in the cornea. *The Journal of physiology*. 221, 43-54.

McAlister JC, Joyce NC, Harris DL, Ali RR , Larkin DF (2005). Induction of replication in human corneal endothelial cells by E2F2 transcription factor cDNA transfer. *Investigative ophthalmology & visual science*. 46, 3597-3603.

McGowan SL, Edelhauser HF, Pfister RR , Whikehart DR (2007). Stem cell markers in the human posterior limbus and corneal endothelium of unwounded and wounded corneas. *Molecular vision*. 13, 1984-2000.

McKenna CC, Munjaal RP , Lwigale PY (2012). Distinct roles for neuropilin1 and neuropilin2 during mouse corneal innervation. *PloS one*. 7, e37175.

Mergler S , Pleyer U (2007). The human corneal endothelium: new insights into electrophysiology and ion channels. *Progress in retinal and eye research*. 26, 359-378.

Mergler S, Valtink M, Taetz K, Sahlmuller M, Fels G, Reinach PS, Engelmann K , Pleyer U (2011). Characterization of transient receptor potential vanilloid channel 4 (TRPV4) in human corneal endothelial cells. *Experimental eye research*. 93, 710-719.

Mimura T , Joyce NC (2006). Replication competence and senescence in central and peripheral human corneal endothelium. *Investigative ophthalmology & visual science*. 47, 1387-1396.

Mimura T, Yamagami S , Amano S (2013). Corneal endothelial regeneration and tissue engineering. *Progress in retinal and eye research*. 35, 1-17.

Mimura T, Yamagami S, Yokoo S, Usui T , Amano S (2010). Selective isolation of young cells from human corneal endothelium by the sphere-forming assay. *Tissue engineering. Part C, Methods*. 16, 803-812.

Mimura T, Yamagami S, Yokoo S, Usui T, Tanaka K, Hattori S, Irie S, Miyata K, Araie M , Amano S (2004). Cultured human corneal endothelial cell transplantation with a collagen sheet in a rabbit model. *Investigative ophthalmology & visual science*. 45, 2992-2997.

Moller-Pedersen T (1997). A comparative study of human corneal keratocyte and endothelial cell density during aging. *Cornea*. 16, 333-338.

Murphy C, Alvarado J, Juster R , Maglio M (1984). Prenatal and postnatal cellularity of the human corneal endothelium. A quantitative histologic study. *Investigative ophthalmology & visual science*. 25, 312-322.

Nau CB, Malihi M, McLaren JW, Hodge DO , Sit AJ (2013). Circadian Variation of Aqueous Humor Dynamics in Older Healthy Adults. *Investigative ophthalmology & visual science*.

Nguyen TT , Bonanno JA (2011). Bicarbonate, NBCe1, NHE, and carbonic anhydrase activity enhance lactate-H+ transport in bovine corneal endothelium. *Investigative ophthalmology & visual science*. 52, 8086-8093.

NIH (2009). Appendix A: Early Development. In Stem Cell Information [World Wide Web site]. Bethesda, MD: National Institutes of Health, U.S. Department of Health and Human Services, 2009 Available at <http://stemcells.nih.gov/info/scireport/pages/appendixa.aspx%3Eed%5Eeds): National Institutes of Health.

Ohkawa K, Saika S, Hayashi Y, Tawara A , Ohnishi Y (2003). Cornea with Peters' anomaly: perturbed differentiation of corneal cells and abnormal extracellular matrix in the corneal stroma. *Japanese journal of ophthalmology*. 47, 327-331.

Okumura N, Koizumi N, Ueno M, Sakamoto Y, Takahashi H, Hirata K, Torii R, Hamuro J , Kinoshita S (2011). Enhancement of corneal endothelium wound healing by Rho-associated kinase (ROCK) inhibitor eye drops. *The British journal of ophthalmology*. 95, 1006-1009.

Okumura N, Ueno M, Koizumi N, Sakamoto Y, Hirata K, Hamuro J , Kinoshita S (2009). Enhancement on primate corneal endothelial cell survival in vitro by a ROCK inhibitor. *Investigative ophthalmology & visual science*. 50, 3680-3687.

Pastrana E, Silva-Vargas V , Doetsch F (2011). Eyes wide open: a critical review of sphere-formation as an assay for stem cells. *Cell stem cell*. 8, 486-498.

Paull AC , Whikehart DR (2005). Expression of the p53 family of proteins in central and peripheral human corneal endothelial cells. *Molecular vision*. 11, 328-334.

Peh GS, Toh KP, Ang HP, Seah XY, George BL , Mehta JS (2013). Optimization of human corneal endothelial cell culture: density dependency of successful cultures in vitro. *BMC research notes*. 6, 176.

Peh GS, Toh KP, Wu FY, Tan DT , Mehta JS (2011). Cultivation of human corneal endothelial cells isolated from paired donor corneas. *PloS one*. 6, e28310.

Pinnamaneni N , Funderburgh JL (2012). Concise review: Stem cells in the corneal stroma. *Stem Cells*. 30, 1059-1063.

Pipparelli A, Arsenijevic Y, Thuret G, Gain P, Nicolas M , Majo F (2013). ROCK inhibitor enhances adhesion and wound healing of human corneal endothelial cells. *PloS one*. 8, e62095.

Reneker LW, Silversides DW, Xu L , Overbeek PA (2000). Formation of corneal endothelium is essential for anterior segment development - a transgenic mouse model of anterior segment dysgenesis. *Development*. 127, 533-542.

Sacca SC , Izzotti A (2013). Focus on molecular events in the anterior chamber leading to glaucoma. *Cellular and molecular life sciences : CMLS*.

Sawada H, Konomi H , Hirosawa K (1990). Characterization of the collagen in the hexagonal lattice of Descemet's membrane: its relation to type VIII collagen. *The Journal of cell biology*. 110, 219-227.

Schmedt T, Chen Y, Nguyen TT, Li S, Bonanno JA , Jurkunas UV (2012). Telomerase immortalization of human corneal endothelial cells yields functional hexagonal monolayers. *PloS one*. 7, e51427.

Schmitt CA (2007). Cellular senescence and cancer treatment. *Biochimica et biophysica acta*. 1775, 5-20.

Sheerin AN, Smith SK, Jennert-Burston K, Brook AJ, Allen MC, Ibrahim B, Jones D, Wallis C, Engelmann K, Rhys-Williams W, Faragher RG , Kipling D (2012). Characterization of cellular senescence mechanisms in human corneal endothelial cells. *Aging cell*. 11, 234-240.

Shima N, Kimoto M, Yamaguchi M , Yamagami S (2011). Increased proliferation and replicative lifespan of isolated human corneal endothelial cells with L-ascorbic acid 2-phosphate. *Investigative ophthalmology & visual science*. 52, 8711-8717.

Shin YJ, Cho DY, Chung TY, Han SB, Hyon JY , Wee WR (2011a). Rapamycin reduces reactive oxygen species in cultured human corneal endothelial cells. *Current eye research*. 36, 1116-1122.

Shin YJ, Seo JM, Chung TY, Hyon JY , Wee WR (2011b). Effect of cysteamine on oxidative stress-induced cell death of human corneal endothelial cells. *Current eye research*. 36, 910-917.

Singh JS, Haroldson TA , Patel SP (2013). Characteristics of the low density corneal endothelial monolayer. *Experimental eye research*. 115, 239-245.

Srinivas SP (2010). Dynamic regulation of barrier integrity of the corneal endothelium. *Optometry and vision science : official publication of the American Academy of Optometry*. 87, E239-254.

Srinivas SP (2012). Cell signaling in regulation of the barrier integrity of the corneal endothelium. *Experimental eye research*. 95, 8-15.

Sun XC , Bonanno JA (2002). Expression, localization, and functional evaluation of CFTR in bovine corneal endothelial cells. *American journal of physiology. Cell physiology*. 282, C673-683.

Swamynathan SK (2013). Ocular surface development and gene expression. *Journal of ophthalmology*. 2013, 103947.

Takahashi K , Yamanaka S (2006). Induction of pluripotent stem cells from mouse embryonic and adult fibroblast cultures by defined factors. *Cell*. 126, 663-676.

Teo BK, Goh KJ, Ng ZJ, Koo S , Yim EK (2012). Functional reconstruction of corneal endothelium using nanotopography for tissue-engineering applications. *Acta biomaterialia*. 8, 2941-2952.

Thorin-Trescases N, Voghel G, Farhat N, Drouin A, Gendron ME , Thorin E (2010). [Age-dependent oxidative stress: toward an irreversible failure in endothelial maintenance]. *Medecine sciences : M/S*. 26, 875-880.

Tripathi BJ, Tripathi RC, Livingston AM , Borisuth NS (1991). The role of growth factors in the embryogenesis and differentiation of the eye. *The American journal of anatomy*. 192, 442-471.

Valavanidis A, Vlachogianni T , Fiotakis C (2009). 8-hydroxy-2' -deoxyguanosine (8-OHdG): A critical biomarker of oxidative stress and carcinogenesis. *Journal of environmental science and health. Part C, Environmental carcinogenesis & ecotoxicology reviews*. 27, 120-139.

Valtink M, Gruschwitz R, Funk RH , Engelmann K (2008). Two clonal cell lines of immortalized human corneal endothelial cells show either differentiated or precursor cell characteristics. *Cells, tissues, organs*. 187, 286-294.

Vastrik I, D'Eustachio P, Schmidt E, Gopinath G, Croft D, de Bono B, Gillespie M, Jassal B, Lewis S, Matthews L, Wu G, Birney E , Stein L (2007). Reactome: a knowledge base of biologic pathways and processes. *Genome biology*. 8, R39.

Wang TJ, Wang IJ, Lu JN , Young TH (2012). Novel chitosan-polycaprolactone blends as potential scaffold and carrier for corneal endothelial transplantation. *Molecular vision*. 18, 255-264.

Watanabe R, Hayashi R, Kimura Y, Tanaka Y, Kageyama T, Hara S, Tabata Y , Nishida K (2011). A novel gelatin hydrogel carrier sheet for corneal endothelial transplantation. *Tissue engineering. Part A*. 17, 2213-2219.

Wen Q, Diecke FP, Iserovich P, Kuang K, Sparrow J , Fischbarg J (2001). Immunocytochemical localization of aquaporin-1 in bovine corneal endothelial cells and keratocytes. *Exp Biol Med (Maywood)*. 226, 463-467.

Whikehart DR, Parikh CH, Vaughn AV, Mishler K , Edelhauser HF (2005). Evidence suggesting the existence of stem cells for the human corneal endothelium. *Molecular vision*. 11, 816-824.

Wilson SE, Weng J, Blair S, He YG , Lloyd S (1995). Expression of E6/E7 or SV40 large T antigen-coding oncogenes in human corneal endothelial cells indicates regulated high-proliferative capacity. *Investigative ophthalmology & visual science*. 36, 32-40.

Wion D, Dematteis M, Nissou MF, Cretallaz C, Berger F , Issartel JP (2008). [Oxygen tension and cancer-cell culture: half a century of artifacts?]. *Medecine sciences : M/S*. 24, 1093-1095.

Yamagami S, Yokoo S, Mimura T, Takato T, Araie M , Amano S (2007). Distribution of precursors in human corneal stromal cells and endothelial cells. *Ophthalmology*. 114, 433-439.

Yoeruek E, Saygili O, Spitzer MS, Tatar O, Bartz-Schmidt KU , Szurman P (2009). Human anterior lens capsule as carrier matrix for cultivated human corneal endothelial cells. *Cornea*. 28, 416-420.

Yokoi T, Seko Y, Yokoi T, Makino H, Hatou S, Yamada M, Kiyono T, Umezawa A, Nishina H , Azuma N (2012). Establishment of functioning human corneal endothelial cell line with high growth potential. *PloS one*. 7, e29677.

Yokoo S, Yamagami S, Yanagi Y, Uchida S, Mimura T, Usui T , Amano S (2005). Human corneal endothelial cell precursors isolated by sphere-forming assay. *Investigative ophthalmology & visual science*. 46, 1626-1631.

Yu WY, Sheridan C, Grierson I, Mason S, Kearns V, Lo AC , Wong D (2011). Progenitors for the corneal endothelium and trabecular meshwork: a potential

source for personalized stem cell therapy in corneal endothelial diseases and glaucoma. *Journal of biomedicine & biotechnology*. 2011, 412743.

Yuan Y, Yeh LK, Liu H, Yamanaka O, Hardie WD, Kao WW , Liu CY (2013). Targeted overexpression of TGF-alpha in the corneal epithelium of adult transgenic mice induces changes in anterior segment morphology and activates noncanonical Wnt signaling. *Investigative ophthalmology & visual science*. 54, 1829-1837.

Zhang Y, Li J, Xie Q , Bonanno JA (2006). Molecular expression and functional involvement of the bovine calcium-activated chloride channel 1 (bCLCA1) in apical HCO3- permeability of bovine corneal endothelium. *Experimental eye research*. 83, 1215-1224.

PARTIE EXPERIMENTALE

Articles en premier auteur

ARTICLE I: Microarray analysis of cell cycle gene expression in adult human corneal endothelium cells

Un des prérequis pour optimiser les cultures primaires des cellules endothéliales cornéennes humaines est la compréhension des mécanismes qui aboutissent à l'arrêt du cycle cellulaire chez l'humain. De nombreux travaux ont été réalisés depuis les années 90, à la suite des travaux principaux de N. Joyce qui a démontré le blocage en début de phase G1 et le potentiel prolifératif résiduel. Aucun des travaux réalisé jusque là n'avait cependant utilisé de microarrays spécifiques du cycle cellulaire pour étudier en une fois un ensemble de transcripts présent dans les CEs. Nous l'avons fait en apportant une originalité supplémentaire en comparant les profils de transcription de 112 gènes (dont 62 impliquées directement dans les différentes phases du cycle) dans 6 modèles biologiques choisis pour avoir un stimulus prolifératif croissant: in vivo sur l'endothélium central de cornées recueillies immédiatement après trépanation lors d'une greffe pour kératocône (modèle jamais utilisée dans la littérature et servant ici de référence), post mortem dans lequel le stress maximal pourrait induire des stimuli «ultimes», conservation en organoculture en milieu contenant 2% de sérum de veau fœtal connue pour induire des lésions endothéliales limitées et permettre un certain degré de cicatrisation, cultures primaires in vitro confluentes avec inhibition de contact, culture primaires non confluente et donc en cours de prolifération, et lignée cellulaire commerciale immortalisée par transfection avec SV40LT.

Les résultats des microarrays ont été vérifiés par qRT-PCR sur 11 gènes choisis.

Nos résultats sont cohérents avec la littérature, compatible avec un arrêt en phase G1 et un état de sénescence due à des dommages à l'ADN; nous mettons en évidence la présence de certains transcrits jamais mis en évidence jusque là comme DIRAS3. Certains d'entre eux pourraient devenir des cibles directes d'intervention destinées à contourner la sénescence ex vivo ou in vitro ou servir de marqueurs pour évaluer l'impact d'autres méthodes de contournement impliquant des petites molécules ou l'interférence ARN.

PLOS ONE

Microarray Analysis of Cell Cycle Gene Expression in Adult Human Corneal Endothelial Cells

--Manuscript Draft--

Manuscript Number:	PONE-D-13-54951
Article Type:	Research Article
Full Title:	Microarray Analysis of Cell Cycle Gene Expression in Adult Human Corneal Endothelial Cells
Short Title:	cell cycle microarray of human corneal endothelium
Corresponding Author:	Gilles Thuret Faculty of Medicine Saint Etienne, FRANCE
Keywords:	human, cornea, endothelium, adult, cell cycle, microarrays, mRNA, DNA damage-induced, check-point, proliferation, senescence
Abstract:	Corneal endothelial cells (ECs) form a monolayer that controls the hydration of the cornea and thus its transparency. Their almost nil proliferative status in humans is responsible, in several frequent diseases, for cell pool attrition that leads to irreversible corneal clouding. To screen for candidate genes involved in cell cycle arrest, we studied human ECs subjected to various environments thought to induce different proliferative profiles compared to ECs in vivo. Donor corneas (a few hours after death), organ-cultured (OC) corneas, in vitro confluent and non-confluent primary cultures, and an immortalized EC line were compared to healthy ECs retrieved in the first minutes of corneal grafts. Transcriptional profiles were compared using a cDNA array of 112 key genes of the cell cycle and analysed using Gene Ontology classification; cluster analysis and gene map presentation of the cell cycle regulation pathway were performed by GenMAPP. Results were validated using qRT-PCR on 11 selected genes. We found several transcripts of proteins implicated in cell cycle arrest and not previously reported in human ECs. Early G1-phase arrest effectors and multiple DNA damage-induced cell cycle arrest-associated transcripts were found in vivo and over-represented in OC and in vitro ECs. Though highly proliferative, immortalized ECs also exhibited overexpression of transcripts implicated in cell cycle arrest. These new effectors likely explain the stress-induced premature senescence that characterizes human adult ECs. They are potential targets for triggering and controlling EC proliferation with a view to increasing the cell pool of stored corneas or facilitating mass EC culture for bioengineered endothelial grafts.
Order of Authors:	Binh Minh HA THI
	Nelly CAMPOLMI
	Zhiguo HE
	Aurélien PIPPARELLI
	Chloé MANISSOLLE
	Jean-Yves THURET
	Simone PISELLI
	Fabien FOREST
	Michel PEOC'H
	Olivier GARRAUD
	Philippe GAIN
	Gilles Thuret
Suggested Reviewers:	Alain BRON, M.D., Ph.D. University of Dijon alain.bron@chu-dijon.fr

Powered by Editorial Manager® and ProduXion Manager® from Aries Systems Corporation

	because of his expertise in the anatomy of the extreme corneal periphery
	Katrin ENGELMANN, M.D., Ph.D. Head of ophthalmology dpt, University of Dresden, Germany katrin.engelmann@uniklinikum-dresden.de In Europe, she is one of the ophthalmologists and scientists to best study strategies for overcoming the non proliferative status of ECs
	Nancy JOYCE, Ph.D. Schepens Eye Research Institute nancy.joyce@schepens.harvard.edu The one who elucidated the cell cycle arrest mechanism in human EC 20 years ago and regularly enriched the literature with rigorous works on this topic.
Opposed Reviewers:	
Additional Information:	
Question	**Response**
Competing Interest For yourself and on behalf of all the authors of this manuscript, please declare below any competing interests as described in the "PLoS Policy on Declaration and Evaluation of Competing Interests." You are responsible for recognizing and disclosing on behalf of all authors any competing interest that could be perceived to bias their work, acknowledging all financial support and any other relevant financial or competing interests. If no competing interests exist, enter: "The authors have declared that no competing interests exist." If you have competing interests to declare, please fill out the text box completing the following statement: "I have read the journal's policy and have the following conflicts" * typeset	The authors have declared that no competing interests exist.
Financial Disclosure Describe the sources of funding that have supported the work. Please include relevant grant numbers and the URL of any funder's website. Please also include this sentence: "The funders had no role in study design, data collection and analysis, decision to publish, or preparation of the manuscript." If this statement is not	Fondation de l'Avenir ET7-468, Agence de la Biomédecine 2013 projet 76. The funders had no role in study design, data collection and analysis, decision to publish, or preparation of the manuscript.

Powered by Editorial Manager® and ProduXion Manager® from Aries Systems Corporation

correct, you must describe the role of any sponsors or funders and amend the aforementioned sentence as needed. * typeset	
Ethics Statement All research involving human participants must have been approved by the authors' institutional review board or equivalent committee(s) and that board must be named by the authors in the manuscript. For research involving human participants, informed consent must have been obtained (or the reason for lack of consent explained, e.g. the data were analyzed anonymously) and all clinical investigation must have been conducted according to the principles expressed in the Declaration of Helsinki. Authors should submit a statement from their ethics committee or institutional review board indicating the approval of the research. We also encourage authors to submit a sample of a patient consent form and may require submission of completed forms on particular occasions. All animal work must have been conducted according to relevant national and international guidelines. In accordance with the recommendations of the Weatherall report, "The use of non-human primates in research" we specifically require authors to include details of animal welfare and steps taken to ameliorate suffering in all work involving non-human primates. The relevant guidelines followed and the committee that approved the study should be identified in the ethics statement. Please enter your ethics statement below and place the same text at the beginning of the Methods section of your manuscript (with the subheading Ethics Statement). Enter "N/A" if you do not require an ethics statement.	All procedures conformed to the tenets of the Declaration of Helsinki for biomedical research involving human subjects. Central corneal buttons removed as waste during surgery were collected as per the usual protocol in force in our University Hospital and by presumed consent further to the written information given to all admitted patients. This protocol was written by our Hospital's commission for clinical research and innovation and accepted by the local ethics committee (CPP Sud Est I, CHU Saint Etienne, Saint Etienne, France). Corneas assigned to scientific use were procured from bodies donated to science (Laboratory of Anatomy, Faculty of Medicine) as permitted by French law. Each donor volunteers their body and gives written consent to the Laboratory of Anatomy; no extra specific approval by the ethics committee is required.

Powered by Editorial Manager® and ProduXion Manager® from Aries Systems Corporation

Cover Letter

Dear Sir,

We are please to submit an original article entitled "**Microarray Analysis of Cell Cycle Gene Expression in Adult Human Corneal Endothelial Cells**" in *Plos One*.

The present research article analyzes, for the first time, the cell cycle gene transcripts of human corneal endothelial cells (EC) placed in different environments liable to alter their replication status. These cells are paramount in visual-system performance because they ensure stability of corneal transparency, but lack significant proliferative capacity in vivo in humans. In physiological conditions, the EC reserve is huge and, despite a gradual age-related decrease in EC density (ECD), a cornea could remain crystal clear for two centuries. Conversely, the situation becomes worrying when pathological mechanisms accelerate EC loss below a minimum threshold. The only solution is thus to replace the missing cells by new ones. To date retrieved from donors, these will probably soon be bioengineered.

The EC cycle has partly been elucidated, mainly by Nancy Joyce's team at the Schepens Eye Research Institute. Its arrest at the G1 phase and the major role of premature stress induced senescence have been elegantly highlighted by numerous complementary experiments performed on animal and human stored corneas (using the American cold storage technique).

In the present paper, we add three innovations: 1/ study of healthy ECs retrieved during corneal graft (performed for keratoconus, a disease well known to leave ECs intact) and analyzed within minutes after their explantation and thus considered as reflecting the in vivo environment; 2/ study of human corneas stored in organ culture at 31°C in a medium containing 2% foetal calf serum and known to allow endothelial wound healing and possibly proliferation, unlike cold storage; and 3/ use of a 112-gene microarray dedicated to cell cycle analysis.

We wish respectfully to suggest Prof. Katrin Engelmann of Dresden University, Germany, as a reviewer. In Europe, she is one of the ophthalmologists and scientists to best study strategies for overcoming the non proliferative status of ECs. We also suggest Prof Alain Bron of Dijon University, France, because of his expertise in the anatomy of the extreme corneal periphery, where EC progenitors may concentrate. Lastly, we would be honored to benefit from Nancy Joyce's expertise. We suggest Michael E Boulton from the Indiana University College of Medicine as Academic Editor.

We declare that all authors have directly participated in the planning, execution, or analysis of the study and resulting paper, and have read and approved the submitted version.

We hope that our manuscript will interest the Editorial Board of *Plos One*.

Sincerely,

Professor Gilles Thuret, MD, PhD, Institut Universitaire de France

Corresponding author:
Laboratory for Biology, engineering and imaging of Corneal Graft, EA 2152, IFR143
Faculty of Medicine
15, Rue Ambroise Paré
F 42023 Saint-Etienne Cedex 2, France.
Tel: +33 (0)4 77 12 77 93
Fax: +33 (0)4 77 12 09 95
E-mail: gilles.thuret@univ-st-etienne.fr

Microarray Analysis of Cell Cycle Gene Expression in Adult Human Corneal Endothelial Cells

Binh Minh T. Ha[1], Nelly Campolmi[1, 2], Zhiguo He[1], Aurélien Pipparelli[1], Jean-Yves Thuret[5], Simone Piselli[1], Fabien Forest [1, 3], Michel Peoc'h[1, 3], Olivier Garraud[1, 4], Philippe Gain[1, 2], Gilles Thuret.[1, 2, 6]

1. Laboratory for corneal graft biology, engineering and imaging', EA2521, IFR143, Faculty of Medicine, Saint-Etienne, France

2. Department of Ophthalmology, University Hospital, Saint-Etienne, France

3. Department of Pathology, University Hospital, Saint-Etienne, France

4. Eye Bank, Etablissement Français du Sang Loire/Auvergne, Saint-Etienne, France

5. Commissariat à l'Energie Atomique, Institut de biologie et de technologies de Saclay (iBiTec-S), Service de Biologie Intégrative et de Génétique Moléculaire (SBIGeM), F-91191, Gif-sur-Yvette, France.

6. Institut Universitaire de France, 103, Boulevard Saint-Michel, 75005 Paris

Abstract

Corneal endothelial cells (ECs) form a monolayer that controls the hydration of the cornea and thus its transparency. Their almost nil proliferative status in humans is responsible, in several frequent diseases, for cell pool attrition that leads to irreversible corneal clouding. To screen for candidate genes involved in cell cycle arrest, we studied human ECs subjected to various environments thought to induce different proliferative profiles compared to ECs in vivo. Donor corneas (a few hours after death), organ-cultured (OC) corneas, in vitro confluent and non-confluent primary cultures, and an immortalized EC line were compared to healthy ECs retrieved in the first minutes of corneal grafts. Transcriptional profiles were compared using a cDNA array of 112 key genes of the cell cycle and analysed using Gene Ontology classification; cluster analysis and gene map presentation of the cell cycle regulation pathway were performed by GenMAPP. Results were validated using qRT-PCR on 11 selected genes. We found several transcripts of proteins implicated in cell cycle arrest and not

previously reported in human ECs. Early G1-phase arrest effectors and multiple DNA damage-induced cell cycle arrest-associated transcripts were found in vivo and over-represented in OC and in vitro ECs. Though highly proliferative, immortalized ECs also exhibited overexpression of transcripts implicated in cell cycle arrest. These new effectors likely explain the stress-induced premature senescence that characterizes human adult ECs. They are potential targets for triggering and controlling EC proliferation with a view to increasing the cell pool of stored corneas or facilitating mass EC culture for bioengineered endothelial grafts.

Key words: human, cornea, endothelium, cell cycle, microarrays, mRNA, DNA damage-induced, check-point, proliferation, senescence

Introduction

The corneal endothelium, which maintains stable corneal transparency in humans, is essential to visual-system performance [1]. It is a monolayer of hexagonal, densely packed corneal endothelial cells (ECs) separating the corneal stroma from the aqueous humor. By actively regulating hydration of the stroma, it prevents the onset of edema which, by disorganizing the collagen fibrils, would impair the passage of light [2]. In humans, corneal ECs lose their proliferative ability during fetal development [3,4] and are consequently vulnerable in vivo. If the endothelium sustains a lesion, its integrity, which is necessary for its function, is only maintained by the migration and enlargement of the ECs adjacent to the lesion, without mitosis. As a result, when endothelial cell density (ECD) falls below a critical threshold (which depends on the type, extent and kinetics of the pathological process), irreversible corneal edema sets in. Endothelial diseases are a frequent cause of corneal blindness, for which the only treatment is corneal graft. The graft, whether full thickness (penetrating keratoplasty, PKP) or endothelial (endothelial keratoplasty, EK), supplies a new pool of functional ECs in the donor cornea. However, after both types of graft, ECD falls rapidly in the first 6 months, then more slowly, but at a higher rate than the physiological EC loss rate of 0.6% a year [5]. Recipients thus frequently need more than one graft during their lifetime.

The absence of corneal EC division is therefore responsible for significant corneal blindness worldwide. Knowing which cellular mechanisms are implicated in human corneal EC cycle arrest would thus allow the development of new therapeutic tools to trigger and control EC proliferation. In vivo, ECs are blocked in G1 phase but maintain a residual proliferative capacity that can be exploited in vitro. The senescent state of central ECs in vivo may result from many simultaneous mechanisms (exposed in [6,7,8]): low level of growth factors in aqueous humor, lack of autocrine stimulation by growth factors synthesized by ECs, cell cycle entry inhibition by TGF-β2 present in aqueous humor, contact inhibition induced by formation of mature cell-cell and cell-substrate junctions, oxidative DNA damage resulting in a permanently high level of mRNA or proteins of the cyclin-dependent kinase inhibitors (CDKI) p27, p21, and p16, and cascades of blocking points for G1-S transition, especially belonging to the p53 pathway.

There are at least three possible areas of development for advanced therapy medicinal products in the field of ECs: 1/Ex vivo enrichment of grafts in EC is a realistic prospect [9] that would improve both the quality (prolonged survival in recipients) and the quantity of available graft tissue (by upgrading corneas whose ECD was initially too low). 2/In vitro mass culture of ECs would also allow bioengineering of endothelial graft tissue. 3/In parallel, it would become conceivable to treat early stages of primitive (Fuch's) or secondary endothelial dystrophies in vivo by injecting ECs in the anterior chamber [10]. Until now, three main approaches were used to trigger human EC proliferation (Table 1): 1/A general approach of improving culture conditions to limit cell death and promote cell cycle stimulating factors. 2/A focused approach focusing on a limited number of key cycle-controlling proteins considered as EC cycle blocking points. 3/Selecting and stimulating potential EC progenitor or stem cells located at the extreme periphery of the endothelium [11,12].

Table 1. *Published experimental methods for triggering human corneal endothelial cell proliferation.*

Approach		Principle	Biological model	Author, year
FOCUSED	Immortalization of primary HCEC	Transduction of **simian virus 40 large T-antigen** expression	human (in vitro)	Wilson 1993[13], Feldman 1993[14]
		Transformation with papillomavirus **E6/E7** oncogenes	human (in vitro)	Wilson 1995[15]
		Retroviral transduction of **Cdk4R24C/CyclinD1** to human corneal endothelial	human (in vitro)	Yokoi 2012[16]
		Transduction of human **telomerase reverse transcriptase expression** (hTERT)	human (in vitro)	Liu 2012[17]
		Transduction of **hTERT** combined with **p53** downregulation or **CDK4** overexpression	human (in vitro)	Sheerin 2012[8]
	E2F2 overexpression	Transduction of **E2F2**	human (ex vivo)	McAlister 2005[18]
	CDKI down regulation	siRNA **p27Kip1**	human (in vitro)	Kikuchi 2006[19]
		Electroporation with **p21+p16** siRNA	human (in vitro)	Joyce 2010[20]
	Anti-apoptotic effect	Transduction of baculoviral **p35** or mammalian **Bcl-xL** for anti-apoptotic gene therapy	human (in vitro)	Fuchsluger 2011[21]
GENERAL	Medium optimization	Organ culture at 32°C with 8% FCS	human (ex vivo)	Slettedal 2008[22]
		Evaluation of 4 basic culture **medias** (DMEM, OptiMEM-I, DMEM/F12, Ham's F12/M199) in isolation & propagation	human (in vitro)	Peh 2011[23]
		Reduction of reactive oxygen species by **rapamycin** & **cysteamine**	human (in vitro)	Shin 2012[24]
	Culture support	**Decellularized bovine corneal posterior lamellae** as carrier matrix for cultivated cells	human & bovin (ex vivo, in vitro)	Bayyoud 2012[25]
		Gelatin hydrogel carrier sheet for corneal endothelial transplantation.	human (in vitro)	Watanabe 2011[26]
	Cell-cell contact release	**EDTA** + organ culture at 37°C + 10% FCS†, 10 ng/mL EGF†, 20 ng/mL FGF†	human (ex vivo)	Senoo 2000[27], Patel 2009[28]
		Localized lesion+ organ culture at 37°C + 10% FCS†, 10 ng/mL EGF†, 20 ng/mL bFGF†	human (ex vivo)	Senoo, 2000[29]
REGENERATION	HCEC precursor	Isolation of **HCEC precursors i**n vitro by sphere-forming assay	human (in vitro)	Yokoo 2005[30]
	Stromal cornea-derived precursors	Differentiation of **stromal cornea-derived precursors** to functional corneal endothelium by cell isolation in medium containing retinoic acid, GSK 3b inhibitor and Rock inhibitor Y-27632	human (in vitro)	Hatou 2012[31]
	Trabecular meshwork stem-like cell	Local progenitors for the corneal endothelium and **trabecular meshwork** personalized stem cell therapy in corneal endothelial diseases and glaucoma (Review)	/	Yu 2012[32]

†FCS: Fœtal calf serum; EGF: Epidermal growth factor; FGF: Fibroblast growth factor

In the present study, we used a specific chip of 112 genes implicated in cell cycle regulation to examine human ECs subjected to six environments thought to induce different proliferative profiles: in vivo, post mortem (PM), organ culture (OC) stored corneas, confluent primary culture (CPC), non-confluent primary culture (NCPC), and immortalized EC line (ECL). Unlike short-term cold storage, OC in fetal calf serum (FCS) supplemented medium maintains EC viability and functionality for up to 5 weeks. OC is not known to promote EC proliferation, although it facilitates endothelial wound healing by migration of cells in the vicinity of local defects in the endothelial layer [33]. Only OC with 8% FCS, a method that remains an exception [34], seems likely to promote cell mitosis [22]. It was thus important to determine whether routine OC induces significant transcriptional profile changes liable to reveal the stimulation of certain ECs with residual proliferative capacity. In vitro, primary cultures of ECs with FCS and growth factors usually have limited proliferative capacity and rapidly become senescent, especially when reaching confluence. Conversely, ECLs obtained by transducing simian virus 40 large T-antigene expression display very high proliferative capacity [35].

Hence, the crossing analysis of these models, from in vivo to the ECL, helps us to understand mechanisms implicated in EC division and senescence, thus giving new potential key points for triggering mitosis. Gottsch's major work on human endothelial cornea genomics proposed an analysis of all transcripts present in normal endothelia [36] and in Fuch's dystrophy [37] by using an ultra-sensitive SAGE method and Affymetrix HU95a microarrays containing about 12000 genes previously characterized in terms of function or disease association. In addition, Gottsch's team created a comprehensive database of human corneal gene expression. To date, no focused analysis has been done on the expression of genes implicated in cell cycle control in human ECs.

Materials and methods

Ethics Statement

All procedures conformed to the tenets of the Declaration of Helsinki for biomedical research involving human subjects. Central corneal buttons removed as

waste during surgery were collected as per the usual protocol in force in our University Hospital and by presumed consent further to the written information given to all admitted patients. This protocol was written by our Hospital's commission for clinical research and innovation and accepted by the local ethics committee (CPP Sud Est I, CHU Saint Etienne, Saint Etienne, France). Corneas assigned to scientific use were procured from bodies donated to science (Laboratory of Anatomy, Faculty of Medicine) as permitted by French law. Each donor volunteers their body and gives written consent to the Laboratory of Anatomy; no extra specific approval by the ethics committee is required

Materials

Serum-free medium (OptiMEM-1), Petri dish, 6-well tissue culture plates, T25 flasks and fetal bovine serum (FBS) were purchased from Fisher Bioblock Scientific (Vaulx-Milieu, France). Medium 199 (M199), epidermal growth factor (EGF; from mouse submaxillary glands), nerve growth factor (NGF; from mouse submaxillary glands), bovine pituitary extract (also known as Keratinocyte Growth Supplement), ascorbic acid, calcium chloride, chondroitin sulphate, 0.02% EDTA solution (EDTA disodium salt), antibiotic-antimycotic solution, gentamicin, trypsin, glutamine, penicillin-streptomycin solution, insulin and RNA loading dye were purchased from Sigma-Aldrich (Saint-Quentin Fallavier, France). Cell attachment reagent (FNC Coating Mix) was purchased from Gentaur (Brussels, Belgium). RNeasy mini Kit, RNase-free DNase I and Taq PCR Master Mix were purchased from Qiagen (Courtaboeuf, France). Oligo$(dT)_{12\text{-}18}$ primer, dNTP Mix (10 mM), Ribonuclease H, dithiothreitol (DTT; 0.1 M), 5X First-Strand Buffer, SuperScript™ II Reverse Transcriptase, Ribosomal protein S27a (RPS27A) forward and reverse primers were purchased from Invitrogen (Cergy Pontoise, France). Biotin-16-UTP was purchased from Roche Applied Science (Meylan, France). Cell Cycle OligoArray (Oligo GEArray Human Cell Cycle OHS-020) and Oligo GEArray Starter Kit (SABiosciences Corporation, SuperArray, Frederick, MD) were purchased from Tebu-bio (Le Perray en Yvelines, France). Inventoried TaqMan® Gene Expression Assays and TaqMan® Universal PCR Master Mix were purchased from Applied Biosystems (Courtaboeuf, France).

Human corneal tissue

In order to study ECs in the physiological in vivo state as closely as possible, ECs from patients undergoing corneal graft for keratoconus were chosen. Keratoconus is a common non-inflammatory, progressive disease in which the endothelial layer is healthy and not known to be involved in the disease pathogenesis. Penetrating keratoplasty consists of replacing the central full-thickness cornea by a normal donor cornea. Consequently, a normal endothelium can be obtained during surgery. After informed consent, eight central corneas (diameter 8.25 mm) were obtained during penetrating grafts for keratoconus, immediately after trephination (in vivo group). ECs were collected as explained above. Time from trephination to endothelial freezing was about 20 minutes. Thirty-four supplementary human corneas assigned to scientific use (procured from bodies donated to science, Laboratory of Anatomy, Faculty of Medicine) were used in this study. Donor and procurement characteristics are presented in Table 2. Except for the in vivo group, corneas were procured by a 16-18 mm diameter in situ excision, as per the procedure recommended in France for corneas intended for transplantation. Twelve corneas, forming the post-mortem group, were immediately used. Eleven corneas, forming the OC group, were immediately placed in 100 mL of OC medium (Corneamax®, Eurobio, Les Ulis, France) at 31°C in a dry incubator. Five corneas were used to carry out confluent primary culture (CPC group). The last six corneas were used to carry out non-confluent primary culture (NCPC group). SV40 immortalized ECs (HCECT-12) were bought from DMSZ (Braunschweig, Germany) [35,38] and are henceforth referred to as the endothelial cell line (ECL).

Table 2. *Characteristics of donor corneas. Values were expressed as mean (min-max).*

Condition	Biological replicate	Age (years)	Death/retrieval time (hours)	Storage time (days)
In vivo	15	44 (27-81)	/	/
Post-mortem	12	79 (49-98)	12h25 (4h-21h45)	/
Organ culture	11	69 (49-85)	11h40 (5h30-15h55)	16 (13-24)
Confluent primary culture	5	78 (65-88)	13h08 (6h30-21h25)	13 (8-18)
Non-confluent primary culture	6	78 (58-89)	15h26 (11h-16h30)	21 (4-48)

Cell culture

Primary culture

ECs were isolated and cultured according to published protocols [19,39,40,41,42,43]. Briefly, Descemet membrane and ECs were peeled off under an operating microscope and separated into small fragments that were immersed in culture medium containing OptiMEM-I, 10% FBS, 5 ng/mL EGF, 20 ng/mL NGF, 100 µg/mL pituitary extract, 20 µg/mL ascorbic acid, 200 mg/L calcium chloride, 0.08% chondroitin sulphate, 50 µg/mL gentamicin, and antibiotic/antimycotic solution diluted 1/100. Isolated cells and pieces of Descemet's membrane that still contained attached cells were plated in six-well tissue culture plates precoated with undiluted FNC Coating Mix. Cultures were then incubated at 37°C in a 5% carbon dioxide, humidified atmosphere. Medium was changed every 2 days. Confluent primary cultured cells were then trypsinized, resuspended in culture medium, and subcultured into T25 flasks that had been precoated and grown to 50% or 100% confluence.

Immortalized cell line

The ECL was cultured as previously described [44] with some technical changes. Briefly, cells were grown in T25 flasks with culture medium F99 (1:2 dilution of medium 199 and Ham's F12) supplemented with 0.3% chondroitin sulphate, 2% glutamine, 0.5% penicillin-streptomycin solution, 0.02% ascorbic acid, 0.02% insulin and 10% FCS. The cultures were maintained in 5% CO_2 at 37°C. Culture medium was changed every 2-3 days.

RNA extraction

Under an operating microscope, Descemet's membrane with endothelium was peeled off from the underlying stroma with forceps to avoid contamination by other cell types. Two corneas were pooled for the OC and post-mortem groups (whole cornea), and four for the in vivo group (8 mm diameter trephination). Microarrays were consequently performed in duplicate for each condition. This approach minimizes inter individual differences and was extensively published [45,46,47]. Non-confluent and confluent primary cultures and ECL cultures were trypsinized and pelleted. Descemets membrane fragments and ECs were then frozen at -80°C until RNA isolation. Total

RNA was isolated using an RNeasy mini kit as per the manufacturer's instructions. Before further use, total RNA was treated with RNase-free DNase I [48]. After extraction, RNA was checked for stability and DNA contamination by running a sample with an RNA loading dye on a 1% agarose gel, and visualization was done by staining with ethidium bromide. Lack of genomic DNA contamination was confirmed by polymerase chain reaction (PCR) amplification of RNA samples that had not been reverse-transcribed. RNA quantity was determined by spectrophotometric absorbance of the sample at 260 nm measurement, and purity was determined based on the ratio at 260 nm to that of 280 nm (A_{260}/A_{280}) using a BioMate™ 3 Series spectrophotometer (Thermo Fisher Scientific, Cergy Pontoise, France). Only RNA samples with A_{260}/A_{280} ratio >1.8 were used for further experiments. Samples were frozen at -80°C until use in microarrays and qRT-PCR.

Polymerase chain reaction

PCR was carried out on RNA of each sample in order to check possible contamination with genomic DNA. Amplification was performed by the standard method on Ribosomal protein S27a (RPS27A) gene using Taq PCR Master Mix as per the manufacturer's instructions. RPS27A is a component of the 40S subunit of the ribosome, and has been previously identified as a valid control gene in expression studies conducted among human malignant and control tissues [49,50]. PCRs were performed in 100 µl reactions using 300 ng RNA, 2.5 units of Taq DNA Polymerase, 1x PCR Buffer (containing 1.5 mM $MgCl_2$), 200 µM of each dNTP and 0.5 µM of each primer. The sequences of human RPS27A primers, described elsewhere [51,52], were as follows: forward primer, 5'-TCGTGGTGGTGCTAAGAAAA-3'; and reverse primer, 5'-TCTCGACGAAGGCGACTAAT-3'. Amplifications were carried out using the following cycling parameters: initial denaturation at 95°C for 10 minutes, denaturation at 95°C for 60 seconds, annealing at 53°C for 60 seconds, and extension at 72°C for 60 seconds. PCR amplification was done for 40 cycles with a final extension at 72°C for 10 minutes. RPS27A cDNA from cell line, obtained after RT, was used as a positive control. For a negative control, PCR was run using PCR reaction mixture with primers but no nucleic acid. Following amplification, the PCR products were characterized in 1% agarose-ethidium bromide gels in Trisacetate buffer. A product

was obtained from PCR performed on positive control but not on RNAs and negative control, indicating that samples were not contaminated by genomic DNA (data not shown).

Reverse transcription

First-strand cDNA synthesis was carried out on 300 ng of total RNA in a final volume of 20 µl with SuperScript™ II Reverse Transcriptase as per the manufacturer's protocol. Briefly, after addition in nuclease-free microcentrifuge tubes of 300 ng of total RNA, 0.1µl Oligo$(dT)_{12\text{-}18}$ (500 µg/ml), 1 µl dNTP Mix (10 mM each) and sterile distilled water to complete the volume at 12 µl, the mixture was heated at 65°C for 5 minutes. 4 µl of 5X First-Strand Buffer and 2 µl of DTT were then added and the mix incubated at 42°C for 2 minutes. Incubation at 42°C for 50 minutes was performed after the addition of 1 µl of SuperScript™ II RT. The reaction was inactivated by heating at 70°C for 15 minutes. To remove RNA complementary to the cDNA, 1 µl of *E. coli* RNase H (two units) was added and the mixture incubated at 37°C for 20 minutes and then chilled on ice. cDNA were stored at -20°C until use in qPCR.

GEArray

Expression levels of cell cycle-specific genes were examined by human cell cycle Oligo GEArray® (OHS-020). The Oligo GEArray® Human cell cycle Microarray profiled the expression of 112 key genes involved in cell cycle regulation, such as cyclin-dependent kinases (CDKs) involved in cell cycle progression and the proteins that regulate them (cyclins, CDK inhibitors, CDK phophatases and kinases). Genes essential for DNA damage and mitotic spindle checkpoints and genes in the SCF (*CUL1, SKP2*) and APC (anaphase promoting complex, with *CDC16-20, ANAPC2-4-5*) ubiquitin-conjugation complexes were also included. Microarrays were performed in two biological replicates for each group. Briefly, as described elsewhere [53,54,55,56,57], using the TrueLabeling-AMP 2.0 kit, 1 µg of purified total RNA was reversely transcribed to obtain cDNA and converted into biotin-labeled cRNA using biotin-16-UTP (Roche) by in vitro transcription. The biotin-labeled cRNA was purified using the cRNA clean-up kit. Prehybridization (2 hours) and hybridization (overnight) was done at 60°C in a hybridization oven using 3 µg purified labeled cRNA target as per manufacturer's protocol. After washing and blocking the array membranes, alkaline phosphatase-conjugated streptavidin was allowed to bind and CDP-Star substrate

chemiluminescence was detected by exposure to x-ray film. The film was acquired using a 16-bit desktop scanner and saved as a grayscale 16-bit TIFF file. Absence of signal saturation (number of grey levels <255) was verified for each image. Array data were analyzed using the web-based GEArray Expression Analysis Suite software (SuperArray Bioscience). All signal intensities were background subtracted (subtraction of minimum value), and normalized to the housekeeping genes (RPS27A; GAPDH; B2M; HSP90AB1 and ACTB). For each set of duplicates, the mean value for each gene was determined and used to calculate the fold-changes: the in vivo group served as reference sample. The cut-off induction determining expression was ≥1.5 fold changes [58,59,60], (fold change = normalized result of groups/normalized result of the control group). Genes suiting both the above criteria were considered to be upregulated or downregulated with biological relevance. To gather reliable data, careful quality control of experiments, data extraction and standardization approaches were maintained throughout the experimental process.

Gene ontology (GO) and Cluster analysis

The enriched biological processes GO terms for each cell cycle phase was determined by uploading the gene list on the Database for Annotation, Visualization, and Integrated Discovery (DAVID) version 6.7, 2013 (http://david.abcc.ncifcrf.gov/ [61,62], (Table 1S supplemental data). Clustering of genes expression by cell cycle phase was conducted with the software R version 2.15.0, 2012 [63]. The fold-change expression values were represented in logarithmic scale in heatmap graph.

Table 1S (Supporting informations). *Functional classification by cell cycle phase (using DAVID version 6.7, 2013 (http://david.abcc.ncifcrf.gov/)) of the 62/112 transcripts obtained with the Oligo GEArray® Human cell cycle Microarray. 40/112 transcripts were not classified in this table.*

Cell cycle process	GO terms	GEarray Entrez Gene Identification
G1 phase	GO:0000080	CDK2 (1017), CDC6 (990), CDC25C (995), CDK6 (1021), CDKN1C (1028), E2F1 (1869)
S phase	GO:0000084	DDX11 (1663), ABL1 (25)
G2 phase	GO:0000085	GTSE1 (51512), KPNA2 (3838)
M phase	GO:0000087	CDC25A (993), BIRC5 (332), CDK2 (1017), DDX11 (1663), CCNB1 (891), ANAPC4 (29945), ANAPC5 (51433), CCNA2 (890), CDC2 (983), MAD2L1 (4085), MAD2L2 (10459), CDC6 (990), CDC25C (995), CCNF (899), CCNG1 (900), CCNG2 (901), CDC20 (991), CDC16 (8881), CCNA1 (8900), PKMYT1 (9088), CCNB2 (9133), KNTC1 (9735), ANAPC2 (29882)
G1/S transition	GO:0000082, GO:0031575	CDKN1A (1026), CDKN2B (1030), NBN (4683), CDC25A (993), GTSE1 (51512), CCND1 (595), BCL2 (596), CCND2 (894), CCNE1 (898), CDC34 (997), CDK4 (1019), CDKN1B (1027), CDKN2A (1029), CDKN2C (1031), CDKN2D

		(1032), CDKN3 (1033), E2F4 (1874), E2F6 (1876), MNAT1 (4331), RB1 (5925), RBBP8 (5932), SKP2 (6502), CUL5 (8065), CDC7 (8317), CUL4A (8451), CUL3 (8452), CUL2 (8453), CUL1 (8454), HUS1 (3364), TP53 (7157)
G2/M transition	GO:0000086, GO:0031576	BIRC5 (332), CDKN1A (1026), CDKN2B (1030), NBN (4683), CDK2 (1017), DDX11 (1663), CCNB1 (891), ANAPC4 (29945), ANAPC5 (51433), CCNA2 (890), CDC2 (983), CHEK1 (1111), GADD45A (1647), DNM2 (1785), BRCA1 (672)
M/G1 (Mitotic spindle checkpoint)	GO:0007094	BIRC5 (332), MAD2L1 (4085), MAD2L2 (10459), ATM (472)

Pathway profile analysis

Gene Map Annotator and Pathway Profiler (GenMAPP) version 2.1 was used to analyze GEArrays results. Fold-change expression values of each biological group versus the in vivo group were related to the Kyoto Encyclopedia of Genes and Genomes (KEGG) pathway of human cell cycle [64,65]. Fold-change absolute values over 1.5 were considered as upregulated or downregulated and classified in three classes: 1.5 to 5 folds, 5 to 10 folds, and 10 folds and more.

Real-time quantitative PCR

To confirm the cDNA arrays findings, real-time quantitative PCR were carried out on 11 selected genes: Cyclin D1; Cyclin E1; p21; p27; p16; p15; GADD45A, DIRAS3, culin 1, MKI67 and PCNA using an AB 7500 Fast Real-Time PCR System (Applied Biosystems). Assays were performed with TaqMan® Universal PCR Master Mix and Inventoried Taqman® Gene Expression Assays (Table 3) as per the manufacturer's instructions. Briefly, in wells of a 0.2 ml optical-grade 96-well PCR plate, we placed a 25 µl reaction mixture of 12.5 µl TaqMan® Universal PCR Master Mix, 900 nM of each unlabeled primers (forward and reverse), 250 nM TaqMan® MGB (minor groove binder) probe and 25 ng cDNA for each of the target genes. The assay's probes incorporated a 5' reporter dye (6-carboxy-fluorescein, 6-FAM™dye label) and a 3' non-fluorescent quencher (NFQ) and spanned an exon junction (Table 3): genomic DNA could not be detected. The thermal cycle conditions, as previously described[66] and as per the manufacturer's instructions, consisted of AmpErase activation (50°C, 2 min) and Taq activation (95°C, 10 min), followed by 40 cycles of denaturation (95°C, 15 sec), annealing and elongation (60°C, 1 min). The AB 7500 system measures a fluorescent accumulation of PCR product by continuous monitoring. 18S rRNA was used as an endogenous control to normalize for variation in the amount of cDNA template. Each sample also consisted of two biological replicates and three technical

replicates. No Template Controls (NTC: PCR mixture without cDNA) were performed to rule out cross contamination of reagents, on each target as well as on endogenous control. All data were analyzed using the 7500 Fast System Detection Software version 1.2.3 (Applied Biosystems). After normalization of measurements using the endogenous control, results were analyzed using the comparative critical threshold (ΔΔCT) method [67,68,69] to compare differences between samples. As for the microarray, the in vivo group served as reference.

Table 3. *TaqMan® gene expression assays for quantitative real-time PCR used to validate microarray results on a subset of 11 genes of interest.*

Assay ID	NCBI Gene Reference	Gene Symbol	Gene Name	Target Exons	Amplicon Length
Hs01026536_m1	NM_001238.1	*CCNE1*	Cyclin E1	11-12	64
Hs00277039_m1	NM_053056.2	*CCND1*	Cyclin D1	2-3	94
Hs00696862_m1	NM_002592.2	*PCNA*	Proliferating cell nuclear antigen	1-2	95
Hs01032443_m1	NM_002417.4	*MKI67*	Antigen identified by monoclonal antibody Ki-67	8-9	66
Hs00190723_m1	NM_004675.2	*DIRAS3*	DIRAS family, GTP-binding RAS-like 3	1-2	115
Hs00169255_m1	NM_001199741.1	*GADD45A*	Growth arrest and DNA-damage-inducible, alpha	2-3	123
	NM_001924.3			3-4	123
Hs00355782_m1	NM_078467.1	*CDKN1A*	Cyclin-dependent kinase inhibitor 1A ($p21^{Cip1}$)	2-3	66
Hs00153277_m1	NM_004064.3	*CDKN1B*	Cyclin-dependent kinase inhibitor 1B ($p27^{Kip1}$)	1-2	71
Hs00233365_m1	NM_058195.2	*CDKN2A*	Cyclin-dependent kinase inhibitor 2A ($p16^{Ink4A}$)	2-3	117
Hs00365249 m1	NM_078487.2	*CDKN2B*	Cyclin-dependent kinase inhibitor 2B ($p15^{INK4B}$)	1-2	128
Hs00269187_m1	NM_003592.2	*CUL1*	Cullin 1	2-3	165
Hs99999901_s1	X03205.1	*18S*	Eukaryotic 18S rRNA (Endogenous Controls)	___	187

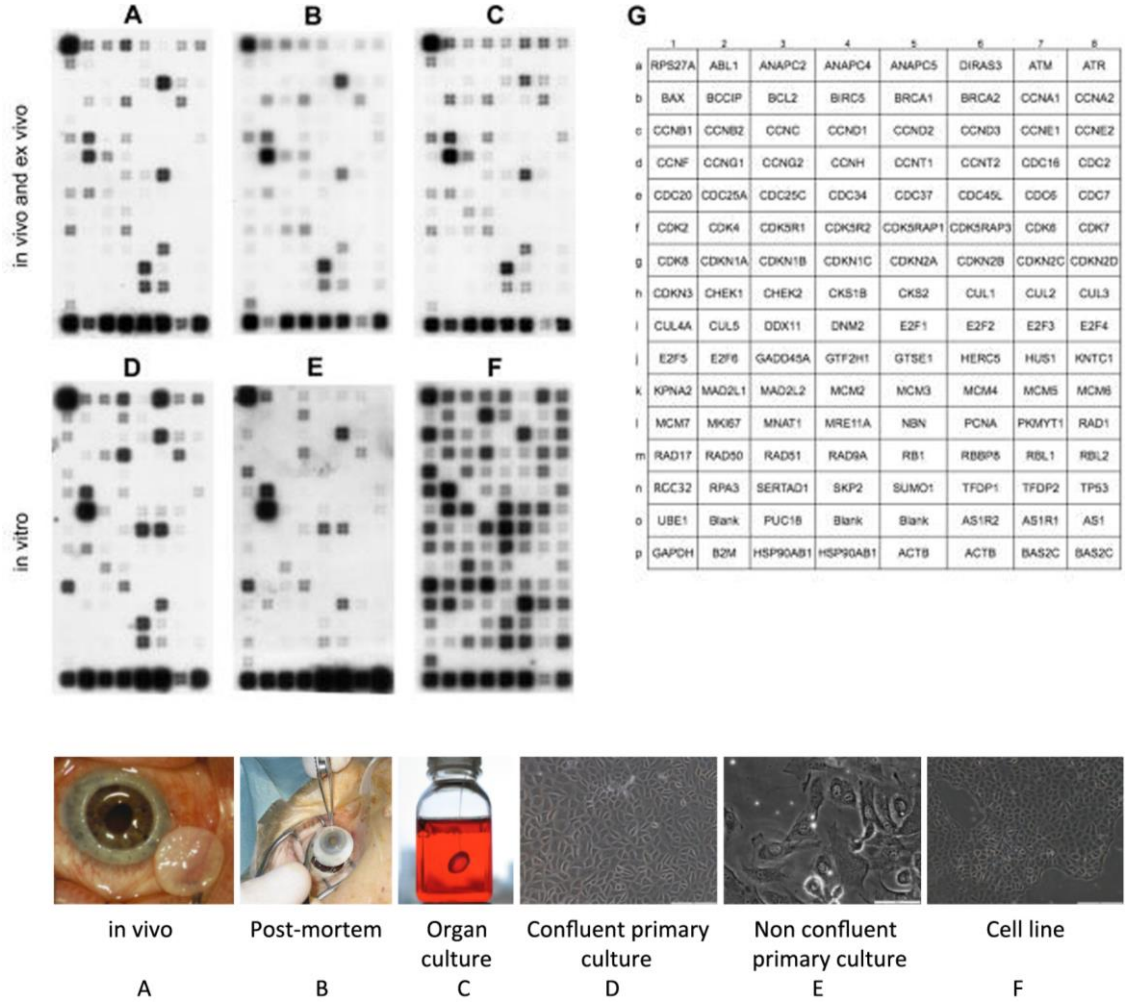
Statistical analysis

Spearman's correlation coefficient (r) was calculated between the biological replicate of each group studied by microarray, in order to estimate reproducibility, and between microarray and qRT-PCR results to estimate the reliability of microarrays. $P < 0.05$ was considered statistically significant.

Results

Gene expression profiles in endothelial cells from different environments

Detection of cell cycle gene transcripts by GEArray was successful for the six types of EC (Fig.1). For each EC type, normalized values of biological duplicates were concordant with Spearman's correlation coefficients between biological replicates respectively of 0.891 for in vivo, 0.881 for PM, 0.972 for OC, 0.974 for CPC, 0.792 for NCPC, and 0.981 for the ECL ($p<0.001$ for each).



	1	2	3	4	5	6	7	8
a	RPS27A	ABL1	ANAPC2	ANAPC4	ANAPC5	DIRAS3	ATM	ATR
b	BAX	BCCIP	BCL2	BIRC5	BRCA1	BRCA2	CCNA1	CCNA2
c	CCNB1	CCNB2	CCNC	CCND1	CCND2	CCND3	CCNE1	CCNE2
d	CCNF	CCNG1	CCNG2	CCNH	CCNT1	CCNT2	CDC16	CDC2
e	CDC20	CDC25A	CDC25C	CDC34	CDC37	CDC45L	CDC6	CDC7
f	CDK2	CDK4	CDK5R1	CDK5R2	CDK5RAP1	CDK5RAP3	CDK8	CDK7
g	CDK8	CDKN1A	CDKN1B	CDKN1C	CDKN2A	CDKN2B	CDKN2C	CDKN2D
h	CDKN3	CHEK1	CHEK2	CKS1B	CKS2	CUL1	CUL2	CUL3
i	CUL4A	CUL5	DDX11	DNM2	E2F1	E2F2	E2F3	E2F4
j	E2F5	E2F6	GADD45A	GTF2H1	GTSE1	HERC5	HUS1	KNTC1
k	KPNA2	MAD2L1	MAD2L2	MCM2	MCM3	MCM4	MCM5	MCM6
l	MCM7	MKI67	MNAT1	MRE11A	NBN	PCNA	PKMYT1	RAD1
m	RAD17	RAD50	RAD51	RAD9A	RB1	RBBP8	RBL1	RBL2
n	RCC32	RPA3	SERTAD1	SKP2	SUMO1	TFDP1	TFDP2	TP53
o	UBE1	Blank	PUC18	Blank	Blank	AS1R2	AS1R1	AS1
p	GAPDH	B2M	HSP90AB1	HSP90AB1	ACTB	ACTB	BAS2C	BAS2C

Figure 1. Microarray analysis of mRNA extracted from endothelial cells collected on six biological models. *(**A**) in vivo corneas (reference group); (**B**) post-mortem corneas; (**C**) organ-cultured corneas; (**D**) confluent primary culture; (**E**) non-confluent primary culture; and (**F**) in vitro confluent cell line. Genes expressed were identified as a specific hybridization signal that appeared as tetra-spots. In addition to the 112 genes of interest, each chip contained five housekeeping genes for normalization (GADPH, beta-2-microglobuline (B2M), 2x HSP90AB1, 2x Actin beta (ACTB)), seven negative controls: PUC18 plasmid DNA, Artificial Sequence 1 related 2 (AS1R2), Artificial Sequence 1 Related 1 (AS1R1), Artificial Sequence 1 (AS1) and three blank spots, and two positive detection controls: two biotinylated Artificial Sequence 2*

*Complementary sequence (BAS2C) at increasing gradient. A key to gene coordinates is shown in panel **G***

Using cluster analysis of normalized values of the 112 cell cycle gene expressions, the heatmap representation (Fig. 2) exhibited the highest similarity between cell cycle gene expression of EC in vivo and PM. Samples collected from donors with short death to retrieval time (under 24h) still had the same properties as the in vivo samples. OC shares similar patterns of expression with CPC and NCPC. The ECL clearly had a completely different profile, with activation of most cell cycle genes, and could consequently be considered a positive control for EC proliferation.

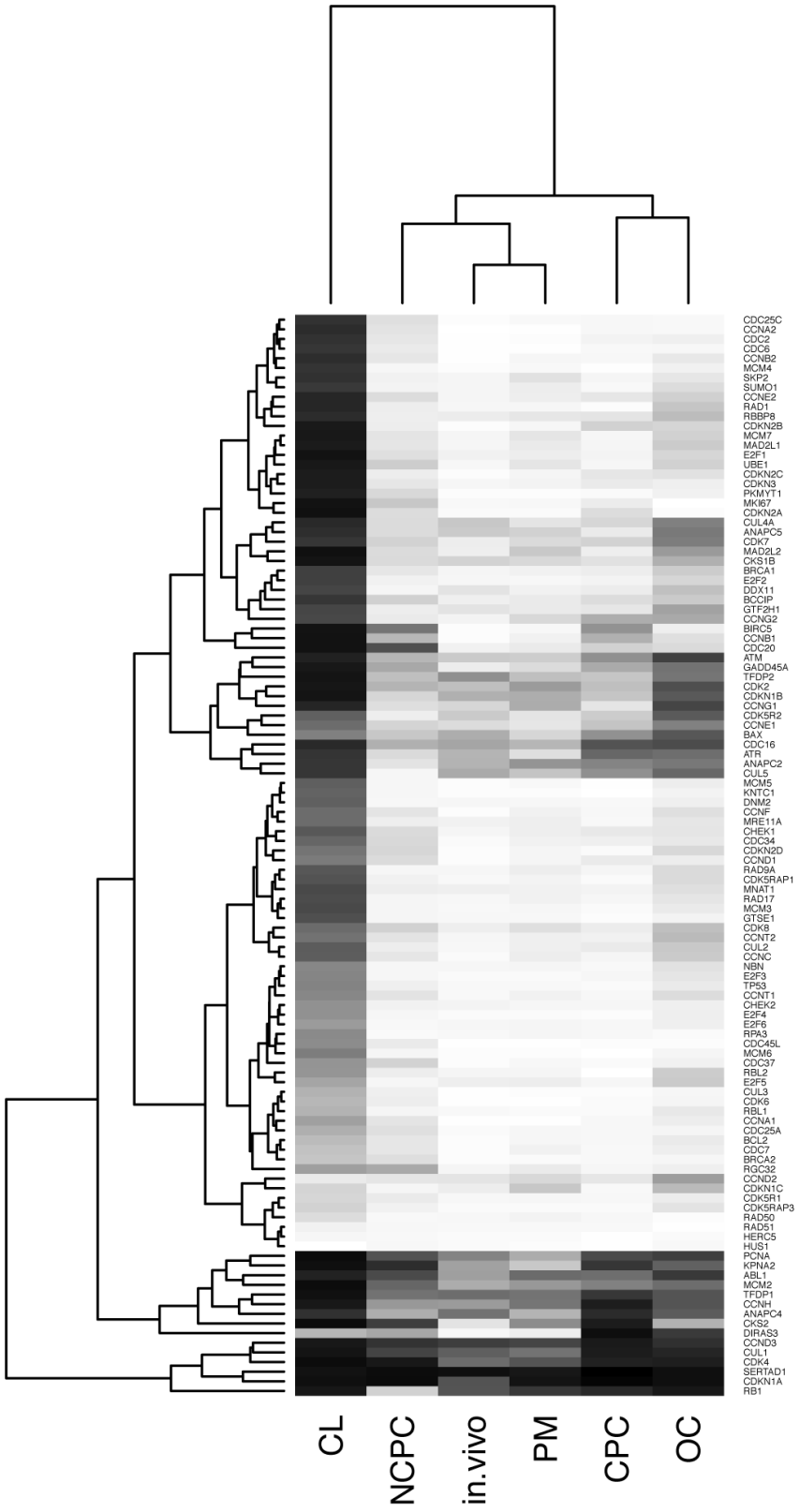


Figure 2. Clustergram analysis of expression of 112 cell cycle genes in endothelial cells of the six different biological models*: in vivo, post mortem (PM), organ culture (OC), in vitro confluent primary culture (CPC), in vitro non confluent primary culture (NCPC), and cell line (ECL). Normalized expressions of all models were represented on the heatmap graph. Gray scale from 0 (blank) to 1 (black) represents variation between minimum and maximum normalized values.*

Based on GO classification, 62 of 112 genes analyzed by GEArray were directly classified in cell cycle phases and checkpoints; 40 other genes were not classified. The percentage of genes over- or underexpressed is presented in Figure 3. In ex vivo EC, compared to in vivo, cell cycle regulator genes were overexpressed progressively in PM and OC conditions. In isolated culture of EC, NCPC overexpressed cell cycle regulators compared to EC in CPC. Immortalized ECs overexpressed 100% of cell cycle regulators. Taken together, this general evaluation showed slight activation of the cell cycle in ECs of corneas shortly after donors' death, and high activation during OC. In vitro, isolated ECs entered the cell cycle but the cycle stabilized when they reached confluence.

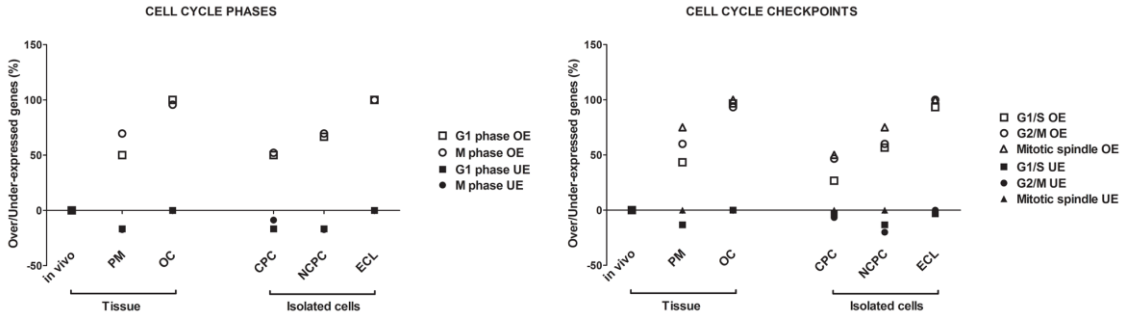


Figure 3. Variations of genes implicated in cell cycle phases and checkpoints. *Percentage of genes overexpressed (OE) or underexpressed (UE) compared to in vivo condition (fold-change ≥ 1.5) in ECs of the different biological models: post mortem (PM), organ culture (OC), confluent primary culture (CPC), non-confluent primary culture (NCPC), and endothelial cell line (ECL). S and G2-phase genes (n=4, see Table 1S), were not shown.*

Cell cycle signaling in endothelial cells

In vivo (reference)

Transcripts present and those absent in the reference group were represented in Figure 4 and detailed in Table 2S (supplemental data). The profile was compatible with early G1 phase arrest. For early G1 phase, CCND2 (Cyclin D2), CCND3 (Cyclin D3), CDK4 were present but not CDK6. For late G1 phase, CDK2 was present but not CCNE1 (Cyclin E1) or CCNE2 (Cyclin E2) transcripts, preventing CyclinE/CDK2 complexes from forming and entering the S phase. The presence of two CDK inhibitors CDKN1A ($p21^{CIP1}$) and CDKN1B ($p27^{KIP1}$) suggested inhibition of CDK2 and CDK4, preventing formation of CyclinE/CDK2 and CyclinD/CDK4 complexes. For

progression from G1 to the S phase, RBL1 transcript was present but not E2F transcription factors (except for E2F5), *CDC7* (G1/S), *CDC45* (S) or MKI67 (Ki67). The CDC25A transcript required for activation of CDKs was also absent. Markers of G2 and S phase entry were absent: CCNA1 (Cyclin A1), CCNA2 (Cyclin A2), CCNB1 (Cyclin B1), CCNB2 (Cyclin B2). For the G2 to M phase, the presence of ATR and ATM transcripts suggested the activation of DNA damage checkpoints. The presence of NBN (Nibrin), GADD45A and CDKN1A ($p21^{CIP1}$) transcripts may result in CDK2 inactivation and cell cycle arrest. The absence of M phase transcripts, such as MCM complexes (except for MCM2), confirmed the absence of cell division. Several transcripts whose proteins are involved in the large ubiquitin-mediated degradation complex were expressed: three anaphase-promoting complex (APC) subunits, three culins, and *CDC16*. Notably, no transcript of Cyclin D1, or p53 or $p16^{Ink4A}$, was found. The five other EC types were compared to this baseline expression profile.

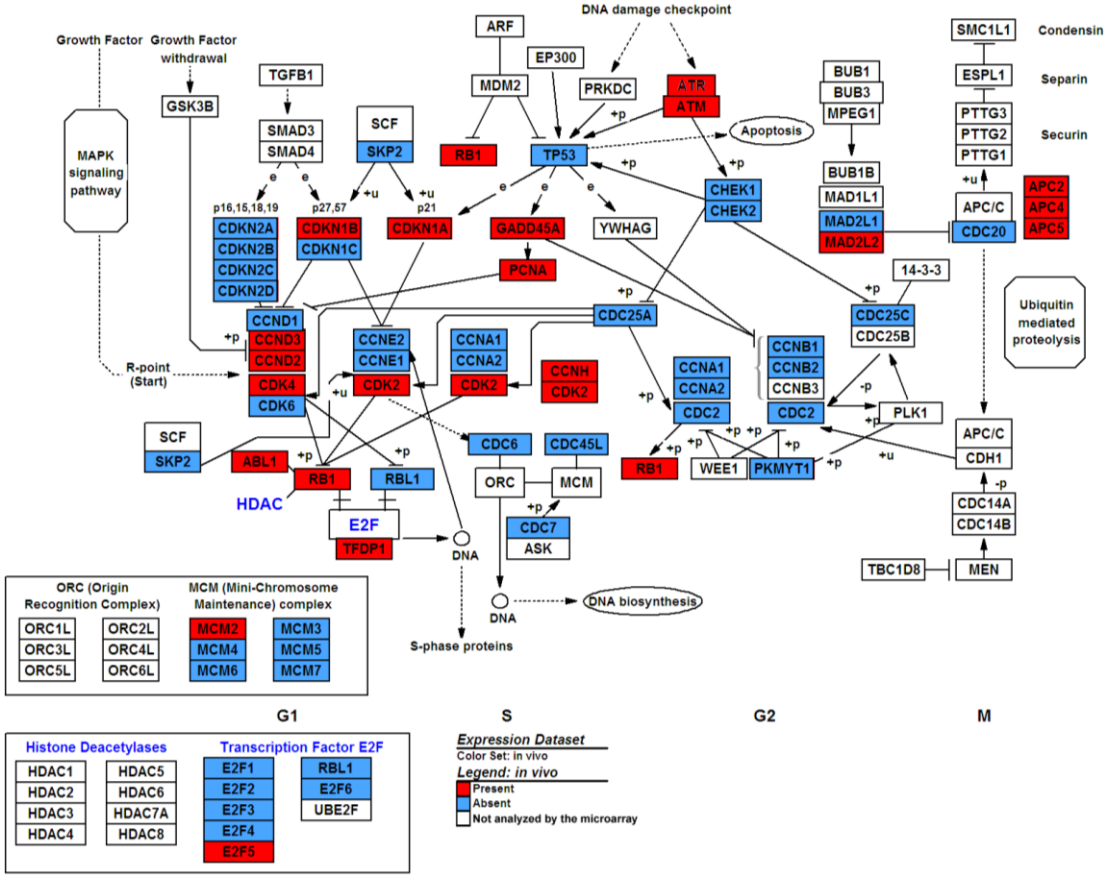


Figure 4. Baseline cell cycle gene expression profile in human corneal endothelial cells in vivo. *Graphic representation of the presence/absence of gene expression on KEGG cell cycle pathway using GenMAPP version 2.1 (http://www.genmapp.org/).*

Table 2S. (supporting informations). *Baseline gene expression profile in human corneal endothelial cells in vivo. Highlighted in gray: transcripts that remained absent in all six experimental conditions.*

Position	*Symbol*	*Description*	genebank No.	Absent/Present
2	ABL1	V-abl Abelson murine leukemia viral oncogene homolog 1	NM_005157	P
3	ANAPC2	Anaphase promoting complex subunit 2	NM_013366	P
4	ANAPC4	Anaphase promoting complex subunit 4	NM_013367	P
5	ANAPC5	Anaphase promoting complex subunit 5	NM_016237	P
6	DIRAS3	DIRAS family, GTP-binding RAS-like 3	NM_004675	A
7	ATM	Ataxia telangiectasia mutated (includes complementation groups A, C and D)	NM_000051	P
8	ATR	Ataxia telangiectasia and Rad3 related	NM_001184	P
9	BAX	BCL2-associated X protein	NM_004324	P
10	BCCIP	BRCA2 and CDKN1A interacting protein	NM_016567	A
11	BCL2	B-cell CLL/lymphoma 2	NM_000633	A
12	BIRC5	Baculoviral IAP repeat-containing 5 (survivin)	NM_001168	A
13	BRCA1	Breast cancer 1, early onset	NM_007294	A
14	BRCA2	Breast cancer 2, early onset	NM_000059	A
15	CCNA1	Cyclin A1	NM_003914	A
16	CCNA2	Cyclin A2	NM_001237	A
17	CCNB1	Cyclin B1	NM_031966	A
18	CCNB2	Cyclin B2	NM_004701	A
19	CCNC	Cyclin C	NM_005190	A
20	CCND1	Cyclin D1	NM_053056	A
21	CCND2	Cyclin D2	NM_001759	P
22	CCND3	Cyclin D3	NM_001760	P
23	CCNE1	Cyclin E1	NM_001238	A
24	CCNE2	Cyclin E2	NM_057735	A
25	CCNF	Cyclin F	NM_001761	A
26	CCNG1	Cyclin G1	NM_004060	P
27	CCNG2	Cyclin G2	NM_004354	A
28	CCNH	Cyclin H	NM_001239	P
29	CCNT1	Cyclin T1	NM_001240	A
30	CCNT2	Cyclin T2	NM_001241	A
31	CDC16	Cell division cycle 16 homolog (S. cerevisiae)	NM_003903	P
32	CDC2	Cell division cycle 2, G1 to S and G2 to M	NM_001786	A
33	CDC20	Cell division cycle 20 homolog (S. cerevisiae)	NM_001255	A
34	CDC25A	Cell division cycle 25 homolog A (S. pombe)	NM_001789	A
35	CDC25C	Cell division cycle 25 homolog C (S. pombe)	NM_001790	A
36	CDC34	Cell division cycle 34 homolog (S. cerevisiae)	NM_004359	A
37	CDC37	Cell division cycle 37 homolog (S. cerevisiae)	NM_007065	A
38	CDC45L	CDC45 cell division cycle 45-like (S. cerevisiae)	NM_003504	A
39	CDC6	Cell division cycle 6 homolog (S. cerevisiae)	NM_001254	A

40	CDC7	Cell division cycle 7 homolog (S. cerevisiae)	NM_003503	**A**
41	CDK2	Cyclin-dependent kinase 2	NM_001798	**P**
42	CDK4	Cyclin-dependent kinase 4	NM_000075	**P**
43	CDK5R1	Cyclin-dependent kinase 5, regulatory subunit 1 (p35)	NM_003885	**A**
44	CDK5R2	Cyclin-dependent kinase 5, regulatory subunit 2 (p39)	NM_003936	**P**
45	CDK5RAP1	CDK5 regulatory subunit associated protein 1	NM_016408	**A**
46	CDK5RAP3	CDK5 regulatory subunit associated protein 3	NM_176096	**A**
47	CDK6	Cyclin-dependent kinase 6	NM_001259	**A**
48	CDK7	Cyclin-dependent kinase 7	NM_001799	**A**
49	CDK8	Cyclin-dependent kinase 8	NM_001260	**P**
50	CDKN1A	Cyclin-dependent kinase inhibitor 1A (p21, Cip1)	NM_000389	**P**
51	CDKN1B	Cyclin-dependent kinase inhibitor 1B (p27, Kip1)	NM_004064	**P**
52	CDKN1C	Cyclin-dependent kinase inhibitor 1C (p57, Kip2)	NM_000076	**A**
53	CDKN2A	Cyclin-dependent kinase inhibitor 2A (p16)	NM_000077	**A**
54	CDKN2B	Cyclin-dependent kinase inhibitor 2B (p15)	NM_004936	**A**
55	CDKN2C	Cyclin-dependent kinase inhibitor 2C (p18)	NM_078626	**A**
56	CDKN2D	Cyclin-dependent kinase inhibitor 2D (p19)	NM_001800	**A**
57	CDKN3	Cyclin-dependent kinase inhibitor 3	NM_005192	**A**
58	CHEK1	CHK1 checkpoint homolog (S. pombe)	NM_001274	**A**
59	CHEK2	CHK2 checkpoint homolog (S. pombe)	NM_007194	**A**
60	CKS1B	CDC28 protein kinase regulatory subunit 1B	NM_001826	**P**
61	CKS2	CDC28 protein kinase regulatory subunit 2	NM_001827	**P**
62	CUL1	Cullin 1	NM_003592	**P**
63	CUL2	Cullin 2	NM_003591	**A**
64	CUL3	Cullin 3	NM_003590	**A**
65	CUL4A	Cullin 4A	NM_003589	**P**
66	CUL5	Cullin 5	NM_003478	**P**
67	DDX11	DEAD/H (Asp-Glu-Ala-Asp/His) box polypeptide 11	NM_004399	**P**
68	DNM2	Dynamin 2	NM_004945	**A**
69	E2F1	E2F transcription factor 1	NM_005225	**A**
70	E2F2	E2F transcription factor 2	NM_004091	**A**
71	E2F3	E2F transcription factor 3	NM_001949	**A**
72	E2F4	E2F transcription factor 4, p107/p130-binding	NM_001950	**A**
73	E2F5	E2F transcription factor 5, p130-binding	NM_001951	**P**
74	E2F6	E2F transcription factor 6	NM_198256	**A**
75	GADD45A	Growth arrest and DNA-damage-inducible, alpha	NM_001924	**P**
76	GTF2H1	General transcription factor IIH, polypeptide 1, 62kDa	NM_005316	**P**
77	GTSE1	G-2 and S-phase expressed 1	NM_016426	**A**
78	HERC5	Hect domain and RLD 5	NM_016323	**A**
79	HUS1	HUS1 checkpoint homolog (S. pombe)	NM_004507	**A**
80	KNTC1	Kinetochore associated 1	NM_014708	**A**
81	KPNA2	Karyopherin alpha 2 (RAG cohort 1, importin alpha 1)	NM_002266	**P**
82	MAD2L1	MAD2 mitotic arrest deficient-like 1 (yeast)	NM_002358	**A**

83	MAD2L2	MAD2 mitotic arrest deficient-like 2 (yeast)	NM_006341	**P**
84	MCM2	MCM2 minichromosome maintenance deficient 2, mitotin (S. cerevisiae)	NM_004526	**P**
85	MCM3	MCM3 minichromosome maintenance deficient 3 (S. cerevisiae)	NM_002388	**A**
86	MCM4	MCM4 minichromosome maintenance deficient 4 (S. cerevisiae)	NM_005914	**A**
87	MCM5	MCM5 minichromosome maintenance deficient 5, cell division cycle 46 (S. cerevisiae)	NM_006739	**A**
88	MCM6	Minichromosome maintenance deficient 6 homolog (S. cerevisiae)	NM_005915	**A**
89	MCM7	MCM7 minichromosome maintenance deficient 7 (S. cerevisiae)	NM_005916	**A**
90	MKI67	Antigen identified by monoclonal antibody Ki-67	NM_002417	**A**
91	MNAT1	Menage a trois homolog 1, cyclin H assembly factor (Xenopus laevis)	NM_002431	**P**
92	MRE11A	MRE11 meiotic recombination 11 homolog A (S. cerevisiae)	NM_005590	**A**
93	NBN	Nibrin	NM_002485	**A**
94	PCNA	Proliferating cell nuclear antigen	NM_182649	**P**
95	PKMYT1	Protein kinase, membrane associated tyrosine/threonine 1	NM_182687	**A**
96	RAD1	RAD1 homolog (S. pombe)	NM_002853	**A**
97	RAD17	RAD17 homolog (S. pombe)	NM_002873	**A**
98	RAD50	RAD50 homolog (S. cerevisiae)	NM_005732	**A**
99	RAD51	RAD51 homolog (RecA homolog, E. coli) (S. cerevisiae)	NM_002875	**A**
100	RAD9A	RAD9 homolog A (S. pombe)	NM_004584	**A**
101	RB1	Retinoblastoma 1 (including osteosarcoma)	NM_000321	**P**
102	RBBP8	Retinoblastoma binding protein 8	NM_002894	**P**
103	RBL1	Retinoblastoma-like 1 (p107)	NM_002895	**A**
104	RBL2	Retinoblastoma-like 2 (p130)	NM_005611	**A**
105	RGC32/C13orf15	Response gene to complement 32/chromosome 13 open reading frame 15	NM_014059	**A**
106	RPA3	Replication protein A3, 14kDa	NM_002947	**A**
107	SERTAD1	SERTA domain containing 1	NM_013376	**A**
108	SKP2	S-phase kinase-associated protein 2 (p45)	NM_005983	**A**
109	SUMO1	SMT3 suppressor of mif two 3 homolog 1 (S. cerevisiae)	NM_003352	**P**
110	TFDP1	Transcription factor Dp-1	NM_007111	**P**
111	TFDP2	Transcription factor Dp-2 (E2F dimerization partner 2)	NM_006286	**A**
112	TP53	Tumor protein p53 (Li-Fraumeni syndrome)	NM_000546	**A**
113	UBE1	Ubiquitin-activating enzyme E1 (A1S9T and BN75 temperature sensitivity complementing)	NM_003334	**P**

Functional analysis (Fig. 5)

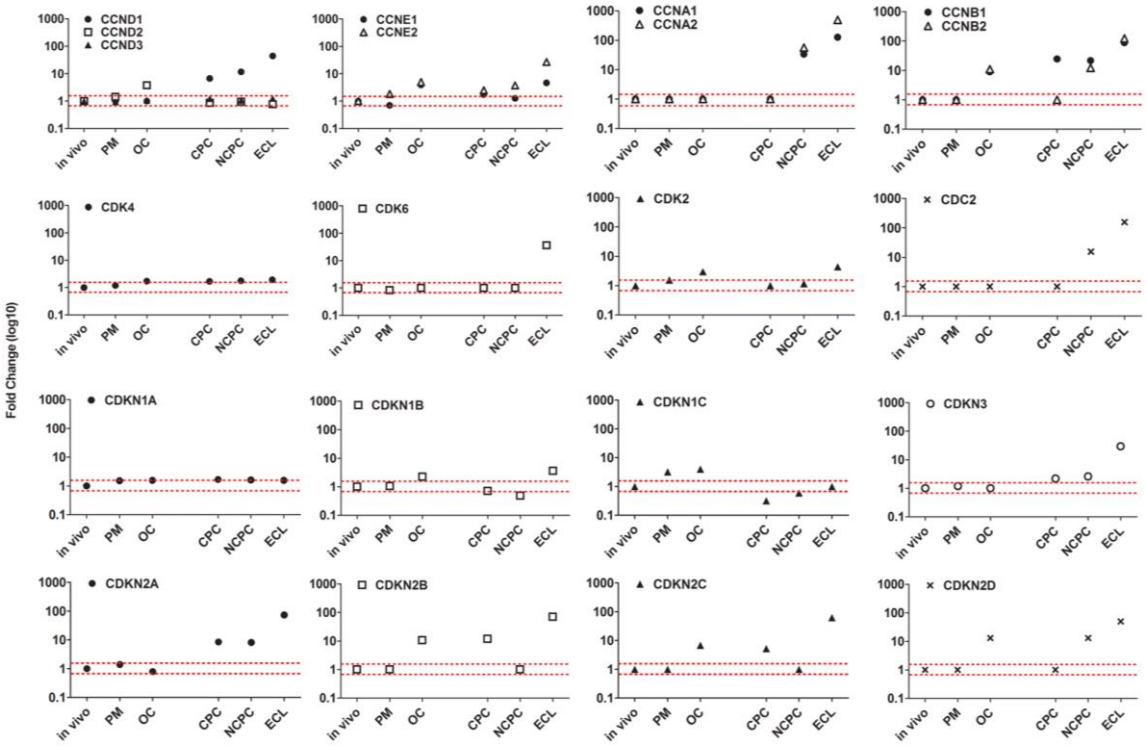


Figure 5. Analysis of mRNA expression of cyclins, CDKs and CKIs in endothelial cells exposed to 6 different environments. *Fold-change expressions of in vivo (reference), post mortem (PM), organ culture (OC), confluent primary culture (CPC), non-confluent primary culture (NCPC), and endothelial cell line (ECL) models were represented in logarithmic scale. The red dotted lines show limits of under/overexpression (fold-change ≥ 1.5).*

Expression of Cyclins and Cyclin-Dependent Kinases

For G1 to S phase, in tissue models, only cyclin D2 was overexpressed in OC. Cyclin D1 and D3 showed no significant change in any conditions. Cyclin D1, not detected in vivo, was increasingly expressed in CPC, NCPC and the ECL. Similarly, cyclin E1 and E2, not detected in vivo, were expressed in OC and primary cultures. For the formation of cyclin/CDK complexes, the level of CDK4 expression detected in vivo did not change significantly in any conditions. Only CDK6 expression, not detected in vivo, was present in the ECL. These observations suggest that the lack of expression of cyclin D1, E1, E2 and CDK6 may be responsible for EC cell-cycle arrest in G1 phase. S to G2 and M phase cyclins (A1, A2, B1, B2) and CDC2 not detected in vivo were expressed only in NCPC and the ECL. These findings were consistent with

proliferation observed in both cell types. CDK2 level increased slightly only in OC and the ECL.

Cyclin-dependent kinase inhibitors

Notably, CDKN1A (p21) expression was unchanged in all conditions. CDKN2A (p16) was overexpressed in the three in vitro cell culture models. CDKN2B (p15), CDKN2C (p18), and CDKN2D (p19) were overexpressed in OC and also in vitro. CDKN3 significantly increased only in the three in vitro cell culture models.

Analysis by biological model (Fig. 6)

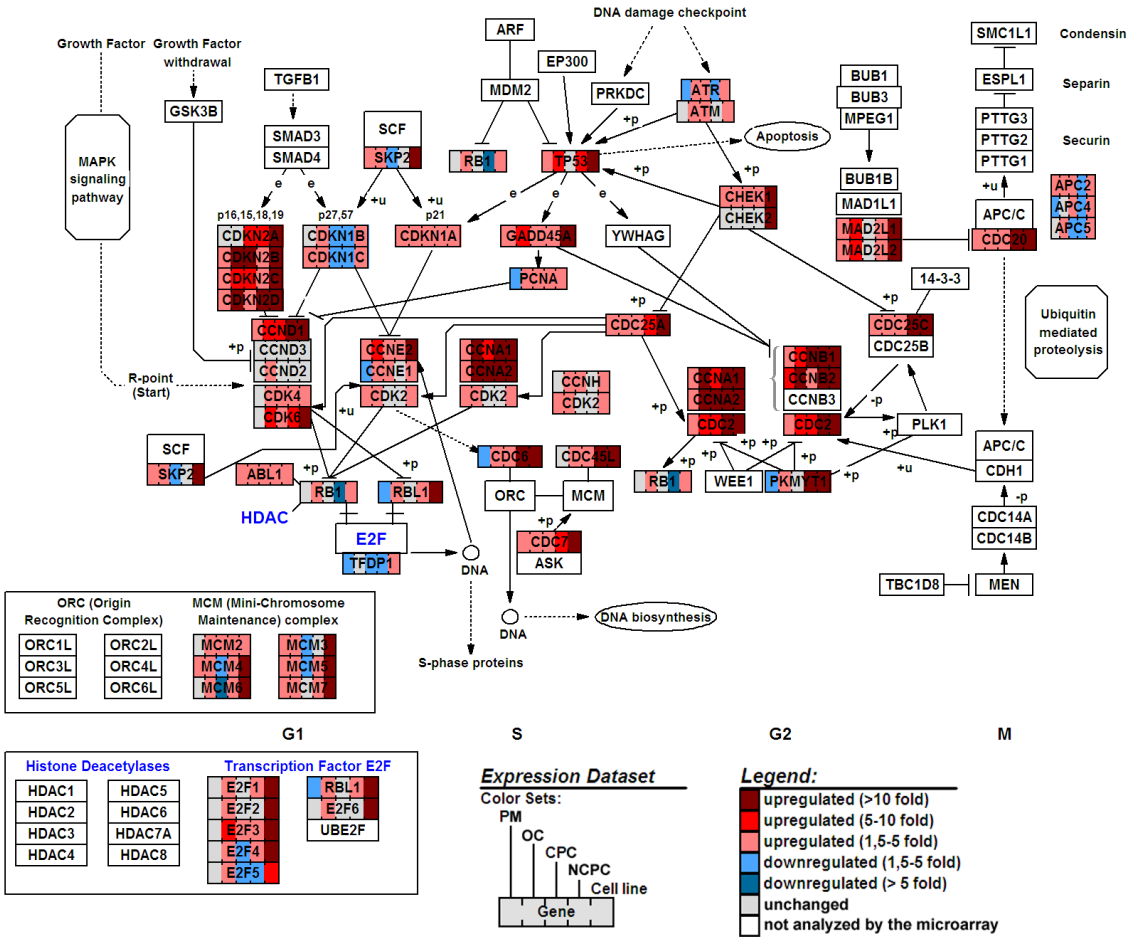


Figure 6. Gene map of cell cycle genes differentially expressed by human corneal endothelial cells in six biological models. *Post mortem (PM), corneal organ culture (OC), in vitro confluent primary culture (CPC), in vitro non-confluent primary culture (NCPC), and immortalized endothelial cell line (ECL). Results were compared with in vivo endothelial cells. The representation of the pathway was generated by GenMAPP version 2.1 (http://www.genmapp.org/) using the cell cycle pathway provided by KEGG.*

Table 4. *Top gene expression changes.*

	OVEREXPRESSION			UNDEREXPRESSION		
	Gene symbol	**Gene title**	**Fold change**	**Gene symbol**	**Gene title**	**Fold change**
Post-mortem	CKS2	CDC28 protein kinase regulatory subunit 2	4.27	ATR	Ataxia telangiectasia and Rad3 related	-2.47
	TP53	Tumor protein p53 (Li-Fraumeni syndrome)	3.56	BAX	BCL2-associated X protein	-2.10
	MAD2L2	MAD2 mitotic arrest deficient-like 2 (yeast)	3.39	CUL4A	Cullin 4A	-2.08
	CCNC	Cyclin C	3.35	CDK5R2	Cyclin-dependent kinase 5, regulatory subunit 2 (p39)	-2.05
	SERTAD1	SERTA domain containing 1	3.26	ANAPC4	Anaphase promoting complex subunit 4	-1.98
	CDKN1C	Cyclin-dependent kinase inhibitor 1C (p57, Kip2)	3.22	TFDP1	Transcription factor Dp-1	-1.80
	CCNG2	Cyclin G2	3.00	KPNA2	Karyopherin alpha 2 (RAG cohort 1, importin alpha 1)	-1.74
	MCM7	MCM7 minichromosome maintenance deficient 7 (S. cerevisiae)	2.64	PCNA	Proliferating cell nuclear antigen	-1.54
	MAD2L1	MAD2 mitotic arrest deficient-like 1 (yeast)	2.25			
	CCNG1	Cyclin G1	2.15			
	CDK7	Cyclin-dependent kinase 7 (MO15 homolog, Xenopus laevis, cdk-activating kinase)	1.99			
OC	DIRAS3	DEAD/H (Asp-Glu-Ala-Asp/His) box polypeptide 11 (CHL1-like helicase homolog, S. cerevisiae)	32.08			
	CCNF	Cyclin F	13.14			
	CDKN2D	Cyclin-dependent kinase inhibitor 2D (p19, inhibits CDK4)	13.05			
	CCNB2	Cyclin B2	10.95			
	CDKN2B	Cyclin-dependent kinase inhibitor 2B (p15, inhibits CDK4)	10.52			
	CCNC	Cyclin C	9.88			
	CCNB1	Cyclin B1	8.97			
	GADD45A	Growth arrest and DNA-damage-inducible, alpha	7.96			
	CUL2	Cullin 2	7.84			
	CCNT2	Cyclin T2	7.71			
	CDK5RAP3	CDK5 regulatory subunit associated protein 3	7.35			
	CDK7	Cyclin-dependent kinase 7 (MO15 homolog, Xenopus laevis, cdk-activating kinase)	7.27			
	CCNG2	Cyclin G2	6.78			
CPC	DIRAS3	DEAD/H (Asp-Glu-Ala-Asp/His) box polypeptide 11 (CHL1-like helicase homolog, S. cerevisiae)	43.06	UBE1	Ubiquitin-activating enzyme E1 (A1S9T and BN75 temperature sensitivity complementing)	-3.33
	BIRC5	Baculoviral IAP repeat-containing 5 (survivin)	38.92	ANAPC5	Anaphase promoting complex subunit 5	-2.49
	CCNB1	Cyclin B1	24.30	TFDP1	Transcription factor Dp-1	-2.01
	CDKN2B	Cyclin-dependent kinase inhibitor 2B (p15, inhibits CDK4)	11.83	CCNG1	Cyclin G1	-1.62
	CKS2	CDC28 protein kinase regulatory subunit 2	9.64	DDX11	DEAD/H (Asp-Glu-Ala-Asp/His) box polypeptide 11 (CHL1-like helicase homolog, S. cerevisiae)	-1.56

	OVEREXPRESSION			UNDEREXPRESSION		
	Gene symbol	**Gene title**	**Fold change**	**Gene symbol**	**Gene title**	**Fold change**
	CDKN2A	Cyclin-dependent kinase inhibitor 2A (melanoma, p16, inhibits CDK4)	8.51			
	CCND1	Cyclin D1	6.66			
	CCNG2	Cyclin G2	6.44			
	CDKN2C	Cyclin-dependent kinase inhibitor 2C (p18, inhibits CDK4)	5.19			
	GADD45 A	Growth arrest and DNA-damage-inducible, alpha	4.51			
NCPC	CCNA2	Cyclin A2	56.21	RB1	Retinoblastoma 1 (including osteosarcoma)	-4.06
	BIRC5	Baculoviral IAP repeat-containing 5 (survivin)	50.85	ANAPC2	Anaphase promoting complex subunit 2	-2.78
	CCNA1	Cyclin A1	33.75	CDKN1 B	Cyclin-dependent kinase inhibitor 1B (p27, Kip1)	-2.03
	CCNB1	Cyclin B1	21.65	ATR	Ataxia telangiectasia and Rad3 related	-1.99
	CDC2	Cell division cycle 2, G1 to S and G2 to M	15.54	ANAPC4	Anaphase promoting complex subunit 4	-1.81
	BRCA2	Breast cancer 2, early onset	14.96	TFDP1	Transcription factor Dp-1	-1.80
	CDC20	Cell division cycle 20 homolog (S. cerevisiae)	14.53	CUL4A	Cullin 4A	-1.62
	CDC37	Cell division cycle 37 homolog (S. cerevisiae)	13.89	ANAPC5	Anaphase promoting complex subunit 5	-1.51
	CDKN2D	Cyclin-dependent kinase inhibitor 2D (p19, inhibits CDK4)	13.10			
	DIRAS3	DEAD/H (Asp-Glu-Ala-Asp/His) box polypeptide 11 (CHL1-like helicase homolog, S. cerevisiae)	12.81			
ECL	CCNA2	Cyclin A2	492.07			
	CDC2	Cell division cycle 2, G1 to S and G2 to M	156.81			
	CDC6	Cell division cycle 6 homolog (S. cerevisiae)	135.25			
	CCNA1	Cyclin A1	127.09			
	CCNB2	Cyclin B2	123.42			
	BIRC5	Baculoviral IAP repeat-containing 5 (survivin)	99.46			
	CCNB1	Cyclin B1	87.46			
	CDC25C	Cell division cycle 25 homolog C (S. pombe)	76.85			
	CDKN2A	Cyclin-dependent kinase inhibitor 2A (melanoma, p16, inhibits CDK4)	73.44			
	PKMYT1	Protein kinase, membrane associated tyrosine/threonine 1	70.07			

Post-mortem group

The total quantity of over/under-represented transcripts was lower than in other groups. The pair-wise comparison of RNA normalized expression values between in vivo and post-mortem identified 59/112 transcripts with ≥1.5-fold changes in

expression (48 overexpressed, 11 underexpressed). The most over-represented transcripts were *CKS2* (+4.3 fold), *TP53* (p53) (+3.6 fold), *MAD2L2* (+3.4 fold), *CCNC* (+3.3 fold) (Table 4). Over-represented transcripts mainly comprised genes potentially associated with cell cycle arrest: *TP53* and *GADD45A*, both cyclin G, which are associated with DNA-induced damage (Cyclin G1 is associated with the p53 pathway [70]; cyclin G2 inhibits proliferation in models of ovarian [71] or gastric [72] cancers); cyclin C, which is a candidate tumor suppressor gene in osteosarcoma [73] and actively maintains quiescence in hematopoietic stem/progenitor cells [74]; *MAD2-1* and *MAD2-2*, two of the essential mitotic spindle checkpoint regulators, which have been associated with limitation of proliferation in a gastric-cancer model [75]; and p57Kip2, a strong inhibitor of several G1 phase cyclin/Cdk complexes and a negative regulator of cell proliferation [76]. In contrast, only three transcripts of pro-proliferative genes were found to be over-represented: CKS2, essential for cell cycle progression and associated with proliferation in gastric cancer [77]; *CDK7*, which functions as a CDK-activating kinase (CAK) and has also been identified as an essential component of the transcription factor TFIIH, which is involved in transcription initiation and DNA repair [78,79,80]; and *MCM7*, critical for cell proliferation and maintaining genome stability [81]. Other genes were absent or under-represented.

Organ Culture group

The pair-wise comparison of RNA normalized expression values between in vivo and OC identified 58/112 transcripts with >1.5-fold changes in expression (all overexpressed). Among the transcripts with the largest fold change in expression (Table 4), the most interesting observation was that several over-represented transcripts, not previously reported, encoded proteins implicated in cell cycle arrest. The most over-represented transcripts were *DIRAS 3*(ARH1) (+32.1 fold), *CCNF* (cyclin F) (+13.1 fold), *CDKN2D* ($p19^{Ink4d}$), (+13.1 fold), *CDKN2B* ($p15^{Ink4b}$) (+11.8 fold). Notably, multiple transcripts of proteins implied in cell cycle arrest in response to DNA damage were over-represented. Several other transcripts encoding pro-proliferative proteins were over-represented: *CCNE1, CCNE2, CCND2, CDK2, CDK4, E2F2.*

Confluent primary culture

The pair-wise comparison of RNA normalized expression values between in vivo and confluent primary cultures identified 32 transcripts with ≥1.5 fold changes in

expression (23 overexpressed, 9 underexpressed). Among the transcripts with the largest fold changes in expression (Table 4) were six of the top 10 encoded proteins implicated in cell cycle arrest (DNA-damaged induced or CKI) and four of the top 10 encoded proteins implicated in proliferation and cell survival. The four most over-represented transcripts were *DIRAS3* (+43.1 fold), *BIRC5* (Survivin) (+38.9 fold), *CCNB1* (cyclin B1)(+24.3 fold), and *CDKN2B* ($p15^{Ink4b}$) (+11.8 fold). The most under-represented transcripts were *UBE1* (-3.3 fold), *ANAPC5* (-2.5 fold), *TFDP1* (-2.0 fold), *E2F5* (-1.9 fold). Confluent primary culture also exhibited overexpression of transcripts of the proliferation marker *Ki67*, underexpression of *CDKN1B* ($p27^{KIP1}$) but overexpression of three other CKIs (*CDKN2B* ($p15^{Ink4b}$), *CDKN2A* ($p16^{Ink4a}$), *CDKN2C* ($p18^{Ink4c}$)), the associated cdk2 inhibitor transcript *CDKN3*, and $p21^{CIP1}$associated transcript *BCCIP*.

Non-confluent primary culture

Confluent and non-confluent primary cultures exhibited similar profiles. The pair-wise comparison of RNA normalized expression values between in vivo and confluent primary cultures identified 36 transcripts with ≥1.5 fold changes in expression (22 overexpressed, 14 underexpressed). Among the transcripts with the largest fold change in expression (Table 4) were three of the top 10 encoded proteins implicated in cell cycle progression and four encoded proteins implicated in cell cycle inhibition. The four most overrepresented transcripts were *BIRC5* (survivin) (+50.9 fold), *CCNB1* (cyclin B1) (+21.7 fold), *BRCA2* (+15.0 fold), and *CDC20* (+14.5 fold). The most underrepresented transcripts were *CUL5* (-8.8 fold), *RB1* (-4.1 fold), *CDK5R2* (-3.3 fold), and *DDX11* (-2.9 fold). Transcripts of proliferation markers (*Ki67* and *MCM2*) were overrepresented. Non-confluent culture overexpressed fewer CKIs than confluent culture.

Cell line

The proliferative cell line exhibited a completely different transcriptional profile. The pair-wise comparison of RNA normalized expression values between in vivo and cell line identified 85 transcripts with ≥1.5 fold changes in expression (all overexpressed). Among the transcripts with the largest fold change in expression (Table 4), the most interesting observation was that several transcripts overrepresented in the cell line encoded proteins implicated in cell proliferation. The most overrepresented

transcripts were *CCNA2* (+492.1 fold), *CDC2* (+156.8 fold), *CDC6* (+135.3 fold), *CCNB2* (+123.4 fold). The cell line exhibited expression changes in several groups of genes; and interestingly, numerous transcripts of cell cycle negative regulators were overrepresented too. Note that *DIRAS3*, overrepresented in OC and in both in vitro cultures, was not found in the ECL.

Real-time PCR confirmation of microarrays

A subset of 11 transcripts, over- or under-represented in microarrays depending on EC type, was tested using qRT-PCR. Differential gene expression was consistent between the two independent methods of analysis, and the level of expression of the 11 genes changed in the same direction, although there were quantitative differences between the results of gene array analysis and of quantitative real-time PCR (Fig. 7). Spearman's correlation coefficient (rho) between microarray and qRT-PCR results was 0.8218 ($p<0.001$), confirming a very high level of agreement.

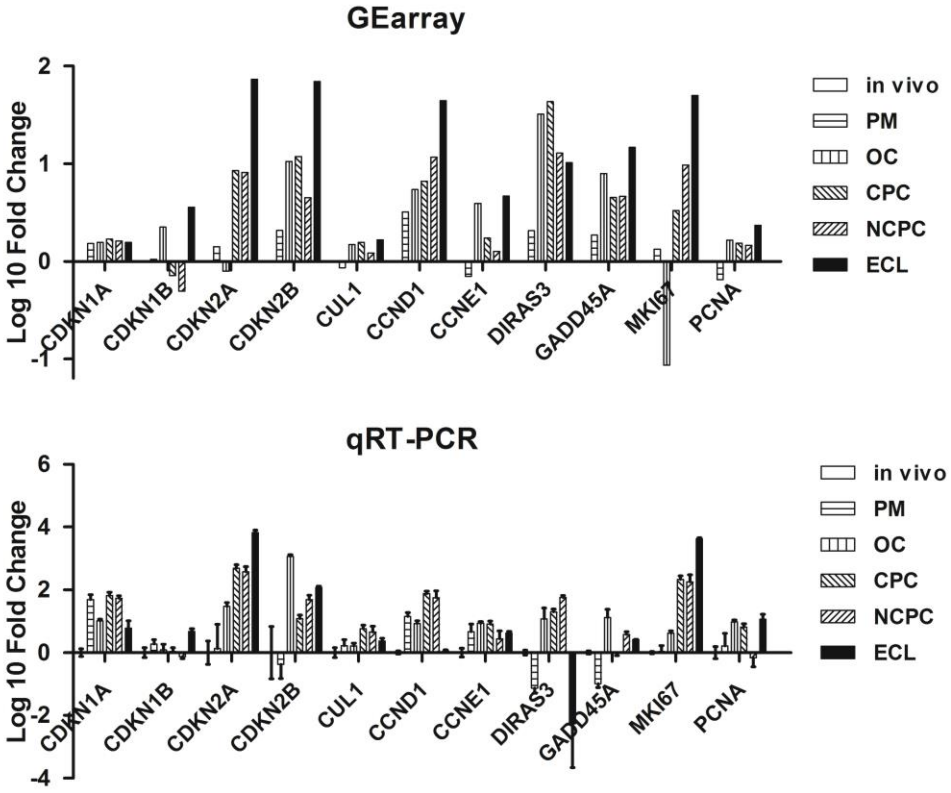


Figure 7. Differentially expressed genes by endothelial cells of the six different biological models, confirmed by real-time PCR. *RNA (300 ng) was characterized using qRT-PCR profiling kit on a subset of 11 genes. Corresponding microarray results are shown.*

Discussion

In the present study, gene array technology was used to examine differential cell cycle gene expression in human corneal ECs that exhibit different proliferation status. A focused cDNA array was chosen. We previously identified unknown differentially expressed genes, especially those implicated in G1-phase arrest and in DNA damage-induced cell cycle arrest in other cell types. While it is beyond the scope of this report to highlight the potential significance of each altered gene, some are of unique interest and warrant specific mention. Although less sensitive than SAGE, SADE or the most recent RNA-sequencing techniques, microarrays enable focused assessment of gene expression in a given tissue. In Gottsh, 10% of SAGE tags were devoted to cell growth and regulation, so it was likely that specific arrays could identify specific variations in cell cycle-related transcripts in ECs. Focused analysis and transcript classification confirmed the logical evolution of the profiles from in vivo to CL, or from the least to the most proliferative status.

Study limitations

Despite a high level of agreement between qRT-PCR and microarrays, the changes in expression detected by microarray analysis were generally smaller than those derived by qRT-PCR as previously described [55]. This may be due to the different detection ranges of these two techniques. It has been demonstrated that microarrays tend to have a low dynamic range, which could lead to under-representation of changes in gene expression, whereas qRT-PCR has a high dynamic range [82]. This may also explain why *CCND1*, *CDNK1A*, and *MKI67*, or changes thereto, were not detected by microarray in certain groups but were detected by real-time PCR.

Ages in the in vivo group were lower than in the other groups because keratoconus patients are younger than corneal donors. In most European countries and particularly in France, where no upper age limit exists for corneal donation, mean donor age is 72 years [34]. The corneas studied in this paper are thus close in age to those routinely grafted, making it difficult to distinguish differences in transcription levels due respectively to donor aging and to environment (post-mortem stress, OC, in vitro cell culture). Donor age was significantly higher than in other studies, and our

results are consequently difficult to compare, since a systemic decrease in transcription and translation with age has been described [83].

The in vivo group comprised only central endothelial cells, whereas the other groups involved the whole endothelium, in which substantial differences in proliferative capacity between center and periphery were demonstrated [41,42]. This likely explains the specific profile found in the in vivo group, where most transcripts were associated with cell cycle arrest and more specifically growth arrest following DNA damage; and the presence in the other groups of both cell cycle arrest and pro-proliferative signatures, because neither central nor peripheral cells were separated.

Confluent and non-confluent primary cultures were grown from independent donors.

Microarrays are limited by the finite number of oligonucleotide sequences on a chip, and are not able to identify the expression of novel genes, contrary to SAGE or genome-wide assays.

Protein expression remains to be demonstrated and quantified on selected candidates to validate microarrays and qRT-PCR findings, given that post-transcriptional modifications are likely to occur, increasing the complexity of cell cycle controls.

Baseline transcription profile in vivo

For the first time, the cell cycle-related transcription profile of human ECs very close to in vivo physiological condition has been described using normal ECs collected immediately after explantation during a corneal graft. This profile is consistent with the previously known proliferative status determined using study of proteins involved in cell cycle regulation performed with donor corneas stored for 24-36 hours at 4°C [84], but provides much complementary information. We found multiple transcripts compatible with early G1 phase arrest of the cell cycle. *GADD45A, Nibrin (NBN* or *NBS1), ATM* and *ATR,* four transcripts associated with DNA damage-induced cell cycle arrest, have been identified. These results are consistent with the recent findings of Joyce et al. [85] using PCR-based microarray (and Western blots for GADD45A and ATM) and with the previously described nuclear oxidative DNA damage in ECs of donors aged over 50 years, with a predominance of lesions in the central corneal area

[83]. These lesions are likely induced by cumulative low-dose exposure to UV radiation throughout life (the major part of UV wavelengths being attenuated by the epithelial and stromal layers) and may be modulated by frequent temperature variations of the cornea. At chromosome level, an age-related accumulation of errors was described in human ECs, with an age-related increase in the relative number of polyploid cells with >4N DNA content and cells with multiple nuclei in otherwise healthy human corneal endothelium [86,87]. Similar increases in DNA content were observed in adult endothelium in response to injury [88].

Several actors in the ubiquitin/proteasome complex implicated in the regulation of CDK/Cyclin and CKI have also been found, confirming that ECs actively regulate their non-proliferative profile and are not excluded from the cell cycle. Our results differ sightly from the literature regarding three transcripts: CCND1, TP53 and CDN2A. We found no expression of CCND1 or CDKN2A in microarrays, only in qRT PCR (see above for technical discussion). Until now, the three cyclin-D isoforms had not been studied separately in human ECs [84,89]. The CCND1 protein (cyclin D1) had been described only in in vitro rat corneal endothelial cells [90]. Cyclin D isoform may have redundant functions and is not distributed equally in all tissues [91]. Nevertheless, the absence of cyclin D1 may be associated with the non-proliferative status of ECs in vivo, as overexpression was observed in OC and in the three types of cell culture. Notably, it has recently been demonstrated that the forced overexpression of CDK4/Cyclin D1 in human ECs led to the establishment of functioning ECL with high growth potential [16]. *CDKN2A* ($p16^{Ink4a}$) was not found either, although expression of the corresponding protein in EC nuclei has already been described, with expression increasing with donor age [43,89,92]. This difference is unlikely explained by the donor age in our experiments because *CDKN2A* was not more strongly expressed in the OC group, although donors were older than in the in vivo group. The difference in tissue origin and storage method may be partly responsible, $p16^{Ink4a}$ having been described in post-mortem cornea with short-term cold storage [43,89,92]. Conversely we found *CDKN2A* in cell cultures, as already described [43]. *TP53* transcript was not found either in microarrays (not tested with qRT-PCR), although the protein has previously been described in human donor cornea after short-term cold storage [89,93,94]. The difference could be explained by the absence of post-mortem and storage-induced stress in our in vivo samples. Moreover, p53 transcript was one of the

most overrepresented in the post-mortem group. Lastly, we found only one of the EF2 transcription factors, E2F5, whose particular role in the early G1 phase has already been described [95].

Donor cornea

High post-mortem stress is liable to induce profound changes in gene transcription. Unsurprisingly, the level of change in our study remained low, indicating a global decrease in cell metabolism. Nevertheless, the well-known long survival of corneal EC after donor death (successful grafts with corneas retrieved up to 72 hours post death are regularly observed, and longer post-mortem times have also been described more anecdotally) explains the possibility of observing significant transcriptional changes. DNA damage appears to activate cell cycle arrest mechanisms through overexpression of several genes involved in the p53-dependent or -independent pathways. Interestingly, culin4A, implicated in the limitation of DNA-damage repair capacity in UV-induced skin cancers [96], is under-represented in this group, and this may correspond to a response adopted to increase cellular DNA repair capacity.

Organ-cultured corneas

Genomic study of OC corneas is also original because only corneas stored at 4°C had previously been studied. Routine OC with conventional medium (MEM + 2% FCS) is the main method used for cornea storage in Europe. By promoting cell metabolism in cell culture-derived medium at 31-34°C (as per eye bank protocol) it allows storage for up to 5 weeks, unlike the current 5-6 days allowed by the cold storage at 4°C common in the USA. OC is not known to promote EC proliferation, although it facilitates endothelial wound healing by migration of cells in the vicinity of the local defect in the endothelial layer [33]. Only OC with 8% FCS, a method that remains an exception,[34] seems likely to promote cell mitosis [22]. It was thus important to determine whether routine OC induces significant transcriptional profile changes liable to reveal the stimulation of certain ECs with residual proliferative capacity. In our samples, the majority of the transcripts are associated with cell cycle arrest mechanisms, but several others were implicated in G1/S transition, suggesting that ECs did not behave homogeneously in OC. The percentage of cells progressing in the cell cycle remains to be determined, but similar focused microarrays were sensitive enough to detect as little as 10% contamination from a specific cell subpopulation [97].

Up to now, the role of three CKIs ($p21^{Cip1}$, $p27^{Kip1}$, and $p16^{Ink4a}$) has been demonstrated. We have highlighted the probable role of the third CIP/KIP $p57^{Kip2}$ and the three other INK4 family members $p15^{Ink4b}$, $p18^{Ink4c}$, $p19^{Ink4d}$, whose transcripts were found to be overexpressed. The absence of $p16^{Ink4a}$ transcript has been discussed above. Our results suggest that cell cycle inhibition is redundantly controlled in OC. Interestingly, other transcripts associated with cell cycle arrest were over-represented, especially DIRAS3 (also over-represented in primary cell cultures but absent in the ECL). DIRAS3, also known as A ras homologue member 1 (ARHI) is a maternally imprinted human tumor suppressor gene that encodes a small G protein with 50-60% aminoacide homology to Rap and Ras. It has been extensively studied in various cancer types. In ovarian and breast cancer, reexpression of ARH1 inhibits cancer cell growth in vitro and in vivo, induces $p21^{WAF1}$ and downregulates cyclin D1 promoter activity [98]. In pancreatic cancer, ARH1 blocks cell progression in cell cycle phase G1, and increases $p21^{Cip1}$ through the accumulation of p53 protein. ARHI enhances expression of $p27^{Kip1}$ through inhibition of PI-3K/AKT signaling [99]. Note that the Pi-3K/AKT signaling pathway has been described in rabbit ECs in response to FGF-2 stimulation in vitro [100]. However, *DIRAS3* was not found in the CorneaNet database nor in the recent study by Joyce et al [85]. Besides *DIRAS3*, several transcripts whose proteins are involved in cell cycle arrest and DNA damage repair in response to DNA damage were described in OC: *GADD45A*, *NBN*, *ATM* and *ATR* already present in the in vivo group, associated with *RAD1*, *RAD9A*, *TP53*, *BCRA1*, and *CCNG1*.

The role of CUL4 should also be further investigated because of its particular relevance in controlling DNA repair capacities. We found its transcript in in vivo EC, underexpressed in the primary cultures, and over-represented in OC and the CL. The CUL4A-E3 ligase is involved in the ubiquitination of various protein substrates around the site of UV-induced DNA damage.[101] It is associated with UV-damaged DNA-binding protein 2 that has been described as highly expressed in human EC [102]. By analogy with descriptions made in UV-induced skin carcinogenesis in mice, in which CUL4 ubiquitin ligase restricts cellular repair capacity [96], overexpression of CUL4 in OC or the CL may suggest that ECs do not operate at their full DNA repair potential, and highlight the potential increase in cell repair proficiency by pharmacological CUL4A inhibition.

In vitro primary cell cultures

Confluent and non-confluent cultures did not differ fundamentally in profile. Like ECs from OC corneas, they exhibited cell cycle arrest-associated transcripts, be they CKIs, cell cycle checkpoints, or DNA damage-induced. Conversely, they also logically expressed transcripts associated with proliferation such as G1/S and G2/M cyclins, or proliferation markers. One of the most overexpressed transcripts was that of the anti-apoptotic protein survivin, which may be stimulated by cell culture-associated stress. Interestingly, the CKI $p27^{KIP1}$ was found to be under-represented, although it was associated with mitotic inhibition induced by cell-cell contact in neonatal rat ECs [103,104]. This result suggests that contact inhibition in confluent culture may be less efficient than in vivo, and/or that the mechanism in humans may involve other CKIs than only $p27^{Kip1}$.

Cell line

The SV40LT transformed CL overexpressed almost all cell cycle-related genes in the microarray. The most up-regulated genes were logically associated with cell cycle progression and were consistent with the mechanisms of SV40LT transformation [105]: CDK/cyclin of the G1/S and G2/M transitions, E2F transcription factors, proliferation markers and MCM replication complex, with *CCNA2* and *CDC2* (both G2/M) being the two most over-represented. Conversely, cycle inhibitors (CKIs, checkpoints, DNA damage-induced inhibitors) were also strongly over-represented. A first hypothesis for the double profile relies on good contact inhibition of the cell line that, despite high proliferative capacity, strictly grows in a monolayer until it reaches very high cell density. A second explanation could be the existence of a double population in the cell line, with opposite differentiation and proliferation profiles [35,38]. High expression of anti-apoptotic proteins is common in immortalized cells, especially IAPs [106]. Notably, the absence of overexpression of *DIRAS3* in those proliferative cells suggests it plays a role in mitosis inhibition in non-transformed ECs, where it is always present.

Conclusions

Cell cycle-specific cDNA arrays identified several candidate genes that may actively repress EC proliferation in humans and thus help us understand the premature senescence in human ECs previously described [8,42,107]. These genes are thus a useful resource for further mechanistic studies. Several of them could be targets for triggering and controlling cell proliferation, with a view to developing a cell therapy for corneal endothelial dystrophies.

References

1. Stocker FW (1953) The endothelium of the cornea and its clinical implications. Trans Am Ophthalmol Soc 51: 669.

2. Maurice DM (1970) The transparency of the corneal stroma. Vision Res 10: 107-108.

3. Murphy C, Alvarado J, Juster R, Maglio M (1984) Prenatal and postnatal cellularity of the human corneal endothelium. A quantitative histologic study. Invest Ophthalmol Vis Sci 25: 312-322.

4. Ko MK, Park WK, Lee JH, Chi JG (2001) A histomorphometric study of corneal endothelial cells in normal human fetuses. Exp Eye Res 72: 403-409.

5. Bourne WM, Nelson LR, Hodge DO (1997) Central corneal endothelial cell changes over a ten-year period. Invest Ophthalmol Vis Sci 38: 779-782.

6. Joyce NC (2003) Proliferative capacity of the corneal endothelium. Prog Retin Eye Res 22: 359-389.

7. Joyce NC (2012) Proliferative capacity of corneal endothelial cells. Exp Eye Res 95: 16-23.

8. Sheerin AN, Smith SK, Jennert-Burston K, Brook AJ, Allen MC, et al. (2012) Characterization of cellular senescence mechanisms in human corneal endothelial cells. Aging Cell 11: 234-240.

9. Insler MS, Lopez JG (1991) Heterologous transplantation versus enhancement of human corneal endothelium. Cornea 10: 136-148.

10. Okumura N, Koizumi N, Ueno M, Sakamoto Y, Takahashi H, et al. (2012) ROCK inhibitor converts corneal endothelial cells into a phenotype capable of regenerating in vivo endothelial tissue. Am J Pathol 181: 268-277.

11. McGowan SL, Edelhauser HF, Pfister RR, Whikehart DR (2007) Stem cell markers in the human posterior limbus and corneal endothelium of unwounded and wounded corneas. Mol Vis 13: 1984-2000.

12. He Z, Campolmi N, Gain P, Minh Hathi B, Dumollard JM, et al. (2012) Revisited Microanatomy of the Corneal Endothelial Periphery: New Evidence for Continuous Centripetal Migration of Endothelial Cells in Humans. Stem Cells 30: 2523-2534.

13. Wilson SE, Lloyd SA, He YG, McCash CS (1993) Extended life of human corneal endothelial cells transfected with the SV40 large T antigen. Invest Ophthalmol Vis Sci 34: 2112-2123.

14. Feldman ST, Gjerset R, Gately D, Chien KR, Feramisco JR (1993) Expression of SV40 virus large T antigen by recombinant adenoviruses activates proliferation of corneal endothelium in vitro. J Clin Invest 91: 1713-1720.

15. Wilson SE, Weng J, Blair S, He YG, Lloyd S (1995) Expression of E6/E7 or SV40 large T antigen-coding oncogenes in human corneal endothelial cells indicates regulated high-proliferative capacity. Invest Ophthalmol Vis Sci 36: 32-40.

16. Yokoi T, Seko Y, Makino H, Hatou S, Yamada M, et al. (2012) Establishment of functioning human corneal endothelial cell line with high growth potential. PloS one 7: e29677.

17. Liu Z, Zhuang J, Li C, Wan P, Li N, et al. (2012) Long-term cultivation of human corneal endothelial cells by telomerase expression. Exp Eye Res 100: 40-51.

18. McAlister JC, Joyce NC, Harris DL, Ali RR, Larkin DF (2005) Induction of replication in human corneal endothelial cells by E2F2 transcription factor cDNA transfer. Invest Ophthalmol Vis Sci 46: 3597-3603.

19. Kikuchi M, Zhu C, Senoo T, Obara Y, Joyce NC (2006) p27kip1 siRNA induces proliferation in corneal endothelial cells from young but not older donors. Invest Ophthalmol Vis Sci 47: 4803-4809.

20. Joyce NC, Harris DL (2010) Decreasing expression of the G1-phase inhibitors, p21Cip1 and p16INK4a, promotes division of corneal endothelial cells from older donors. Mol Vis 16: 897-906.

21. Fuchsluger TA, Jurkunas U, Kazlauskas A, Dana R (2011) Anti-apoptotic gene therapy prolongs survival of corneal endothelial cells during storage. Gene Ther.

22. Slettedal JK, Lyberg T, Roger M, Beraki K, Ramstad H, et al. (2008) Regeneration with proliferation of the endothelium of cultured human donor corneas with extended postmortem time. Cornea 27: 212-219.

23. Peh GS, Toh KP, Wu FY, Tan DT, Mehta JS (2011) Cultivation of human corneal endothelial cells isolated from paired donor corneas. PloS one 6: e28310.

24. Shin YJ, Cho DY, Chung TY, Han SB, Hyon JY, et al. (2011) Rapamycin reduces reactive oxygen species in cultured human corneal endothelial cells. Curr Eye Res 36: 1116-1122.

25. Bayyoud T, Thaler S, Hofmann J, Maurus C, Spitzer MS, et al. (2012) Decellularized bovine corneal posterior lamellae as carrier matrix for cultivated human corneal endothelial cells. Curr Eye Res 37: 179-186.

26. Watanabe R, Hayashi R, Kimura Y, Tanaka Y, Kageyama T, et al. (2011) A novel gelatin hydrogel carrier sheet for corneal endothelial transplantation. Tissue Eng Part A 17: 2213-2219.

27. Senoo T, Obara Y, Joyce NC (2000) EDTA: a promoter of proliferation in human corneal endothelium. Invest Ophthalmol Vis Sci 41: 2930-2935.

28. Patel SP, Bourne WM (2009) Corneal endothelial cell proliferation: a function of cell density. Invest Ophthalmol Vis Sci 50: 2742-2746.

29. Senoo T, Joyce NC (2000) Cell cycle kinetics in corneal endothelium from old and young donors. Invest Ophthalmol Vis Sci 41: 660-667.

30. Yokoo S, Yamagami S, Yanagi Y, Uchida S, Mimura T, et al. (2005) Human corneal endothelial cell precursors isolated by sphere-forming assay. Invest Ophthalmol Vis Sci 46: 1626-1631.

31. Hatou S, Yoshida S, Higa K, Miyashita H, Inagaki E, et al. (2013) Functional corneal endothelium derived from corneal stroma stem cells of neural crest origin by retinoic acid and Wnt/beta-catenin signaling. Stem Cells Dev 22: 828-839.

32. Yu WY, Sheridan C, Grierson I, Mason S, Kearns V, et al. (2011) Progenitors for the corneal endothelium and trabecular meshwork: a potential source for personalized stem cell therapy in corneal endothelial diseases and glaucoma. J Biomed Biotechnol 2011: 412743.

33. Nejepinska J, Juklova K, Jirsova K (2010) Organ culture, but not hypothermic storage, facilitates the repair of the corneal endothelium following mechanical damage. Acta Ophthalmol 88: 413-419.

34. European Eye Bank Association Directory. eighteenth edition. 2010. Amsterdam.

35. Valtink M, Gruschwitz R, Funk RH, Engelmann K (2008) Two clonal cell lines of immortalized human corneal endothelial cells show either differentiated or precursor cell characteristics. Cells Tissues Organs 187: 286-294.

36. Gottsch JD, Seitzman GD, Margulies EH, Bowers AL, Michels AJ, et al. (2003) Gene expression in donor corneal endothelium. Arch Ophthalmol 121: 252-258.

37. Gottsch JD, Bowers AL, Margulies EH, Seitzman GD, Kim SW, et al. (2003) Serial analysis of gene expression in the corneal endothelium of Fuchs' dystrophy. Invest Ophthalmol Vis Sci 44: 594-599.

38. Bednarz J, Teifel M, Friedl P, Engelmann K (2000) Immortalization of human corneal endothelial cells using electroporation protocol optimized for human corneal endothelial and human retinal pigment epithelial cells. Acta Ophthalmol Scand 78: 130-136.

39. Chen KH, Azar D, Joyce NC (2001) Transplantation of adult human corneal endothelium ex vivo: a morphologic study. Cornea 20: 731-737.

40. Zhu C, Joyce NC (2004) Proliferative response of corneal endothelial cells from young and older donors. Invest Ophthalmol Vis Sci 45: 1743-1751.

41. Konomi K, Zhu C, Harris D, Joyce NC (2005) Comparison of the proliferative capacity of human corneal endothelial cells from the central and peripheral areas. Invest Ophthalmol Vis Sci 46: 4086-4091.

42. Mimura T, Joyce NC (2006) Replication competence and senescence in central and peripheral human corneal endothelium. Invest Ophthalmol Vis Sci 47: 1387-1396.

43. Enomoto K, Mimura T, Harris DL, Joyce NC (2006) Age differences in cyclin-dependent kinase inhibitor expression and rb hyperphosphorylation in human corneal endothelial cells. Invest Ophthalmol Vis Sci 47: 4330-4340.

44. Mergler S, Dannowski H, Bednarz J, Engelmann K, Hartmann C, et al. (2003) Calcium influx induced by activation of receptor tyrosine kinases in SV40-transfected human corneal endothelial cells. Exp Eye Res 77: 485-495.

45. Saghizadeh M, Kramerov AA, Tajbakhsh J, Aoki AM, Wang C, et al. (2005) Proteinase and growth factor alterations revealed by gene microarray analysis of human diabetic corneas. Invest Ophthalmol Vis Sci 46: 3604-3615.

46. Tanwar MK, Gilbert MR, Holland EC (2002) Gene expression microarray analysis reveals YKL-40 to be a potential serum marker for malignant character in human glioma. Cancer Res 62: 4364-4368.

47. Desai KV, Michalowska AM, Kondaiah P, Ward JM, Shih JH, et al. (2004) Gene expression profiling identifies a unique androgen-mediated inflammatory/immune signature and a PTEN (phosphatase and tensin homolog deleted on chromosome 10)-mediated apoptotic response specific to the rat ventral prostate. Mol Endocrinol 18: 2895-2907.

48. Bustin SA (2002) Quantification of mRNA using real-time reverse transcription PCR (RT-PCR): trends and problems. J Mol Endocrinol 29: 23-39.

49. Menendez L, Benigno BB, McDonald JF (2004) L1 and HERV-W retrotransposons are hypomethylated in human ovarian carcinomas. Mol Cancer 3: 12.

50. Lee PD, Sladek R, Greenwood CM, Hudson TJ (2002) Control genes and variability: absence of ubiquitous reference transcripts in diverse mammalian expression studies. Genome Res 12: 292-297.

51. Zweitzig DR, Smirnov DA, Connelly MC, Terstappen LW, O'Hara SM, et al. (2007) Physiological stress induces the metastasis marker AGR2 in breast cancer cells. Mol Cell Biochem 306: 255-260.

52. Kosaka Y, Mimori K, Fukagawa T, Ishikawa K, Etoh T, et al. (2007) Identification of the high-risk group for metastasis of gastric cancer cases by vascular endothelial growth factor receptor-1 overexpression in peripheral blood. Br J Cancer 96: 1723-1728.

53. Veeriah S, Kautenburger T, Habermann N, Sauer J, Dietrich H, et al. (2006) Apple flavonoids inhibit growth of HT29 human colon cancer cells and modulate expression of genes involved in the biotransformation of xenobiotics. Mol Carcinog 45: 164-174.

54. DenBesten PK, Machule D, Zhang Y, Yan Q, Li W (2005) Characterization of human primary enamel organ epithelial cells in vitro. Arch Oral Biol 50: 689-694.

55. Bryan BA, Dyson OF, Akula SM (2006) Identifying cellular genes crucial for the reactivation of Kaposi's sarcoma-associated herpesvirus latency. J Gen Virol 87: 519-529.

56. Qu R, Li Y, Gao Q, Shen L, Zhang J, et al. (2007) Neurotrophic and growth factor gene expression profiling of mouse bone marrow stromal cells induced by ischemic brain extracts. Neuropathology 27: 355-363.

57. Kucukzeybek Y, Gul MK, Cengiz E, Erten C, Karaca B, et al. (2008) Enhancement of docetaxel-induced cytotoxicity and apoptosis by all-trans retinoic acid (ATRA) through downregulation of survivin (BIRC5), MCL-1 and LTbeta-R in hormone- and drug resistant prostate cancer cell line, DU-145. J Exp Clin Cancer Res 27: 37.

58. Chang HY, Sneddon JB, Alizadeh AA, Sood R, West RB, et al. (2004) Gene expression signature of fibroblast serum response predicts human cancer progression: similarities between tumors and wounds. PLoS Biol 2: E7.

59. Bittel DC, Kibiryeva N, Sell SM, Strong TV, Butler MG (2007) Whole genome microarray analysis of gene expression in Prader-Willi syndrome. Am J Med Genet A 143: 430-442.

60. Schippert R, Schaeffel F, Feldkaemper MP (2008) Microarray analysis of retinal gene expression in chicks during imposed myopic defocus. Mol Vis 14: 1589-1599.

61. Huang da W, Sherman BT, Lempicki RA (2009) Systematic and integrative analysis of large gene lists using DAVID bioinformatics resources. Nat Protoc 4: 44-57.

62. Huang da W, Sherman BT, Lempicki RA (2009) Bioinformatics enrichment tools: paths toward the comprehensive functional analysis of large gene lists. Nucleic Acids Res 37: 1-13.

63. Computing RFfS (2012) R: A language and environment for statistical computing. In: Team RDC, editor. Vienna.

64. Kanehisa M, Goto S (2000) KEGG: kyoto encyclopedia of genes and genomes. Nucleic Acids Res 28: 27-30.

65. Kanehisa M, Goto S, Sato Y, Furumichi M, Tanabe M (2012) KEGG for integration and interpretation of large-scale molecular data sets. Nucleic Acids Res 40: D109-114.

66. Lanfranco MF, Seitz PK, Morabito MV, Emeson RB, Sanders-Bush E, et al. (2009) An innovative real-time PCR method to measure changes in RNA editing of the serotonin 2C receptor (5-HT(2C)R) in brain. J Neurosci Methods 179: 247-257.

67. Schefe JH, Lehmann KE, Buschmann IR, Unger T, Funke-Kaiser H (2006) Quantitative real-time RT-PCR data analysis: current concepts and the novel "gene expression's CT difference" formula. J Mol Med 84: 901-910.

68. Livak KJ, Schmittgen TD (2001) Analysis of relative gene expression data using real-time quantitative PCR and the 2(-Delta Delta C(T)) Method. Methods 25: 402-408.

69. Wong ML, Medrano JF (2005) Real-time PCR for mRNA quantitation. Biotechniques 39: 75-85.

70. Bates S, Rowan S, Vousden KH (1996) Characterisation of human cyclin G1 and G2: DNA damage inducible genes. Oncogene 13: 1103-1109.

71. Xu G, Bernaudo S, Fu G, Lee DY, Yang BB, et al. (2008) Cyclin G2 is degraded through the ubiquitin-proteasome pathway and mediates the antiproliferative effect of activin receptor-like kinase 7. Mol Biol Cell 19: 4968-4979.

72. Choi MG, Noh JH, An JY, Hong SK, Park SB, et al. (2009) Expression levels of cyclin G2, but not cyclin E, correlate with gastric cancer progression. J Surg Res 157: 168-174.

73. Ohata N, Ito S, Yoshida A, Kunisada T, Numoto K, et al. (2006) Highly frequent allelic loss of chromosome 6q16-23 in osteosarcoma: involvement of cyclin C in osteosarcoma. Int J Mol Med 18: 1153-1158.

74. Miyata Y, Liu Y, Jankovic V, Sashida G, Lee JM, et al. (2010) Cyclin C regulates human hematopoietic stem/progenitor cell quiescence. Stem Cells 28: 308-317.

75. Wang L, Yin F, Du Y, Chen B, Liang S, et al. (2010) Depression of MAD2 inhibits apoptosis and increases proliferation and multidrug resistance in gastric cancer cells by regulating the activation of phosphorylated survivin. Tumour Biol 31: 225-232.

76. Matsuoka S, Edwards MC, Bai C, Parker S, Zhang P, et al. (1995) p57KIP2, a structurally distinct member of the p21CIP1 Cdk inhibitor family, is a candidate tumor suppressor gene. Genes Dev 9: 650-662.

77. Kang MA, Kim JT, Kim JH, Kim SY, Kim YH, et al. (2009) Upregulation of the cycline kinase subunit CKS2 increases cell proliferation rate in gastric cancer. J Cancer Res Clin Oncol 135: 761-769.

78. Schwartz BE, Larochelle S, Suter B, Lis JT (2003) Cdk7 is required for full activation of Drosophila heat shock genes and RNA polymerase II phosphorylation in vivo. Mol Cell Biol 23: 6876-6886.

79. Matsuno M, Kose H, Okabe M, Hiromi Y (2007) TFIIH controls developmentally-regulated cell cycle progression as a holocomplex. Genes Cells 12: 1289-1300.

80. Gentile A, Ditt RF, Dias FO, Da Silva MJ, Dornelas MC, et al. (2009) Characterization of ScMat1, a putative TFIIH subunit from sugarcane. Plant Cell Rep 28: 663-672.

81. Gladden AB, Diehl JA (2003) The cyclin D1-dependent kinase associates with the pre-replication complex and modulates RB.MCM7 binding. J Biol Chem 278: 9754-9760.

82. Mutch DM, Berger A, Mansourian R, Rytz A, Roberts MA (2002) The limit fold change model: a practical approach for selecting differentially expressed genes from microarray data. BMC Bioinformatics 3: 17.

83. Joyce NC, Zhu CC, Harris DL (2009) Relationship among oxidative stress, DNA damage, and proliferative capacity in human corneal endothelium. Invest Ophthalmol Vis Sci 50: 2116-2122.

84. Joyce NC, Meklir B, Joyce SJ, Zieske JD (1996) Cell cycle protein expression and proliferative status in human corneal cells. Invest Ophthalmol Vis Sci 37: 645-655.

85. Joyce NC, Harris DL, Zhu CC (2011) Age-related gene response of human corneal endothelium to oxidative stress and DNA damage. Invest Ophthalmol Vis Sci 52: 1641-1649.

86. Ikebe H, Takamatsu T, Itoi M, Fujita S (1984) Cytofluorometric nuclear DNA determinations on human corneal endothelial cells. Exp Eye Res 39: 497-504.

87. Ikebe H, Takamatsu T, Itoi M, Fujita S (1986) Age-dependent changes in nuclear DNA content and cell size of presumably normal human corneal endothelium. Exp Eye Res 43: 251-258.

88. Ikebe H, Takamatsu T, Itoi M, Fujita S (1988) Changes in nuclear DNA content and cell size of injured human corneal endothelium. Exp Eye Res 47: 205-215.

89. Joyce NC, Navon SE, Roy S, Zieske JD (1996) Expression of cell cycle-associated proteins in human and rabbit corneal endothelium in situ. Invest Ophthalmol Vis Sci 37: 1566-1575.

90. Kikuchi M, Harris DL, Obara Y, Senoo T, Joyce NC (2004) p27kip1 Antisense-induced proliferative activity of rat corneal endothelial cells. Invest Ophthalmol Vis Sci 45: 1763-1770.

91. Pagano M, Jackson PK (2004) Wagging the dogma; tissue-specific cell cycle control in the mouse embryo. Cell 118: 535-538.

92. Joyce NC (2005) Cell cycle status in human corneal endothelium. Exp Eye Res 81: 629-638.

93. Paull AC, Whikehart DR (2005) Expression of the p53 family of proteins in central and peripheral human corneal endothelial cells. Mol Vis 11: 328-334.

94. Song Z, Wang Y, Xie L, Zang X, Yin H (2008) Expression of senescence-related genes in human corneal endothelial cells. Mol Vis 14: 161-170.

95. Sardet C, Vidal M, Cobrinik D, Geng Y, Onufryk C, et al. (1995) E2F-4 and E2F-5, two members of the E2F family, are expressed in the early phases of the cell cycle. Proc Natl Acad Sci U S A 92: 2403-2407.

96. Liu L, Lee S, Zhang J, Peters SB, Hannah J, et al. (2009) CUL4A abrogation augments DNA damage response and protection against skin carcinogenesis. Mol Cell 34: 451-460.

97. Luo Y, Schwartz C, Shin S, Zeng X, Chen N, et al. (2006) A focused microarray to assess dopaminergic and glial cell differentiation from fetal tissue or embryonic stem cells. Stem Cells 24: 865-875.

98. Bao JJ, Le XF, Wang RY, Yuan J, Wang L, et al. (2002) Reexpression of the tumor suppressor gene ARHI induces apoptosis in ovarian and breast cancer cells through a caspase-independent calpain-dependent pathway. Cancer Res 62: 7264-7272.

99. Lu X, Qian J, Yu Y, Yang H, Li J (2009) Expression of the tumor suppressor ARHI inhibits the growth of pancreatic cancer cells by inducing G1 cell cycle arrest. Oncol Rep 22: 635-640.

100. Lee HT, Kay EP (2003) Regulatory role of PI 3-kinase on expression of Cdk4 and p27, nuclear localization of Cdk4, and phosphorylation of p27 in corneal endothelial cells. Invest Ophthalmol Vis Sci 44: 1521-1528.

101. Sugasawa K (2009) UV-DDB: a molecular machine linking DNA repair with ubiquitination. DNA Repair (Amst) 8: 969-972.

102. Inoki T, Endo H, Inoki Y, Hamamoto T, Tsuru T, et al. (2004) Damaged DNA-binding protein 2 accelerates UV-damaged DNA repair in human corneal endothelium. Exp Eye Res 79: 367-376.

103. Joyce NC, Harris DL, Zieske JD (1998) Mitotic inhibition of corneal endothelium in neonatal rats. Invest Ophthalmol Vis Sci 39: 2572-2583.

104. Joyce NC, Harris DL, Mello DM (2002) Mechanisms of mitotic inhibition in corneal endothelium: contact inhibition and TGF-beta2. Invest Ophthalmol Vis Sci 43: 2152-2159.

105. Lee C, Cho Y (2002) Interactions of SV40 large T antigen and other viral proteins with retinoblastoma tumour suppressor. Rev Med Virol 12: 81-92.

106. LaCasse EC, Baird S, Korneluk RG, MacKenzie AE (1998) The inhibitors of apoptosis (IAPs) and their emerging role in cancer. Oncogene 17: 3247-3259.

107. Konomi K, Joyce NC (2007) Age and topographical comparison of telomere lengths in human corneal endothelial cells. Mol Vis 13: 1251-1258.

ARTICLE II: Corneal endothelial cells from old donors: differentiation, senescence, proliferative capacities and optimized culture conditions

La culture primaire de CEs est théoriquement la méthode la plus susceptible de conduire à des cellules ayant le bon phénotype final mais les capacités prolifératives résiduelles exploitées in vitro restent le plus souvent limitées. Elles ont mis en échec pendant 30 ans la plupart des tentatives de production de masse de CEs. Récemment, une équipe de Singapore Eye Research Institute a publié le premier protocole obtenant suffisamment de CEs pour envisager une application clinique prochaine, mais les cultures sont établies à partir de donneur de 30 ans et moins, ce qui est un frein majeur à l'utilisation du protocole en Europe. Rappelons que la moyenne d'âge y est de 70 ans et que les donneurs de moins de 30 ans sont réellement anecdotiques.

Nous envisageons une autre approche destinée à utiliser de façon réaliste les donneurs dont nous disposons régulièrement. Dans ce travail, nous avons caractérisé la différenciation, la sénescence et les capacités prolifératives résiduelles des CEs de donneurs de plus de 50 ans, et proposons un procédé de culture optimisé. Ce procédé de culture de courte durée associe une courte incubation dans un milieu de survie facilitant aussi l'adhérence au support, suivi d'une incubation en milieu de stabilisation. Le but est plus d'augmenter la DCE en concentrant les CEs que de les forcer à proliférer. Cette stratégie garantit le maintien du bon phénotype en évitant la transition mésenchymateuse de ces CEs sénescentes. A terme, celui-ci pourrait permettre d'utiliser les 20% de cornées détruites dans les banques pour endothélium insuffisant pour enrichir des cornées entières ou coloniser des supports pour reconstruire des greffons endothéliaux.

Cover letter

Dear Editor,

We are please to submit an original article entitled "**Corneal endothelial cells from old donors: differentiation, senescence, proliferative capacities and optimized culture conditions**." in *Aging Cell*.

La greffe de cornée est la plus fréquente des greffes dans le monde mais l'offre est très loin de couvrir les besoins sans cesse croissants. Le déséquilibre est inégal dans la monde et, bien entendu, les populations qui en ont le plus besoin sont celles qui en bénéficient le moins; Le don de cornée, seule source actuelle de tissue, reste limité pour de multiples raisons, éducationnelle, religieuses mais aussi logistiques et il est probable qu'il ne connaitra jamais une évolution suffisante pour couvrir les besoins. Des alternatives à l'utilisation de cornées de donneurs sont d'ores et déjà en cours de développement. Le bioengineering de greffons endothéliaux représente la solution la plus réaliste à moyen terme car le cahier des charges est plus simple que celui de la reconstruction d'une cornée entière en échec depuis 30 ans. Le prérequis commun à toutes les stratégies de bioengineering est le développement de culture de masse de cellules endothéliales (CEs) à partir d'un petit nombre de cornées de donneurs pour multiplier les ressources. Ces cellules ont la particularité de ne pas proliférer in vivo et de façon très limitée in vitro. De nombreuses méthodes ont été décrites, essentiellement à but scientifique, et toutes en utilisant des donneurs de 30 ans et moins, ce qui n'est pas réaliste pour un procédé de bioengineering qui doit utiliser une ressource plus facilement disponible.

Le travail que nous présentons caractérise la différenciation et les capacités prolifératives résiduelles de l'endothélium des cornées de donneurs âgés. Nous mettons en évidence que la périphérie cornéenne est composée de cellules moins bien différenciées et que certaines cellules peuvent exprimer des marqueurs de progéniteurs ; Nous montrons également, pour la première fois qu'il existe de rare label-retaining cells à l'extrême périphérie de l'endothélium, probablement des vestiges du développement embryonnaire de l'endothélium sans traduction clinique cependant. Enfin, nous proposons une méthode de culture spécifique des CEs de donneurs âges, qui permet de pooler les CEs afin d'obtenir une quantité de CEs bien différenciées et d'éviter l'endothelial-mensenchymal transformation habituellement décrite dans la plupart des méthodes de cultures. Notre technique pourrait permettre de « recycler » les 20% des cornées de donneurs âgés habituellement détruites par les banques de cornées à cause d'un nombre insuffisant de CEs.

We declare that all authors have directly participated in the planning, execution, or analysis of the study and resulting paper, and have read and approved the submitted version.

We hope that our manuscript will interest the Editorial Board of *Aging Cell*.

Sincerely,

Professor Gilles Thuret, MD, PhD, Institut Universitaire de France
Corresponding author:
Laboratory for Biology, engineering and imaging of Corneal Graft, EA 2152, IFR143
Faculty of Medicine
15, Rue Ambroise Paré
F 42023 Saint-Etienne Cedex 2, France.
Tel: +33 (0)4 77 12 77 93
Fax: +33 (0)4 77 12 09 95
E-mail: gilles.thuret@univ-st-etienne.fr

Corneal endothelial cells from old donors: differentiation, senescence, proliferative capacities and optimized culture conditions.

Binh Minh Thi Ha[1], Nelly Campolmi[1, 2], Zhiguo He[1], Jean-Yves Thuret[5], Simone Piselli[1], Fabien Forest [1, 3], Jean-Marc Dumollard[1, 3], Michel Peoc'h[1, 3], Olivier Garraud[1, 4], Philippe Gain[1, 2], Gilles Thuret[1, 2, 6]

1. Laboratory for corneal graft biology, engineering and imaging', EA2521, SFR143, Faculty of Medicine, Saint-Etienne, France

2. Department of Ophthalmology, University Hospital, Saint-Etienne, France

3. Department of Pathology, University Hospital, Saint-Etienne, France

4. Eye Bank, Etablissement Français du Sang Loire/Auvergne, Saint-Etienne, France

5. Commissariat à l'Energie Atomique, Institut de biologie et de technologies de Saclay (iBiTec-S), Service de Biologie Intégrative et de Génétique Moléculaire (SBIGeM), F-91191, Gif-sur-Yvette, France.

6. Institut Universitaire de France, 103, Boulevard Saint-Michel, 75005 Paris

Summary

The intrinsically low proliferative capacity of human corneal endothelial cells (HCECs) and their rapid senescence during in vitro expansion constitute major limitations for cell bioengineering destined to treat endothelial dysfunctions that result in corneal blindness. A recent success was obtained with donors below 30 years old in Asia, but, in Europe, the mean donor age of 70 adds a supplementary difficulty to the complex equation. This study aims at clarifying whether old donor corneas could be however used for cell expansion.

The morphology and differentiation of central and peripheral HCECs were analysed by immunostaining of ion transport-related proteins, progenitor and neuronal markers in whole corneas retrieved in donor >50 years. The proliferative capacity of HCECs from organ-cultured corneas was quantified by 5-ethynyl-2′-deoxyuridine proliferation assay. The differences of central versus peripheral HCECs were further characterized in vitro by studying their migration, proliferation and differentiation in serum-containing medium.

Central HCECs highly expressed specific ion transport-related proteins, and showed a high senescence level. On the contrary, cells located in the periphery or extreme periphery were less specialized, expressed progenitors and neuronal markers and were more prone to endothelial-mesenchymal transformation in serum-containing medium. With a new culture sequence that limited proliferation and maintained differentiation, corneas from donors >70 years old, could successfully be used to reconstitute a monolayer of stable endothelial phenotype with endothelial cell density (ECD) of 2000 cells/mm^2 but require pooling of corneas. This will allow to "recycle" the 20% of corneas usually discarded by eye banks because of age-related ECD decline.

Key words (6): corneal endothelium, aging, donor, senescence, bioengineering, graft.

Introduction

The corneal endothelium functions as a permeability barrier that restricts the movement of ions and water into the hydrophilic stroma to control corneal transparency(Maurice 1972; Bonanno 2012). In human, the deregulation of cornea transparency due to endothelium degeneration is irreversible because of the absence of efficient regeneration mechanisms of corneal endothelium. In vivo, human corneal endothelial cells (HCECs) are blocked at G1 phase but maintain a residual proliferative capacity. The senescence state of HCEC in vivo may result from many simultaneous mechanisms(Joyce 2003; Joyce 2012; Sheerin *et al.* 2012): low level of growth factors in aqueous humour, lack of autocrine stimulation by growth factors synthesized by EC, cell cycle entry inhibition by TGF-β2 present in the aqueous humour, contact inhibition induced by the formation of mature cell-cell and cell-substrate junctions, oxidative DNA damage resulting in a permanent high level of cyclin-dependent kinase inhibitors (CDKI) p27, p21, p16 (proteins or transcripts) and cascades of blocking points for G1-S transition (Sheerin *et al.* 2012).

Recent findings confirmed that proliferative capacity of human endothelium depend highly on age and cellular topography (center or periphery). First, aging is highly related to the increase of oxidative DNA damage in central endothelium, in ex vivo and in vitro condition (Joyce *et al.* 2009). Compared to ex vivo HCEC from young donor (< 30 years), ex vivo HCEC from old donor (> 50 years) cornea stains most strongly for senescence-associated β-galactosidase (Mimura & Joyce 2006), giving

enlarged cells and low-density monolayer when isolated in primary culture (Liu *et al.* 2012). Consequently, the most recent reports of in vitro HCEC expansion were done mainly using young donor cornea(Levis *et al.* 2012; Liu *et al.* 2012; Schmedt *et al.* 2012; Yokoi *et al.* 2012; Peh *et al.* 2013). Secondly, proliferative capacity of HCECs also depends on their central or peripheral localization. The high level of oxidative DNA damage and the senescence state of HCEC in old donor were found principally in central HCEC compared with peripheral HCEC (Mimura & Joyce 2006; Joyce *et al.* 2009). Further morphology observations of the centre and the periphery showed a relationship between cell localization and differentiation state. HCEC density is higher in peripheral cornea than central cornea (Schimmelpfennig 1984; Amann *et al.* 2003). Central HCECs form a flat hexagonal monolayer on a smooth Descemet membrane (DM), whereas peripheral cells are organized in radial rows between DM furrows, and, in the extreme periphery, form cells clusters between DM mushroom-shaped DM excrescents called Hassall-Henle bodies(He *et al.* 2012). Replication competences of HCECs are better in the periphery than in the centre, which exhibits little or no mitotic activity (Bednarz *et al.* 1998; Mimura & Joyce 2006). In particular, the rate of sphere formation by peripheral HCEC is 4 times higher than by central HCEC(Yokoo *et al.* 2005). About progenitor markers, the expression of nestin, telomerase, ABCG2 were occasionally detected in extreme periphery endothelium of cornea retrieved with short post-mortem delay (He *et al.* 2012). Recently, the expression of LGR5 detected in peripheral HCEC and the implication of Wnt signalling (Hirata-Tominaga *et al.* 2013) suggests the existence of stem cell in corneal endothelium. Further, progenitors were detected at the edge of DM (in a region called transition zone) with stem cell markers expression as nestin, alkaline phosphatase and telomerase (McGowan *et al.* 2007). This transition zone was supposed to be a potential stem cell source for endothelial renewal in case of wounding (Yu *et al.* 2011). Nevertheless, despite many evidence supporting the hypothesis of progenitor existence in corneal endothelium, this potential regeneration source is not efficient in vivo in case of severe corneal endothelial damage. Even in physiological conditions, the number of HCEC decreases by 0.56% per year during adulthood (Murphy *et al.* 1984).

Despite more than 100000 corneal grafts performed each year in the world thanks to donor corneas, there is a huge scarcity for donation, especially in Asia and Africa where the estimated needs are the most elevated. Moreover, corneal blindness increases in the world mainly because of population aging, and new surgical

techniques, namely lamellar grafts increase the number of patients eligible for surgery(Tan *et al.* 2012), thus increasing even further the needs. Therefore, the bioengineering of endothelial substitutes is considered as the most realistic solution to reduce the general supply-demand imbalance. Indeed, endothelial dystrophies may represent one third of all corneal graft indications and consequently, replacing endothelial grafts prepared from donor corneas by bioengineered endothelial substitutes would allow redistributing of donors corneas for the other indications. Two types of bioengineered endothelial substitutes are now envisaged: HCECs suspension destined to be injected into the anterior chamber behind the diseased cornea in association with strategy promoting cell adherence onto the cornea, and in vitro reconstruction of an endothelial graft simply consisting in establishing a continuous mosaic of densely packed monolayered HCECs on a thin biocompatible transparent carrier. In both processes the first step is to obtain a stable, GMP-compatible mass culture of functioning HCECs. Among the different developing strategies, the expansion of HCECs retrieved from donor corneas has the theoretical advantage of producing cells directly with the right phenotype, compared with emerging strategy of stem cells differentiation into HCECs. Furthermore, starting from corneal tissue, for a corneal application would also certainly facilitate acceptance by health authorities during transfer into patients. Nevertheless, 35 years after the description of mass HCECs cultures from very young donors (Baum *et al.* 1979), and despite regular reports of culture successes, no translation into patients has been done yet. On the one hand, successes were usually, if not always, reported with young donors (>30 years old) who are by definition scarce, at least in Europe and in the USA. It seems not therefore easily conceivable to build a bioengineered process on a rare cell source. Indeed, the average donor age in 2011 was 61 years old in European eye banks (EBAA 2012) and 59 years old in the USA, with 83% retrieved from donors from 41-80 years old (EBAA 2012). On the second hand, many HCECs expansion processes rapidly result in cell morphology alterations likely to correspond to partial or total function loss. The most common alteration appears as endothelial-mesenchymal transformation (EMT) with elongated and fibroblast-like abnormal phenotype (Schmedt *et al.* 2012), a phenomenon also described in vivo during retrocorneal fibrous membrane formation for instance in end stage Fuchs dystrophy (Leung *et al.* 2000). To avoid this alteration, Peh et al. recently proposed a new two-step protocol composed of one proliferation phase and

one stabilisation phase. However, even with young donors, seeding HCECs at low density still resulted in EMT (Peh *et al.* 2013).

In this manuscript, we used complementary techniques to better characterize the differentiation state and proliferative capacities of HCECS of corneas retrieved in donors over 50 years old, to determined whether they could be suitable for establishing reliable HCECs cultures in view of an endothelial bioengineering process. We suggest a culture protocol that, rather than expanding the cell pool, allows recycling corneas with poor endothelial cell density (ECD) in order to obtain well differentiated mosaics of acceptable ECD.

Results

HCECs are less specialized in the periphery than in the center of the endothelium

The differentiation of HCECs was firstly assessed by studying their morphology and their expression of specific ions transport proteins. The expression of ZO-1 and of the 3 pumps, $Na^{+/}K^{+}$ATPase, CLCN3, and VDAC3, was assessed by immunostaining on flat-mounted cornea ($n \geq 2$) retrieved with low postmortem delay (4.5 to 9 hours) (Fig. 1A). Central HCECs formed regular monolayer of hexagonal cells with tight-junction component ZO-1, highly expressed Na^{+}/K^{+}ATPase in lateral membrane, CLCN3 in both apical and basolateral membrane and VDAC3 in apical membrane as expected(Bonanno 2003; Bonanno 2012). Peripheral HCECs formed a less organized tight junction belt in their apical pole and express Na^{+}/K^{+}ATPase but were organized in radial rows between Hassal-Henle bodies. Nevertheless, in extreme periphery, HCECs lost their tight junction and pumps expression in the vicinity of the transition zone (Fig. 1A).

Additionally, considering the origin of corneal endothelium from the periocular mesenchyme derived from neural crest, the expression of mesenchymal markers (αSMA), and neuronal markers (NRP2, NSE, NCAM1, and β-III tubulin) were assessed by immunostaining in the same samples (Fig. 1). The expression of NCAM1 was detected in lateral membrane of central, peripheral and extreme peripheral HCECs. NSE expression was detected exclusively in central HCEC. On the contrary, αSMA, NRP2, and β-III tubulin were occasionally found exclusively in the extreme periphery, mostly in cell clusters nested between Hassal-Henle bodies. Furthermore, in the

transition zone previously reported as a possible progenitor cell niches(McGowan *et al.* 2007), cells expressed αSMA, β-III tubulin and occasionally NRP2 (Fig. 1B). The contact between the extreme periphery and the transition zone and the shared expression of αSMA, β-III tubulin and NRP2, suggested cell migration from the transition zone towards corneal endothelium.

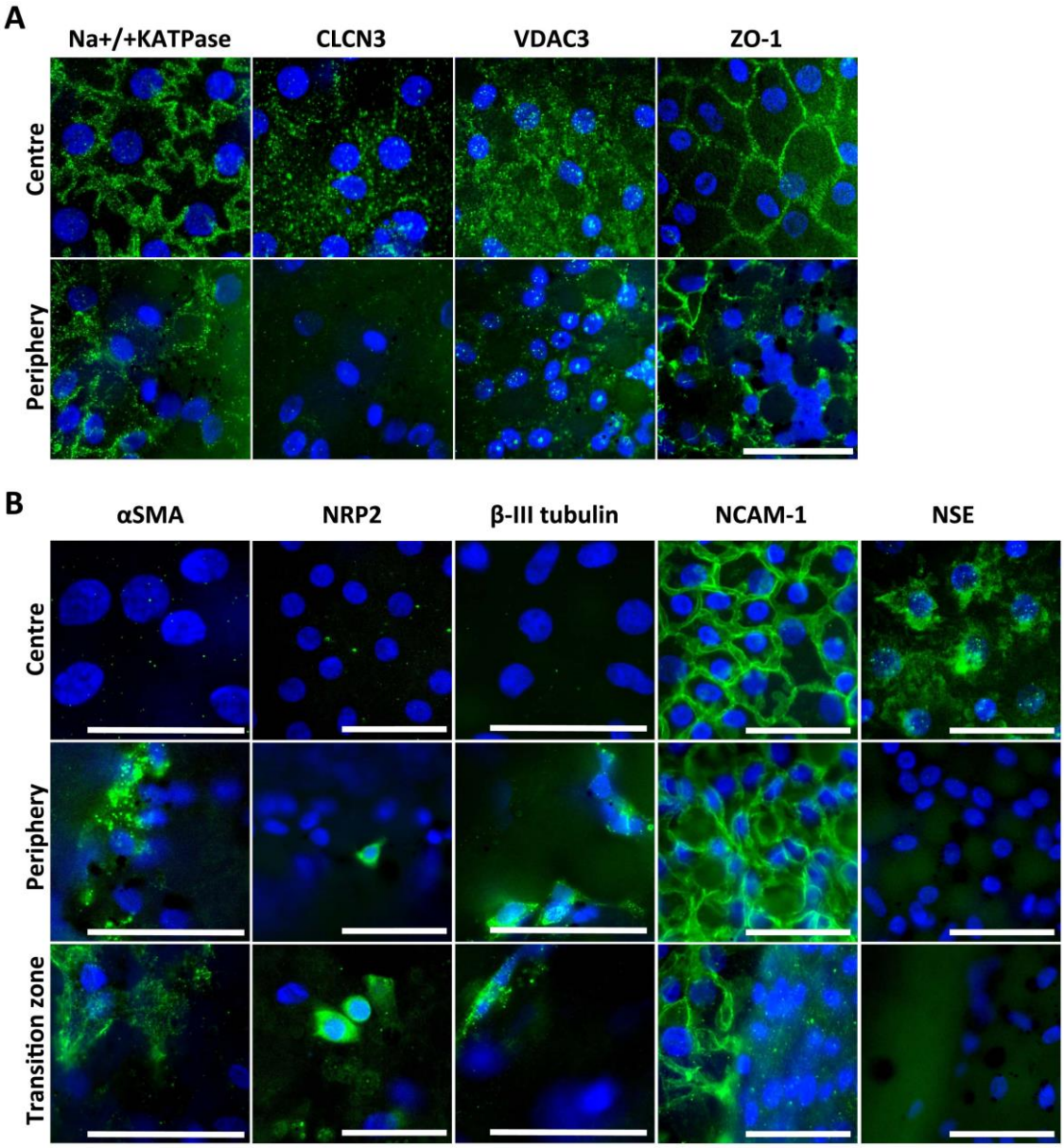


Fig. 1 *Immunostaining of differentiation markers (pseudocolored in green) in human corneal endothelial cells (HCEC) of fresh whole corneas (5 corneas of 73-79 years old donors) with extremely short post mortem times. (A) Proteins most often used to characterize HCEC (ion transporters Na^+/K^+ATPase, CLCN3, and VDAC3, and the tight junction protein ZO-1) were labelled and observed in the center and periphery of the endothelium. (B) expression of mesenchymal and neuronal markers: αSMA, NRP2, β-III tubulin, NCAM1 NSE in the same regions and also just ouside the endothelium in a short band called transition zone, that makes transition with the trabecular meshwork. Nuclei were counterstained with Hoechst 33342 (pseudocolored in blue). Scale bar 50µm.*

Proliferation capacity of HCEC depends on endothelial cell density but rare label-retaining cells are localised in the extreme periphery of the endothelium of all corneas

After 30 days of incubation with EdU, corneas with endothelial cell density (ECD) over 2000 cells/mm^2 carried only a few EdU+ ECs located exclusively at the extreme periphery, whereas corneas with ECD < 1500 cells/mm^2 had significantly more EdU+ ECs, located in both the center and the periphery (Fig.2). The EdU+ ECs number was negatively correlated with ECD with Spearman r coefficient at -0,43 (P = 0,0117). In order to study the regeneration mechanism nearest to physiological conditions, only high-ECD corneas (> 2000 cell/mm^2) were chosen to eliminate mechanisms activated by low ECD. Corneas were incubated with EdU during 30 days following by another 30 days period without EdU to select only label retaining cells. Very rare slow-cycling cells (1 to 5 per cornea) were detected in all corneas exclusively in the extreme periphery next to the transition zone.

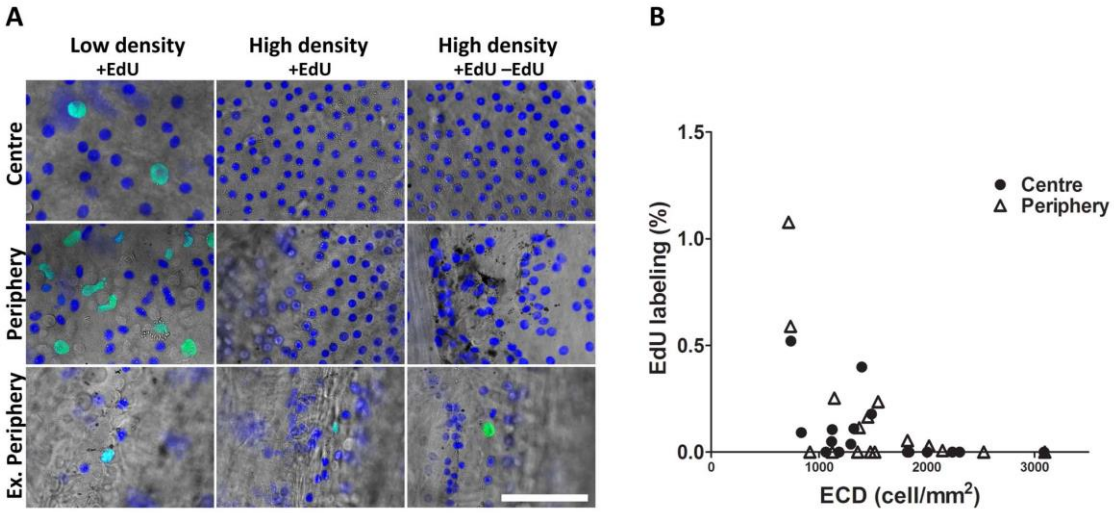


Fig. 2 *Characterization of cell cycle activation in intact endothelium of donor corneas stored in organ culture in a medium containing 2% foetal calf serum. EdU+ cells (nuclei pseudocolored in green) were counted in low-density (<1500 cells/mm^2) and high-density endothelium (>2000 cells/mm^2) in the center, the periphery and the extreme periphery (A). Number of EdU+ ECs was negatively correlated with ECD (B) In order to detect label-retaining cells directly in situ in intact tissue, organ-cultured corneas with ECD>2000 cells/mm^2 were incubated with for 30 days with EdU (+EdU) following of 30 days without EdU (-EdU) (18 corneas of 59-83 year-old donors). Very rare label retaining cells were found exclusively at the extreme periphery. Nuclei were counterstained with Hoechst 33342 (pseudocolored in blue). All images are merged with bright field view. Scale bar 100µm*

In vitro, peripheral HCEC can easily migrate from Descemet membrane but rapidly undergo mesenchymal transformation

Considering the variation in expression of differentiation markers, progenitor markers and proliferative capacity from the centre to the periphery in HCEC of OC corneas, the behaviour of HCEC was further studied in vitro after isolation in primary culture. HCEC migration was observed firstly from peripheral DM fragments, starting 3 days after peeling-off, whereas migration from central DM started only after 5 days with a lower extend (Fig. 3A). After 2 weeks of in vitro culture, central HCECs formed homogenous endothelial monolayer cells with tight junctions whereas HCECs from peripheral DM underwent mesenchymal transformation with heterogeneous fibroblastic-like morphology.

Almost all central HCECs incubated with EdU during 7 days fully retained the label 1 week after EdU removal (Fig. 3A), indicating a limited mitotic activity (S phase without subsequent significant division). Peripheral HCECs divisions were also detected but most of fibroblastic-like cell displayed a partial EdU labeling, providing evidence for a continuous proliferation after EdU removal from culture medium. Furthermore, HCECs having migrated outside the DM divided quickly and lost the EdU marker, but those that remained attached to the DM kept slow-cycling with full labelled nuclei (Fig. 3B).

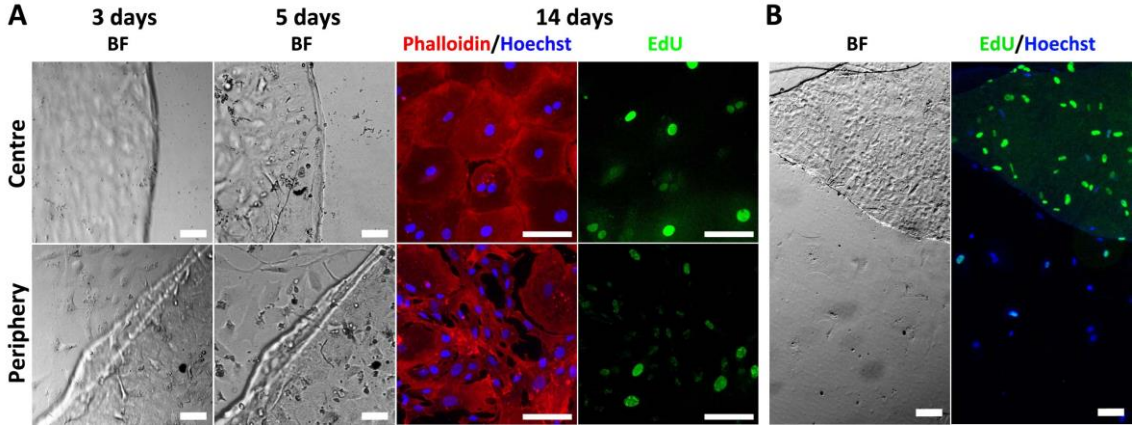


Fig. 3 *In vitro migration of human corneal endothelial cells (HCEC) from Descemet membrane explants and differentiation in adherent culture. Brightfield images of HCEC migration at 3rd and 5th days, and fluorescence image of Phalloidin (red) and EdU (green) at 14th day characterized central HCEC by slow migration (from 5th day), low division activity (full EdU label) and homogenous morphology of endothelial cell after complete migration (14 days), compared to faster migration of peripheral HCEC (from 3rd day), high division activity (partial EdU label) and mesenchymal transformation after 2 weeks of culture (A). Detection of slow-cycling cell in HCEC remained attached on the Descemet membrane after 7 days in EdU and 7 days without EdU (B). Scale bar 100 µm. (4 corneas of 50-83 year-old donors).*

Old donor corneas contain endothelial progenitors located in their periphery

In sphere culture from old donors (63, 65 and 86 years old), no significant increase in sphere diameter with time was observed for both central and peripheral HCEC. The expression of progenitor and differentiation markers in spheres was analyzed by immunostaining. Cells located in the core of spheres expressed neuronal progenitor marker nestin exclusively in sphere bigger than 100 µm of diameter. β-III tubulin, a marker of neuronal differentiation, and αSMA, a mesenchymal marker, were expressed in the peripheral cells. NCAM1 was expressed in all cells, from the core to the envelope (Fig. 4A).

After inducing adherence of sphere by liquid FCS-containing medium in order to promote differentiation, cells from sphere reformed a monolayer of pseudo hexagonal cells. They expressed ZO-1 in apical tight-junctions, Na+/K+ATPase, NCAM1 and β-III tubulin (Fig. 4B).

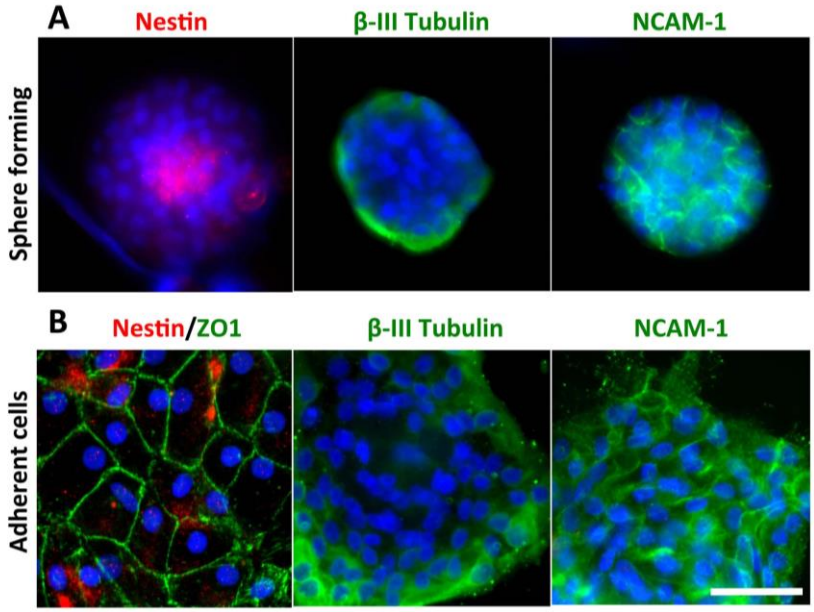


Fig. 4 *Expression of progenitor and differentiation markers after sphere-forming assay with HCECs isolated from a very old donor (3 pairs of corneas of 63, 65 and 86 year-old donors) (A) and subsequent culture in adherent conditions (B). Immunostaining of nestin, β-III tubulin, NCAM1 and ZO-1. Nuclei were counterstained with Hoechst 33342 (pseudocolored in blue). Scale bar 50 µm.*

New strategy for HCEC culture from old donor corneas

After having shown that old donor cornea retained endothelial progenitor at least in their periphery but that peripheral HCECs rapidly underwent endothelial-mesenchymal transformation (EMT) during in vitro proliferation in serum containing

medium we designed a specific culture sequence able to provide well-differentiated mosaics with acceptable ECD. HCECs were isolated from whole corneas (center and periphery separately) by peel-digest method, seeded directly at confluent density (2000 cells/mm^2) in OptiMEM-I medium containing 8% FCS for only 4h to promote cells survival and adherence and then cultured in stabilisation serum free medium to avoid EMT. Central and peripheral HCECs cultured separately maintained both a stable monolayer with strong expression of ZO-1, Na^+/K^+ATPase for at least 2 weeks (Fig. 5). Using corneas from 70 and 75 years old donors that had initially 1700-2300 cells/mm^2 after retrieval, second passage culture of HCECs reached 8 to 8.5 x10^4 cells by pooling both corneas from the same donor. It is therefore possible to pool 2 corneas to cover a 7mm diameter disc with HCECs slightly higher than 2000 cells/mm^2.

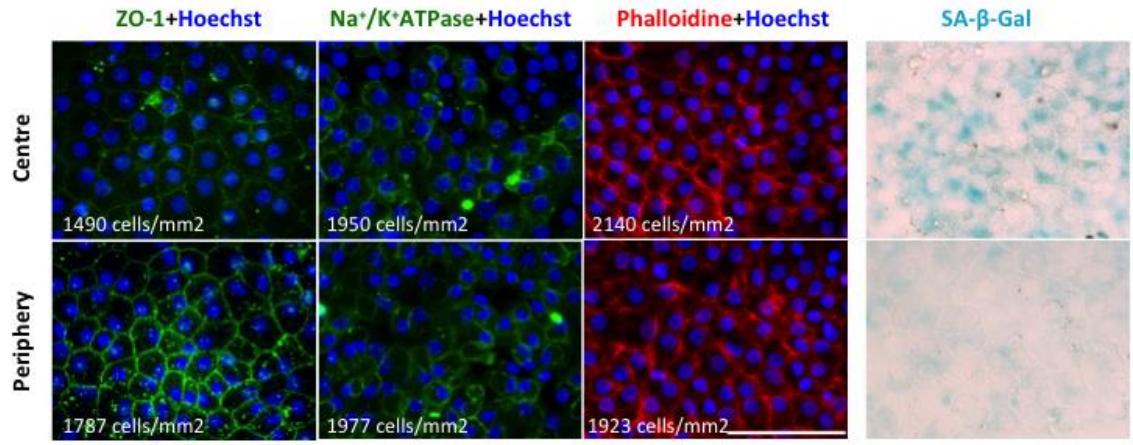


Fig. 5 *Evaluation of in vitro HCEC culture from old donor cornea (donors of 85 and 75 years old). Morphology and functionality after 7 days of culture of HCEC. Immunostaining of ZO-1 and Na^+/K^+ATPase, staining of actin by phalloidine and SA-α-Gal assay for senescence level (n=2). Nuclei were counterstained with Hoechst 33342 (pseudocolored in blue). Scale bar 100µm.*

Discussion

The prerequisite for corneal endothelial bioengineering is to obtain, in a reproducible manner, a mass culture of cells with a perfect corneal endothelial phenotype. Nevertheless, a balance has to be found between proliferation and differentiation, since high proliferation goes along with fibroblastic transformation (EMT), and highly differentiated mosaics with strong contact inhibition automatically triggering cell cycle arrest. Until now, the main obstacles for the development of efficient corneal endothelium bioengineering strategies are the alteration of HCEC

morphology (highly suggesting loss of pump functions) and limited survival during in vitro expansion of the cell pool that acquires a senescent fibroblastic morphology. This phenotype is highly related to the well-characterized limited proliferative capacity of HCECs retrieved mainly in old donor corneas (EEBA 2012). In this study, we highlight that these alterations are caused mainly by the peripheral HCECs that, in old donors, remain less differentiated than in the center and consequently more prone to fibroblastic transformation when submitted to external stimulations like during organ culture or in vitro culture in serum containing media. Using a new culture sequence combining short time incubation at high density in serum containing medium followed by incubation in serum free medium, we show that HCECs from old donors successfully maintains the endothelial morphology with acceptable ECD. We were able to obtain 5.2 x 10^4 HCECs at a ECD of 2000 cells/mm^2 from 1 pair of cornea, suggesting that HCECs of 4 donor corneas not suitable for graft because of low ECD could be pooled to repopulate one 8mm diameter carrier (50,2 mm^2) to reconstruct an endothelial graft.

Center versus periphery differentiation heterogeneity

Human corneal endothelium is not homogeneous from the periphery to the centre in regards to ECD (Schimmelpfennig 1984), proliferating capacities(Bednarz *et al.* 1998; Joyce 2012), density of progenitors (Yokoo *et al.* 2005) and microanatomy (He *et al.* 2011). Here we show in old donors, that HCECs do not express exactly the same differentiation markers suggesting that they progressively acquire their complete phenotype and function during their centripetal migration. Additionally, subpopulations of HCECs from the extreme periphery and of cells of the transition zone express progenitor markers. We described two new markers in the transition zone and extreme endothelial periphery potentially implicated in endothelial formation. NRP was previously reported in a chicken embryogenesis model, implicated in endothelium differentiation from periocular mesenchyme derived from neural crest, induced by crystalline epithelium (Lwigale & Bronner-Fraser 2009). Presence of β-III tubulin, a neuronal marker potentially implicated in neurogenesis and axon guidance (NCBI ressource for TUBB3 (Gene ID: 10381) updated on 21-Dec-2013) was not previously reported. Being found in both locations, both markers are new evidence for the continuous differentiation process from the extreme periphery toward cornea centre that we previously described (He *et al.* 2012) even in old donor. These new findings

complete the list of progenitor markers already described in this area as telomerase, nestin, and alkaline phosphatase (McGowan *et al.* 2007; He *et al.* 2012).

Proliferation and label retaining cells

Proliferation assay in OC corneas reveals that a few central and peripheral HCECs proliferate only in corneas below 2000 cells/mm^2. Although we cannot rule out a certain toxicity of prolonged incubation with EdU itself that could induce underestimation of proliferation rate, our results are consistent with the findings of Patel et al. in a different model in which activation of HCECs division was achieved by artificial contact inhibition release by EDTA and incubation in culture medium supplemented by 10% FCS and growth factors(Patel & Bourne 2009). The threshold of 2000 cells/mm^2 may represent a limit in the cohesion of the mosaics under which cell contact inhibition can be efficiently released in central and peripheral endothelium. In organ culture with CorneaMax we previously showed that the mosaic was not evenly covered with viable cells(Pipparelli *et al.* 2011). We suggest that random small lesions present in the endothelium of OC corneas could stimulate HCECs proliferation in corneas with low ECD in a medium comprising only 2% FCS and no other growth factors. Additionally, for the first time, the EdU labeling in intact whole OC corneas with high ECD revealed the existence of rare isolated label-retaining HCECs in the extreme periphery. These cells may be at the origin of the sphere observed during the sphere-forming assay. Although spheres remained small in diameter they expressed neuronal progenitor and differentiation markers, and were able to reform monolayer of functional endothelial cells upon adherent culture conditions. The slow-cycling cells that we described may be residual endothelial progenitors that extremely slowly divide giving rise to transient amplifying cells migrating from the extreme periphery to the centre of the endothelium. However, this hypothetical regeneration mechanism is clinically insufficient to restore ECD after traumatism or even to maintain ECD constant with age, and may be consequently only a vestige of the embryonic activity. Furthermore, EdU labeling during primary culture also clearly show that DM play a major role in limiting HCECs proliferation. Further analysis of the HCECs/DM contact inhibition should help understand how to overcome this blockage during expansion phase and to arrest proliferation during stabilization phase of bioengineering.

Increased risk of endothelial-mesenchymal transformation with foetal calf serum

Complementary to the differences between central and peripheral differentiation profiles observed on ex vivo corneas, we found a faster migration of peripheral HCECs and observed their ability to undergo EMT during in vitro culture with serum-containing medium. EMT of HCECs was previously described in 8% serum-containing medium without specifying the localization of the transformed HCEC sub-population(Schmedt *et al.* 2012). Taken together, all these coherent results define two populations of HCECs at least in old donor corneas: central HCECs keep a stable endothelial phenotype with extremely low proliferative capacity, and peripheral HCECs have higher proliferation capacity but are more sensitive to serum component and can be transformed into another cell type under inappropriate culture conditions. This specificity of peripheral HCECs likely explains the peripheral deterioration that we previously observed during organ culture in commercial media containing 2% serum(He *et al.* 2012). Consequently, these results suggest that OC in serum-containing media may alter peripheral HCECs and hinder subsequent efficient cell expansion for bioengineering purposes.

Optimization of corneal endothelial culture from old donors

Recently, Peh et al.(Peh *et al.* 2013) proposed a two-phase protocol able to provide sufficiently high number of differentiated HCECs to envisage endothelial cell therapy (injection therapy) or endothelial bioengineering. It consisted of a proliferation phase in F99 medium + 5% FBS and a stabilization phase in Human Endothelial - SFM + 5% FBS. From three very young donors of <30 years old, like we only exceptionally have in France, the amplification phase with initial minimal seeding density at 10 000 cells/cm^2 obtained 4.5x10^6 to 7.5x10^6 cells at the 2nd passage from one pair of cornea. In order to adapt such protocol to old donors corneas that are continuously available, and avoid EMT of peripheral cells that we described above, we used serum-free media and removed the proliferation phase in order to allow eventually further division in vivo to repair surgery-induced cell death and kept only the stabilization phase for the purification of HCECs from extracellular matrix debris. Our first results demonstrated the possibility to obtain a monolayer with acceptable ECD (approximately 2000 cells/mm^2) with stable endothelial morphology and with the main markers of pump function from both central and peripheral HCECs isolated from old donor cornea (70 -

75 years old) in a serum-free medium. Calculation of number of HCECs obtained suggests that our method allows the transfer of cells form cornea to culture support rather than expansion of the cell pool. The limited proliferation of HCECs in these conditions may only compensate the mandatory cell loss during cell culture preparation, without risking EMT. Even if considerably less efficient than cell expansion from very young donors, our culture protocol could potentially allow to use the 20% corneas discarded by European eye banks for insufficient ECD(EEBA 2012). Note that these corneas are most of the time not ideal for anterior graft either, because of age-related stromal transparency alterations(Borderie *et al.* 2013). Further improvements, namely supplementation of culture media with Rapamycin or its derivatives (mTor inhibitor, the drug of rejuvenation) in order to reduce senescence(Shin *et al.* 2011) and culture in controlled hypoxemia are undergoing in our laboratory and may help limiting additional oxidative DNA damage that are already elevated in old donors(Mimura & Joyce 2006).

From a practical perspective, our findings indicate that the specificity of peripheral HCECs isolated on corneas from old donor does not allow sufficient proliferation to obtain significant expansion of the cell pool with simple cell culture protocol. Nevertheless, first, by pooling HCECs from several corneas, in conditions that favor survival adherence and differentiation in densely packed mosaics rather than proliferation, it will be possible to “recycle” the corneas from old donors usually discarded by eye banks. Secondly, more sophisticated interventions that could reverse senescence(Gomes *et al.* 2013) would eventually allow real cell expansion of HCECs from old donors that, logically and fortunately remain the most numerous.

Experimental methods

Human corneas

Forty-two corneas were retrieved from twenty-six donors by in situ excision, the routine method for clinical use. Twenty-two corneas were obtained from the Department of Anatomy of the Faculty of Medicine of Saint-Etienne (body donation to science). Twenty corneas not suitable for corneal graft but with a normal endothelium were obtained from the Eye Banks of Saint-Etienne and of Besançon. Donor age (mean±standard deviation, (range, median) was 73±10 years, (50 to 83, 74), and time

from death to procurement was 17±13 hours (4.5 to 54.5, 14). Ex vivo corneas were stored in organ culture (OC) at 31 °C for 15±7 days (2 to 26, 15) in a commercial medium containing 2% foetal calf serum (CorneaMax, Eurobio, Les Ulis, France) before specific experiments. Handling of the donor tissues adhered to the tenets of the Declaration of Helsinki of 1975 and its 1983 revision in protecting donor confidentiality.

Definition of centre, periphery, extreme periphery, and transition zone

Cell characteristics were studied in the surgical or anatomical regions of the posterior surface of the cornea previously described(He *et al.* 2012). Briefly, from center to periphery: (1) endothelial center with a 4.0 mm radius, corresponding to the disk usually trephined by the surgeon for corneal graft; (2) endothelial periphery (P) of approximately 1.5- 2 mm width (depending on corneal diameter), stopping at the anatomic endothelium edge i.e. the end of the DM, also called Schwalbe's line; (3) for our work, we had to define a supplementary zone inside the periphery corresponding to the last 0.2 mm of the endothelial periphery, which we named endothelial extreme periphery (EP), a zone comprising most of the Hassal-Henle bodies that correspond to age-related Descemetic mushroom-shaped expansions; (4) transition zone (TZ), 0.15 mm wide, characterized by absence of DM and of fibers typical of the TM. The zone is often confused in the literature with Schwalbe's ring, which is only prominent in 15% of corneas (Hogan *et al.* 1971); (5) and finally TM, approximately 0.5 mm wide.

Primary corneal endothelial cell culture

Standard protocol

For the evaluation of HCEC migration and differentiation in serum-containing medium, HCEC primary cultures were obtained from four OC corneas using protocol previously reported by Joyce et al. (Zhu & Joyce 2004). Corneal centre was separated from the periphery using a 7.5 mm diameter trephine. Central en peripheral DM fragments carrying HCECs were separately peeled off the cornea (n=2) and incubated on 6-well FNC (FNC coating mix ®) coated plate in seeding medium composed of OPTIMEM-1 (Invitrogen Life technologies, St-Aubin, France) supplemented with 8% fetal bovine serum (FBS) (Eurobio), 20 ng/ml of nerve growth factor (NGF, Cell signaling), 5 ng/ml of epidermal growth factor (EGF), 20 mg/ml of ascorbic acid, 200

µg/l of calcium chloride, 0.08% chondroitin sulfate, 100 µg/ml bovin pituitary extract, 1X antibiotic solution (Sigma) (the last six from Sigma, St Quentin Fallavier, France), and 50 µg/ml gentamicin (Invitrogen). Medium was carefully changed every 2 days. The migration of HCEC was observed daily by phase contrast microscopy during 14 days. Cultures were maintained in a humidified incubator at 37°C and 5% CO_2.

Optimized protocol

For the adherent culture of central versus peripheral HCECs from old donors corneas, the protocol was modified from the method recently described by Peh et al. (Peh *et al.* 2013). Briefly, center and periphery of the cornea were separated as described above and DM with the attached ECs was incubated in 0,1% collagenase type IV-S (Sigma) for 1 hour at 37°C. Cells of both corneas from one donor were pooled. HCEC dissociated from DM were washed in phosphate buffered saline (PBS) and seeded in 10 µg/ml laminin and 5 mg/ml chondroitin sulfate (LC) coated 48-well plates (75 mm^2). For the first 4 hours only, cells were incubated with the same seeding FBS-containing medium as the standard method in order to enhance cell adhesion and survival without allowing proliferation and risking EMT. The prolonged maintenance of HCEC in vitro was carried out by culture in a stabilisation medium composed of Human Endothelium serum-free Medium (Invitrogen) only supplemented with 10 ng/ml fibroblast growth factor (FGF-2, Sigma), and was changed every two days. For passaged culture, cells were washed in PBS, dissociated with TrypLE™ Express (Invitrogen) for 10 min at 37°C and washed with stabilisation medium before seeding into new LC coated 384-well plates at density of 2000 cells/mm^2.

Sphere forming culture

HCEC sphere forming cultures were performed following previously described protocols (Yokoo *et al.* 2005; Mimura *et al.* 2010; Bi *et al.* 2013) using 3 pairs of corneas of 63, 65 and 86 year-old donors OC corneas. Cells were isolated as described in primary culture by peel-digest protocol. After collagenase digestion, cells were washed with PBS and resuspended in sphere medium containing 1.5% Methylcellulose (Sigma), DMEM/F12 (invitrogen), 20ng/ml FGFb, 20ng/ml EGF into uncoated plate. Sphere cultures were maintained at 37°C in a 5% carbon dioxide humidified atmosphere. Medium was changed every 2 days.

Senescence-associated β galactosidase assay (SA-β-Gal)

SA-β-Gal activity was performed using the Senescence Cells Histochemical Staining Kit (Sigma) according to the manufacturer's instructions. Briefly, in vitro HCEC were washed with balanced salt solution (BSS), fixed with fixation solution for 10 minutes at room temperature (RT), followed by staining mix solution incubation overnight at 37°C. The following day, cell were washed with PBS and visualized under bright field microscope (IX81, Olympus, Tokyo, Japan). The blue stained cells corresponding to the SA-β-Gal activity were counted using x40 magnificated pictures. Staining intensity (light or dark blue) was also considered as indicative of low or high level of senescence and quantified (Kurz *et al.* 2000).

Proliferation assay

The activation of cell cycle in HCEC was detected using a Click-iT EdU Imaging kit (invitrogen). 5-ethynyl-2´-deoxyuridine (EdU) is an analog of thymidine that is incorporated into DNA during replication. In vitro cell cultures were incubated during 7 days and whole corneas during 30 days in media containing 10µM EdU. For certain experiments destined to indentified rapid and slow cycling cells, this first period was followed by a similar incubation time in their respective media without EdU. After fixation of cell cultures with 4% paraformaldehyde (PFA) for 10 minutes at RT and whole corneas with 0,5% paraformaldehyde (PFA) for 45 minutes at RT (He *et al.* 2011), EdU labeling was revealed according to the manufacturer's protocol. EdU staining could be combined with other immunostainings. Cells and flat-mounted corneas were observed under a fluorescent microscope (IX81, Olympus). Three proliferative profiles were distinguished: 1/ partial EdU labeling corresponding to rapid-cycling cells that incorporated EdU which was subsequently diluted during the following successive cell divisions in medium without EdU; 2/ full EdU labeling corresponding to slow-cycling cells that incorporated EdU once during the first time and stay quiescence; and 3/ EdU negative cells, corresponding to non-proliferating cells that did not incorporate EdU. The rate of EdU+ ECs was expressed as the percentage of EdU positive nuclei per total number of Hoechst 33342 positive nuclei counted in each sample region observed with a 10X or 40X objectives. The final value of was obtained by the average of EdU+ percentages in four sample regions. For whole corneas, EdU+ percentage was calculated for the centre and the periphery of each cornea.

Immunostaining

Immunostainings were based on previous optimized protocols (He *et al.* 2011). Briefly, corneas were rinsed in BSS before fixation in 0,5% PFA or 100% methanol for 45 minutes at RT. Cell membranes were permeabilized by 0,5% Triton x-100 in PBS for 10 min at RT. The non-specific binding sites were then saturated by incubation with 2% bovine serum albumin (BSA) and 2% goat serum for 30 min at 37°C. Primary antibodies diluted at 1:200 in PBS containing 2% BSA and 2% goat serum were incubated for 1 h at 37°C. Incubation with secondary antibodies diluted 1:500 in PBS containing 2% BSA and 2% goat serum was done for 45 min at 37°C. Nuclei were finally counterstained with Hoechst 33342 (Sigma) 10 µg/ml in PBS at RT for 2 min. Three rinses in PBS were performed between all steps, except between saturation of non-specific protein binding sites and incubation with primary antibody. Corneas were flat-mounted between a glass slide and a glass coverslip. Images were performed by a fluorescence inverted microscope IX81 (Olympus) equipped with the Cell^P imaging software (Soft Imaging System GmbH, Munster, Germany). Immunocytochemistry used a similar protocol as for whole corneas, except that the fixation was performed with 4% PFA or 100% methanol for 10 minutes only.

The primary antibodies and their dilutions are listed in Table 1. Secondary antibodies were Alexa Fluor 488 goat anti-mouse IgG or/and Alexa Fluor 555 goat anti-rabbit IgG (Invitrogen, Eugene, OR).

Table 1. *List of primary antibodies.*

Target protein	**Animal source**	**Clonality**	**Laboratory**	**Dilution**
Na^+/K^+ATPase	mouse	monoclonal	Millipore	1/200
ZO-1	mouse	monoclonal	Invitrogen	1/500
CLCN3	rabbit	polyclonal	Abcam	1/200
VDAC3	rabbit	polyclonal	GeneTex	1/200
αSMA	rabbit	polyclonal	GeneTex	1/200
NRP2	rabbit	polyclonal	Cell Signaling	1/200
β-III tubulin	mouse	monoclonal	Sigma	1/500
NCAM-1	rabbit	polyclonal	Cell Signaling	1/500
NSE	mouse	monoclonal	GeneTex	1/200
Nestin	rabbit	polyclonal	Abcam	1/200

Acknowledgments

This work was funded by the Fondation de l'Avenir (ET7-468) and the Agence de la Biomédecine 2013

Author Contributions

Binh Minh Thi Ha: conceived the work, retrieved corneas, acquired and analyzed the data, drafted the work, approved its final version, agreed to be accountable for all aspects of the work

Nelly Campolmi: acquired and analyzed the data, drafted the work, approved its final version, agreed to be accountable for all aspects of the work

Zhiguo He: retrieved corneas, acquired and analyzed the data, drafted the work, approved its final version, agreed to be accountable for all aspects of the work

Jean-Yves Thuret: conceived the work, analyzed the data, revised the work, approved its final version, agreed to be accountable for all aspects of the work

Simone Piselli: acquired the data, drafted the work, approved its final version, agreed to be accountable for all aspects of the work

Fabien Forest: conceived the work, acquired the data, drafted the work, approved its final version, agreed to be accountable for all aspects of the work

Jean-Marc Dumollard: conceived the work, acquired and analyzed the data, drafted the work, approved its final version, agreed to be accountable for all aspects of the work

Michel Peoc'h: conceived the work, acquired and analyzed the data, revised the work, approved its final version, agreed to be accountable for all aspects of the work

Olivier Garraud: conceived the work, acquired and analyzed the data, revised the work, approved its final version, agreed to be accountable for all aspects of the work

Philippe Gain: conceived the work, acquired and analyzed the data, wrote the article, approved its final version, agreed to be accountable for all aspects of the work

Gilles Thuret: conceived the work, acquired and analyzed the data, wrote the article, approved its final version, agreed to be accountable for all aspects of the work

References

Amann J, Holley GP, Lee SB , Edelhauser HF (2003). Increased endothelial cell density in the paracentral and peripheral regions of the human cornea. *Am J Ophthalmol*. **135**, 584-590.

Baum JL, Niedra R, Davis C , Yue BY (1979). Mass culture of human corneal endothelial cells. *Arch Ophthalmol*. **97**, 1136-1140.

Bednarz J, Rodokanaki-von Schrenck A , Engelmann K (1998). Different characteristics of endothelial cells from central and peripheral human cornea in primary culture and after subculture. *In Vitro Cell Dev Biol Anim*. **34**, 149-153.

Bi YL, Zhou Q, Du F, Wu MF, Xu GT , Sui GQ (2013). Regulation of functional corneal endothelial cells isolated from sphere colonies by Rho-associated protein kinase inhibitor. *Exp Ther Med*. **5**, 433-437.

Bonanno JA (2003). Identity and regulation of ion transport mechanisms in the corneal endothelium. *Prog Retin Eye Res*. **22**, 69-94.

Bonanno JA (2012). Molecular mechanisms underlying the corneal endothelial pump. *Exp Eye Res*. **95**, 2-7.

Borderie VM, Sandali O, Basli E, Goldschmidt P , Laroche L (2013). Donor tissue selection for anterior lamellar keratoplasty. *Cornea*. **32**, 1105-1109.

EBAA (2012). EBAA 2011 Statistical Report on Eye Bankinged^eds): Eye Bank Association of America.

EEBA (2012). European Eye Bank Association Directory. Twentieth edition. 2012ed^eds). Amsterdam.

Gomes AP, Price NL, Ling AJ, Moslehi JJ, Montgomery MK, Rajman L, White JP, Teodoro JS, Wrann CD, Hubbard BP, Mercken EM, Palmeira CM, de Cabo R, Rolo AP, Turner N, Bell EL , Sinclair DA (2013). Declining NAD(+) Induces a Pseudohypoxic State Disrupting Nuclear-Mitochondrial Communication during Aging. *Cell*. **155**, 1624-1638.

He Z, Campolmi N, Gain P, Minh Hathi B, Dumollard JM, Duband S, Peoc'h M, Piselli S, Garraud O , Thuret G (2012). Revisited Microanatomy of the Corneal Endothelial Periphery: New Evidence for Continuous Centripetal Migration of Endothelial Cells in Humans. *Stem Cells*. **30**, 2523-2534.

He Z, Campolmi N, Ha Thi BM, Dumollard JM, Peoc'h M, Garraud O, Piselli S, Gain P , Thuret G (2011). Optimization of immunolocalization of cell cycle proteins in human corneal endothelial cells. *Mol Vis*. **17**, 3494-3511.

Hirata-Tominaga K, Nakamura T, Okumura N, Kawasaki S, Kay EP, Barrandon Y, Koizumi N , Kinoshita S (2013). Corneal endothelial cell fate is maintained by LGR5 through the regulation of hedgehog and Wnt pathway. *Stem Cells*. **31**, 1396-1407.

Hogan MJ, Alvarado JA , Weddell JS (1971). *Histology of the human eye: An Atlas and Text*. Philadelphia: W.B. Saunders.

Joyce NC (2003). Proliferative capacity of the corneal endothelium. *Prog Retin Eye Res*. **22**, 359-389.

Joyce NC (2012). Proliferative capacity of corneal endothelial cells. *Exp Eye Res*. **95**, 16-23.

Joyce NC, Zhu CC , Harris DL (2009). Relationship among oxidative stress, DNA damage, and proliferative capacity in human corneal endothelium. *Invest Ophthalmol Vis Sci*. **50**, 2116-2122.

Kurz DJ, Decary S, Hong Y , Erusalimsky JD (2000). Senescence-associated (beta)-galactosidase reflects an increase in lysosomal mass during replicative ageing of human endothelial cells. *J Cell Sci*. **113 (Pt 20)**, 3613-3622.

Leung EW, Rife L, Smith RE , Kay EP (2000). Extracellular matrix components in retrocorneal fibrous membrane in comparison to corneal endothelium and Descemet's membrane. *Molecular Vision*. **6**, 15-23.

Levis HJ, Peh GS, Toh KP, Poh R, Shortt AJ, Drake RA, Mehta JS , Daniels JT (2012). Plastic compressed collagen as a novel carrier for expanded human corneal endothelial cells for transplantation. *PLoS One*. **7**, e50993.

Liu Z, Zhuang J, Li C, Wan P, Li N, Zhou Q, Zhou C, Huang Z , Wang Z (2012). Long-term cultivation of human corneal endothelial cells by telomerase expression. *Exp Eye Res*. **100**, 40-51.

Lwigale PY , Bronner-Fraser M (2009). Semaphorin3A/neuropilin-1 signaling acts as a molecular switch regulating neural crest migration during cornea development. *Developmental biology*. **336**, 257-265.

Maurice DM (1972). The location of the fluid pump in the cornea. *J Physiol*. **221**, 43-54.

McGowan SL, Edelhauser HF, Pfister RR , Whikehart DR (2007). Stem cell markers in the human posterior limbus and corneal endothelium of unwounded and wounded corneas. *Mol Vis*. **13**, 1984-2000.

Mimura T , Joyce NC (2006). Replication competence and senescence in central and peripheral human corneal endothelium. *Invest Ophthalmol Vis Sci*. **47**, 1387-1396.

Mimura T, Yamagami S, Yokoo S, Usui T , Amano S (2010). Selective isolation of young cells from human corneal endothelium by the sphere-forming assay. *Tissue Eng Part C Methods*. **16**, 803-812.

Murphy C, Alvarado J, Juster R , Maglio M (1984). Prenatal and postnatal cellularity of the human corneal endothelium. A quantitative histologic study. *Invest Ophthalmol Vis Sci*. **25**, 312-322.

Patel SP , Bourne WM (2009). Corneal endothelial cell proliferation: a function of cell density. *Invest Ophthalmol Vis Sci*. **50**, 2742-2746.

Peh GS, Toh KP, Ang HP, Seah XY, George BL , Mehta JS (2013). Optimization of human corneal endothelial cell culture: density dependency of successful cultures in vitro. *BMC Res Notes*. **6**, 176.

Pipparelli A, Thuret G, Toubeau D, He Z, Piselli S, Lefevre S, Gain P , Muraine M (2011). Pan-corneal endothelial viability assessment: application to endothelial grafts predissected by eye banks. *Invest Ophthalmol Vis Sci*. **52**, 6018-6025.

Schimmelpfennig BH (1984). Direct and indirect determination of nonuniform cell density distribution in human corneal endothelium. *Invest Ophthalmol Vis Sci*. **25**, 223-229.

Schmedt T, Chen Y, Nguyen TT, Li S, Bonanno JA , Jurkunas UV (2012). Telomerase immortalization of human corneal endothelial cells yields functional hexagonal monolayers. *PLoS One*. **7**, e51427.

Sheerin AN, Smith SK, Jennert-Burston K, Brook AJ, Allen MC, Ibrahim B, Jones D, Wallis C, Engelmann K, Rhys-Williams W, Faragher RG , Kipling D (2012). Characterization of cellular senescence mechanisms in human corneal endothelial cells. *Aging Cell*. **11**, 234-240.

Shin YJ, Cho DY, Chung TY, Han SB, Hyon JY , Wee WR (2011). Rapamycin reduces reactive oxygen species in cultured human corneal endothelial cells. *Curr Eye Res*. **36**, 1116-1122.

Tan DT, Dart JK, Holland EJ , Kinoshita S (2012). Corneal transplantation. *Lancet*. **379**, 1749-1761.

Yokoi T, Seko Y, Makino H, Hatou S, Yamada M, Kiyono T, Umezawa A, Nishina H , Azuma N (2012). Establishment of functioning human corneal endothelial cell line with high growth potential. *PLoS One*. **7**, e29677.

Yokoo S, Yamagami S, Yanagi Y, Uchida S, Mimura T, Usui T , Amano S (2005). Human corneal endothelial cell precursors isolated by sphere-forming assay. *Invest Ophthalmol Vis Sci*. **46**, 1626-1631.

Yu WY, Sheridan C, Grierson I, Mason S, Kearns V, Lo AC , Wong D (2011). Progenitors for the corneal endothelium and trabecular meshwork: a potential source for personalized stem cell therapy in corneal endothelial diseases and glaucoma. *J Biomed Biotechnol*. **2011**, 412743.

Zhu C , Joyce NC (2004). Proliferative response of corneal endothelial cells from young and older donors. *Invest Ophthalmol Vis Sci*. **45**, 1743-1751.

ARTICLE III: Electric pulses trigger mitosis in human corneal endothelial cells

Dans la littérature, la description de figures de mitoses de CEs reste exceptionnelle sur des cornées humaines entières. La plupart des travaux décrivant la prolifération de CEs dans des conditions expérimentales montre l'incorporation de BrdU caractérisant la phase S du cycle cellulaire et ou un marquage des phases G1 tardive, S, G2 mais rarement M par Ki67. Par ailleurs, la prolifération est habituellement obtenue dans des milieux comprenant de 8 à 20 % de sérum de veaux fœtal et des facteurs de croissance spécifiques des CEs, EGF et FGF. Nous montrons pour la première fois qu'un stimulus physique constitué d'un train d'impulsions carrées de courant constant habituellement destiné à l'électroporation, déclenche un nombre considérable de mitoses de CEs de cornées simplement conservées en milieux d'organoculture standard avec seulement 2% de SVF et sans supplément de facteur de croissance. Toutes les phases de la mitose sont observées. L'enthousiasme est cependant modéré par le fait que la prolifération est limitée à des zones de DCE < 2000 cellules/mm^2 qui suggèrent que le stimulus est insuffisant pour les zones où l'inhibition de contact reste forte.

Cover letter

Dear Editor,

We are please to submit an original article entitled "**Electric pulses trigger mitosis in human corneal endothelial cells.**" in *IOVS*.

In this article we present for the first time the triggering of proliferation of human corneal endothelial cells (HCECs) directly in situ on whole donor corneas after a single stimulus by a train of electric pulses similar to those used in electroporation. In situ proliferation have been described by the past after localized mechanical wound or contact inhibition release always followed by incubation in culture medium supplemented with 8 to 10% fetal calf serum and growth factors. Here, we only used basal organ culture medium containing only 2% fetal calf serum without other additives. We first observed this unexpected phenomenon during development of custom made electrodes designed for gene electrotransfer in HCECs on organ culture corneas [1].

We propose some clues for explaining the phenomenon, but concede that it remain to be further explored. Nevertheless we think that results are robust enough to deserve communication to the community in order to stimulate works in this field, considering that all new orientation that could help expanding the HCECs pool could have significant clinical applications.

We declare that all authors have directly participated in the planning, execution, or analysis of the study and resulting paper, and have read and approved the submitted version.

We hope that our manuscript will interest the Editorial Board of *IOVS*.

Sincerely,

Professor Gilles Thuret, MD, PhD, Institut Universitaire de France
Corresponding author:
Laboratory for Biology, engineering and imaging of Corneal Graft, EA 2152, IFR143
Faculty of Medicine
15, Rue Ambroise Paré
F 42023 Saint-Etienne Cedex 2, France.
Tel: +33 (0)4 77 12 77 93
Fax: +33 (0)4 77 12 09 95
E-mail: gilles.thuret@univ-st-etienne.fr

References

1. He Z, Pipparelli A, Manissolle C, et al. Ex vivo gene electrotransfer to the endothelium of organ cultured human corneas. *Ophthalmic Res* 2010;43:43-55.

Electric pulses trigger mitosis in human corneal endothelial cells

Binh Minh Thi Ha[1], Nelly Campolmi[1, 2], Zhiguo He[1], Jean-Yves Thuret[5], Simone Piselli[1], Fabien Forest [1, 3], Jean-Marc Dumollard[1, 3], Michel Peoc'h[1, 3], Olivier Garraud[1, 4], Philippe Gain[1, 2], Gilles Thuret[1, 2, 6]

1. Laboratory for corneal graft biology, engineering and imaging', EA2521, SFR143, Faculty of Medicine, Saint-Etienne, France

2. Department of Ophthalmology, University Hospital, Saint-Etienne, France

3. Department of Pathology, University Hospital, Saint-Etienne, France

4. Eye Bank, Etablissement Français du Sang Loire/Auvergne, Saint-Etienne, France

5. Commissariat à l'Energie Atomique, Institut de biologie et de technologies de Saclay (iBiTec-S), Service de Biologie Intégrative et de Génétique Moléculaire (SBIGeM), F-91191, Gif-sur-Yvette, France.

6. Institut Universitaire de France, 103, Boulevard Saint-Michel, 75005 Paris

Abstract

Purpose: Human corneal endothelial cells (HCECs) have no clinically significant proliferative capacity but can however proliferate ex vivo and in vitro in response to mitotic stimuli. Up to now, only small mechanical wound or contact inhibition release by EDTA followed by incubation in medium with 10% fetal calf serum (FCS), or adenoviral transfection with E2F2 successfully triggered significant proliferation in the endothelium of whole corneas. We report here the triggering of HCECs proliferation after electrostimulation of whole corneas stored in a basal organ culture (OC) medium.

Methods: Human donor corneas stored in a commercial OC medium containing 2% FCS were treated with 8 square pulses of 100ms, 1 Hz, 135 mA with stainless steel custom-made electrodes previously designed for gene electrotransfer selectively in HCECs of stored corneas. Paired corneas remained untreated for control experiments. They were returned to their OC medium for 12 hours (H), 24H, 3 days (D), or 7D.

Proliferation was studied at this 4 times points using Ki67 immunostaining and with 5-ethynyl-2´-deoxyuridine (EdU), an analog of thymidin that reveals the S-phase. Additionally, immunostaining for ZO-1 was used to study the mosaic integrity. Preincubation with 10 µM of Rock inhibitor or verapamil were also performed.

Results: At D3 all corneas carried proliferating HCECs with a significant 4.0 fold increase $_{95\%CI}$(1.5-6.5) in electrostimulated corneas. Total number of KI67+ and EdU+ HCECs was 1028 (230-3251) (median, range) per cornea. All cell cycle phase were observed from late G1 to daughter cells but the majority of cells were in S phase at D3. At D7 proliferating HCECs were still present but numerous fragmented nuclei consistent with apoptosis were also noted. We observed significant regional endothelial lesions at H12 and H24 that healed à D3. Distribution of proliferating HCECs was heterogeneous with significantly more numerous stained cells in the periphery than in the central 8mm, and more numerous in area with ECD<2000 cells/mm^2. Rock-inh decreased the number of proliferating cells whereas verapamil had no effect.

Conclusion: A single stimulation of HCECs with a train of electric pulses triggers mitosis probably in response to transient disorganization of the intercellular junctions and direct modulation of cell cycle regulators. This new phenomenon could help find innovative strategy of HCECs expansion for clinical applications.

Key words (6): corneal endothelium, cell cycle, proliferation, electroporation, human, organ-culture

Introduction

Cornea transparency is controlled by the barrier and ionic pump functions of the corneal endothelial monolayer. Approximately 3 to 450000 cells (2000 to 4000 cells/mm^2 depending mainly on age) in each cornea ensure this essential function. However the lack of significant proliferative capacity of the human corneal endothelial cells (HCECs) (for review see[1]) explained their implication in about one third of all corneal blindness [2]. Indeed, when their number falls under a threshold varying between 300-500 cells/mm^2, they cannot further adequately deswell the collagenic corneal stroma that, in response, spontaneously swells and become irreversibly cloudy. Multiple pathological processes can results in HCECs premature death leading to

blindness that can, up to now, only be treated by corneal grafts performed with donor corneas and consequently conditioned by regular corneal donation. However, the recognized worldwide scarcity for corneal donation and the multiple societal, educational, religious and logistic obstacles to its increase, make it necessary the search for alternatives to donation. In this respect, stimulation of the residual proliferative capacities of the HCECs would have significant applications. In vivo, it could allow treating stages of corneal diseases where corneal stroma has not been yet permanently opacified. Recently a pharmacological approach using Rock-inhibitor has been proposed[3] and the first-in-man applications reported for Fuchs endothelial dystrophy, the most frequent primary endothelial dystrophy[4]. Ex vivo, taking advantage of the possibility of long-term corneal storage using the European organ-culture eye banking system, strategies that could force HCECs to proliferate would allow enrichment of the endothelium either to obtain super high endothelial cell density (ECD) susceptible to survive longer or to restore a sufficient ECD (>2000 cell/mm^2) to the 20% of corneas usually discarded because of too low ECD in Europe[5]. In vitro, triggering and controlling HCECs proliferation would certainly facilitate the difficult task of cultivating sufficient number of cells to develop bioengineering of graft substitutes, either HCECs suspension for injection therapy of reconstruction of endothelial grafts composed of a biocompatible thin transparent carrier evenly covered with HCECs.

Up to now, direct stimulation of proliferation of HCECs in situ on whole corneas has been obtained mainly for experimental purposes in order to better characterize the residual capacities of HCECs according to donor age[6, 7], central or peripheral topography[8] of HCECs, and ECD[9]. Two stimuli have been regularly reported: creation of a localized calibrated mechanical wound with a silicon canula in order to obtain a response of neighbour cells[7, 8], and partial release of intercellular junctions using a calcium chelators (EDTA)[6, 9] in order to temporarily weakened the contact inhibition strongly involved in the late G1 phase arrest of HCECs. In all these experiments, corneas were systematically incubated in culture medium containing 8 to 10% FCS and growth factors (namely epidermal growth factor and beta fibroblast growth factor) after stimulation and sometimes even before. Additionally in situ proliferation of HCECs was also reported after adenoviral transfection with the transcription factor E2F2 to stimulate G1 to S phase transition in corneas subsequently incubated in EMEM with only 2% FCS and no additional growth factors [10]. Lastly, cases of in situ proliferation were obtained more simply by incubating donor corneas

with impaired HCECs due to long post mortem times, during 3 days in organ culture medium (EMEM) supplemented with 8% FCS without other growth factors[11]. In all these works proliferation was classically studied using Ki67 antibody, a robust marker of cell cycle from late G1 to the end of mitosis with specific staining patterns easily identifiable and/or incorporation of BrdU, an analog of thymidine that reveals the S-phase, and/or immunostaining for other proliferating markers (MCM2[8] and PCNA[11]). In all above cited experiments, Ki67+ and/or BrdU+ HCECs were identified. All phases of the cell cycle were reported until daughter cells but, notably, mitosis figures remained scarce on published images, most of the visible cells being in the G1, S or G2 phases.

We previously reported a method of gene electrotransfer directly into HCECs of whole corneas stored in organ culture thanks to custom made electrodes that does not touch the endothelium[12]. Although efficient this technique lacks reproducibility for reasons that remains to be further explained but likely to be related with variable ions and water contain of the stored corneas. During the assessment of this method with discovered that all electrostimulated corneas unexpectedly presented some HCECs with condensed nuclei consistent with mitosis features that were never observed in control corneas. Considering this observation worth of interest we went one step ahead to characterized this phenomenon, and present here the first evidence that a train of electric pulses can trigger proliferation in HCECs of organ cultured corneas.

Materials and methods

Human corneas

All procedures conformed to the tenets of the Declaration of Helsinki for biomedical research involving human cadaver tissue. Scientific corneas were procured from bodies donated to the Laboratory of Anatomy in the Faculty of Medicine and from the Eye Bank of Saint-Etienne, including seven paired corneas. Mean donor age was 75±9 years (range: 60–90, median: 77). Mean time from death to procurement was 14±4 hours. Mean storage time in organ-culture at 31°C in CorneaMax (Eurobio, Les Ulis, France) before experiments was 15±4 days. CorneaMax is a conventional medium based on DMEM medium supplemented with 2% of fetal calf serum (FCS) and contained no additional growth factor. The corneal endothelial cell density (ECD) was determined 24 hours before treatment by a calibrated image analysis software

(Sambacornea, Tribvn, Chatillon, France)[13, 14]. Pairs of corneas were selected only if their ECD did not differ for more than 10%.

Electro-stimulation

The stimulation of endothelium of OC corneas was based on the same protocol as for gene transfer and used custom made stainless steel electrodes as previously described [12]. Briefly, the cornea was placed endothelial side up on the concavity of the anode, 125 µL of 0.9% NaCl (Sigma, St Quentin Fallavier, France) were added on the endothelium into the corneal concavity and the convex cathode was placed in contact with the liquid without touching the cornea. Electrodes were designed to have parallel surfaces. The GET42 generator (EIP, Jonzieux, France) delivered 8 square pulses lasting 100 ms, at 1 Hz frequency and 125 mA constant intensity. The entire sequence was performed under a laminar flow hood at room temperature. Corneas were then returned to their OC medium without FCS nor growth factor supplementation. Control corneas with similar donor characteristics were subjected to the same manipulations without electric pulses. Contrary to gene electrotransfer, no DNA was added in the endothelial concavity during experiments.

Analysis of cell cycle activation

The activation of HCECs cell cycle was analyzed 12 hours, 24 hours, 3 days and 7 days after electro-stimulation. Cell cycle phases were characterized by two complementary methods: a proliferation assay and immunostaining of Ki67, both performed directly on whole corneas to avoid artifacts caused by single cell separation. Proliferation assay was performed using a Click-iT EdU Imaging kit (invitrogen-Life Technologies, St-Aubin, France). 5-ethynyl-2′-deoxyuridine (EdU) is an analog of thymidine that can be incorporated in cellular DNA during its replication and is consider as S phase marker. The saturation of culture medium with EdU allowed its incorporation in DNA of all dividing cells. Compared to the widely used 5-bromo-2'-deoxyuridine (BrdU), EdU, a more recent technique, is revealed by a chemical reaction with a fluorescent probe much smaller than antibody anti-BrdU, making this technique more convenient than BrdU. After electro-stimulation, corneas were stored in 25 mL CorneaMax supplemented with 10µM EdU. EdU labeling was revealed according to the manufacturer's protocol. Briefly, after fixation of the whole corneas

with 0.5% paraformaldehyde (PFA) for 45 minutes at room temperature (RT), HCECs were permeabilized with 0.5% triton X-100 followed by an incubation in EdU cocktail mixture for 30 minutes at RT. Corneas were washed twice by phosphate buffer saline (PBS) between each steps. EdU staining remained compatible with subsequent immunostaining. We used a protocol optimized for HCECs immunolabeling on whole corneas as previously described [12]. Two primary antibodies were used: rabbit monoclonal antibody anti-Ki67 (abcam, UK), as proliferation marker, and mouse monoclonal antibody anti-ZO-1 (Invitrogen, Eugene, OR), as apical tight junction marker. Second antibodies were Alexa Fluor 488 goat anti-mouse IgG and Alexa Fluor 555 goat anti-rabbit IgG (Invitrogen). Nuclei were counterstained with Hoechst 33342 (Sigma) 10µg/ml in PBS for 1 minute. Flat-mounted corneal were observed under a fluorescent microscope (IX81, Olympus, Tokyo, Japan). The number of Ki67 positive HCECs was counted in the whole cornea surface at 4x magnification. ECD was determined by averaging the number of nuclei counted in four fields taken at random with a x10 objective. Nuclei were automatically counted in large region of interest using the image analysis software Cell^P (Olympus Soft Imaging Solutions, Berlin, Germany). Central (within a 4mm radius central disc) and peripheral (outside the center) ECD were calculated separately as well as percentage of Ki67 positive HCECs.

Analysis of activation mechanisms

To further determine the mechanism of cell cycle activation, experiments were repeated with corneas treated either with Rock-inhibitor in order to stabilize HCECs cytoskeleton or verapamil, a voltage-dependent calcium channel blocker in order to limit Ca2+ movements. Corneas were incubated at 31°C in CorneaMax supplemented with 10µM of the Rock-inhibitor Y-27632 (Sigma) or 10 µM of verapamil (Sigma) during one hour before electrostimulation. The paired cornea remained untreated and was electrostimulated simultaneously. The CorneaMax medium was not changed after the electric treatment, to avoid additional environment stimulation of corneal endothelium cell cycle like renewal of foetal calf serum.

Definition of centre, periphery, extreme periphery, and transition zone

Cell characteristics were studied in the surgical or anatomical regions of the posterior surface of the cornea previously described [15]. Briefly, from center to

periphery: (1) endothelial center with a 4.0 mm radius, corresponding to the disk usually trephined by the surgeon for corneal graft; (2) endothelial periphery (P) of approximately 1.5- 2 mm width (depending on corneal diameter), stopping at the anatomic endothelium edge i.e. the end of the DM, also called Schwalbe's line; (3) for our work, we had to define a supplementary zone inside the periphery corresponding to the last 0.2 mm of the endothelial periphery, which we named endothelial extreme periphery (EP), a zone comprising most of the Hassal-Henle bodies that correspond to age-related Descemetic mushroom-shaped expansions; (4) transition zone (TZ), 0.15 mm wide, characterized by absence of DM and of fibers typical of the TM. The zone is often confused in the literature with Schwalbe's ring, which is only prominent in 15% of corneas [16]; (5) and finally TM, approximately 0.5 mm wide.

Statistical analysis

Considering the limited number of corneas, data were expressed as median (range). Data were compared using Wilcoxon non-parametric rank test. Percentages of Ki67 positives cells were compared using Khi^2 test. Relationship between ECD and total number of Ki67= HCECs was assess by calculating the Spearman correlation coefficient. Analyses were performed using IBM SPSS Statistics Version 20 (IBM Corporation, NY). with $P<0.05$ considered as significant.

Results

Electric pulses systematically triggered HCECs mitosis

Median ECD was 2023 cells/mm^2 (818-2454) (n=20) and difference in ECD between paired corneas was 6±3% (mean±SD). An increase of Ki67 expression in HCECs nuclei and the corresponding EdU staining were observed in all electro-stimulated corneas at D3 (**Fig 1A**). Ki67+ HCECs were found in both electro-stimulated and control corneas, but total number of Ki67+ was significantly higher in electrostimulated corneas with 1028 (230-3251) Ki67+ HCECs versus 464 (29-784) in controls (n = 7 pairs) (P=0.018) corresponding to a mean fold change of 4.0 $_{95\%CI}$(1.5-6.5). No Ki67+ HCECs was observed at H12 and only a few at H24. Double staining with EdU and Ki67 facilitated cell cycle phases' classification with Ki67+/EdU- corresponding to G1 to S transition. Afterwards, the double staining pattern of

chromatin or chromosomes easily indicated the different mitosis phases. All mitosis phases were observed in each cornea (Fig 1B). At D3, proliferating HCECs were found mostly in S phase.

Notably, most proliferating HCECs were located in endothelium periphery with 473 (25-2701) Ki67+ HCECs versus 146 (4-550) in the center P=0.002 corresponding to a mean fold change of 3.6 $_{95\%CI}$(2.2-7.8) (n = 7 pairs of corneas) (**Fig 2A**). The activation of division process in CEs was heterogeneous within a cornea, with most of proliferating HCECs located in area with ECD <2000 cells/mm^2 (**Fig 2B**) but the number of Ki67 +HCECs did not correlate with ECD determined before electrostimulation r= -0.409 P=0.146.

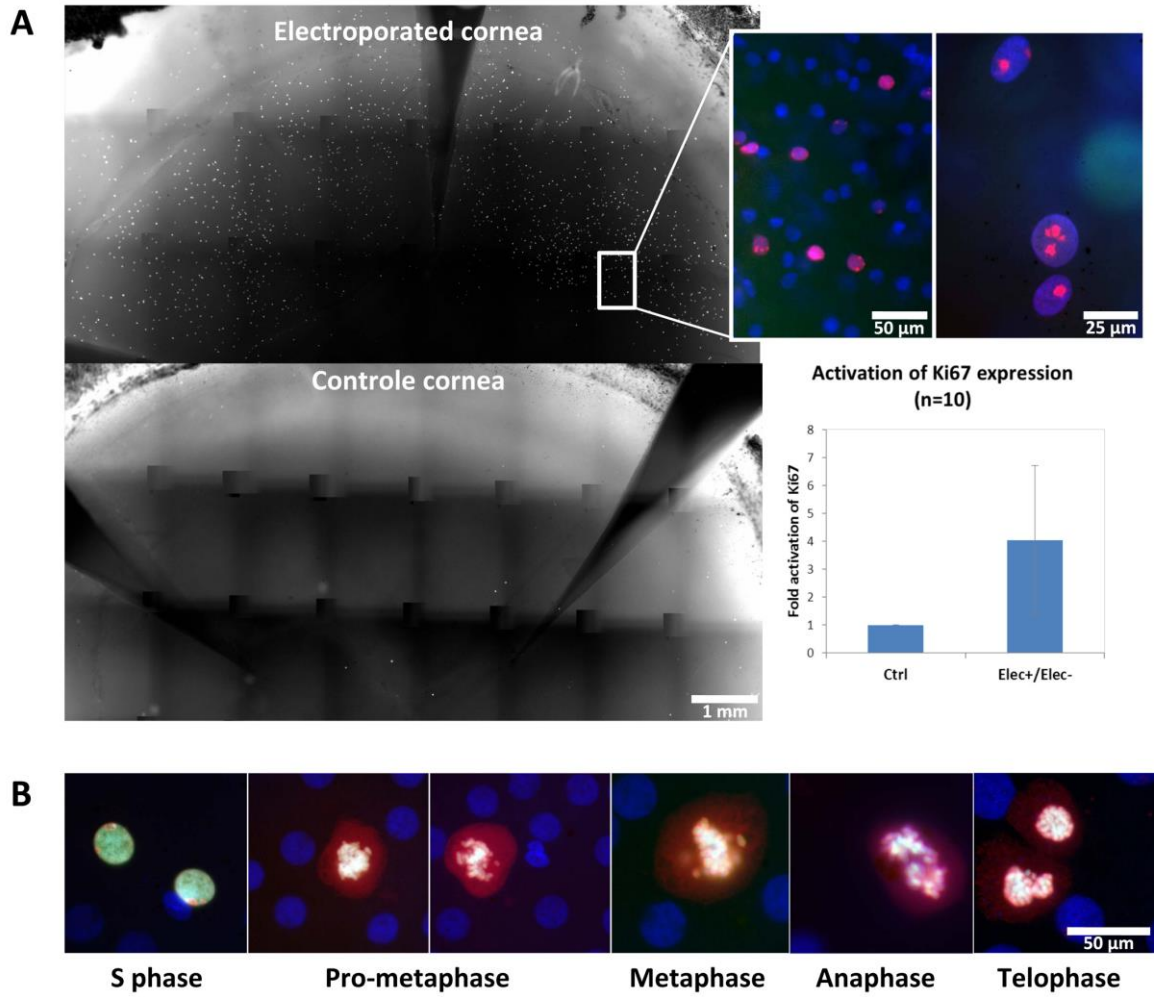


Figure 1. Activation of endothelial cell cycle three days after stimulation with electric pulses. *(A) Immunostaining of Ki67 (red) in electroporated and control corneas. (B). Detection of cell cycle at different phases from G1 to mitosis. Scale bar = 50 µm. Nuclei were counterstained by Hoechst 33342.*

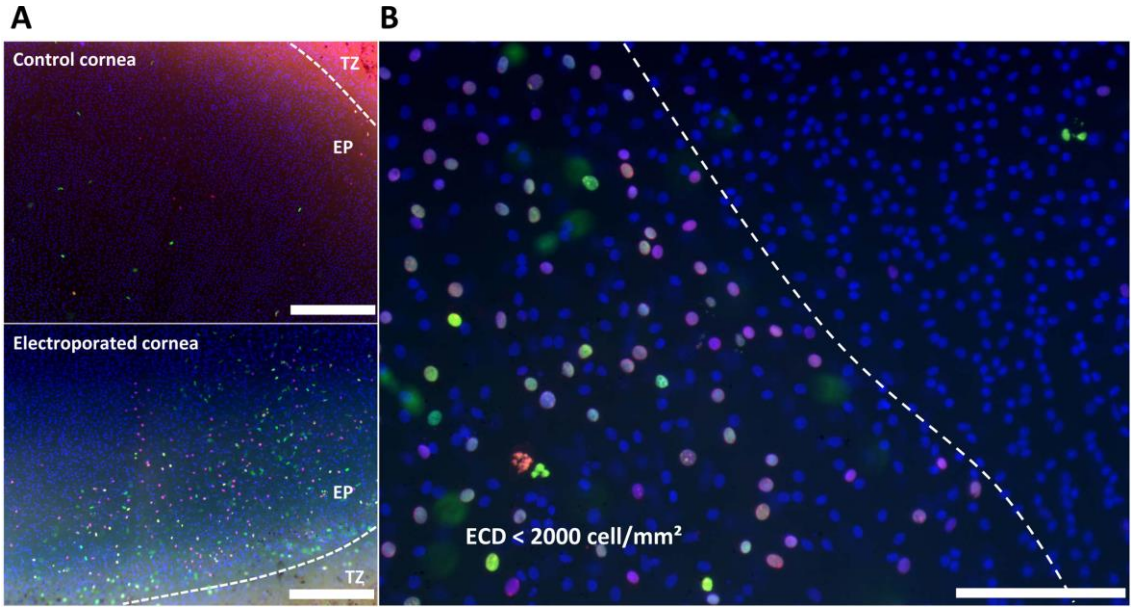


***Figure 2. Corneal endothelial cell division activation in the periphery** (A) **and in low-density region** (B). Immunostaining of Ki67 (red) and EdU labelling (green). Nuclei counterstain by Hoechst 33342. TZ: transition zone, EP: extreme periphery. Scale bar 50 µm.*

Kinetic of cell cycle activation (Fig 3)

The immunostaining of ZO-1 expression provided additional information about the integrity of tight junctions formation between HCECs. Twelve hours after electro-stimulation, HCECs monolayer was highly damaged, only in the endothelial periphery, with areas of denuded Descemet membrane. At H24, wound-healing features were observed with enlargement of HCECs situated at the proximity of denuded areas. At D3, Ki67+ and EdU+ HCECs covered the healed endothelial areas. At D7, numerous EdU+ HCECs were still present in these areas, among which many pairs of EdU+ HCECs were observed. Notably several had also fragmented nuclei suggesting abortive mitosis and apoptosis.

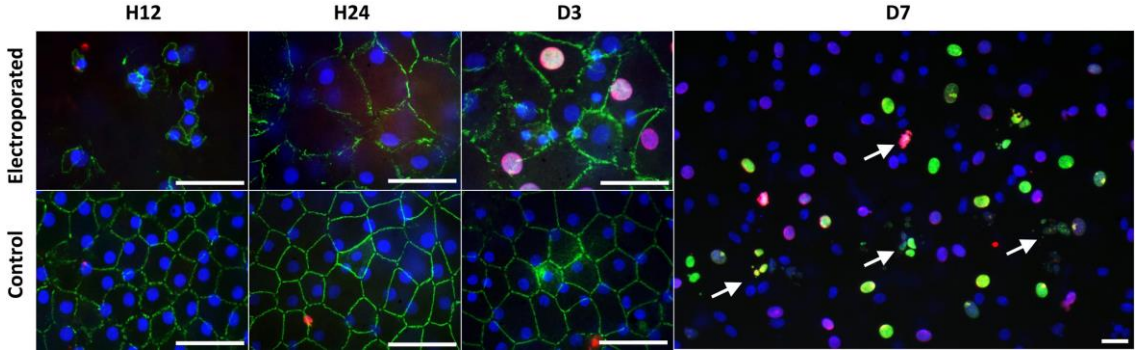


***Figure 3: Kinetic of cell cycle activation of ex vivo corneal endothelium after electro-stimulation**. Immunostainng of Ki67 (red), ZO-1 (green, intercellular junction) and EdU*

labelling (green, nuclear). At day 7, pairs of proliferative cells (arrowheads) and several fragmented nuclei were observed (arrows). Scale bars 50 µm

Effect of ROCK inhibitor and verapamil

Pretreatment of corneas with Y-27632 significantly decreased the number of Ki67+ HCECs compared with the control suggesting a relationship between destabilization of cytoskeleton and intercellular junctions by electric pulses and stimulation of proliferation. Conversely, pretreatment with verapamil had no effect on the percentage of proliferative HCECs triggered by electric pulses.

Discussion

Application of electric field pulses to cells results in a temporary increase of the membrane permeability due to a reversible electric breakdown of the cell membrane. This well known property is exploited to transfect cells with diverse molecules including DNA in a technique called electroporation or gene electrotransfer that has been applied to multiple cells and tissues types, in vitro, ex vivo and in vivo. We previously adapted the technique to the gene transfer into HCECs of whole corneas stored in classical OC medium [12]. Here we show that electric pulses with the same parameter as those used for gene transfer induce proliferation of HCECs by themselves.

Biological effects of electric pulses have been assessed for years mainly with two opposite goals: stimulation of cell death in cancers[17, 18] and stimulation of cell proliferation for regenerative medicine. Indeed, depending on cell types[19] and electric pulses parameters (intensity, voltage, frequency, duration) both opposite results (death of proliferation) have been observed, but deleterious effect on cell survival were more often searched and demonstrated. For instance, induction of apoptosis in cell suspension has already been demonstrated with high intensity short pulses (between 4.5 and 8.1 kV/cm strength and 40 microsec duration) for Jurkatt cells [20]. Occasionally pro-proliferative effects were however reported years ago [21, 22].

Two mutually non-exclusive hypotheses for the stimulation of HCECs proliferation have to be considered. First, the reversible local permeabilization on the membrane by trains of short and intense electric pulses allows almost free movements of hydrophilic species across the envelope. Ions can either enter or escape from the cytoplasm [23]. Among ions species, Ca2+ signaling plays a major role in numerous

fundamental cell processes including regulation of proliferation [24]. Depending on the quantity of free Ca^{2+} present in the medium and the characteristics of current, electric pulses can trigger a true calcium wave liable to stimulate intracellular metabolic pathway including cell cycle or apoptosis. Additionally, excess of intracellular calcium can result in rapid cell necrosis. When cell survive, usually the basic cytoplasmic level is set back spontaneously within a few minutes thanks to Ca^{2+} channels. In our study verapamil, a voltage dependent calcium channel blocker that should have limited the outflow of Calcium after the electro-stimulation did not modified cell proliferation. Logically, verapamil cannot inhibit calcium entry because electric pulses-induced permeability is not dependent on ions channels but on transient artificial membrane pores. Further experiments using modified concentration of Ca^{2+} in the OC medium and imaging of intracellular calcium concentration after electric pulses will help defining its potential role in the stimulation of proliferation.

Secondly, we observed that electric pulses induced regional short-term toxicity on HCECs, disrupting the monolayer of hexagonal cells. This early phenomenon was not seen in our initial description because the first assessments were done 3 hours and the second 3 days after electroporation, therefore missing the time window when local toxicity became apparent [12]. The release of intercellular junctions has been shown to be a major determinant of HCECs proliferation[6, 9] because contact inhibition is one of the mechanism involved in the late G1 phase arrest of the HCECs cell cycle. Additionally, the local toxicity automatically decreases the local ECD and when falling 2000 cells/mm^2, may have favored proliferation as described by Patel et al. [9]. Furthermore, Rock-inhibitor may have delayed the cytosqueletic actin constriction via Rho-A kinase inhibition [25] in response to electric pulses. The stabilized mosaic may therefore be less prone to proliferate after electrostimulation. Notably effects of Rock inhibitor on the reduction of the electroporation cytotoxicity have to be further assessed.

As expected, the proliferative response was higher in the periphery than in the center. Several previous works have shown that the endothelial periphery (usually admitted as the ring outside the central 4mm radius disc) is populated by HCECs that retain higher proliferative capacities in relation with lower stress induced DNA damage[26, 27], by HCECs progenitors[15, 28, 29]. Complementarily, the potential mechanisms discussed above for proliferation induction suggest here that peripheral HCECs are more easily disorganized by electric pulses because of weaker intercellular junctions.

Two other points remain notable in our serie: age of donors were significantly higher than in series with in situ stimulation of proliferation [6-8] and culture medium was significantly poorer (only 2% FCS without additional growth factors) but we nevertheless observed a high number of proliferating cells, from the G1 to daughter cells. Both points suggest that the proliferative stimulus obtained with electric pulses is very robust, probably because it combines different mechanisms like release of contact inhibition and direct modulation of cell cycle regulators by intracellular calcium level. Further experiments on corneas form younger donors and with supplemented medium (8% FCS + EGF + bFGF) are ongoing in our laboratory to better explain the relationship between age, ECD, pro-proliferative growth factors and efficiency of electric pulses.

Other experiments cited above were all done using corneas stored à 4°C in Optisol until experiments. We used corneas stored at 31°C in OC during approximately 2 weeks before stimulation. It is likely that, contrary to cold storage, OC realized a preconditioning of HCECs that may become more prone to answer to proliferating stimuli but this remained to be explore by direct comparison of paired corneas stored in Optisol and in OC prior to electrostimulation.

We observed numerous fragmented nuclei among proliferating HCECs at D7. These features compatible with apoptosis are indicative of abortive mitosis. Although we cannot eliminate an artefact linked to long-term genotoxicity of EdU recognized by the mitotic spindle checkpoint, this observation also suggest that physiologic DNA damages accumulated into HCECs with age may ultimately result in abortion of artificially induced cell division.

In conclusion, it is, at the best of our knowledge, the first time that a unique stimulation with a train of electric pulses have been shown to induce proliferation of a significant number of HCECs directly in situ in the endothelium of intact corneas stored in organ culture without growth factor supplementation. Although the cascade of molecular events responsible for the triggering of progression through cell cycle remains unknown, we believe that it could contribute to improve endothelial cell expansion methods for future therapeutic applications.

References

1. Joyce NC. Proliferative capacity of corneal endothelial cells. *Exp Eye Res* 2012;95:16-23.
2. Tan DT, Dart JK, Holland EJ, Kinoshita S. Corneal transplantation. *Lancet* 2012;379:1749-1761.
3. Koizumi N, Okumura N, Kinoshita S. Development of new therapeutic modalities for corneal endothelial disease focused on the proliferation of corneal endothelial cells using animal models. *Exp Eye Res* 2012;95:60-67.
4. Koizumi N, Okumura N, Ueno M, Nakagawa H, Hamuro J, Kinoshita S. Rho-associated kinase inhibitor eye drop treatment as a possible medical treatment for Fuchs corneal dystrophy. *Cornea* 2013;32:1167-1170.
5. EEBA. European Eye Bank Association Directory. Twentieth edition. 2012. Amsterdam; 2012.
6. Senoo T, Obara Y, Joyce NC. EDTA: a promoter of proliferation in human corneal endothelium. *Invest Ophthalmol Vis Sci* 2000;41:2930-2935.
7. Senoo T, Joyce NC. Cell cycle kinetics in corneal endothelium from old and young donors. *Invest Ophthalmol Vis Sci* 2000;41:660-667.
8. Mimura T, Joyce NC. Replication competence and senescence in central and peripheral human corneal endothelium. *Invest Ophthalmol Vis Sci* 2006;47:1387-1396.
9. Patel SP, Bourne WM. Corneal endothelial cell proliferation: a function of cell density. *Invest Ophthalmol Vis Sci* 2009;50:2742-2746.
10. McAlister JC, Joyce NC, Harris DL, Ali RR, Larkin DF. Induction of replication in human corneal endothelial cells by E2F2 transcription factor cDNA transfer. *Invest Ophthalmol Vis Sci* 2005;46:3597-3603.
11. Slettedal JK, Lyberg T, Roger M, Beraki K, Ramstad H, Nicolaissen B. Regeneration with proliferation of the endothelium of cultured human donor corneas with extended postmortem time. *Cornea* 2008;27:212-219.
12. He Z, Pipparelli A, Manissolle C, et al. Ex vivo gene electrotransfer to the endothelium of organ cultured human corneas. *Ophthalmic Res* 2010;43:43-55.
13. Deb-Joardar N, Thuret G, Gavet Y, et al. Reproducibility of endothelial assessment during corneal organ culture: comparison of a computer-assisted analyzer with manual methods. *Invest Ophthalmol Vis Sci* 2007;48:2062-2067.
14. Deb-Joardar N, Thuret G, Zhao M, et al. Comparison of two semiautomated methods for evaluating endothelial cells of eye bank corneas. *Invest Ophthalmol Vis Sci* 2007;48:3077-3082.
15. He Z, Campolmi N, Gain P, et al. Revisited Microanatomy of the Corneal Endothelial Periphery: New Evidence for Continuous Centripetal Migration of Endothelial Cells in Humans. *Stem Cells* 2012;30:2523-2534.
16. Hogan MJ, Alvarado JA, Weddell JS. *Histology of the human eye: An Atlas and Text*. Philadelphia: W.B. Saunders; 1971:102-103.
17. Miklavcic D, Sersa G, Brecelj E, et al. Electrochemotherapy: technological advancements for efficient electroporation-based treatment of internal tumors. *Med Biol Eng Comput* 2012;50:1213-1225.
18. Frandsen SK, Gissel H, Hojman P, Tramm T, Eriksen J, Gehl J. Direct therapeutic applications of calcium electroporation to effectively induce tumor necrosis. *Cancer Res* 2012;72:1336-1341.

19. Stacey M, Stickley J, Fox P, et al. Differential effects in cells exposed to ultra-short, high intensity electric fields: cell survival, DNA damage, and cell cycle analysis. *Mutat Res* 2003;542:65-75.
20. Hofmann F, Ohnimus H, Scheller C, Strupp W, Zimmermann U, Jassoy C. Electric field pulses can induce apoptosis. *J Membr Biol* 1999;169:103-109.
21. Black J. Electrical stimulation of hard and soft tissues in animal models. *Clin Plast Surg* 1985;12:243-257.
22. Maddin WS, Bell PW, James JH. The biological effects of a pulsed electrostatic field with specific reference to hair. Electrotrichogenesis. *Int J Dermatol* 1990;29:446-450.
23. Golzio M, Gabriel B, Boissier F, Deuwille J, Rols MP, Teissie J. [Calcium and electropermeabilized cells]. *J Soc Biol* 2003;197:301-310.
24. Capiod T. Cell proliferation, calcium influx and calcium channels. *Biochimie* 2011;93:2075-2079.
25. Srinivas SP. Dynamic regulation of barrier integrity of the corneal endothelium. *Optom Vis Sci* 2010;87:E239-254.
26. Joyce NC, Zhu CC, Harris DL. Relationship among oxidative stress, DNA damage, and proliferative capacity in human corneal endothelium. *Invest Ophthalmol Vis Sci* 2009;50:2116-2122.
27. Joyce NC, Harris DL, Zhu CC. Age-related gene response of human corneal endothelium to oxidative stress and DNA damage. *Invest Ophthalmol Vis Sci* 2011;52:1641-1649.
28. Yokoo S, Yamagami S, Yanagi Y, et al. Human corneal endothelial cell precursors isolated by sphere-forming assay. *Invest Ophthalmol Vis Sci* 2005;46:1626-1631.
29. McGowan SL, Edelhauser HF, Pfister RR, Whikehart DR. Stem cell markers in the human posterior limbus and corneal endothelium of unwounded and wounded corneas. *Mol Vis* 2007;13:1984-2000.

Article en temps que co-auteur

ARTICLE I: Revisited microanatomy of the corneal endothelial periphery: new evidence for continuous centripetal migration of endothelial cells in humans

STEM CELLS®
TISSUE-SPECIFIC STEM CELLS

Revisited Microanatomy of the Corneal Endothelial Periphery: New Evidence for Continuous Centripetal Migration of Endothelial Cells in Humans

ZHIGUO HE,[a] NELLY CAMPOLMI,[a] PHILIPPE GAIN,[a] BINH MINH HA THI,[a] JEAN-MARC DUMOLLARD,[a,b] SÉBASTIEN DUBAND,[a,b] MICHEL PEOC'H,[a,b] SIMONE PISELLI,[a] OLIVIER GARRAUD,[c] GILLES THURET[a]

[a]Corneal Graft Biology, Engineering and Imaging Laboratory, Federative Institute of Research in Sciences and Health Engineering, Faculty of Medicine, Jean Monnet University, Saint-Etienne, France; [b]Department of Pathology, University Hospital of Saint-Etienne, Saint-Etienne, France; [c]Eye Bank of Saint-Etienne, Auvergne Loire Blood Center, Saint-Etienne, France

Key Words. Human • Cornea • Endothelium • Stem cell • Limbus • Rows • Clusters • Periphery

ABSTRACT

The control of corneal transparency depends on the integrity of its endothelial monolayer, which is considered nonregenerative in adult humans. In pathological situations, endothelial cell (EC) loss, not offset by mitosis, can lead to irreversible corneal edema and blindness. However, the hypothesis of a slow, clinically insufficient regeneration starting from the corneal periphery remains debatable. The authors have re-evaluated the microanatomy of the endothelium in order to identify structures likely to support this homeostasis model. Whole endothelia of 88 human corneas (not stored, and stored in organ culture) with mean donor age of 80 ± 12 years were analyzed using an original flat-mounting technique. In 61% of corneas, cells located at the extreme periphery (last 200 μm of the endothelium) were organized in small clusters with two to three cell layers around Hassall-Henle bodies. In 68% of corneas, peripheral ECs formed centripetal rows 830 ± 295 μm long, with Descemet membrane furrows visible by scanning electron microscopy. EC density was significantly higher in zones with cell rows. When immunostained, ECs in the extreme periphery exhibited lesser differentiation (ZO-1, Actin, Na/K ATPase, CoxIV) than ECs in the center of the cornea but preferentially expressed stem cell markers (Nestin, Telomerase, and occasionally breast cancer resistance protein) and, in rare cases, the proliferation marker Ki67. Stored corneas had fewer cell clusters but more Ki67-positive ECs. We identified a novel anatomic organization in the periphery of the human corneal endothelium, suggesting a continuous slow centripetal migration, throughout life, of ECs from specific niches. STEM CELLS *2012;30:2523–2534*

Disclosure of potential conflicts of interest is found at the end of this article.

INTRODUCTION

Corneal endothelial cells (ECs) are crucial for vision because they control movement of ions and water into the hydrophilic stroma and thus regulate corneal transparency [1]. Derived from the cranial neural crest [2], they form a monolayer of hexagonal cells organized in a tessellated mosaic on their basal membrane, the Descemet's membrane (DM). They uniformly cover the whole posterior corneal surface, and at its periphery reach the trabecular meshwork (TM) in the angle between the cornea and iris root. Central endothelial cell density (ECD, expressed in cells per mm^2) physiologically decreases by 0.6% per year during adulthood [3, 4] without impairing corneal transparency, even in centenarians. However, several endothelial dystrophies and certain traumatisms dramatically accelerate this pace: ECD falls below the threshold of 300–500 cells per mm^2, where irreversible corneal edema occurs, causing permanent vision loss. Such endothelial dysfunctions represent one-third of the indications for corneal grafts performed yearly worldwide.

In vivo, corneal endothelium has limited wound-healing capacity, using residual ECs which, by enlargement and migration, cover the defects left by lost cells [5] without cell division. Joyce et al. [6, 7] have demonstrated that human corneal ECs in vivo are arrested in the G1 phase of the cell cycle. They express negative regulators of the cell cycle belonging to the CIP/KIP family (p21 and p27), to the INK4 family (p16, p15, and p19), and to the p53 family of proteins (p53, TAp63) [8]. Mitotic inhibition may be caused by the presence of

Author contributions: Z.H.: conception and design, collection and/or assembly of data, data analysis and interpretation, and manuscript writing; N.C., J-M.D., S.D., and M.P.: collection and/or assembly of data, data analysis and interpretation, and final approval of manuscript; P.G.: conception and design, provision of study material or patients, manuscript writing, and final approval of manuscript; B.M.H.T.: collection and/or assembly of data and data analysis and interpretation; S.P.: collection and/or assembly of data; O.G.: conception and design, manuscript writing, and final approval of manuscript; G.T.: conception and design, provision of study material or patients, collection and/or assembly of data, data analysis and interpretation, manuscript writing, and final approval of manuscript.

Correspondence: Gilles Thuret, M.D., Ph.D., Corneal Graft Biology, Engineering and Imaging Laboratory, EA 2125, SFR143, Faculty of Medicine, Jean Monnet University, 15, Rue Ambroise Paré, F 42023 Saint-Etienne Cedex 2, France. Telephone: +33-(0)4-77-12-77-93, Fax: +33-(0)4-77-12-09-95; e-mail: gilles.thuret@univ-st-etienne.fr Received October 26, 2011; accepted for publication June 7, 2012; first published online in STEM CELLS *EXPRESS* September 4, 2012. © AlphaMed Press 1066-5099/2012/$30.00/0 doi: 10.1002/stem.1212

transforming growth factor β (TGF-β) in aqueous humor, by contact inhibition of densely packed ECs in a joint mosaic [9], and by stress-induced premature senescence [10–12].

However, a series of clinical and experimental arguments suggest the existence of endothelial regeneration in the human corneal periphery. Higher ECD in the endothelial periphery was described more than 25 years ago [13–15]. The possibility of centripetal migration of ECs from the periphery is suggested by at least two observations: the reported colonization of donors' DM by recipients' ECs after full-thickness corneal graft [16, 17]; and the demonstrated longer survival of corneal grafts in recipients with high ECD in the endothelial periphery [18, 19], namely in keratoconus, a noninflammatory corneal disease affecting young people and characterized by progressive stromal thinning and ecstasy but an endothelium that remains normal. This second observation suggests that the central endothelium is continuously sustained by the peripheral reserve. Furthermore, the continuous insidious destruction of peripheral ECs by certain artificial lenses implanted during cataract surgery in the 1980s, in contact with the corneal periphery, led 10–15 years later to edematous decompensation of the cornea, thus constituting an iatrogenic demonstration of the importance of peripheral ECs in endothelial and corneal homeostasis. Similarly, there is undoubtedly a rapid decrease in central ECD after corneal graft when no ECs persist in the recipient's corneal periphery, typically in edematous decompensation of the cornea. This suggests that central ECs that die cannot be replaced by peripheral ECs.

In experimental conditions, human corneal ECs retain residual proliferative capacity, even in very old donors [20]. In vitro, peripheral ECs have higher mitotic activity than central ones, as their morphology in primary culture is less typically hexagonal and their intercellular junctions loosen [21]. These differences may be due partly to the higher density of precursors in the endothelial periphery [22]. Whikehart et al. [23] and McGowan et al. [24] suggested that human corneal endothelial stem cells (SCs) may be sequestered in niches located deep in the TM or in the so-called transition zone (TZ) between the endothelial edge and the TM, and supply new cells to heal corneal endothelial wounds, at least during in vitro experiments.

In this study, we present a large series of corroborating observations that combine optical and electron microscopy with immunolocalization done on flat-mounts of whole human endothelia. This provides evidence that EC proliferation exists in the extreme periphery of human corneas in vivo. Cell organization in clusters and radial rows, first described in this article, progresses by one step the hypothesis that ECs continuously migrate centripetically from the extreme periphery, where SCs may nest, to the center of the cornea.

Materials and Methods

Cornea Characteristics

Three groups of corneas were studied. Group 1 (nonstored corneas) comprised 39 corneas obtained from the Anatomy Department of the Faculty of Medicine of Saint-Etienne thanks to body donations to science and processed immediately after procurement with no immersion in storage medium. Group 2 (stored corneas) comprised 45 corneas studied after storage in our eye bank. These were normal tissues procured after relatives had been informed, as authorized by French bioethics law. They were not suitable for transplantation owing to inconclusive donor serology despite normal endothelial characteristics, in particular central ECD >2,000 cells per mm^2, the conventional cutoff value for corneal graft qualification. They were stored in organ culture (OC), the prevalent method used in European eye banks, which maintains cell metabolic activity for at least 5 weeks [25]. Corneas were immersed in a closed vial of 100 ml of a commercial medium containing 2% fetal calf serum (FCS; CorneaMax, Eurobio, Les Ulis, France, http://www.eurobio.fr) at 31°C, renewed after 2 weeks. Forty corneas were studied just before medium renewal, and five 3 days after. Corneas in groups 1 and 2 were procured from donors placed in 4°C mortuary chambers, by in situ excision with 18 mm diameter trephination, thus comprising the whole cornea and a rim of adjacent sclera with TM and iris root, as per the procedure recommended in France for corneas intended for transplantation. Group 3 (fresh corneas) comprised four central corneal buttons (8.25 mm in diameter) obtained, after patients' informed consent, directly in the operating theater during full-thickness graft for keratoconus in Saint-Etienne University Hospital. Time from procurement to fixation was only 15–30 minutes.

In group 1, donor age was (mean ± SD) 84 ± 8 years and death-to-procurement time 20 ± 16 hours. In group 2, donor age was 77 ± 10 years. In group 3, donor ages were 23, 28, 30, and 30 years. Handling of the donor tissues adhered to the tenets of the Declaration of Helsinki of 1975 and its 1983 revision in protecting donor confidentiality.

Observation of Flat-Mounted Corneas (En Face Observation)

Cell Morphology. ECs were stained using Alizarin red to visualize cell borders of the whole endothelial mosaic. Prior to staining, the endothelial side was rinsed with balanced salt solution (BSS, Alcon, Rueil Malmaison, France, http://www.alcon.fr). The dye (0.5% Alizarin red [Sigma, St Louis, MO, http://www.sigmaaldrich.com] dissolved in 0.9% sodium chloride with a pH adjusted to 5.2) was filtered through a 0.2-μm filter and placed in the corneal concavity for 90 seconds. After removal of excess dye, corneas were fixed for 2 minutes in 4% paraformaldehyde (PFA) in phosphate buffered saline (PBS) of pH 7.45. Corneas were then immersed in PBS and shaken until detachment of the dark red deposit that had formed on the endothelial surface. Nuclei were counterstained either with 0.4% trypan blue solution (Sigma) for 2 minutes or Hoechst 33342 (Sigma) 10 μg/ml in PBS for 1 minute. After a brief rinse in PBS, corneas were flat-mounted with four radial cuts. A large coverslip was maintained using adhesive tape to ensure mount stability. In a few corneas, the endothelium was observed using phase contrast combined with fluorescence imaging of nuclei stained with Hoechst but not Alizarin red.

Cell Count. ECD was determined in various endothelial zones (see below) using image analysis with the Cell^P software (Olympus Soft Imaging Solutions, Berlin, Germany, http://www.olympus-sis.com). Briefly, cell nuclei were automatically isolated after Hoechst image thresholding. Systematic manual controls prevented false-negative and false-positive cases. Nuclei were then numbered in large regions of interest (ROIs) comprising at least 1,000 nuclei. Half of the nuclei truncated by the ROI edges were taken into account.

Cell Mortality Assessment. In order to assess local differences on the whole endothelium in susceptibility to death after stresses caused by donor death and/or corneal storage, EC viability was determined using trypan blue staining or a live/dead assay with ethidium homodimer/calcein-AM (calcein acetoxymethyl ester) combined with Hoechst 33342, in a

subset of corneas randomly chosen from groups 1 and 2. For group 1, corneas were studied within minutes of procurement. Vital staining with trypan blue is routinely used in eye banks during organ culture. We recently optimized triple labeling with Hoechst-ethidium-calcein (HEC) for experimental assessment of endothelial viability over the whole endothelial area [26]. The endothelial side was exposed for 1 minute to 0.4% trypan blue solution (Sigma) or submitted to HEC triple labeling as previously described [26]. After two rinses in BSS to remove excess dye, the cornea was fixed for 2 minutes in 4% PFA. For trypan blue stained corneas, after a brief rinse in PBS, nuclei were counterstained with Hoechst 33342 (Sigma) 10 μg/ml in PBS for 1 minute. All corneas were flat-mounted as previously described.

Histology on Cross-Sections

To compare the en face view and conventional histology on cross-sections, corneas were fixed in 4% PFA for 24 hours, then dehydrated in successive ethanol baths, and embedded in paraffin. Serial 6-μm-thick sections were cut on a microtome, deparaffinized, and stained with hematoxylin eosin safran. On a subset of 10 corneas selected at random, the thickness of DM was measured on $\times$40 images using the Cell^P image analysis software. For each cornea, thickness was measured on three cross-sections selected in different quadrants, and results were averaged. On each section, thickness was measured in the area where DM was deemed the thickest then repeated 0.5, 1, 2, and 5 mm nearer the center. Distance between DM edge and the area of maximum thickness was measured.

Immunostaining on Flat-Mounted Corneas: Proliferation, Differentiation, SC Markers

EC differentiation was studied using the expression pattern of four proteins: hexagonal apical organization of the tight junction protein ZO-1; hexagonal organization of the cytoplasmic F-actin belt; basolateral localization of Na^+/K^+ ATPase that participates in EC pump functions; and cytoplasmic expression of cytochrome C oxidase (COX) IV, which stains mitochondriae. Stemcellness was studied using Nestin, Telomerase, breast cancer resistance protein (BCRP/ABCG2), Oct-4, and P63-α antibodies. EC proliferation was studied with the ubiquitous proliferation marker Ki67 already validated for human corneal ECs [27].

Specific primary antibodies were IgG from either mouse or rabbit (supporting information Table 1). Nonspecific rabbit IgG (Zymed, Carlsbad, CA, http://www.zymed.com; 02-6102) and mouse IgG (Zymed; 02-6502) were used for negative controls. Secondary antibodies used at 1/500 were Alexa Fluor488 goat anti-mouse IgG (Invitrogen, Carlsbad, CA, http://www.invitrogen.com; A11001) and Alexa Fluor 555 goat anti-rabbit IgG (Invitrogen, A21428). Each cornea was cut radially into four or eight pie-shaped wedges. Fixation was done at room temperature (RT) for 45 minutes either in 0.5% PFA in PBS pH 7.45 or in methanol, depending on the antigen. Fixation was followed by antigen retrieval with 0.5% sodium dodecyl sulfate (SDS) in water for 5 minutes at RT to reveal telomerase. Membrane permeabilization with 1% Triton X-100 in PBS was necessary for PFA-fixed corneas except the corneal wedges treated with SDS. These experimental conditions were optimized after previous experiments recently published (data not shown) [28]. Heat-inactivated goat serum was used to block the nonspecific binding sites for 30 minutes at 37°C. Corneal pieces were immersed in primary antibodies diluted in 2% inactivated goat serum and 2% bovine serum albumin in PBS for 1 hour at 37°C. After three rinses in PBS, pieces were incubated with the secondary antibody for 45 minutes at 37°C. The counterstain was done with Hoechst 33342 10 μg/ml in PBS for 1 minute at RT. Finally, the corneas were flat-mounted in PBS just before observation. All images were captured using an IX81 fluorescence microscope (Olympus, Tokyo, Japan, http://www.olympus-global.com) with Cell^P imaging software.

Scanning Electron Microscopy of DM

Five corneas (two from group 1 with death-to-procurement time of 11–66 hours and three from group 2 stored for 10, 20, and 23 days) with mean donor age of 85 $\pm$ 19 years (53–100 years) were observed after removal of ECs, to give access to the bare DM. ECs were removed by incubation with 1% SDS in water followed by vigorous washing in distilled water. The corneas were fixed in 0.1 N cacodylate-buffered 2% glutaraldehyde pH 7.4 at 4°C for 24 hours. They were washed with 0.2 N cacodylate and then distilled water. The fixed specimens were dehydrated through ascending concentrations of acetone up to pure acetone. They were then dried using a critical point dryer (E3000, Quarum Technologies, East Sussex, U.K., http://www.quorumtech.com). After coating with gold-palladium in a mini sputter coater (Polaron SC 7620, Quorum Technologies) and mounting on metal stubs, the specimens were observed using a Hitachi S-3000N SEM at an electron accelerating voltage of 5 kV.

Definition of Observation Zones of the Posterior Surface of the Cornea

Cell characteristics were studied systematically in the surgical or anatomic regions of the posterior surface of the cornea, which were defined as follows, from center to periphery (Fig. 1): (a) endothelial center with a 4.0 mm radius, corresponding to the disk usually trephined by the surgeon for corneal graft; (b) endothelial periphery (P) of approximately 1.5–2 mm width (depending on corneal diameter), stopping at the anatomic endothelium edge, that is, the end of the DM, also called Schwalbe's line; (c) for our work, we had to define a supplementary zone inside the periphery corresponding to the last 0.2 mm of the endothelial periphery, which we named endothelial extreme periphery, a zone comprising most of the Hassal-Henle bodies that correspond to age-related Descemetic mushroom-shaped expansions; (d) TZ, 0.15 mm wide, characterized by absence of DM and of fibers typical of the TM. The zone is often confused in the literature with Schwalbe's ring, which is only prominent in 15% of corneas [29]; and (e) finally TM, approximately 0.5 mm wide. Outside these structures, residues of the iris root, gently detached during procurement, remained as a pigmented ring, followed by bare sclera cut at a 9-mm radius.

RESULTS

En Face and Cross-Section Observations

Cell Clusters in the Extreme Periphery. On the flat-mounts, cell clusters were observed in the extreme periphery in nearly two-thirds of cases (61% (n = 23/38): 80% of group 1 corneas (n = 16/20) and 39% of those in group 2 (n = 7/18) (p = .01 (χ^2)) (Fig. 1). These clusters were organized between the Hassall-Henle bodies and were not clearly separated and so impossible to count precisely. However, we estimate that on average they occupied one-third of the circumference of each cornea. On the cross-sections, they always comprised two or three cell layers 7–12 μm deep. The cells in the clusters had spherical or ovoid nuclei with smaller diameters than those of the central ECs, which had flat, strictly round nuclei of larger diameter.

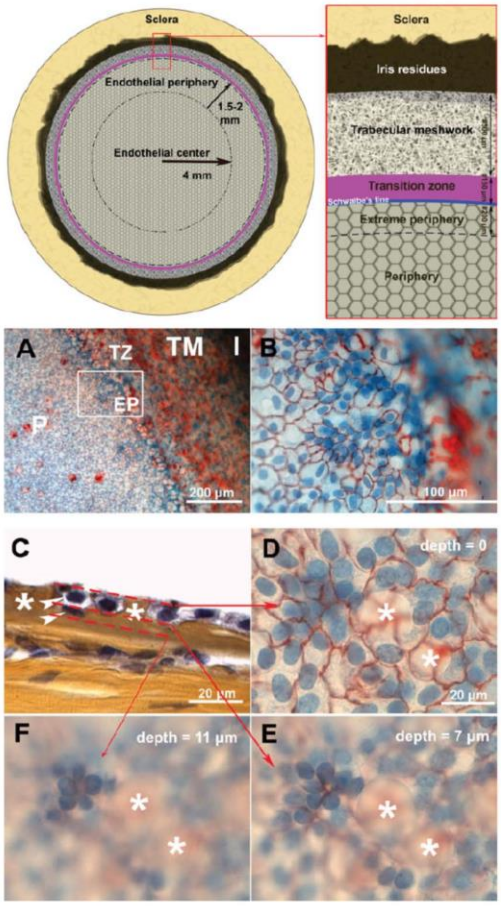


Figure 1. Top: Zones of interest on the posterior surface of a human cornea. The sclera has been trephined to a diameter of 18 mm and the iris removed. Bottom: Cell clusters. **(A, B):** En face view of the corneal endothelial periphery (P). Cell clusters were localized in the EP in contact with the TZ. TM and iris root residues (I) are indicated. A ×10, B ×40. Alizarin red and trypan blue on fixed tissue. **(C–F):** (×96) Multilayered organization (arrowheads) of cell clusters, always localized in immediate vicinity of Hassall-Henle bodies (asterisk). (C): Cross-section (hematoxylin eosin safran). (D–F): En face view (Alizarin + trypan blue). Abbreviations: EP, extreme periphery; I, iris root residues; P, periphery; TM, trabecular meshwork; TZ, transition zone.

Radial EC Rows in the Periphery

General description. In the periphery, EC organization in radial rows was observed in more than two-thirds of cases (68% [$n = 26/38$]): 67% ($n = 12/18$) of group 1 corneas and 70% (14/20) of those in group 2 (nonsignificant difference) (Fig. 2). These rows on average occupied 86% ± 24% of the corneal circumference, leaving some zones with none. These rows were variable in length in the same cornea and also between corneas, varying from 350 to 1,465 μm (mean 827 ± 295 μm). There was no difference in donor age or in central ECD between corneas presenting rows and the other corneas (data not shown). ECs of rows consistently had elongated nuclei (compared with those of the central ECs, which were always strictly round), the longitudinal axis of which most often coincided with the axis of the rows. Cells in rows had increased polymorphism and weaker Alizarin red staining than central ECs.

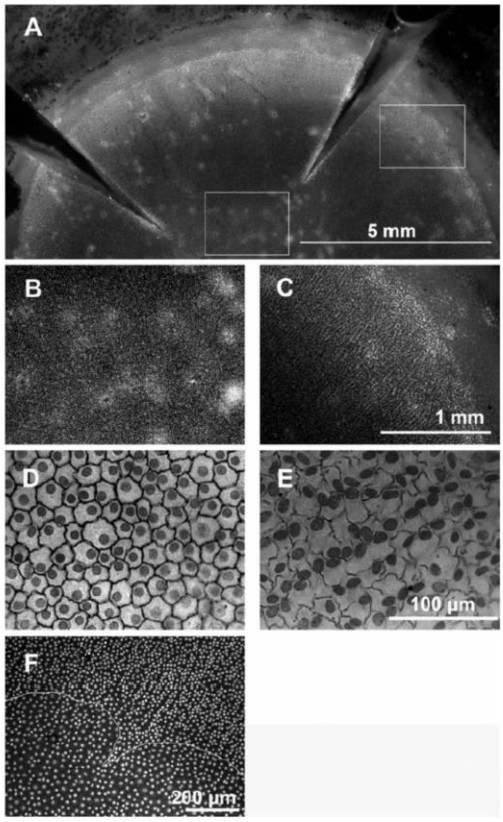


Figure 2. Radial endothelial rows in the corneal periphery. **(A):** General view of half cornea flat-mounted thanks to radial cuts. Hoechst 33342 staining, ×4. **(B, C):** Zoom with ×10 objective on center (B) and periphery (C) where cell rows were clearly present. **(D, E):** Difference of endothelial cell morphology between center (D) and periphery (E). Alizarine red and Hoechst staining, ×40. **(F):** Transition between cell rows and more central endothelium in a non-stored cornea. The white line indicates an artificial boundary between the zones. Hoechst staining, ×10.

EC density in radial rows. Of the seven corneas in group 1 (age = 83 ± 13 years, death-to-procurement time = 19 ± 20 hours) picked randomly from among those organized in rows, ECD was significantly higher (by 69% ± 41%) in the cell rows than in the immediately adjacent zone not organized thus, respectively, 3,483 ± 558 versus 2,141 ± 507 EC per mm^2 ($p < .05$). The highest maximum difference observed was 4,344 versus 1,786 cells per mm^2, or +143% in a group 1 cornea (donor aged 72 years, death-to-procurement time of 4.5 hours). This difference was less marked in the 10 group-2 corneas (age = 80 ± 14 years, death-to-procurement time = 17 ± 11 hours, time in organ culture 14 ± 6-day): 23% ± 27% higher in the cell rows, respectively, 1,993 ± 698 versus 1,705 ± 750 ECs per mm^2.

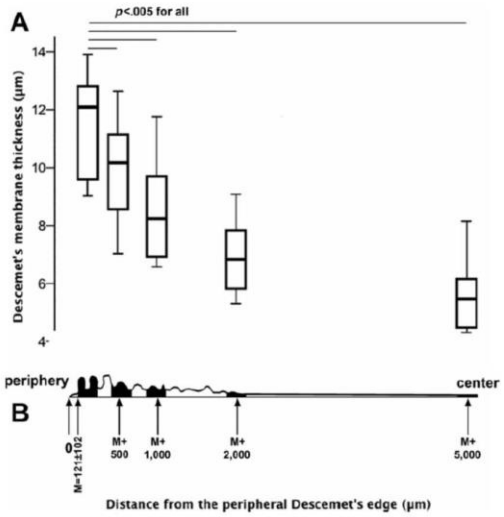


Figure 3. Descemet's membrane thickness from periphery to center. **(A):** Box plots of measurements performed in the thickest area (M), then 500, 1,000, 2,000, and 5,000 μm more centrally. The thickest area was constantly those starting just after the first Hassal-Henle bodies and was located 121 ± 102 μm after the Descemet edge. **(B):** Diagram of the measurement method on a histologic cross-section. Hassal-Henle bodies and Descemet excrescents are deliberately hypertrophied. To reduce biais, the mean thickness of each area was determined by image analysis, taking into account the area of Descemet's cross-section visible on a ×40 image of the whole field, that is, a width of 230 μm (area schematized in black).

DM furrows in radial rows. Viewed by light microscopy on flat-mounts, the peripheral DM contained imprints of the linear organization of the ECs, in the form of furrows at the base of which EC nuclei were lodged. On the cross-sections, the DM periphery was thicker (Fig. 3) and more irregular than its center and the furrows were defined by DM excrescences covered by EC cytoplasm (Fig. 4). In scanning electron microscope (SEM), the furrows appeared as the dotted line formed by DM plots (Fig. 4).

Relationship between cell clusters and radial rows. In all corneas, cell rows were separated from cell clusters by a narrow 150–200 μm band comprising polymorph ECs with an ECD lower than that in cell rows (see above) (Fig. 2; supporting information Fig. 1). Alterations to EC morphology were greater in group-2 corneas. In cross-sections, the DM of this band presented warts more elongated than typical Hassal-Henle bodies.

EC Mortality. In all corneas (groups 1 and 2), small clusters of cells with high cell mortality (>50% of cells) were systematically observed in the extreme periphery, with mortality decreasing very rapidly toward the center (Fig. 5).

Immunolocalization

Differentiation Markers. The cells in the extreme periphery did not have the expression patterns typical of central ECs for ZO-1 (absence of apical organization tight-junctions, hexagonal aspect), Actin (absence of submembranal apical belt, hexagonal aspect), Na^+/K^+ ATPase (absence of enzyme activity associated with ionic-pump function, located on the basolateral membranes on cell interdigitations, giving a distinctive star aspect), and COX IV (absence of dense mitochondrial network) (Fig. 6).

SC Markers. Expression of Nestin (nuclear and/or cytoplasmic) and Telomerase (cytoplasmic) was found in ECs in the extreme periphery (Fig. 6; supporting information Table 2). Weak expression of Nestin was observed in the cytoplasm of the scarce isolated ECs elsewhere in the endothelium. Expression of BCRP/ABCG2 was detected not only in a few ECs of the extreme periphery but also in the center of both corneas from one group-1 donor, procured very shortly after death (4.5 hours). Neither Oct-4 nor P63-α was detected (data not shown). There was no difference of expression of any of the five markers between corneas of groups 1 and 2 (data not shown).

Proliferation Marker Ki67. In the nonstored corneas (group 1), scarce Ki67-positive ECs were present but only in clusters in the extreme periphery of the endothelium of two corneas with very short death-to-procurement times (4.5 and 5 hours) (Fig. 7). In the stored corneas (group 2), many Ki67-positive ECs were observed in the periphery and slightly beyond but only in corneas of which the OC medium had been renewed 3 days before observation. In the group-3 corneas, no labeling was observed.

Discussion

The corneal periphery is a complex region that is essential for ocular embryogenesis and for homeostasis of the adult cornea. Superficially, the limbus, a heavily vascularized junction zone between the cornea and sclera, contains epithelial SCs located in specific niches called limbal epithelial crypts (LECs) [30, 31] as well as many transient amplifying cells (TACs) [32]. The epithelium is a multilayered tissue with regular turnover and capable of rapid *ad integrum* healing even after total mechanical destruction, provided the limbus is intact. Epithelial SCs seem to be activated in case of massive epithelial damage, whereas physiological turnover is thought to be provided by TACs [32, 33]. While the existence of epithelial SCs in the limbus is an old premise, the anatomic description of their specific niches is more recent [30, 34]. These LECs are located at the ends of the palisades of Vogt, which are solid radial cords of cells in the extreme periphery of the corneal epithelium. The periphery of the corneal stroma probably also houses keratocyte progenitors, at greater depth [35]. Finally, the posterior, that is, truly intraocular, face of the cornea is even more complex than its surface, as it contains the posterior limbus (TM, Schlemms'canal, TZ) implicated in the regulation of intraocular pressure and the edges of the corneal endothelium. It may house corneal endothelial progenitors or SCs [22–24]. In the hypothesis of slow endothelial renewal, however, their proliferative capacity remains very limited and in particular, unlike the epithelium, they cannot respond to massive endothelial damage, even when the posterior-limbus structures remain intact. This limitation has yet to be explained.

For the first time, using a large number of human corneas, some of which were studied without storage, and complementary methods of observation, we were able to describe a new microanatomic organization of ECs in the endothelial periphery, which we termed cell clusters and radial cell rows (summarize in supporting information Fig. 1), and which suggests

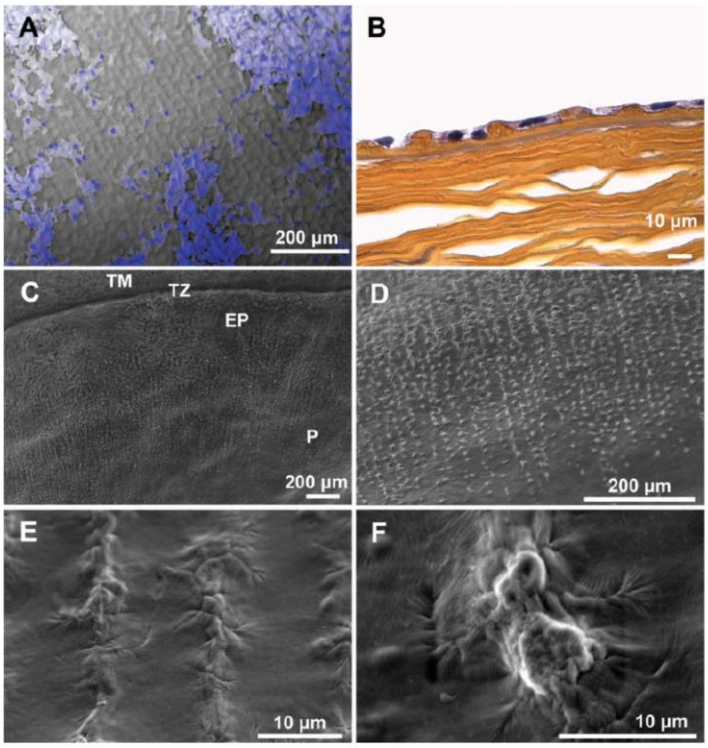


Figure 4. Radial Descemet's membrane (DM) furrows in the corneal periphery. Furrows were made visible after partial **(A)** or complete **(C–F)** removal of endothelial cells. (A): Flat-mount observed with phase contrast to highlight DM excrescences and with Hoechst 33342 to locate cell nuclei at the base of the furrows. **(B):** Cross-sections orthogonal to the cell rows, stained with hematoxylin eosin safran in order to highlight position of nuclei with regards to Descemet excrescents. (C–F): Scanning electron microscopy of the bare DM, showing furrows defined by real plots and starting near the TZ. Abbreviations: EP, extreme periphery; P, periphery; TM, trabecular meshwork; TZ, transition zone.

that ECs slowly and continuously migrate from periphery to center throughout life.

EC organization in the extreme periphery of the human cornea, in small clusters of two to three layers between Hassall-Henle bodies, had never been described. Hassall-Henle bodies were described in the late 19th century and are associated with aging of the normal cornea [36]. These mushroom-shaped Descemetic structures are solely observed in the endothelial periphery. They are absent in children and may progressively appear after 30 years, initially near Schwalbe's line and extending centripetically more than 1 mm [37]. They are constant in humans, but their number varies among individuals. Two hypotheses may explain their association with the peripheral cell clusters we describe. First, that Hassall-Henle bodies are synthesized throughout life by the cells of the clusters that perpetually reside in the periphery. Second, that clusters do not initially exist and Hassall-Henle bodies progressively develop during the continuous centripetal migration of cells that emerge from the posterior limbus and synthesize collagen at their emerging site. Secondarily, Hassall-Henle bodies, with aging, become obstacles that progressively slow cell migration and are consequently responsible for cell accumulation in clusters. Further studies on younger donors are necessary to ascertain whether cell clusters are present independently of Hassall-Henle bodies.

Clusters of cells located in Schwalbe's line were described in 1982 by Raviola [38] in seven *Macaca mulatta* (rhesus monkeys) aged from 3 to 17 years (life span 25 years) and were interpreted as "giving the impression that they originated from the endothelium and successively migrated deeply, toward the meshwork." Retrospectively, these clusters of tightly packed spherical cells with high nucleus/cytoplasmic ratio located at the tapering end of Descemet's membrane appear identical to the clusters we describe here. Their distribution was discontinuous like ours, but their presence was constant in all specimens studied, independently of animal age.

In 1957, Vrabec noted peculiar fan-shaped groups of ECs in the human corneal periphery that were closely related to the anterior anchorage of the ciliary muscle tendons [39] but did not describe multilayered clusters. As it is very unlikely that endothelial SCs nest at the surface, the finding of a deeper structure, closer to the vascularization, may indicate a potential niche. The apparent smallness and round nuclei of these cells is also consistent with SCs or stem-like cells. These clusters are not directly connected with the cell rows we describe, remaining separated by an irregular zone where Descemet warts do not have the round shape typical of Hassall-Henle bodies. Cells in this zone are not fully differentiated, as we demonstrated using immunostaining, as they do not have structural and functional proteins typical of mature

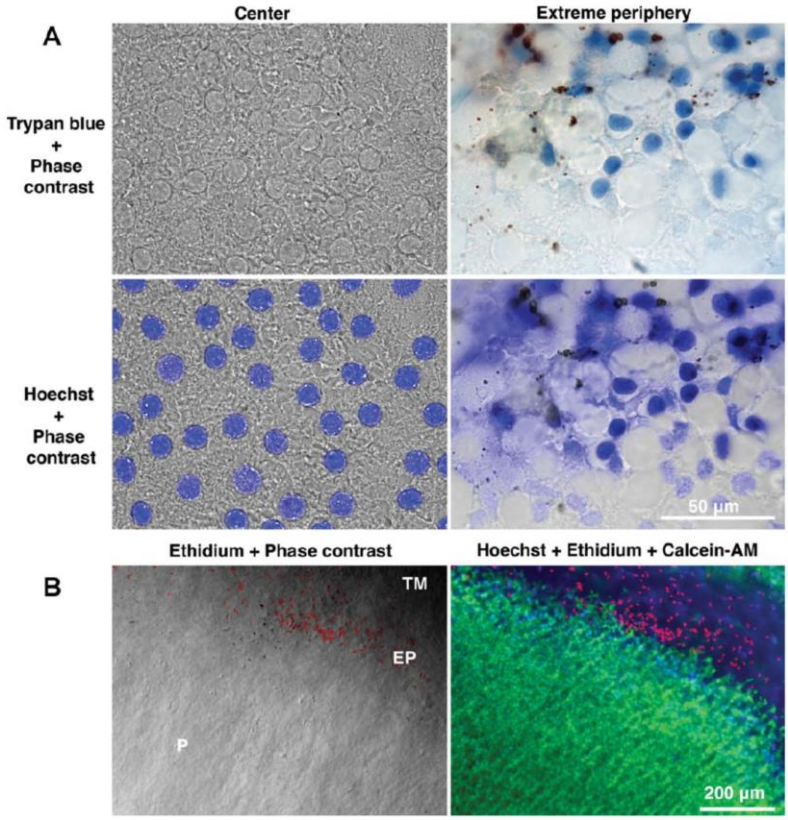


Figure 5. Cell mortality in the extreme periphery compared to the center. **(A):** Representative example of a nonstored cornea (age 69 years, death-to-procurement time 20 hours). Trypan blue and Hoechst staining. ×40 **(B):** Representative example of a stored cornea (age 72 years, 14 days of organ culture without medium renewal). Triple labeling with Hoechst, Ethidium homodimer, Calcein-AM. ×10. Dead cells (E+, C-) locally accumulated at the EP and TM, whereas in the periphery (P), endothelial cells remained viable (H+E-C+). Abbreviations: EP, extreme periphery; TM, trabecular meshwork.

ECs, nevertheless they already form a monolayer which is one feature of ECs. Our staining pattern for SC and TAC markers is consistent with previous reports by Whikehart and McGowan but with certain differences. They described telomerase activity only in ECs located in a zone 4–12 mm from the center and not in the center, TM or TZ [23], whereas protein expression was described in the TM, TZ, and endothelial periphery on cross-sections and only in the TM on flat-mounted whole corneas [24]. This team described the apparition of Oct-4 positive cells in the TM after central trephination followed by subsequent 24–48 hours storage at 4°C and suggested migration of stem-like cells from the TM toward the endothelium. In our series, with immunostaining of flat-mounted whole corneas, telomerase expression seems restricted to the extreme periphery. We found Nestin predominantly in the extreme periphery, whereas it was present only in the TM and TZ (similar on cross-sections and flat-mounts) for Whikehart [23]. BCRP/ABCG2 has been described as a marker for hematopoietic [40] and corneal epithelial SCs [41], among other cell types. We found it expressed occasionally in isolated ECs. These results, associated with negativity for Oct-4 [42, 43], another SC marker, suggest that cells in clusters may be progenitors rather than SCs. Negativity for P63, shown to identify SCs in the basal layer of stratified surface limbal and skin epithelia [44], was consistent with the fact that this marker has never been shown positive in nonepithelial tissues. In any case, both explanations indicate that other markers need to be assessed in this subpopulation of cells. The absence of immunostaining for cells located more deeply in the clusters may be due to our choice of staining only on flat-mounts in order to screen for rare cells among an intact endothelial population [28].

Unlike the LECs described for the corneal epithelial SCs in the limbus [30] and which meet all niche criteria (anatomic protection, specific niche cells, proximity to vascularization, specific microenvironment, adhesion molecules, extracellular matrix components) [45, 46], we did not expect to find similar structures for the endothelium, owing to the absence of clinically significant proliferative capacity. Nevertheless, our microanatomic observations supply fresh arguments in favor of niche-like structures in the extreme periphery of the cornea.

We found overmortality in the extreme periphery, in the zone of the presumed TACs, in nonstored corneas very soon after donor death. Post-mortem ischemia of this heavily vascularized zone probably plays an important role. Increased

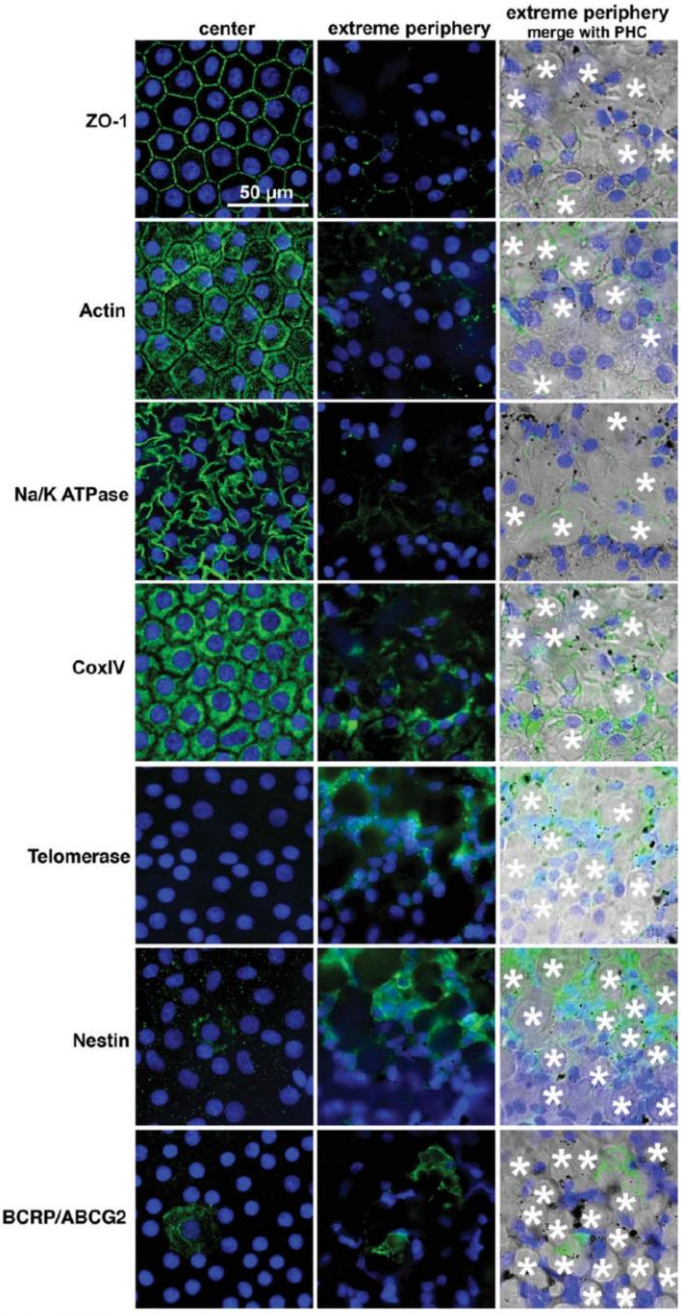


Figure 6. Immunolocalization of differentiation and stem cells markers in endothelial cells. The typical expression patterns of ZO-1, Actin, Na/K ATPase, and CoxIV observed in the center were absent in the extreme periphery, in the cell-cluster zone. Telomerase and Nestin were largely expressed in the cell-cluster zone of almost all corneas. By contrast, BCRP/ABCG2 was found only in two nonstored corneas. PHC was used only for the extreme periphery to allow visualization of Hassal Henle bodies (asterisk), which by definition were absent in the center ×40. Abbreviations: BCRP, breast cancer resistance protein; PHC, phase contrast.

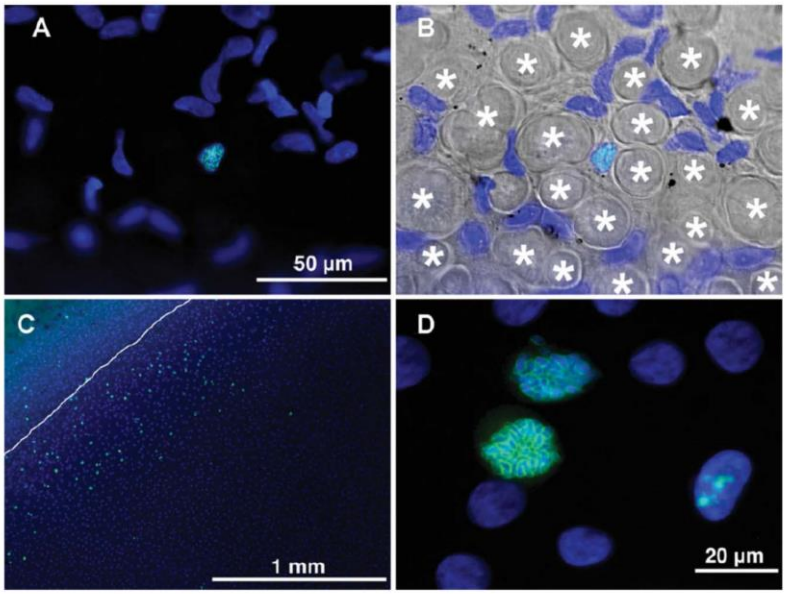


Figure 7. Immunolocalization of the proliferation marker Ki67. **(A, B):** Nonstored cornea with death-to-procurement time of 4.5 hours. Only a few isolated endothelial cells (ECs) located in the extreme periphery were positive. (A): Hoechst + Ki67, (B): Merge with phase contrast to highlight Hassall-Henle bodies (asterisk). **(C, D):** Stored cornea observed 3 days after storage medium renewal. Multiple Ki67-positive ECs were visible, with metaphases indicating active cell cycling. The line in (C) delineated the transition zone.

susceptibility to post-mortem oxidative stress is a hypothesis for these poorly differentiated cells [47], which may have limited protective systems such as, for example, the heat shock proteins in the more central ECs [48]. The literature does not report any particular fragility of SCs or TACs, but, except in corneal-epithelium studies, the other SC types were always procured from beating-heart donors. For the corneal epithelium, however, it has been shown that long death-to-procurement time reduces the proliferative capacity of TACs [49, 50], which may indicate specific mortality of limbic epithelial SCs due to postmortem ischemia. In our study, this apparent higher sensitivity of peripheral cells to cell death soon after donor death may also partly explain the extreme scarcity of Ki67-positive cells in nonstored corneas.

Notably, we also observed overmortality in the extreme periphery of stored corneas, accompanied by lesser frequency of cell clusters and higher EC polymorphism. OC is a storage method derived from cell culture and used since the early 1970s [51]. Contrary to short-term 4°C storage (5–8 days), it lasts up to 5 weeks. Storage-induced cell alterations have been extensively studied in the central cornea, the area of interest for corneal graft. Despite general satisfactory preservation of corneal viability, attested by constant good clinical results identical to 4°C short-term storage [52, 53], death of central ECs increases dramatically during OC, with approximately 1% cell loss per day [54, 55] compared with 0.6% per year throughout life [3, 4]. However, OC-specific alterations of ECs in the extreme periphery have never been described. As OC is known to promote endothelial wound healing [56], we suppose that dead cells in the cell clusters rapidly desquamate and are replaced by neighboring ECs, explaining both why EC clusters were less frequent and why EC polymorphism increased. Moreover, the continuous overmortality that we observed in the extreme periphery may be explained by a specific sensitivity to ischemia reperfusion-like syndrome, as OC conditions restore metabolic activity after prolonged post-mortem ischemia. This specific overmortality in corneas of nonstored or stored corneas, not previously reported, may seriously limit further study of EC proliferation ex vivo. The possibility, independently of donor age, of triggering EC division after intercellular junction loosening with EDTA and incubation at 37°C in mitogen-rich medium was demonstrated by Senoo et al. [57]. Cell division was nevertheless not reported to be restricted in the extreme periphery, even if proliferation capacity was higher in the periphery regardless of donor age [58]. In a similar study on 13 corneas (from donors aged 15–68 years) stored for 7 days at 4°C in OptisolGS, subsequently exposed to EDTA, and cultured at 37°C in a cell-culture medium with 10% FCS plus growth factors for 48 and 96 hours to promote cell proliferation, more Ki67-positive ECs were found in the center than in the periphery [59]. The number of Ki67-positive cells was inversely proportional to ECD. No proliferation was observed when initial ECD exceeded 2,000 cells per mm^2. Having showed that cell death occurs preferentially in the extreme periphery where TACs may reside, we suppose that, in most previous studies, the initial 4°C storage time may have been deleterious to the peripheral TACs already weakened by donor death-induced cellular stress, precluding observation of a higher number of Ki67-positive ECs in the extreme periphery, even after mitotic stimulation.

Interestingly, we observed numerous proliferating ECs in the periphery of organ-cultured corneas but only shortly after medium renewal. We suppose that proliferation was not higher in the extreme periphery for the reasons set out above. OC media, typically containing 2% FCS, are not

known to promote EC division. EC mitosis has only been described in corneas with numerous endothelial lesions due to extended death-to-procurement time and subsequently stored in a specific OC medium supplemented with 8% FCS [60]. In our study, we suppose that the initial storage time triggered cell loss sufficient to locally loosen cell–cell contact and that the rapid increase in nutrients and growth factors during medium renewal stimulated division of several ECs near the local lesions, in a way similar to the experiments reported above with EDTA followed by incubation with mitogens [57].

In our study, the occasional expression of Ki67 in only one nonstored cornea with very short death-to-procurement time (probably with limited ischemia) may indicate that in vivo cell division in this zone concerns only a limited number of cells. Considering cell cycle duration, Ki67 staining of only a few cells is consistent with clinical experience.

To our knowledge, the EC organization in radial rows observed in two-thirds of corneas has never previously been described. In vivo, neither the biomicroscopy used for clinical corneal observation nor the specular microscopy used for endothelial observation allows analysis of the periphery of the posterior face of the cornea. Using SEM, Svedbergh exhaustively described the natural history of the human corneal endothelium of 14 subjects aged 13–88 years without reporting radial rows [61]. His study was done on intact endothelia, whereas Descemetic furrows are only visible after EC removal. Also with SEM, and this time after EC removal by sonication, Inaba studied the periphery of the DM of 87 corneoscleral rims (from donors aged 2 to 100 years), which are postoperative residues of full-thickness corneal graft after central trephination. However, he only examined the TZ and the Hassall-Henle bodies, that is, a zone slightly more peripheral than that of the radial cell rows, and so neither could he describe organization in rows [37]. Indeed, it is likely that the zone comprising the rows was damaged by trepanation. Finally, when the endothelium is observed on histological cross-sections, the most common technique in the literature, rows are not visible and clusters are very hard to see, in the absence of serial cross-sections. Cell clusters and radial rows were frequent but not constant in our series, suggesting inter-individual variability. This is not surprising and can be compared with the variability of healing capacity clinically observed at the ocular surface as well as with the success rate of epithelial culture from limbal explants [49]. Organization in radial cell rows is associated with much higher local ECD than in zones not organized thus. This strongly suggests that continuous proliferation in the periphery regularly "pushes" ECs centripetally. The radial cell rows occupy a narrow peripheral band (mean 827 ± 295 μm), which may be relatively well protected by a cornea that is naturally less transparent in this zone, particularly due to the presence of an arcus senilis, frequent in elderly subjects and in our donor population. We also observed by SEM that this likely cell migration throughout life leaves a highly visible imprint on the DM. In particular, we observed plot structures that perfectly match the images obtained by third harmonic multiphoton microscopy which Aptel and colleagues recently published and titled "Descemetic fibrous patches connecting EC to the stroma" [62]. The DM contains a nonbanded layer that is synthesized by ECs throughout life and gradually thickens from 2 to 10 μm between 10 and 80 years [63]. The largest mean thickness found in the periphery, and the association with the plots, indicate increased collagen synthesis by peripheral ECs, linked to their greater number and/or more intense activity. However, the linear organization of the plots, which form clear furrows, reflects the deposit of collagen along the EC path throughout life. The function of these plots, located between the ECs and potentially at the intercellular junctions, has yet to be determined. The heterogeneous distributions of cell-line length indicate that cell migration is heterogeneous in the same cornea and between individuals. Cell lines have never been found in the central endothelium of normal corneas. This indicates that corneal-endothelium regeneration is a very slow process limited to the peripheral endothelium of normal corneas. The age-related decrease in ECD in the central endothelium indicates that this regenerative mechanism may only partially offset cell loss in the central endothelium during adulthood. Again, the absence of young donors in our series prevents us from verifying at what point in life this organization appears.

In the radial cell row zone of nonstored corneas, we found weaker Alizarin red staining and higher polymorphism than in central ECs. These characteristics had already been described years ago using silver cell border staining in ECs of the TZ (although a linear organization was not described) [39]. This may indicate looser intercellular junctions and therefore higher cell-mobility potential than in the center, where the intensity of alizarin red staining and the regular morphometry correlate with the stability of the cell mosaic. Note that both modifications are actually observed in the center during wound healing, when cell migration becomes necessary to cover a defect left by dead cells. The possibility for ECs to easily move in from the extreme periphery is a supplementary argument for slow centripetal migration from stem/progenitor cell niches and may explain why they seem to accumulate in a zone where cells are more uniform and probably more stable, as shown in Figure 3F. Cell nuclei in radial cell rows were always elongated and radially oriented, whereas nuclei of central ECs were perfectly round. This morphological difference between peripheral and central ECs suggests that the endothelium is more stable around the optical axis, and is supplied by a peripheral store of cells that are less differentiated and liable to migrate slowly toward the central zone. In this peripheral zone, which is not needed for vision, the pump function of the endothelium for deturgescence of the corneal stroma, which incidentally is thicker in its periphery than in its center, is probably less efficient.

Conclusion and Summary

To summarize, we suggest a unifying model of human corneal endothelial homeostasis. This model comprises, in the "non-visual" periphery of the cornea, a renewal zone where ECs divide very slowly and migrate toward the center but probably desquame, while the central ECD in the optical axis remains stable. Cell clusters located in the extreme periphery may be SC niches or at least emerging points for progenitors migrating from deeper niches. Once they make contact with aqueous humor, their dividing capacity, but not their migrating potential, may be partly repressed by cell cycle inhibition by TGF β and by cell contact inhibition as soon as they form a monolayer. These cells may then be continuously pushed toward the center and retain some proliferative capacity in experimental conditions, but as they never divide in vivo after reaching the endothelial monolayer, they do not shorten their telomeres [10, 64]. During migration, they acquire full differentiation and slowly lose their residual proliferative capacity owing to environmental stresses (ultra-violet light, temperature changes, aqueous humor soluble factors) [11, 65] that are probably more pronounced in the corneal center, far from limbal vascularization. These mechanisms may contribute to the

stability of the central endothelium, which, as an ionic pump, is devoted solely to maintaining a transparent optical axis.

ACKNOWLEDGMENTS

We thank Jean-Yves Thuret for his comments on the manuscript and fruitful discussions; Isabelle Anselme from the Centre de Microscopie Electronique Stéphanois (CMES) for her contribution to scanning electron microscopy; Sophie Acquart from the Eye Bank of Saint-Etienne and Gérard Guillain from the Anatomy Department at the Faculty of Medicine of Saint-Etienne, both for providing precious human corneas.

DISCLOSURE OF POTENTIAL CONFLICTS OF INTEREST

The authors indicate no potential conflicts of interest.

REFERENCES

1 Maurice DM. The location of the fluid pump in the cornea. J Physiol 1972;221:43–54.
2 Hayashi K, Sueishi K, Tanaka K et al. Immunohistochemical evidence of the origin of human corneal endothelial cells and keratocytes. Graefes Arch Clin Exp Ophthalmol 1986;224:452–456.
3 Murphy C, Alvarado J, Juster R et al. Prenatal and postnatal cellularity of the human corneal endothelium. A quantitative histologic study. Invest Ophthalmol Vis Sci 1984;25:312–322.
4 Bourne WM, Nelson LR, Hodge DO. Central corneal endothelial cell changes over a ten-year period. Invest Ophthalmol Vis Sci 1997;38: 779–782.
5 Sherrard ES. The corneal endothelium in vivo: its response to mild trauma. Exp Eye Res 1976;22:347–357.
6 Joyce NC, Meklir B, Joyce SJ et al. Cell cycle protein expression and proliferative status in human corneal cells. Invest Ophthalmol Vis Sci 1996;37:645–655.
7 Joyce NC, Navon SE, Roy S et al. Expression of cell cycle-associated proteins in human and rabbit corneal endothelium in situ. Invest Ophthalmol Vis Sci 1996;37:1566–1575.
8 Paull AC, Whikehart DR. Expression of the p53 family of proteins in central and peripheral human corneal endothelial cells. Mol Vis 2005; 11:328–334.
9 Joyce NC, Harris DL, Mello DM. Mechanisms of mitotic inhibition in corneal endothelium: Contact inhibition and TGF-beta2. Invest Ophthalmol Vis Sci 2002;43:2152–2159.
10 Konomi K, Joyce NC. Age and topographical comparison of telomere lengths in human corneal endothelial cells. Mol Vis 2007;13: 1251–1258.
11 Joyce NC, Zhu CC, Harris DL. Relationship among oxidative stress, DNA damage, and proliferative capacity in human corneal endothelium. Invest Ophthalmol Vis Sci 2009;50:2116–2122.
12 Xiao X, Wang Y, Gong H et al. Molecular evidence of senescence in corneal endothelial cells of senescence-accelerated mice. Mol Vis 2009;15:747–761.
13 Schimmelpfennig BH. Direct and indirect determination of nonuniform cell density distribution in human corneal endothelium. Invest Ophthalmol Vis Sci 1984;25:223–229.
14 Daus W, Volcker HE, Meysen H et al. Vital staining of the corneal endothelium–increased possibilities of diagnosis. Fortschr Ophthalmol 1989;86:259–264.
15 Amann J, Holley GP, Lee SB et al. Increased endothelial cell density in the paracentral and peripheral regions of the human cornea. Am J Ophthalmol 2003;135:584–590.
16 Wollensak G, Green WR. Analysis of sex-mismatched human corneal transplants by fluorescence in situ hybridization of the sex-chromosomes. Exp Eye Res 1999;68:341–346.
17 Lagali NS, Stenevi U, Claesson M et al. Donor and recipient endothelial cell population of the transplanted human cornea: A two-dimensional imaging study. Invest Ophthalmol Vis Sci 2010;51:1898–1904.
18 Thompson RW,Jr., Price MO, Bowers PJ et al. Long-term graft survival after penetrating keratoplasty. Ophthalmology 2003;110: 1396–1402.
19 Williams KA, Coster DJ. The immunobiology of corneal transplantation. Transplantation 2007;84:806–813.
20 Joyce NC. Proliferative capacity of the corneal endothelium. Prog Retin Eye Res 2003;22:359–389.
21 Bednarz J, Rodokanaki-von Schrenck A, Engelmann K. Different characteristics of endothelial cells from central and peripheral human cornea in primary culture and after subculture. In Vitro Cell Dev Biol Anim 1998;34:149–153.
22 Yamagami S, Yokoo S, Mimura T et al. Distribution of precursors in human corneal stromal cells and endothelial cells. Ophthalmology 2007;114:433–439.
23 Whikehart DR, Parikh CH, Vaughn AV et al. Evidence suggesting the existence of stem cells for the human corneal endothelium. Mol Vis 2005;11:816–824.
24 McGowan SL, Edelhauser HF, Pfister RR et al. Stem cell markers in the human posterior limbus and corneal endothelium of unwounded and wounded corneas. Mol Vis 2007;13:1984–2000.
25 Pels L. Organ culture: The method of choice for preservation of human donor corneas. Br J Ophthalmol 1997;81:523–525.
26 Pipparelli A, Thuret G, Toubeau D et al. Pan-corneal endothelial viability assessment: Application to endothelial grafts predissected by eye banks. Invest Ophthalmol Vis Sci 2011;52:6018–6025.
27 Senoo T, Joyce NC. Cell cycle kinetics in corneal endothelium from old and young donors. Invest Ophthalmol Vis Sci 2000;41:660–667.
28 He Z, Campolmi N, Ha Thi BM et al. Optimization of immunolocalization of cell cycle proteins in human corneal endothelial cells. Mol Vis 2011;17:3494–3511.
29 Hogan MJ, Alvarado JA, Weddell JS. Histology of the Human Eye: An Atlas and Text. Philadelphia: W.B. Saunders, 1971:102–103.
30 Dua HS, Shanmuganathan VA, Powell-Richards AO et al. Limbal epithelial crypts: A novel anatomical structure and a putative limbal stem cell niche. Br J Ophthalmol 2005;89:529–532.
31 Shortt AJ, Secker GA, Munro PM et al. Characterization of the limbal epithelial stem cell niche: Novel imaging techniques permit in vivo observation and targeted biopsy of limbal epithelial stem cells. Stem Cells 2007;25:1402–1409.
32 Barrandon Y. Crossing boundaries: Stem cells, holoclones, and the fundamentals of squamous epithelial renewal. Cornea 2007;26: S10–S12.
33 Majo F, Rochat A, Nicolas M et al. Oligopotent stem cells are distributed throughout the mammalian ocular surface. Nature 2008;456: 250–254.
34 Kulkarni BB, Tighe PJ, Mohammed I et al. Comparative transcriptional profiling of the limbal epithelial crypt demonstrates its putative stem cell niche characteristics. BMC Genomics 2010;11:526.
35 Du Y, Funderburgh ML, Mann MM et al. Multipotent stem cells in human corneal stroma. Stem Cells 2005;23:1266–1275.
36 Vrabec F. Age changes of the inner surface of the trabecular meshwork shown by the replica technique. Invest Ophthalmol 1974;13: 950–953.
37 Inaba K, Tanishima T, Hirosawa K. Electron microscopic observations of Descemet's membrane of peripheral cornea. Jpn J Ophthalmol 1986;30:1–13.
38 Raviola G. Schwalbe line's cells: A new cell type in the trabecular meshwork of *Macaca mulatta*. Invest Ophthalmol Vis Sci 1982;22: 45–56.
39 Vrabec F. Studies on the corneal and trabecular endothelium. II. Endothelium of the zone of transition. Br J Ophthalmol 1958;42: 667–673.
40 Bunting KD. ABC transporters as phenotypic markers and functional regulators of stem cells. Stem Cells 2002;20:11–20.
41 Budak MT, Alpdogan OS, Zhou M et al. Ocular surface epithelia contain ABCG2-dependent side population cells exhibiting features associated with stem cells. J Cell Sci 2005;118:1715–1724.
42 Pesce M, Scholer HR. Oct-4: Gatekeeper in the beginnings of mammalian development. Stem Cells 2001;19:271–278.
43 Zangrossi S, Marabese M, Broggini M et al. Oct-4 expression in adult human differentiated cells challenges its role as a pure stem cell marker. Stem Cells 2007;25:1675–1680.
44 Reis-Filho JS, Schmitt FC. Taking advantage of basic research: p63 is a reliable myoepithelial and stem cell marker. Adv Anat Pathol 2002; 9:280–289.
45 Scadden DT. The stem-cell niche as an entity of action. Nature 2006; 441:1075–1079.
46 Discher DE, Mooney DJ, Zandstra PW. Growth factors, matrices, and forces combine and control stem cells. Science 2009;324:1673–1677.
47 Ekshyyan O, Aw TY. Decreased susceptibility of differentiated PC12 cells to oxidative challenge: Relationship to cellular redox and

expression of apoptotic protease activator factor-1. Cell Death Differ 2005;12:1066–1077.
48 Gain P, Thuret G, Chiquet C et al. In situ immunohistochemical study of Bcl-2 and heat shock proteins in human corneal endothelial cells during corneal storage. Br J Ophthalmol 2001;85:996–1000.
49 Kim HS, Jun Song X, de Paiva CS et al. Phenotypic characterization of human corneal epithelial cells expanded ex vivo from limbal explant and single cell cultures. Exp Eye Res 2004;79:41–49.
50 Shanmuganathan VA, Rotchford AP, Tullo AB et al. Epithelial proliferative potential of organ cultured corneoscleral rims; implications for allo-limbal transplantation and eye banking. Br J Ophthalmol 2006;90:55–58.
51 Summerlin W, Miller G, Harris J et al. The organ-cultured cornea: An in vitro study. Invest Ophthalmol Vis Sci 1973;12:176–180.
52 Rijneveld WJ, Beekhuis WH, van Rij G et al. Clinical comparison of grafts stored in McCarey-Kaufman medium at 4°C and in corneal organ culture at 31°C. Arch Ophthalmol 1992;110:203–205.
53 Frueh BE, Bohnke M. Prospective, randomized clinical evaluation of Optisol vs organ culture corneal storage media. Arch Ophthalmol 2000;118:757–760.
54 Thuret G, Chiquet C, Bernal F et al. Prospective, randomized clinical and endothelial evaluation of 2 storage times for cornea donor tissue in organ culture at 31 degrees C. Arch Ophthalmol 2003;121:442–450.
55 Thuret G, Manissolle C, Campos-Guyotat L et al. Animal compound-free medium and poloxamer for human corneal organ culture and deswelling. Invest Ophthalmol Vis Sci 2005;46:816–822.
56 Nejepinska J, Juklova K, Jirsova K. Organ culture, but not hypothermic storage, facilitates the repair of the corneal endothelium following mechanical damage. Acta Ophthalmol 2010;88:413–419.
57 Senoo T, Obara Y, Joyce NC. EDTA: A promoter of proliferation in human corneal endothelium. Invest Ophthalmol Vis Sci 2000;41:2930–2935.
58 Mimura T, Joyce NC. Replication competence and senescence in central and peripheral human corneal endothelium. Invest Ophthalmol Vis Sci 2006;47:1387–1396.
59 Patel SP, Bourne WM. Corneal endothelial cell proliferation: A function of cell density. Invest Ophthalmol Vis Sci 2009;50:2742–2746.
60 Slettedal JK, Lyberg T, Roger M et al. Regeneration with proliferation of the endothelium of cultured human donor corneas with extended postmortem time. Cornea 2008;27:212–219.
61 Svedbergh B, Bill A. Scanning electron microscopic studies of the corneal endothelium in man and monkeys. Acta Ophthalmol (Copenh) 1972;50:321–336.
62 Aptel F, Olivier N, Deniset-Besseau A et al. Multimodal nonlinear imaging of the human cornea. Invest Ophthalmol Vis Sci 2010;51:2459–2465.
63 Johnson DH, Bourne WM, Campbell RJ. The ultrastructure of Descemet's membrane. I. Changes with age in normal corneas. Arch Ophthalmol 1982;100:1942–1947.
64 Egan CA, Savre-Train I, Shay JW et al. Analysis of telomere lengths in human corneal endothelial cells from donors of different ages. Invest Ophthalmol Vis Sci 1998;39:648–653.
65 Zhu C, Rawe I, Joyce NC. Differential protein expression in human corneal endothelial cells cultured from young and older donors. Mol Vis 2008;14:1805–1814.


See www.StemCells.com for supporting information available online.

ARTICLE II: Optimization of immunolocalization of cell cycle proteins in human corneal endothelial cells.

Molecular Vision 2011; 17:3494-3511 <http://www.molvis.org/molvis/v17/a376>
Received 12 December 2011 | Accepted 26 December 2011 | Published 29 December 2011

© 2011 Molecular Vision

Optimization of immunolocalization of cell cycle proteins in human corneal endothelial cells

Zhiguo He,[1] Nelly Campolmi,[1] Binh-Minh Ha-Thi,[1] Jean-Marc Dumollard,[1,2] Michel Peoc'h,[1,2] Olivier Garraud,[3] Simone Piselli,[1] Philippe Gain,[1] Gilles Thuret[1]

[1] "Biology, Engineering and Imaging of Corneal Grafts" Laboratory JE2521, SFR143, Faculty of Medicine, University Jean Monnet, Saint-Etienne, France; [2] Eye Bank of Saint-Etienne, Auvergne Loire Blood Center, Saint-Etienne, France; [3] Department of Pathology, University Hospital of Saint-Etienne, Saint-Etienne, France

Purpose: En face observation of corneal endothelial cells (ECs) using flat-mounted whole corneas is theoretically much more informative than observation of cross-sections that show only a few cells. Nevertheless, it is not widespread for immunolocalization (IL) of proteins, probably because the endothelium, a superficial monolayer, behaves neither like a tissue in immunohistochemistry (IHC) nor like a cell culture in immunocytochemistry (ICC). In our study we optimized IL for EC of flat-mounted human corneas to study the expression of cell cycle-related proteins.

Methods: We systematically screened 15 fixation and five antigen retrieval (AR) methods on 108 human fresh or stored corneas (organ culture at 31 °C), followed by conventional immunofluorescence labeling. First, in an attempt to define a universal protocol, we selected combinations able to correctly localize four proteins that are perfectly defined in ECs (zonula occludens-1 [ZO-1] and actin) or ubiquitous (heterogeneous nuclear ribonucleoprotein L [hnRNP L] and histone H3). Second, we screened protocols adapted to the revelation of 9 cell cycle proteins: Ki67, proliferating cell nuclear antigen (PCNA), minichromosome maintenance 2 (MCM2), cyclin D1, cyclin E, cyclin A, $p16^{Ink4a}$, $p21^{Cip1}$ and $p27^{Kip1}$. Primary antibody controls (positive controls) were performed on both epithelial cells of the same, simultaneously-stained whole corneas, and by ICC on human ECs in in vitro non-confluent cultures. Both controls are known to contain proliferative cells. IL efficiency was evaluated by two observers in a masked fashion. Correct localization at optical microscopy level in ECs was define as clear labeling with no background, homogeneous staining, agreement with previous works on ECs and/or protein functions, as well as a meaningful IL in proliferating cells of both controls.

Results: The common fixation with 4% formaldehyde (gold standard for IHC) failed to reveal 12 of the 13 proteins. In contrast, they were all revealed using either 0.5% formaldehyde at room temperature (RT) during 30 min alone or followed by AR with sodiumdodecyl sulfate or trypsin, or pure methanol for 30 min at RT. Individual optimization was nevertheless often required to optimize the labeling. Ki67 was absent in both fresh and stored corneas, whereas PCNA was found in the nucleus, and MCM2 in the cytoplasm, of all ECs. Cyclin D1 was found in the cytoplasm in a paranuclear pattern much more visible after corneal storage. Cyclin E and cyclin A were respectively nuclear and cytoplasmic, unmodified by storage. P21 was not found in ECs with three different antibodies. P16 and p27 were exclusively nuclear, unmodified by storage.

Conclusions: IL in ECs of flat-mounted whole human corneas requires a specific sample preparation, especially to avoid overfixation with aldehydes that probably easily masks epitopes. En face observation allows easy analysis of labeling pattern within the endothelial layer and clear subcellular localization, neither of which had previously been described for PCNA, MCM2, or cyclin D1.

The corneal endothelium functions as a permeability barrier that restricts the movement of water and solutes into the hydrophilic stroma to control corneal transparency [1]. It is composed of a monolayer of flat (approximately 5 µm) tessellated joint cells forming a mosaic of mainly hexagonal elements (Figure 1). In the adult human, the proliferative capacities of endothelial cells (ECs) are practically nil and cannot offset cell losses in physiologic or pathological cases. Indeed, no increase in EC number has been clinically documented. Although in physiologic conditions the number of ECs decreases very slowly, by about 0.6% per year during adulthood [2,3], this pace accelerates dramatically in several corneal diseases (mainly Fuchs' dystrophy, the most frequent endothelial primary dystrophy) and after accidental or surgical traumatisms: endothelial cell density (ECD) falls below a threshold of 300 to 500 cells/mm^2 (depending on the kinetics of loss) and an irreversible corneal edema occurs, causing permanent visual loss. During corneal storage by eye banks, be it in short-term cold storage at 4 °C in Optisol or in long-term storage at 31 °C to 34 °C in organ culture (OC) media, EC loss also accelerates strongly, causing a decrease in graft quality. In the past two decades Joyce and colleagues

Correspondence to: Professor Gilles Thuret, "Biology, Engineering and Imaging of Corneal Grafts" Laboratory, JE2521, IFR 143, Faculty of Medicine, 15, rue Ambroise Paré, F 42023 Saint-Etienne Cedex 2, France; Phone: +33 (0)4 77 12 77 93; FAX: +33 (0)4 77 12 09 95; email: gilles.thuret@univ-st-etienne.fr

Molecular Vision 2011; 17:3494-3511 <http://www.molvis.org/molvis/v17/a376> © 2011 Molecular Vision

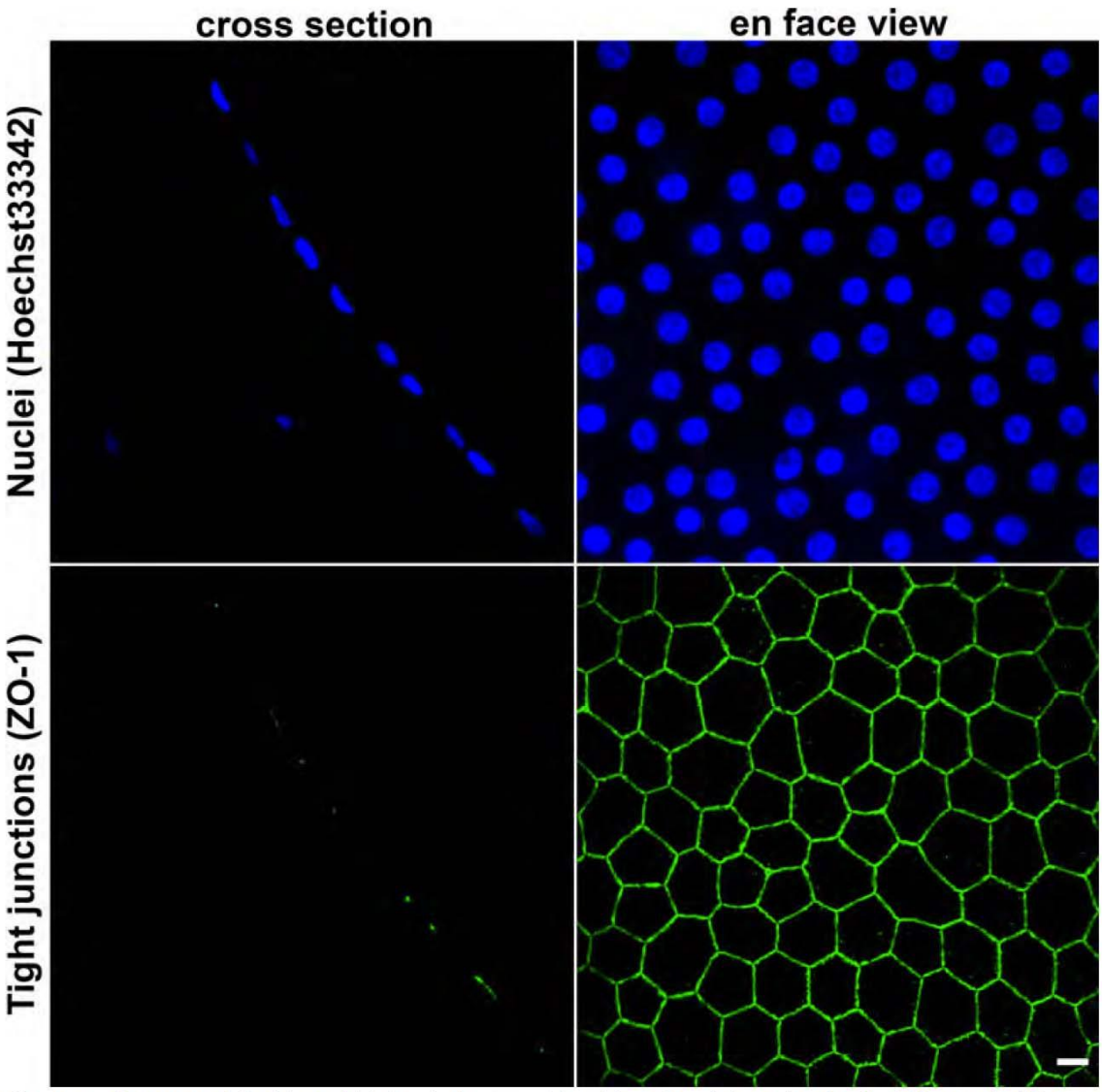


Figure 1. Hoechst 33342 nuclei staining and tight-junction immunostaining with zonula occludens-1 (ZO-1) antibody illustrate the differences between conventional immunohistochemistry on a corneal cross-section where only a few endothelial cells are partially visible, and en face view showing a wide field of intact cells. Original magnification 40×. Bar 10 µm.

have highlighted, mainly based on proteomic studies, that adult ECs in vivo are arrested in the G_1 phase of the cell cycle (reviewed in [4]). However in parallel, they also demonstrated, with other, that ECs retain proliferative capacity [5] even in the elderly, but with an age-related decrease [6,7]. Primary EC cultures from adult donors of all ages can also be routinely obtained in vitro [8].

Stimulation and control of EC proliferation would have high therapeutic impact, making it possible to increase ECD directly in vivo in patients with low ECD and to improve the quantity and quality of donor corneas by increasing ECD ex vivo during storage in eye banks, or by facilitating large-scale development of bioengineered endothelial grafts. Identification of the proteins involved in cell cycle arrest is key to these future endothelial cell therapies.

Molecular Vision 2011; 17:3494-3511 <http://www.molvis.org/molvis/v17/a376> © 2011 Molecular Vision

Immunolocalization (IL) of proteins has been previously used, as a basic tool, on corneal endothelium. Generally, EC can be observed either on corneal cross-sections or on flat-mounts, as the EC monolayer of 300,000 to 400,000 tessellated cells on the innermost face of the cornea is easily visible by en face observation. Although standard immunohistochemistry (IHC) on corneal cross-sections is the prevalent method in the literature, it allows visualization of only a few cells, not a complete view of the unmodified endothelium (Figure 1). Moreover, it does not always give a clear subcellular localization of proteins of interest, a condition required for a proper interpretation [9]. On the contrary, IL on flat-mounted corneas theoretically appears far more informative. It gives access to the whole intact tissue with a possibility to detect regional differences in expression patterns (for example a centripetal gradient) as well as to detect rare isolated cells among an apparently homogeneous cell population. Nevertheless, to date it has been used in very few studies and for few proteins. Moreover, in the only paper reporting the use of both cross-sections and flat-mounts with the same antibodies, immunostaining was not identical, with generally fewer positive results on flat-mounts [10].

In the present study, we systematically screened immunostaining protocols to select those able to correctly reveal proteins in ECs of intact flat-mounted corneas. Fixation and antigen retrieval (AR) are two fundamental steps in all immunostaining processes. They strongly influence the ability of specific antibodies to recognize their targets (retention of antigenicity) while offering good preservation of ultrastructure. Cross-linking fixatives (aldehydes) act by creating covalent chemical bonds between proteins, mainly between lysine residues [11]. They also anchor soluble proteins to the cytoskeleton. Formaldehyde is the most common fixative in histology. Four percent formaldehyde (equivalent to the neutral-buffered formalin (10%) used for clinical pathology) appears as a gold standard in most studies, including those on corneal endothelium. Precipitating, also called denaturing, fixatives (ethanol, methanol, and acetone) reduces the solubility of proteins and disrupts the hydrophobic interactions involved in the tertiary structure of proteins. They are commonly used for immunocytochemistry (ICC), alone or in combination. Metallic fixatives, which denature the proteins and create weak bonds between them, are rarely employed alone in ICC or IHC. Nevertheless, $HgCl_2$ or $ZnCl_2$ containing formaldehyde solutions improve nuclear morphology with various effects on antigenicity [12]. AR, either by heating in specific buffers, enzymatic digestion or chemical reagents, helps unmask certain hidden epitopes. It can be helpful or even crucial during IHC of formalin-fixed paraffin-embedded tissues [13]. Heat-induced antigen retrieval (HIAR), known to hydrolyse protein cross-linking that occurred during aldehyde fixation (but not only [14]), is the most common AR technique [15], but enzymatic digestion by trypsin that cleaves peptide chains mainly at the carboxyl side of lysine, and protein denaturants like sodium dodecyl sulfate (SDS) and urea, have also been used.

In this study, we present optimization of fixation and antigen retrieval (AR) methods for ECs of flat-mounted whole human corneas, and results obtained on a very large series of corneas for IL of proteins involved in cell cycle control.

METHODS

Human corneas: Corneas were retrieved by in situ excision, the routine method for clinical use. Fifty corneas were obtained from the Department of Anatomy of the Faculty of Medicine of Saint-Etienne (body donation to science). Bodies were refrigerated at 4 °C in conditions comparable with those used for donation for clinical use. Donor age (mean±standard deviation, range, median) was 81±11 years, (46 to 99, 82), and time from death to procurement was 27±14 h (7 to 48, 23). They were fixed immediately after procurement and further processed (group 1 of fresh corneas). Seventy-six other corneas were obtained from the Eye Bank of Saint-Etienne, Saint-Etienne, France. They were not suitable for corneal graft because of inconclusive donor serologies, but had a normal endothelium. They were stored in OC at 31 °C for 25±9 days (7 to 35, 27) in CorneaMax medium (Eurobio, Les Ulis, France) before fixation and processing for immunostainings (group 2 of stored corneas). Donor age was 73±12 years (42 to 94, 76), and death-to-procurement time always less than 24 h (13±6 h (4 to 24, 12). Handling of the donor tissues adhered to the tenets of the Declaration of Helsinki of 1975 and its 1983 revision in protecting donor confidentiality.

Primary endothelial cell cultures: Using eight OC corneas from the group described above, ECs were isolated and cultured according to protocols published elsewhere [8]. Briefly, Descemet's membrane with the attached ECs was retrieved under a dissecting microscope, and incubated in 0.2 mg/ml EDTA in Hanks' balanced salt solution (Eurobio), pH 7.4, for 1 h at 37 °C. After centrifugation, cells were resuspended in OPTIMEM-1 (Invitrogen Life technologies, St-Aubin, France) supplemented with 8% fetal bovine serum (Eurobio), 40 ng/ml of fibroblast growth factor, 5 ng/ml of epidermal growth factor, 20 ng/ml of nerve growth factor (the three from Invitrogen), 20 mg/ml of ascorbic acid, 0.005% human lipids, 200 mg/l of calcium chloride, 0.08% chondroitin sulfate, 1% RPMI-1640 multiple vitamin solution, and 50 mg/ml gentamicin (the last six from Sigma, St Quentin Fallavier, France). Cells were incubated in six-well tissue culture plates at 37 °C in a 5% carbon dioxide humidified atmosphere. Medium was changed every other day. After primary cultures reached confluence, cells were transferred to a non-precoated T25 flask and subcultured until confluence. Then, 2000 cells per well were seeded in non-precoated 96-well tissue culture plates and cultured until subconfluence before being used for ICC. These cultures were used as controls (see below).

Molecular Vision 2011; 17:3494-3511 <http://www.molvis.org/molvis/v17/a376> © 2011 Molecular Vision

Table 1. Fixation protocols and antigen retrieval methods assessed on whole corneas.

Number	Fixation protocols
1	4% formaldehyde*, in PBS, pH 7.45 30 min at 4 °C
2	0.5% formaldehyde*, in PBS, pH 7.45 30 min at 4 °C
3	4% formaldehyde*, in PBS, pH 7.45 30 min at RT
4	0.5% formaldehyde*, in PBS, pH 7.45 30 min at RT
5	100% methanol 30 min at −20 °C
6	100% methanol 30 min at RT
7	100% acetone 30 min at −20 °C
8	100% acetone/100% methanol (1:1 v/v) 30 min at −20 °C
9	100% acetone/100% methanol (1:1 v/v) 30 min at RT
10	Carnoy I** 30 min at −20 °C
11	Carnoy I** 30 min at RT
12	Bouin modified*** 45 min at RT
13	0.5% $Zn(OAc)_2$ + 0.5% $ZnCl_2$ + 0.05% $Ca(OAc)_2$ in 0.1M Tris base buffer 45 min at RT (Tris-Zinc)
14	$HgCl_2$ 6 g in formalin (37%–40%) 10 ml + distilled water 90 ml 45 min at RT
15	$ZnCl_2$ 0.16 g + PFA 4 g + NaCl 5 g in distilled water 100 ml 45 min at RT
Number	**Antigen retrieval methods**
1	0.1 M citrate buffer pH 6, 4 h at 55 °C§
2	0.01 M EDTA buffer pH 10, 4 h at 55 °C§
3	0.1% trypsin in PBS, 5 min at 37 °C
4	4 M urea in water, 4 h at RT
5	0.5% sodium dodecyl sulfate in water, 5 min at RT

PBS phosphate buffer saline; RT room temperature; * always made fresh from paraformaldehyde; **100% ethanol/100% acetic acid (3:1 v/v); ***75 ml picric acid saturated in water + 25 ml 4% PFA+5 ml acetic acid; § the highest temperature that did not induce shrinking of fixed corneas.

Study design: The work comprised two steps. First, we studied whether a universal corneal preparation existed for IL in ECs of flat-mounted corneas. We therefore chose four proteins known to be expressed by ECs independently of their proliferative status and localized in four different cell compartments. They were either perfectly characterized in human ECs or ubiquitous proteins: (1) zonula occludens-1 (ZO-1) is a peripheral membrane protein associated with tight junctions [16]; (2) actin is one of the most conserved cytoplasmic proteins in eukaryotes and is distributed in linear circumferential strands that form a hexagonal belt beneath plasmic membrane in ECs [17]; (3) heterogeneous ribonucleoprotein L (hnRNP L) is present in the nucleoplasm as part of the hnRNP complexes that play a major role in the formation, packaging, processing, and function of mRNA; (4) bound with DNA, histone H3 is one of the basic nuclear proteins responsible for the nucleosome structure of chromosomal fibers in eukaryotes.

Considering the large number of fixatives and AR methods to assess, a systematic experiment matrix was built to minimize the number of human corneas necessary. Fixatives and AR were chosen from the general histology and cytology literature [18,19] as well as from current laboratory practices. They were classified as shown in Table 1. To increase the number of experiments while minimizing the number of human corneas necessary, each cornea was cut into eight pie-shaped wedges before or after fixation. Fixatives were then successively assessed and preselected once correct localization seemed to be achieved. Also to reduce the number of corneas necessary, secondary controls and labeling controls (see below) were done only once a protocol had been preselected. When labeling of ECs and positives controls seemed specific in terms of localization but faint and/or non-homogeneous (not all cells), AR methods were assessed successively with the preselected fixative. In case of complete negativity for all fixation protocols, AR methods were assessed only with 0.5% formaldehyde fixation (which, during the previous experiments in the study, had proved to be the most efficient fixative overall).

Second, we applied the previously optimized protocols to 9 proteins involved in cell cycle control: three proteins known as proliferation markers (Ki67, proliferating cell nuclear antigen [PCNA], and mini chromosome maintenance protein 2 [MCM2]); five proteins involved in controlling cell cycle phase G_1 (cyclin D1, cyclin E, $p16^{INK4a}$ (p16), $p21^{WAF1/Cip1}$ (p21), and $p27^{Kip1}$ (p27)); and cyclin A for the S phase. All had previously been studied in human corneas, but only Ki67 and MCM2 on flat-mounted whole corneas. Protocols selected after step one were applied to each of the 9 target proteins. If staining proved unsatisfactory, the systematic selection process was applied from the beginning as in step one, excluding the fixatives and AR methods that consistenly had negative results during step one. Incubations with both primary antibodies were done successively, with three rinses in-between.

Immunolocalization on flat-mounted whole corneas: Corneas were rinsed in PBS before fixation. All tissues were fixed immediately after retrieval or after being removed from OC medium, as a delay between retrieval and fixation is detrimental for immunostaining results [11]. To increase the

Molecular Vision 2011; 17:3494-3511 <http://www.molvis.org/molvis/v17/a376> © 2011 Molecular Vision

Table 2. List of primary antibodies.

Target proteins	Animal source	Clonality	Laboratory	Reference	Dilution
ZO-1	mouse	monoclonal	Zymed, Carlsbad, CA	33–9100	1/200
actin	rabbit	polyclonal	Sigma, Saint Louis, MO	A2066	1/200
hnRNP L	mouse	monoclonal	Abcam, Cambridge, UK	ab6160	1/200
histone H3	rabbit	polyclonal	Abcam	ab1791	1/200
Ki67 clone MIB-1	mouse	monoclonal	Dako, Glostrup, Denmark	M7240	1/100
PCNA	rabbit	polyclonal	Abcam	ab18197	1/200
MCM-2	rabbit	polyclonal	Abcam	ab31159	1/200
*cyclin D1	rabbit	monoclonal	Abcam	ab16663	1/200
*cyclin D1	rabbit	polyclonal	Abcam	ab31450	1/200
cyclin E	rabbit	polyclonal	Abcam	ab7959	1/100
cyclin A	mouse	monoclonal	Abcam	Ab38	1/200
$p16^{INK4a}$	rabbit	polyclonal	Interchim, Fremont, CA	#RB-025-PABX	1/200
*$p21^{Cip/WAF1}$	mouse	monoclonal	Cell Signaling, Danvers, MA	#2946	1/200
*$p21^{Cip/WAF1}$	rabbit	polyclonal	Santa Cruz, Santa Cruz, CA	sc-397	1/200
*$p21^{Cip/WAF1}$	mouse	monoclonal	Zymed, San Francisco, CA	33–7000	1/200
$p27^{kip1}$	mouse	monoclonal	Sigma	P2092	1/200

*For cyclin D1 and p21, different antibodies were tested because of initial negative results.

number of experiments, each cornea was cut into eight pie-shaped wedges before or after fixation, but we occasionally verified that the same results were observed for entire corneas (data not shown) to eliminate artifacts caused by the cut and border effects. Cell membranes were permeabilized by 1% Triton x-100 in PBS for 5 min at room temperature (RT) after fixation. This step was omitted when methanol, acetone or SDS was used, as they alter lipids by themselves. AR methods were then applied each time necessary (for details, see below). The non-specific binding sites were then saturated by incubation with goat serum for 30 min at 37 °C. Primary and secondary antibodies were diluted in PBS containing 2% BSA (BSA) and 2% goat serum. Primary antibodies were diluted in the same blocking buffer and incubated for 1 h at 37 °C. Corneal pieces were totally immersed in 100 µl of this solution in eppendorf microtubes to expose both endothelial and epithelial surfaces. Incubation with secondary antibodies diluted 1:500 in PBS containing 2% BSA and 2% goat serum was done for 45 min at 37 °C. Nuclei were finally counterstained with Hoechst 33342 (Sigma) 10 µg/ml in PBS at RT for 2 min. Three rinses in PBS were performed between all steps, except between saturation of non-specific protein binding sites and incubation with primary antibody. The corneal piece was finally placed on a glass slide, covered with PBS and gently flattened using a large glass coverslip retained by adhesive tape. Experiments were done at RT unless otherwise stated. Images were captured by a fluorescence inverted microscope IX81 (Olympus, Tokyo, Japan) equipped with the Cell^P imaging software (Soft Imaging System GmbH, Munster, Germany). This non-confocal microscope was chosen to obtain large-field images able to tolerate the residual tridimensional (3D) aspect of cell layers after flat-mounting.

The primary antibodies and their dilutions are listed in Table 2. Whenever possible, they were chosen from among antibodies validated for ICC by their manufacturers, which seemed closest to our technique. Non-specific rabbit and/or mouse IgG (ref 02–6102 and 02–6502, respectively; Zymed, Carlsbad, CA,) were used as primary antibodies for negative controls (i.e., secondary antibody control [20]). Complementarily, labeling control was performed by omitting primary and secondary antibodies, to identify potential autofluorescence. Secondary antibodies were Alexa Fluor 488 goat anti-mouse IgG or/and Alexa Fluor 555 goat anti-rabbit IgG (Invitrogen, Eugene, OR).

Controls for primary antibody specificity: To perform the equivalent of a primary antibody control [20] as an indicator for antibody specificity, immunostaining results in ECs of flat-mounted corneas were compared with those of two types of cells: epithelial cells of the same flat-mounted corneal piece, and primary cultures of ECs studied with ICC. Epithelial cells, known to form a highly proliferative layer during OC [21], served as positive controls for the whole process with predictable patterns of expression for proliferation markers and proteins involved in cell cycle control. Primary EC cultures served as positive controls of the same cell type, using conventional ICC techniques.

Molecular Vision 2011; 17:3494-3511 <http://www.molvis.org/molvis/v17/a376> © 2011 Molecular Vision

Immunocytochemistry on endothelial cell cultures: Nonconfluent cell cultures were rinsed in PBS and fixed with 4% formaldehyde in PBS at RT for 15 min without any subsequent AR. Permeabilization, saturation of the non-specific binding sites, immunoreactions, and counterstaining were performed as described above for flat-mounts.

Efficiency criterion: Protocols were deemed optimized once labeling exhibited correct localization at light microscopic level, with homogeneous staining, without zone effect (the first 100 µm near the cutting edges were excluded), and absence of staining in secondary antibody and labeling controls. Defining correct localization was easy for ZO-1, Actin, hnRNP L and histone H3. For the 10 cell cycle-related proteins, for which no absolute certainty existed, localization was considered correct when it agreed with their fundamental characteristics and by comparison with the staining patterns in epithelial cells and EC cultures (both primary antibody controls). Homogeneous staining was the last factor required. In case of equivalence between protocols in terms of specificity, the brightest staining was selected. Whatever the result (positive or negative), each combination was assessed on three independent corneas. The experiment was done twice more before a protocol was rated "optimized." Immunostainings were evaluated independently by two observers experienced in immunohistochemical assessment (Z.H., G.T.) on digital pictures blind to the preparation used. Subcellular localization, extent, homogeneity and intensity (signal/noise ratio) of immunostainings were considered. Intensity of staining was judged weak, moderate, or strong. In case of disagreement, a third judge (P.G.) reviewed the pictures.

RESULTS

Optimization of immulocalization:

ZO-1, actin, hnRNPL, and histone H3—Standard IHC fixation with 4% formaldehyde (at 4 °C or RT) gave unacceptable results for the four proteins: absence of staining for actin, very weak staining or heterogeneous pattern for hnRNPL and ZO-1, or aberrant pattern (cytoplasmic instead of nuclear) for H3. These results clearly demonstrated the need for optimization. Using systematic testing, we found several protocols that provided the expected localization for the four proteins in ECs and epithelial cells, at least for the most superficial layers (Figure 2 and Table 3). Results were similar for both fresh and stored corneas (data not shown). Moreover, results of each protocol, whether correct or not, were always coherent between endothelium and epithelium: no discrepancy (correct localization on one side with aberrant staining on the other) was ever observed, confirming that epithelium can serve as a primary antibody control. Negative controls (with irrelevant antibodies and without antibodies) remained constantly unstained. Fixation in pure methanol at RT for 30 min appeared the best compromise to localize the four proteins present in four different cell compartments, even if not optimal for both nuclear proteins. AR greatly improved H3 labeling.

Cell cycle-related proteins—Methanol for 30 min at RT, found to be the best compromise in the previous step, was not able to provide correct IL for the 10 proteins of interest, indicating that antibody/antigen specific preparations were probably necessary. Selected protocols are summarized in Table 4. There was no ubiquitous protocol but 0.5% formaldehyde alone was nevertheless usable for nine out of 10 cases, even if it was not optimal for four antibodies. Notably, 0.5% formaldehyde alone was the only solution for p21 and p27 antibodies. AR strongly improved immunostaininq quality (brightness and contrast) for PCNA, cyclin E, and p16. It was even the only efficient solution for cyclin A. Each time AR was necessary, it increased the risk of EC detachment from Descemet membrane, so fixation time was increased to 1 h to reduce this risk. As for ZO-1, Actin, hnRNPL, and H3, results of all assessed combinations were coherent between endothelial and epithelial cells of the same cornea. As we could not obtain cyclin D1 or p21 staining in ECs of flat-mounts with any of the protocols with the antibodies initially chosen, we assessed other antibodies using the same procedure. Staining of positive controls was always comparable between antibodies of the same target, using the same protocols. EC results are presented bellow.

For ICC on primary EC cultures, 4% formaldehyde gave reproducible correct IL for all proteins tested except for cyclin A, which required additional AR with 0.5% SDS in water for 5 min at RT.

Summary of optimized protocols obtained on flat-mounted whole corneas—Fixation with 0.5% formaldehyde at RT with or without AR was efficient for 12 antibodies/proteins out of 13, and considered as the best protocol for 10 out of them. Fixation with 0.5% formaldehyde alone for 30 min was efficient for 10 antibodies and considered as the best protocol for five antibodies. Two AR methods combined with 0.5% formaldehyde improved detection for four antibodies: 0.5% SDS in water at RT for 5 min and 0.1% trypsin in PBS at 37 °C for 5 min. Fixation with methanol alone was efficient for six antibodies, and considered as the best protocol for two antibodies.

Cell cycle protein expression:

Proliferation markers—We were first interested in analyzing the presence and localization of proliferation markers widely used in clinical histological studies, and selected Ki67, PCNA and MCM2 (Figure 3 and Table 5). Ki67 positive cells were not detected in ECs of whole corneas. A few positive cells were observed in the epithelium of fresh corneas with death-to-procurement time under 24 h. The number of Ki67 positive cells always increased dramatically in the epithelium of stored corneas. In in vitro ECs, Ki67 positive cells were numerous. Staining pattern characteristics of Ki67 were clearly visible in nuclei. Occasionally epithelial

Molecular Vision 2011; 17:3494-3511 <http://www.molvis.org/molvis/v17/a376> © 2011 Molecular Vision

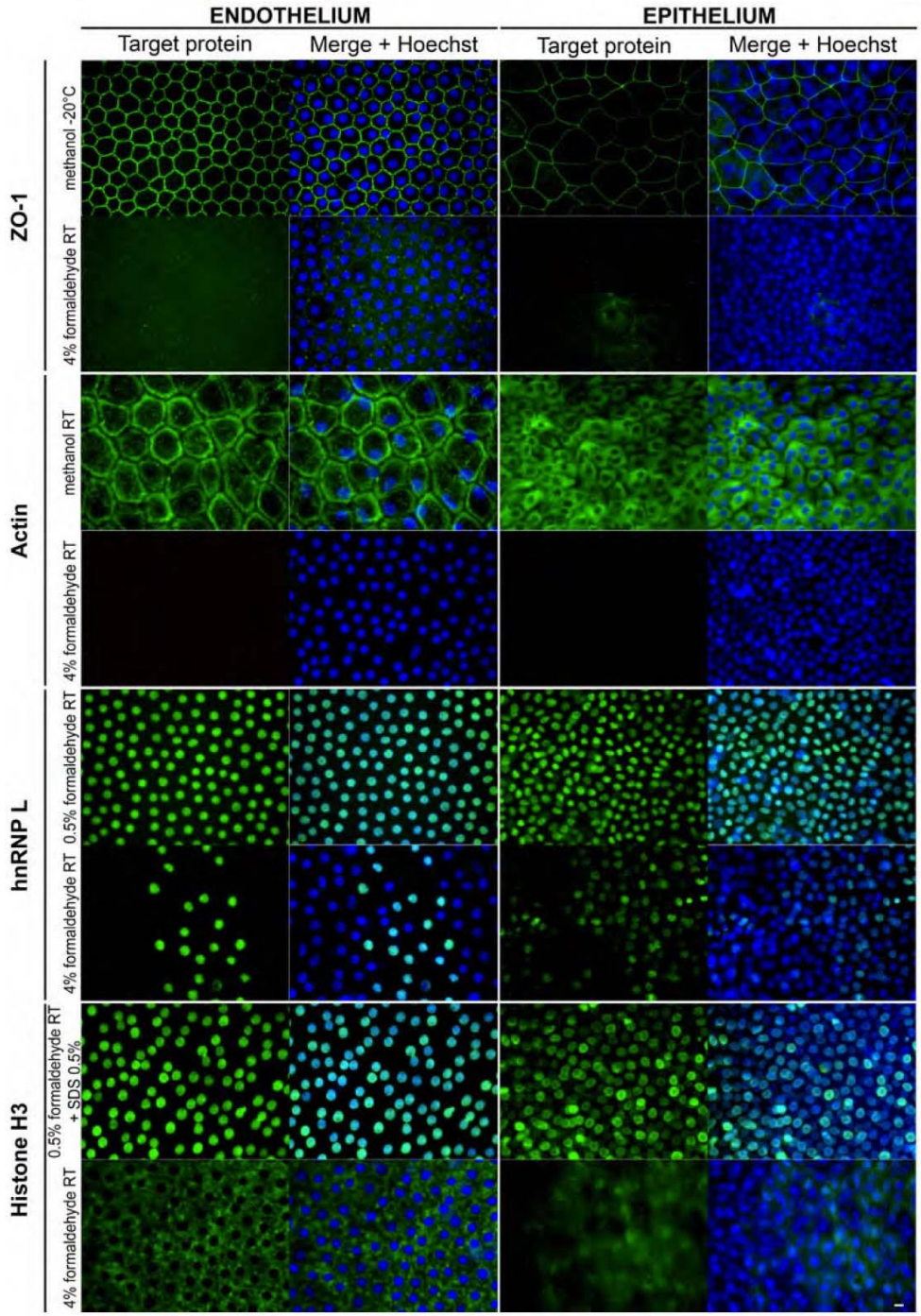


Figure 2. Optimization of immunolocalization of ZO-1, actin, hnRNP L, and histone H3 in endothelial cells on flat-mounted whole human corneas. Only the best combination is shown in the first line, compared with the 4% formaldehyde usually considered as the gold standard in immunohisto- and cytochemistry. Original magnification 40×. Bar 10 µm.

Molecular Vision 2011; 17:3494-3511 <http://www.molvis.org/molvis/v17/a376> © 2011 Molecular Vision

TABLE 3. OPTIMIZATION OF IMMUNOLOCALIZATION OF ZO-1, ACTIN, HNRNP L, AND HISTONE H3 IN ENDOTHELIAL CELLS ON FLAT-MOUNTED WHOLE HUMAN CORNEAS.

Target protein	Classification	Selected protocols
ZO-1	best	methanol at −20 °C
	second choice	methanol at RT; 0.5% formaldehyde at RT; Carnoy I at −20 °C
Actin	best	methanol at RT
	second choice	Carnoy I at −20 °C
hnRNP L	best	0.5% formaldehyde at RT
	second choice	methanol at RT
histone H3	best	0.5% formaldehyde + AR with 0.5% SDS in water 5 min at RT *
	second choice	methanol at RT

* SDS: Sodium dodecyl sulfate. In these cases fixation was prolonged during 1 h to avoid endothelial cell detachment induced by SDS with short time fixation. For all other cases, fixation during 30 min.

TABLE 4. OPTIMIZATION OF IMMUNOLOCALIZATION FOR CELL CYCLE-RELATED PROTEINS IN ENDOTHELIAL CELLS ON FLAT- MOUNTED WHOLE HUMAN CORNEAS.

Target protein	Classification	Selected protocols
Ki67	best	0.5% formaldehyde
	alternatives	4% formaldehyde; methanol
PCNA	best	0.5% formaldehyde 60 min at RT + AR with 0.5% SDS 5 min at RT
	alternatives	0.5% formaldehyde; methanol
MCM-2	best	0.5% formaldehyde
	alternatives	/
cyclin D1 (abcam 31450)	best	Carnoy I at −20 °C
	alternatives	0.5% formaldehyde
cyclin E	best	0.5% formaldehyde 60 min at RT + AR with 0.1% trypsin 5 min at 37 °C
	alternatives	0.5% formaldehyde
cyclin A	best	0.5% formaldehyde 60 min at RT + AR with 0.5% SDS 5 min at RT
	alternatives	/
P16	best	0.5% formaldehyde for 60 min at RT + AR with 0.5% SDS 5 min at RT
	alternatives	0.5% formaldehyde
P21 (cell signaling #2946)	best	0.5% formaldehyde
	alternatives	/
P27	best	0.5% formaldehyde
	alternatives	/

Fixation was at RT during 30 min, unless otherwise stated. /=absence of second choice protocol.

mitosis were observed, confirming completion of the cell cycle.

PCNA was essentially detected with an invariable signal in the nucleus of all ECs on both fresh and stored corneas and of in vitro ECs. Both nuclear and weak cytoplasmic expression was found in a few epithelial cells of fresh corneas. After storage, PCNA was detected in the nucleus of all epithelial cells.

The staining pattern of MCM2 differed totally in ECs and epithelial cells. It was mainly cytoplasmic in most of ECs of both fresh and stored corneas. It filled the lateral expansions of cytoplasm located at the basal Descemetic pole of ECs, giving a characteristic hairy aspect. MCM2 was preferentially detected in the nucleus of in vitro ECs, but cytoplasmic staining was also observed. In the epithelium, MCM2 was exclusively found in the nucleus of only a few cells on fresh corneas but in those of almost all cells on stored corneas.

G_1 and S phase markers—We next analyzed the presence and localization of cyclins involved in the G_1/S transition and S-phase, cyclin D1, cyclin E and cyclin A (Figure 4 and Table 5). The expression pattern of both cyclin D1 and cyclin E also differed totally in ECs and epithelial cells. Surprinsingly, with the monoclonal rabbit antibody (ab16663; Abcam) no staining was observed in ECs whatever the sample preparation. With the polyclonal rabbit antibody (ab31450; Abcam) cyclin D1 was absent or had dim paranuclear staining in fresh corneas' ECs, which increased, after storage. Nuclear and weak cytoplasmic staining was

Molecular Vision 2011; 17:3494-3511 <http://www.molvis.org/molvis/v17/a376> © 2011 Molecular Vision

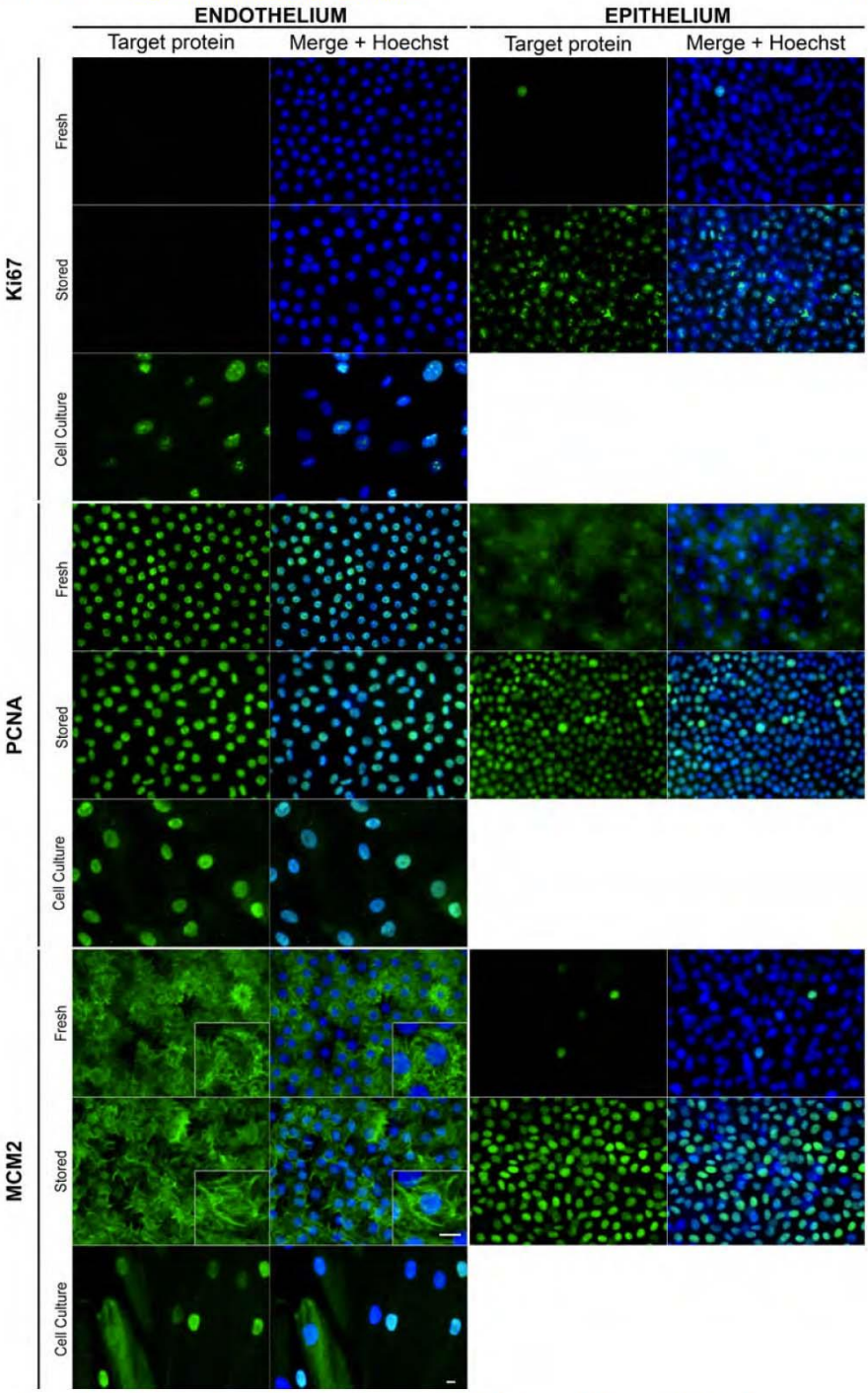


Figure 3. Optimized immunolocalization of proliferation markers in endothelial cells on flat-mounted whole human corneas. Only the best combination of fixative and epitope retrieval is shown for each antibody (see Table 4). Original magnification 40× except insets (96×). Bar 10 µm.

Molecular Vision 2011; 17:3494-3511 <http://www.molvis.org/molvis/v17/a376> © 2011 Molecular Vision

TABLE 5. SUBCELLULAR LOCALIZATION OF THE PROTEINS INVOLVED IN THE CELL CYCLE IN ENDOTHELIAL CELLS AND IN BOTH CONTROLS (IN VITRO ENDOTHELIAL CELLS AND EPITHELIAL CELLS OF WHOLE FLAT-MOUNTED CORNEAS).

	Endothelial cells			Epithelial cells	
Target protein	Fresh	Stored	In vitro cultures	Fresh	Stored
Ki67	A	A	N	N	N
PCNA	N	N	N, N+C	N, C, N+C	N
MCM2	C	C	N, N+C	N	N
cyclin D1	C	C	N, N+C	C, N+C	N
cyclin E	N	N	C	N, C, N+C	N, C, N+C
cyclin A	C	C	N, N+C	C	N, C, N+C
p16	N	N	N, C, N+C	N, C, N/C	C
p21	A	A	N	N, C	N
p27	N	N	N, C, N+C	N, C, N+C	N, C, N+C

A: absence of detection; N: nuclear; C: cytoplasmic, N+C: both nuclear and cytoplasmic.

found in in vitro ECs. In epithelium, with both antibodies, cytoplasmic localization was observed on fresh corneas. After storage, cyclin D1 had a predominant nuclear localization in almost all epithelial cells.

Cyclin E was homogeneously detected in the nucleus of all ECs on both fresh and OC corneas but exclusively in the cytoplasm of in vitro ECs. In contrast, in the epithelium it was heterogeneously detected either in the cytoplasm, the nucleus or both and OC seemed to increase nuclear staining.

Cyclin A was found in almost all ECs on both fresh and stored corneas with a cytoplasmic localization. Hexagonal cytoplamsic patterns were observed in ECs on fresh corneas. Nuclear staining was predominant in in vitro ECs. In the epithelium, cyclin A was mostly cytoplasmic on fresh corneas, but accumulated in the nucleus in numerous cells after storage.

Cell cycle inhibitors—We next analyzed the presence and localization of cyclin-dependent kinase inhibitors, p16, p21, and p27 (Figure 5 and Table 5).

p16, a Cdk4 and Cdk6 inhibitor that play a role at the G_1/S transistion was detected homogeneously in the nucleus of all ECs of both fresh and stored corneas. Weak cytoplasmic or both nuclear and cytoplasmic staining was observed in in vitro ECs as well as in epithelial cells on fresh corneas. After storage, the nuclear accumulation of p16 disappeared in all epithelial cells.

We found no p21, a Cdk1, and Cdk2 inhibitor, in ECs or in fresh or stored corneas, with any of the three antibodies assessed under the various sample preparations. Nevertheless, p21 was found in the nucleus of in vitro ECs in an identical manner with all three antibodies, but the best results were with the mouse monoclonal antibody (#2946; Cell Signaling). In epithelial cells, p21 was predominantly found in the cytoplasm of fresh corneas, with a particular granular pattern in the most superficial cells (especially with death-to-procurement time below 24 h). After storage, p21 was detected exclusively in the nucleus of epithelial cells.

p27, also a Cdk1 and Cdk2 inhibitor, was homogeneously detected in the nucleus of all ECs of both fresh and stored corneas. It was detected in both the nucleus and cytoplasm of in vitro ECs. In epithelial cells on fresh corneas, p27 was heterogeneously detected in cytoplasm, nuclei or both. Similarly to p21, cytoplasmic localization had a particular granular pattern in epithelial cells on fresh corneas with a short death-to-procurement time. After storage, p27 staining dramatically decreased and concerned only a few nuclei.

DISCUSSION

Through systematic testing, on a very large series of human corneas, of most of the fixatives and AR methods that we felt were applicable to the cornea, we determined the optimal preparations for several cell cycle control proteins.

Optimization of immunolocalization on flat-mounted whole corneas: Endothelial immunostaining on flat-mounted corneas offers many advantages over that done on conventional histological cross-sections, but requires adaptation of the usual protocols due to the specificities of the endothelium. IL on flat-mounted whole corneas (intact cell monolayer on intact tissue) possesses the characteristics of both IHC (tissue) and ICC (intact cells). Contrary to IHC, where the content of cross-sectioned cells is easily visible, membrane permeabilization is required for intact ECs of whole flat-mounted corneas to diffuse bulky antibodies and secondary labels. This may be achieved by certain fixatives alone (altering lipids) or require an additional step of membrane permeabilization. Moreover, while dangers of over- [11] and underfixation [22] have been highlighted for IHC on formalin-fixed tissue, they have not been discussed for a superficial cell layer such as ECs. These form a monolayer of cells that are strongly joined together but adhere

Molecular Vision 2011; 17:3494-3511 <http://www.molvis.org/molvis/v17/a376> © 2011 Molecular Vision

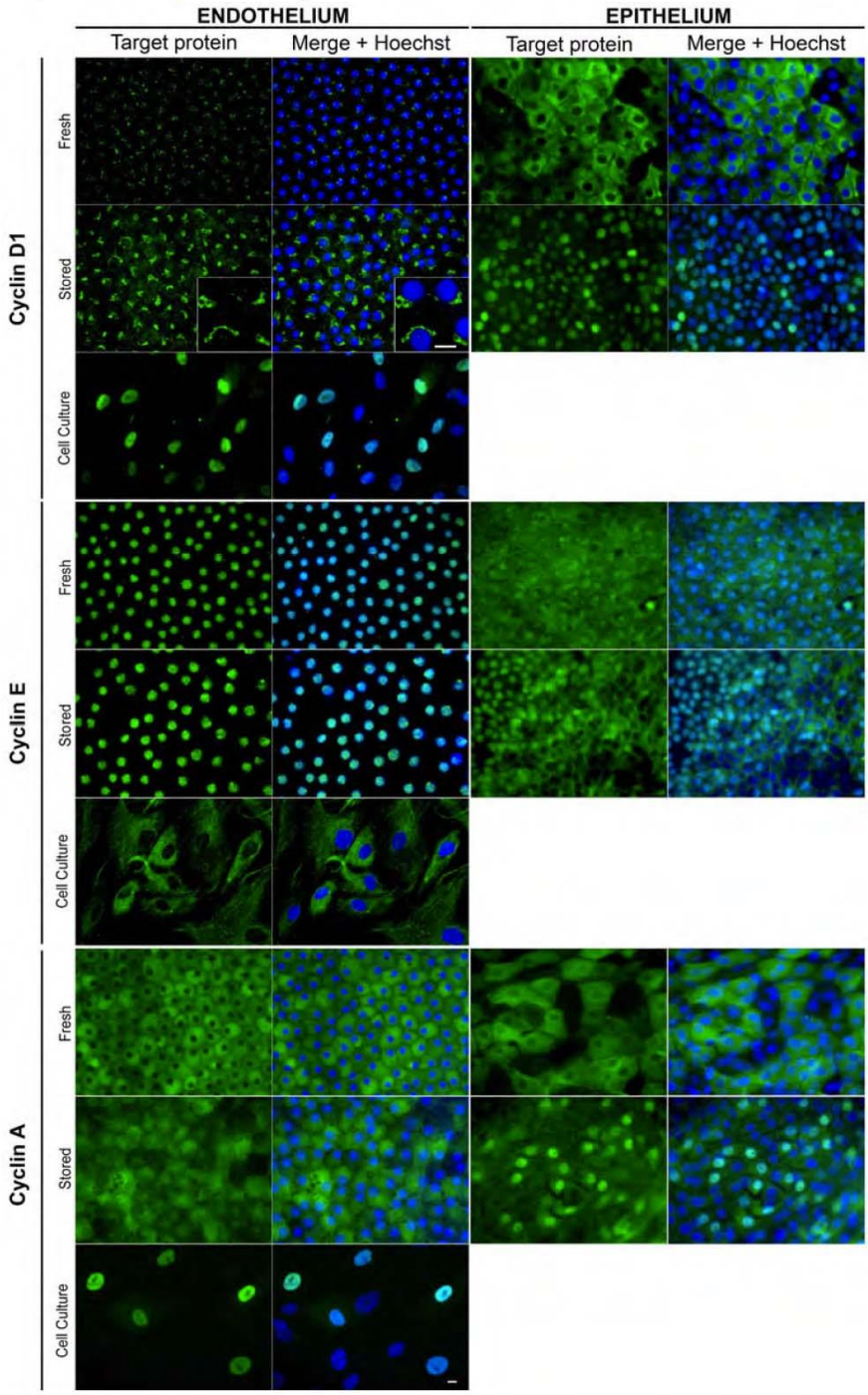


Figure 4. Optimized immunolocalization of cyclins D1, E, and A in endothelial cells on flat-mounted whole human corneas. Only the best combination of fixative and epitope retrieval is shown for each antibody (see Table 4). Original magnification 40× except insets (96×). Bar 10 µm.

Molecular Vision 2011; 17:3494-3511 <http://www.molvis.org/molvis/v17/a376> © 2011 Molecular Vision

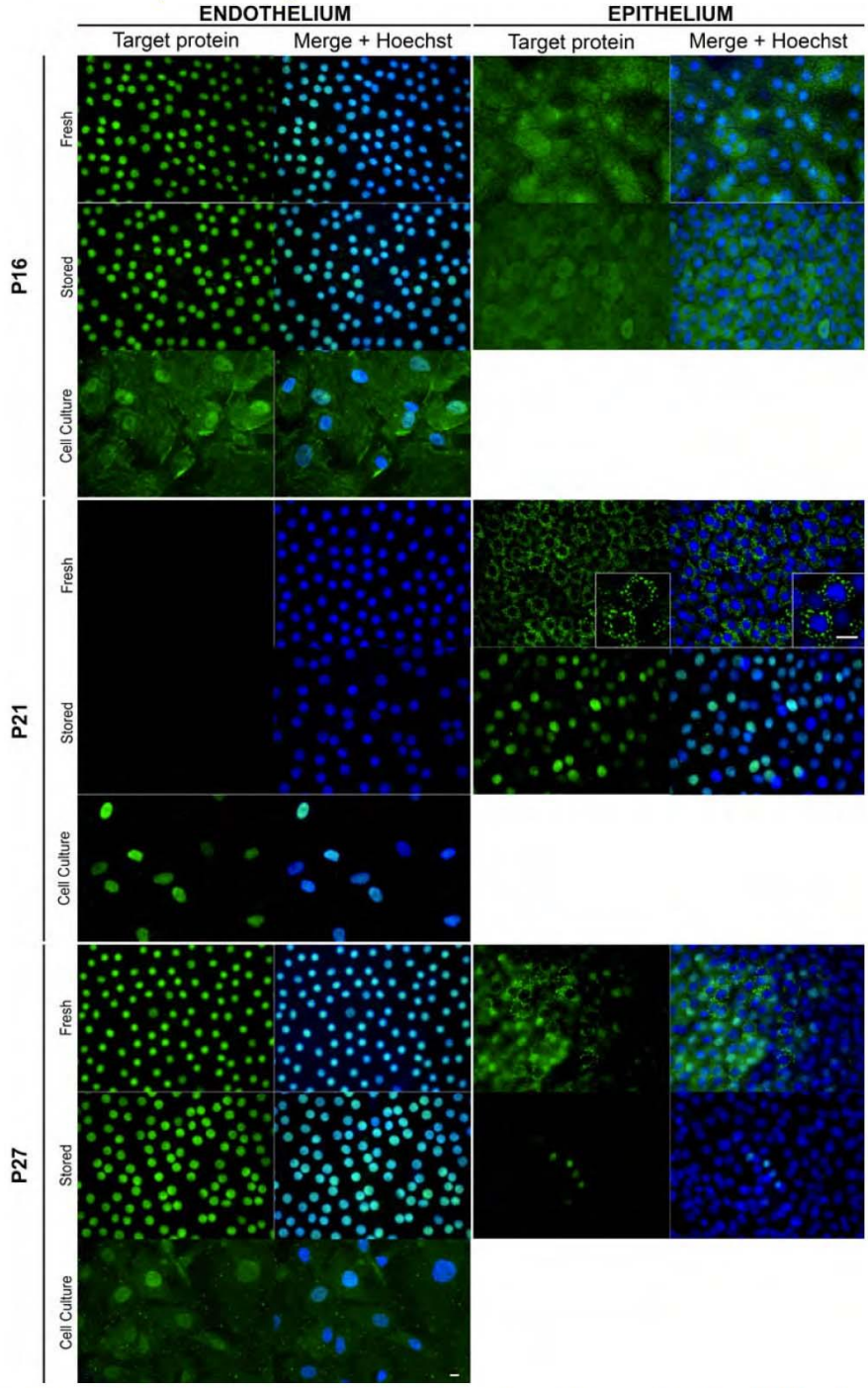


Figure 5. Optimized immunolocalization of three cyclin dependent kinase inhibitors p16, p21, and p27 in endothelial cells on flat-mounted whole human corneas. Only the best combination of fixative and epitope retrieval is shown for each antibody (see Table 4). Original magnification 40× except insets (96×). Bar 10 µm.

Molecular Vision 2011; 17:3494-3511 <http://www.molvis.org/molvis/v17/a376> © 2011 Molecular Vision

relatively poorly to their Descemet membrane. They withstand certain reagents better than cells cultured in vitro on slides, but less well than cells nested in tissue mass. To preserve the integrity of this fragile monolayer, we found a compromise between tissue fixation, permeabilisation of cell membranes to give access to antibodies, and restricted use of AR techniques, which, though useful, carry a high risk of cell detachment or tissue retraction, especially those involving high temperature. In particular, we showed that the most common fixation method, 4% formaldehyde, did not achieve correct localization of most of the proteins studied, irrespective of their cell compartment, probably because there is high and rapid cross-linking of antigenic targets in the directly acccesible superficial cells [23].

We did not find a universal protocol able to satisfactorily reveal all antigens in ECs. Nevertheless, we selected several efficient solutions that could help standardize immunostaining of ECs and facilitate inter-laboratory comparisons. Notably, 0.5% formaldehyde with or without AR or methanol at RT for 30 min are the three simplest and most efficient protocols, as all antigens tested seemed correctly localized by one or another of the protocols. The efficacy of a low concentration of formaldehyde had been described for immunostaining on cytologic preparations [18]. It seems therefore that overfixing was the main obstacle during IL on ECs of flat-mounted corneas.

Interestingly, AR with SDS greatly improved immunolocalization of the three nuclear proteins H3, PCNA, and P16. SDS is a detergent, used in the SDS–PAGE technique and DNA extraction, because it can disrupt non-covalent bonds between proteins, and between proteins and DNA, a property also useful for AR. Histone H3 is one of the proteic constituents of chromatin, while PCNA can be presented in chromatin-associated form [24], and P16 can directly interact with PCNA in nuclei [25]. Our data suggest that SDS enhanced staining quality after formaldehyde fixation by unmasking the epitopic fragments of histone H3 or PCNA, which are probably hidden by their physical interaction with DNA.

We used two complementary positive controls for primary antibodies [20]: epithelial cells of the same cornea, observed at the same time on the opposite side of the flat-mount, and human corneal EC in primary cultures. Both were useful to distinguish negative staining of EC due to absence of expression or due to an unadapted protocol. Observation of the epithelial layer was particularly useful because it was submitted to exactly the same preparation as EC, as corneal pieces were entirely immersed in the different solutions. The difficulty relating to the multilayered organization of the corneal epithelium was taken into account during interpretation. Use of a non-confocal microscope was in this respect an advantage, as we could observe two or three layers of cells at the same time. In vitro ECs did not behave in the same way: stronger fixation (4% formalhedyde) was necessary to avoid cell detachment during the rest of the process. Why 4% formaldehyde allows perfect localization in in vitro ECs and not in situ, where a lesser concentration (0.5%) is far more appropriate, remains unclear. The surface coating layer present in vivo on top of the EC plasma membrane, comprising, among other molecules, membrane proteins, proteoglycans and glycoproteins [26] may form after 4% formaldehyde fixation, a layer relatively impermeable to most of the antibodies.

Expression of the ten cell cycle proteins: To the best of our knowledge, investigation of a large range of proteins involved in the cell cycle had never been performed in fresh human corneas fixed immediately after procurement in donors, without being stored before study. Only Ki67 (clone SP6; Labvision, Fremount, CA) and PCNA (clone PC 10; Dako, Glostrup, Denmark) had been studied on 4% PFA-fixed cross-sections of fresh corneas, but with extended postmortem time (29 to 163 h) [27] and only PCNA on cross-sections of fresh corneas (postmortem time not available) [28]. Modifications in protein expression profile induced by any storage medium (4 °C or OC), even when storage is short, cannot be ruled out. By avoiding this storage time, one is sure to stay as close as possible to physiologic conditions, except for the postmortem metabolic changes that inevitably also occur. Only the study of corneas retrieved from enucleated globes for posterior tumor would ensure true physiologic conditions, but these cases are fortunately scarce and do not provide a sufficient source of human tissue.

We compared fresh corneas with similar corneas after several weeks of storage in OC and highlighted several differences never described before. Conventional OC media are derived from Dulbecco's modified Eagles minimum essential medium supplemented with 2% FCS necessary to ensure EC survival up to 5 weeks. They also stimulate wound healing by cell migration and enlargement [29] but are not known to stimulate EC proliferation. Only in a very specific OC medium containing 8% FCS has EC proliferation been described in situ [27,28]. On the contrary, non-confluent in vitro cultures of human adult ECs contain numerous proliferating cells, explaining a profile totally different from EC in situ. Overall, the profile of cultured ECs is very similar to that of epithelial cells after OC, both being used as primary antibody controls [20]. During OC, the epithelial layer is highly activated and may completely regenerate even after long death-to-retrieval time [21]. Nevertheless, although cells proliferate, the number of cell layers gradually decreased during OC [30], explaining why we observed mainly basal cells where higher proliferative activity occurs. In this article, we have described both a method for systematically assessing antibodies on whole mount en face cornea, and staining patterns for a set of antibodies directed against cell-cycle proteins. We are well aware that the use of a single technique does not allow for definitive interpretation of data, and that

Molecular Vision 2011; 17:3494-3511 <http://www.molvis.org/molvis/v17/a376> © 2011 Molecular Vision

additional primary antibody controls should be added. Several methods could be applicable to ECs, such as immunostaining after knocking down the specific protein expression with siRNA, a combination of immunostaining and fluorescent in situ hybridization, or immunoblots, and will be the subjects for future studies, as they require substantial technical developments. The following interpretation of our data should therefore be seen as open avenues for further investigations.

The Ki67 antibody was originally identified as a reliable marker for a nuclear antigen present in proliferating cells, from late G1 to M phase, and is therefore approved as a ubiquitous proliferation marker [31,32]. As expected, no Ki67 staining was observed in ECs of fresh and stored corneas, whereas it was abundant in epithelial cells and in vitro ECs, two situations where cells proliferate. Ki67 positive ECs and even mitosis have previously been described on wholemounts of human corneas, with clone MIB-1 by Zymed (San Francisco, CA), in experiments of wound healing in presence of 10% FBS and growth factors [33]. In this study, corneal pieces were fixed for 10 min in ice-cold methanol and incubated in 1% Triton X-100 to permeabilize the cells. We also found methanol to be a possible fixative for Ki67, but 0.5% formaldehyde without subsequent cell permeabilization seemed better. From the Ki67 pattern, it appears that whereas the epithelium is highly proliferative in OC, the endothelium is devoid of proliferating cells either in fresh or in stored corneas.

PCNA is another proliferation marker in a wide variety of cell types whose accumulation in the nucleus begins early in the G1 phase. It is a cofactor of DNA polymerase delta [34] but also has numerous other functions in response to DNA damage, cell cycle control, chromatin assembly and cohesion, and in other functions [24]. In ECs, PCNA had only been studied on cross-sections [27,28]: PCNA positive ECs were found in long-term OC corneas but not in fresh corneas [28]. On the contrary, we observed homogeneous nuclear PCNA staining in all ECs of fresh and stored corneas, indicating that PCNA may not be considered as a proliferation marker in this population, whereas staining was more typical in epithelial cells with an increase of nuclear staining after OC. The role of PCNA in ECs remains however to be determined but could be related to nuclear oxidative DNA damage that accumulates in ECs throughout their life [35]. Furthermore, there could be a relationship with the ubiquitous nuclear localization of p16 that we found in ECs of fresh and stored corneas, as p16 can interact directly with PCNA and inhibit DNA polymerase delta activity [25].

MCM2–7 are highly conserved proteins, which form a hexameric complex with replicative helicase activity [36] involved in the regulation of DNA duplication [37]. MCM2 is undetectable in G_0, and accumulates in the nucleus during G_1, peaking on S-phase entry [38], which explains its role as a proliferation marker. MCM2 is then eliminated from the nucleus during the S phase. In ECs in situ, we found no nuclear MCM2 but dense fibrillary cytoplasmic staining, unmodified after storage. The irregular shape of ECs was due simply to the filling by fluorescent markers of the irregular basolateral cytoplasmic expansions previously described [39,40]. In contrast, MCM2 was always detected exclusively in nuclei of the proliferative epithelial cells and preferentially in nuclei of in vitro ECs. Incidentally, a similar pattern in cultured ECs had already been described [41]. Interestingly, the sequestration of MCM proteins in cytoplasm and therefore the inability of MCM to initiate DNA synthesis is one of the mechanisms by which progesterone inhibits estrogen-induced uterin epithelial cell proliferation [42]. We propose that MCM2 sequestration in ECs could play a role in G_1-phase arrest. Nuclear localization of MCM2 had previously been described in nuclei of ECs using corneal pieces fixed for 10 min in ice-cold methanol and incubated in 1% Triton X-100 to permeabilize the cells (MCM2 antibody; BD PharMingen, San Diego, CA) [7]. In the latter experiments, designed to analyze proliferation in response to a calibrated wound, corneas initially stored at 4 °C for several days were subsequently incubated at 37 °C in culture medium supplemented with 8% FCS and various growth factors. MCM2 positive nuclei were observed between 36 to 72 h after wounding and only in ECs close to the wound. These results do not contradict our own, since our OC conditions differ greatly from these proliferation-promoting conditions. In our hands, only 0.5% formaldehyde was able to make the Abcam MCM2 antibody react. Methanol did not help reveal cytoplasmic MCM2.

Cyclins and their catalytic partner cyclin-dependent kinases (CDKs), regulate cell cycle progression in eukaryotes. The three D cyclins (D1, D2, D3) accumulate during G_1 phase in response to mitogenic stimulation, and assemble with CDK4 and 6. Cyclin D1 is an important actor in G_1 to S progression by inactivating the cell cycle-inhibiting functions of the retinoblastoma protein through phosphorylation. In addition, cyclin D/CDK complexes sequester CDK inhibitors such as p21 and p27. Nevertheless, once assembled with CDK within the cytoplasm, complexes need to be imported into the nucleus to be active. For example, it has been demonstrated that the prevention of their nuclear import plays a critical role in the maintenance of cardiomyocytes in their non-proliferative state acquired soon after birth [43]. It has also been shown that postmitotic normal neurons lose their ability to import cyclin D/CDK complexes into the nucleus and that this ectopic cytoplasmic localization plays a role in neuron survival [44]. Aside from its role in cell cycle control, cyclin D1 also possesses other CDK-independent functions [45] such as chromatin remodelling, cell metabolism, and cell migration [46]. The exclusive cytoplasmic localization of cyclin D1 that we found in all ECs, without nuclear translocation after storage whereas it localized in nuclei of proliferating in vitro ECs and in basal epithelial cells after

Molecular Vision 2011; 17:3494-3511 <http://www.molvis.org/molvis/v17/a376> © 2011 Molecular Vision

storage, agrees with its non-proliferative status but suggests that cyclin D1 has CDK-independent functions in ECs. It also suggests that ECs might have passed the restriction point (after which, in a normal cell cycle, cyclin D1 is exported from the nucleus).

Cyclin E/CDK2 complexes act normally after cyclin D/CDK4–6 complexes during G_1 phase. Their activity rises in late G_1 phase, peaks at G_1/S transition, and declines quickly during the S phase [47,48]. Nevertheless, cyclin E accumulation in nuclei with inactive cyclinE/cdk2 complexes is compatible with arrest in the G_1 phase related to senescence [49] and when overexpressed in nontransformed HC11 mouse mammary epithelial cell line, cyclin E localizes exclusively in nuclei, induces an increase in p27 expression, and inhibits cell proliferation [50]. Our results, showing constant localization of cyclin E in nuclei of all ECs in fresh and stored corneas, are therefore compatible with non-proliferative status, and suggest again that ECs in situ might be arrested after the restriction point and before the entry in S-phase. In epithelial cells, staining was heterogeneous and nucleocytoplasmic in most cells in fresh corneas with a predominant nuclear translocation after storage, suggesting progression through the cell cycle. In in vitro ECs cyclin E was mostly localized in the cytoplasm, suggesting that they crossed the restriction point of the cell cycle.

Cyclin A is nomally expressed from late G_1 to late G_2 phases. Cyclin A/CDK complexes have substrates in both the nucleus and the cytoplasm and shuttle between the two compartments [51]. It initially assembles with CDK2 to form a complex imported in the nucleus, where it phosphorylates nuclear substrates implicated in DNA replication, thus promoting progression through the S phase [52]. In proliferating epithelial cells and in vitro ECs, cyclin A is mainly nuclear which is a hallmark of proliferating cells. We found it exclusively expressed in the cytoplasm of ECs of fresh and stored corneas, which again hints at cells having passed the restriction point. It is possible that the cytoplasmic retention of cyclin A hinders progression through S-phase. It would be interesting to assess cyclin A/CDK complexes activity in ECs in situ, as cytoplasmic substrates of the complexes might play a role in ECs physiology.

Our results for cyclins D1, E and A in whole corneas were consistent with the previous studies by Joyce et al. on cross-sections of corneas from seven donors aged 6 weeks to 67 years and stored at 4 °C during 24 to 36 h (Antibodies from Upstate Biotechnology, Lake Placid, NY) [53,54]. Flat mounts now allow clearer subcellular localization as well as observation of a larger population of ECs.

We detected p16 in the nuclei of ECs of both fresh and stored corneas. This is consistent with previous results of IHC done on cross-sections of human corneas, although subcellular localization was in either cytoplasm [54] or nuclei [55,56] of ECs. P16 inhibits cyclin D/CDK4–6. It is thus considered to have a pivotal role in G_1-phase arrest of ECs and stress-induced premature senescence [57]. Furthermore, p16 could interact directly with nuclear PCNA found in ECs and inhibit DNA polymerase delta activity [25]. In epithelial cells, cytoplasmic translocation occurred after OC, corresponding to prominent proliferative status. In in vitro ECs, p16 was found in both nuclei and cytoplasm, indicating cytoplasmic translocation compatible with cell cycle progression.

We did not detect p21 in ECs of flat-mounted fresh or OC-stored corneas despite systematic assessment of a wide variety of fixatives and AR and the use of three antibodies. P21 positivity in the nuclei of epithelial cells of the same corneal piece and in in vitro ECs eliminates a false-negative result in ECs. This apparently contradicts two previous studies that used IHC on cross-sections of 4 °C stored human corneas. In one case, a p21 antibody C-19 from Santa Cruz Biotechnology was used on six corneas stored at 4 °C and confirmed by western blots of proteins extracted from in vitro EC cultures [55]. In the second case, a p21 mouse monoclonal antibody from Lab Vision Corp (Fremont, CA) was used on four corneoscleral rims left off after corneal graft and confirmed with quantitative RT–PCR on RNA extracted from other corneo-scleral rims [56]. Both found nuclear staining for p21. It remains unclear why we did not reveal p21 in ECs in flat-mounted cornea methods. It is possible that fresh and OC corneas with preserved metabolic activities may behave differently from corneas stored for several days at 4 °C. As we found that in vitro EC cultures expressed p21 in nuclei, it is not surprising that WB was found positive by Enomoto et al. [55]. Moreover, the presence of p21 transcripts in ECs from whole corneas is not incompatible with post-transcriptional alterations resulting in absence of protein expression. At present, no other study has revealed p21 expression using immunolocalization in ECs. A direct comparison of paired corneas, one stored at 4 °C and the other either studied fresh or after OC, seems necessary to answer the question. We detected p21 in the nucleus of proliferative cells: epithelial cells of OC corneas and in vitro EC cultures. P21 is one of the main CKIs implicated in late G_1-phase arrest by inhibiting cyclin E/CDK2 complexes [58], but p21 can also contribute to initial G1 progression by promoting the nuclear import of cyclin D/CDK4–6 complexes [59] and by preventing the nuclear export of cyclin D [60].

P27, another CIP/KIP family member, also strongly inhibits cyclin E/CDK2 complexes and arrests the cell cycle in G_1 [61]. It is implicated in cell cycle arrest triggered by contact inhibition and TGFβ [62]. Its role has been demonstrated in rats [63] and the protein has been detected in nuclei of ECs on cross-sections of two corneas from donors aged 18 and 74 years [55] and in one cornea from a 54-year-old donor [56]. The three corneas had been stored shortly at 4 °C beforehand. In our study, in epithelial cells, the near-complete disappearance of p27 after OC strongly suggests cell cycle progression as, at the end of the G_1 phase, cyclin E/

Molecular Vision 2011; 17:3494-3511 <http://www.molvis.org/molvis/v17/a376> © 2011 Molecular Vision

CDK2 complexes (which we found in epithelial cell nuclei and cytoplasm) phosphorylate p27 that is subsequently ubiquitinated by Skp1/Skp2 and degraded by the proteasome [64]. In cultured ECs, p27 in both nuclei and cytoplasm also suggests possible progression beyond the restriction point.

In conclusion, IL on flat-mounted whole corneas seems possible for a large number of proteins, provided that substantial adaptations in corneal fixation and further processing are adopted. Continued efforts to refine methods of antigen preservation or retrieval in human corneas will ultimately allow standardization of IL and elimination of inter-laboratory discrepancies in results, thus allowing accurate research. 0.5% formaldehyde or methanol without AR should be recommended as first-line fixatives during experimental developments, given that in situ ECs seem particularly sensitive to overfixation by aldehydes and that AR methods often harm the integrity of the endothelial monolayer. Conventional OC medium containing 2% FCS does not modify the non-proliferative status of ECs, which is compatible with G_1-phase arrest. Nevertheless, our data suggest that ECs are arrested after the restriction point in the G_1 phase. The role of MCM2 in cytoplasm, the subcellular localization of cycle D1, and the absence of p21 are the main characteristics highlighted by our optimized protocols. Further studies are necessary to explain these particularities of fresh and OC-stored corneas.

ACKNOWLEDGMENTS

This work was funded by a grant from the Fondation de l'Avenir (ET7-468). We thank Jean-Yves Thuret from the CEA, iBiTec-S, Service de Biologie Intégrative et Génétique Moléculaire (Saclay, France), for his comments on the manuscript and fruitful discussions.

REFERENCES

1. Maurice DM. The location of the fluid pump in the cornea. J Physiol 1972; 221:43-54. [PMID: 5016991]
2. Murphy C, Alvarado J, Juster R, Maglio M. Prenatal and postnatal cellularity of the human corneal endothelium. A quantitative histologic study. Invest Ophthalmol Vis Sci 1984; 25:312-22. [PMID: 6698749]
3. Bourne WM, Nelson LR, Hodge DO. Central corneal endothelial cell changes over a ten-year period. Invest Ophthalmol Vis Sci 1997; 38:779-82. [PMID: 9071233]
4. Joyce NC. Proliferative capacity of the corneal endothelium. Prog Retin Eye Res 2003; 22:359-89. [PMID: 12852491]
5. Wilson SE, Weng J, Blair S, He YG, Lloyd S. Expression of E6/E7 or SV40 large T antigen-coding oncogenes in human corneal endothelial cells indicates regulated high-proliferative capacity. Invest Ophthalmol Vis Sci 1995; 36:32-40. [PMID: 7822156]
6. Zhu C, Joyce NC. Proliferative response of corneal endothelial cells from young and older donors. Invest Ophthalmol Vis Sci 2004; 45:1743-51. [PMID: 15161835]
7. Mimura T, Joyce NC. Replication competence and senescence in central and peripheral human corneal endothelium. Invest Ophthalmol Vis Sci 2006; 47:1387-96. [PMID: 16565372]
8. Chen KH, Azar D, Joyce NC. Transplantation of adult human corneal endothelium ex vivo: a morphologic study. Cornea 2001; 20:731-7. [PMID: 11588426]
9. Cheuk W, Chan JK. Subcellular localization of immunohistochemical signals: knowledge of the ultrastructural or biologic features of the antigens helps predict the signal localization and proper interpretation of immunostains. Int J Surg Pathol 2004; 12:185-206. [PMID: 15306932]
10. McGowan SL, Edelhauser HF, Pfister RR, Whikehart DR. Stem cell markers in the human posterior limbus and corneal endothelium of unwounded and wounded corneas. Mol Vis 2007; 13:1984-2000. [PMID: 17982423]
11. Werner M, Chott A, Fabiano A, Battifora H. Effect of formalin tissue fixation and processing on immunohistochemistry. Am J Surg Pathol 2000; 24:1016-9. [PMID: 10895825]
12. Bonds LA, Barnes P, Foucar K, Sever CE. Acetic acid-zinc-formalin: a safe alternative to B-5 fixative. Am J Clin Pathol 2005; 124:205-11. [PMID: 16040290]
13. Shi SR, Shi Y, Taylor CR. Antigen retrieval immunohistochemistry: review and future prospects in research and diagnosis over two decades. J Histochem Cytochem 2011; 59:13-32. [PMID: 21339172]
14. Yamashita S. Heat-induced antigen retrieval: mechanisms and application to histochemistry. Prog Histochem Cytochem 2007; 41:141-200. [PMID: 17197287]
15. Krenacs L, Krenacs T, Stelkovics E, Raffeld M. Heat-induced antigen retrieval for immunohistochemical reactions in routinely processed paraffin sections. Methods Mol Biol 2010; 588:103-19. [PMID: 20012825]
16. Barry PA, Petroll WM, Andrews PM, Cavanagh HD, Jester JV. The spatial organization of corneal endothelial cytoskeletal proteins and their relationship to the apical junctional complex. Invest Ophthalmol Vis Sci 1995; 36:1115-24. [PMID: 7730021]
17. Kim EK, Geroski DH, Holley GP, Urken SI, Edelhauser HF. Corneal endothelial cytoskeletal changes in F-actin with aging, diabetes, and after cytochalasin exposure. Am J Ophthalmol 1992; 114:329-35. [PMID: 1524124]
18. Suthipintawong C, Leong AS, Vinyuvat S. Immunostaining of cell preparations: a comparative evaluation of common fixatives and protocols. Diagn Cytopathol 1996; 15:167-74. [PMID: 8872443]
19. Jamur MC, Oliver C. Cell fixatives for immunostaining. Methods Mol Biol 2010; 588:55-61. [PMID: 20012819]
20. Burry RW. Controls for immunocytochemistry: an update. J Histochem Cytochem 2011; 59:6-12. [PMID: 20852036]
21. Slettedal JK, Lyberg T, Ramstad H, Beraki K, Nicolaissen B. Regeneration of the epithelium in organ-cultured donor corneas with extended post-mortem time. Acta Ophthalmol Scand 2007; 85:371-6. [PMID: 17559462]
22. De Marzo AM, Fedor HH, Gage WR, Rubin MA. Inadequate formalin fixation decreases reliability of p27 immunohistochemical staining: probing optimal fixation time using high-density tissue microarrays. Hum Pathol 2002; 33:756-60. [PMID: 12196928]
23. Helander KG. Kinetic studies of formaldehyde binding in tissue. Biotech Histochem 1994; 69:177-9. [PMID: 8068812]

Molecular Vision 2011; 17:3494-3511 <http://www.molvis.org/molvis/v17/a376> © 2011 Molecular Vision

24. Naryzhny SN. Proliferating cell nuclear antigen: a proteomics view. Cell Mol Life Sci 2008; 65:3789-808. [PMID: 18726183]
25. Souza-Rodrigues E, Estanyol JM, Friedrich-Heineken E, Olmedo E, Vera J, Canela N, Brun S, Agell N, Hubscher U, Bachs O, Jaumot M. Proteomic analysis of p16ink4a-binding proteins. Proteomics 2007; 7:4102-11. [PMID: 17955473]
26. Lydataki S, Lesniewska E, Tsilimbaris MK, Le Grimellec C, Rochette L, Goudonnet JP, Pallikaris IG. Observation of the posterior endothelial surface of the rabbit cornea using atomic force microscopy. Cornea 2003; 22:651-64. [PMID: 14508261]
27. Slettedal JK, Lyberg T, Roger M, Beraki K, Ramstad H, Nicolaissen B. Regeneration with proliferation of the endothelium of cultured human donor corneas with extended postmortem time. Cornea 2008; 27:212-9. [PMID: 18216579]
28. Gan L, Fagerholm P, Ekenbark S. Expression of proliferating cell nuclear antigen in corneas kept in long term culture. Acta Ophthalmol Scand 1998; 76:308-13. [PMID: 9686843]
29. Nejepinska J, Juklova K, Jirsova K. Organ culture, but not hypothermic storage, facilitates the repair of the corneal endothelium following mechanical damage. Acta Ophthalmol 2010; 88:413-9. [PMID: 19604163]
30. Crewe JM, Armitage WJ. Integrity of epithelium and endothelium in organ-cultured human corneas. Invest Ophthalmol Vis Sci 2001; 42:1757-61. [PMID: 11431439]
31. Gerdes J, Schwab U, Lemke H, Stein H. Production of a mouse monoclonal antibody reactive with a human nuclear antigen associated with cell proliferation. Int J Cancer 1983; 31:13-20. [PMID: 6339421]
32. Gerdes J, Lemke H, Baisch H, Wacker HH, Schwab U, Stein H. Cell cycle analysis of a cell proliferation-associated human nuclear antigen defined by the monoclonal antibody Ki-67. J Immunol 1984; 133:1710-5. [PMID: 6206131]
33. Senoo T, Joyce NC. Cell cycle kinetics in corneal endothelium from old and young donors. Invest Ophthalmol Vis Sci 2000; 41:660-7. [PMID: 10711678]
34. Maga G, Hubscher U. Proliferating cell nuclear antigen (PCNA): a dancer with many partners. J Cell Sci 2003; 116:3051-60. [PMID: 12829735]
35. Joyce NC, Zhu CC, Harris DL. Relationship among oxidative stress, DNA damage, and proliferative capacity in human corneal endothelium. Invest Ophthalmol Vis Sci 2009; 50:2116-22. [PMID: 19117931]
36. Ishimi Y. DNA helicase activity is associated with an MCM4, −6, and −7 protein complex. J Biol Chem 1997; 272:24508-13. [PMID: 9305914]
37. Labib K, Tercero JA, Diffley JF. Uninterrupted MCM2–7 function required for DNA replication fork progression. Science 2000; 288:1643-7. [PMID: 10834843]
38. Kearsey SE, Maiorano D, Holmes EC, Todorov IT. The role of MCM proteins in the cell cycle control of genome duplication. Bioessays 1996; 18:183-90. [PMID: 8867732]
39. Ringvold A, Davanger M, Olsen EG. On the spatial organization of the cornea endothelium. Acta Ophthalmol (Copenh) 1984; 62:911-8. [PMID: 6524316]
40. Sherrard ES, Ng YL. The other side of the corneal endothelium. Cornea 1990; 9:48-54. [PMID: 2297995]
41. Konomi K, Zhu C, Harris D, Joyce NC. Comparison of the proliferative capacity of human corneal endothelial cells from the central and peripheral areas. Invest Ophthalmol Vis Sci 2005; 46:4086-91. [PMID: 16249484]
42. Pan H, Deng Y, Pollard JW. Progesterone blocks estrogen-induced DNA synthesis through the inhibition of replication licensing. Proc Natl Acad Sci USA 2006; 103:14021-6. [PMID: 16966611]
43. Tamamori-Adachi M, Ito H, Sumrejkanchanakij P, Adachi S, Hiroe M, Shimizu M, Kawauchi J, Sunamori M, Marumo F, Kitajima S, Ikeda MA. Critical role of cyclin D1 nuclear import in cardiomyocyte proliferation. Circ Res 2003; 92:e12-9. [PMID: 12522130]
44. Sumrejkanchanakij P, Tamamori-Adachi M, Matsunaga Y, Eto K, Ikeda MA. Role of cyclin D1 cytoplasmic sequestration in the survival of postmitotic neurons. Oncogene 2003; 22:8723-30. [PMID: 14647467]
45. Coqueret O. Linking cyclins to transcriptional control. Gene 2002; 299:35-55. [PMID: 12459251]
46. Fu M, Wang C, Li Z, Sakamaki T, Pestell RG. Minireview: Cyclin D1: normal and abnormal functions. Endocrinology 2004; 145:5439-47. [PMID: 15331580]
47. Keyomarsi K, Herliczek TW. The role of cyclin E in cell proliferation, development and cancer. Prog Cell Cycle Res 1997; 3:171-91. [PMID: 9552414]
48. Mazumder S, Plesca D, Almasan A. A jekyll and hyde role of cyclin E in the genotoxic stress response: switching from cell cycle control to apoptosis regulation. Cell Cycle 2007; 6:1437-42. [PMID: 17581275]
49. Stein GH, Dulic V. Origins of G1 arrest in senescent human fibroblasts. Bioessays 1995; 17:537-43. [PMID: 7575495]
50. Sgambato A, Han EK, Zhou P, Schieren I, Weinstein IB. Overexpression of cyclin E in the HC11 mouse mammary epithelial cell line is associated with growth inhibition and increased expression of p27(Kip1). Cancer Res 1996; 56:1389-99. [PMID: 8640830]
51. Jackman M, Kubota Y, den Elzen N, Hagting A, Pines J. Cyclin A- and cyclin E-Cdk complexes shuttle between the nucleus and the cytoplasm. Mol Biol Cell 2002; 13:1030-45. [PMID: 11907280]
52. Yam CH, Fung TK, Poon RY. Cyclin A in cell cycle control and cancer. Cell Mol Life Sci 2002; 59:1317-26. [PMID: 12363035]
53. Joyce NC, Meklir B, Joyce SJ, Zieske JD. Cell cycle protein expression and proliferative status in human corneal cells. Invest Ophthalmol Vis Sci 1996; 37:645-55. [PMID: 8595965]
54. Joyce NC, Navon SE, Roy S, Zieske JD. Expression of cell cycle-associated proteins in human and rabbit corneal endothelium in situ. Invest Ophthalmol Vis Sci 1996; 37:1566-75. [PMID: 8675399]
55. Enomoto K, Mimura T, Harris DL, Joyce NC. Age differences in cyclin-dependent kinase inhibitor expression and rb hyperphosphorylation in human corneal endothelial cells. Invest Ophthalmol Vis Sci 2006; 47:4330-40. [PMID: 17003423]
56. Song Z, Wang Y, Xie L, Zang X, Yin H. Expression of senescence-related genes in human corneal endothelial cells. Mol Vis 2008; 14:161-70. [PMID: 18334933]
57. Joyce NC, Harris DL. Decreasing expression of the G1-phase inhibitors, p21Cip1 and p16INK4a, promotes division of

Molecular Vision 2011; 17:3494-3511 <http://www.molvis.org/molvis/v17/a376> © 2011 Molecular Vision

corneal endothelial cells from older donors. Mol Vis 2010; 16:897-906. [PMID: 20508865]

58. Harper JW, Adami GR, Wei N, Keyomarsi K, Elledge SJ. The p21 Cdk-interacting protein Cip1 is a potent inhibitor of G1 cyclin-dependent kinases. Cell 1993; 75:805-16. [PMID: 8242751]
59. Cheng M, Olivier P, Diehl JA, Fero M, Roussel MF, Roberts JM, Sherr CJ. The p21(Cip1) and p27(Kip1) CDK 'inhibitors' are essential activators of cyclin D-dependent kinases in murine fibroblasts. EMBO J 1999; 18:1571-83. [PMID: 10075928]
60. Alt JR, Gladden AB, Diehl JA. p21(Cip1) Promotes cyclin D1 nuclear accumulation via direct inhibition of nuclear export. J Biol Chem 2002; 277:8517-23. [PMID: 11751903]
61. Toyoshima H, Hunter T. p27, a novel inhibitor of G1 cyclin-Cdk protein kinase activity, is related to p21. Cell 1994; 78:67-74. [PMID: 8033213]
62. Polyak K, Kato JY, Solomon MJ, Sherr CJ, Massague J, Roberts JM, Koff A. p27Kip1, a cyclin-Cdk inhibitor, links transforming growth factor-beta and contact inhibition to cell cycle arrest. Genes Dev 1994; 8:9-22. [PMID: 8288131]
63. Joyce NC, Harris DL, Mello DM. Mechanisms of mitotic inhibition in corneal endothelium: contact inhibition and TGF-beta2. Invest Ophthalmol Vis Sci 2002; 43:2152-9. [PMID: 12091410]
64. Bloom J, Pagano M. Deregulated degradation of the cdk inhibitor p27 and malignant transformation. Semin Cancer Biol 2003; 13:41-7. [PMID: 12507555]

Articles are provided courtesy of Emory University and the Zhongshan Ophthalmic Center, Sun Yat-sen University, P.R. China. The print version of this article was created on 26 December 2011. This reflects all typographical corrections and errata to the article through that date. Details of any changes may be found in the online version of the article.

ARTICLE III: Effects of fixatives temperature on immunolocalization in flat-mounted human corneal endothelial cells.

Effect of fixative temperature on immunolocalization on flat-mounted human corneal endothelium and applications

Zhiguo He[1], Nelly Campolmi[1], Fabien Forest[1,2], Binh-Minh Ha Thi[1], Jean-Marc Dumollard[1,2], Michel Peoc'h[1,2], Olivier Garraud[3], Simone Piselli[1], Philippe Gain[1], Gilles Thuret[1,4]

(1) "Biology, Engineering and Imaging of Corneal Grafts" Laboratory, EA2521, SFR 143, Faculty of Medicine, University of Jean Monnet, Saint-Etienne, France

(2) Department of Pathology, University Hospital of Saint-Etienne, France

(3) Eye Bank of Saint-Etienne, Auvergne Loire Blood Center, Saint-Etienne, France

(4) Institut Universitaire de France, 103 Boulevard Saint-Michel, 75005 Paris, France

Corresponding author

Prof. Gilles Thuret,

"Biology, Engineering and Imaging of Corneal Grafts" Laboratory, EA 2521, IFR 143

Faculty of Medicine

15, rue Ambroise Paré

F 42023 Saint-Etienne Cedex 2, France.

Tel: +33 (0)4 77 12 77 93

Fax: +33 (0)4 77 12 09 95

E-mail: gilles.thuret@univ-st-etienne.fr

Key words: temperature, fixation, cornea, endothelium, immunolocalization, immunocytochemistry, immunohistochemistry, flat-mount, Fuchs' dystrophy, Ki67, neural cell adhesion molecule (NCAM)

Abstract

Corneal endothelium control corneal hydration and are essential for the maintenance of corneal transparency. It is a monolayer of hexagonal flat cells at the posterior surface of the cornea. Immunolocalization on endothelial cells (EC) of flat-mounted whole corneas present two mains advantages over conventional immunohistochemistry (IHC) on cross-sections of cornea: overview of entire endothelium and precise subcellular protein localization. It nevertheless requires several technical adaptations comparing with conventional IHC or immunocytochemistry (ICC) which is applied in cells outside tissue. We had previously developed adapted protocols by defining the critical elements: the fixatives (0,5%PFA and methanol), fixative time (30 minutes), antibody concentration (1/200), antigen retrieval methods, etc. In this experiment, we showed a flagrant effect of fixative temperature to immunolocalization on EC of flat mounted cornea by investigating four increasing temperature during fixation of pure methanol and 0.5% formaldehyde. Four proteins with different expression patterns in EC (Zo-1, hnRNPL, actin and histone H3) were chosen to explain this fact. In order to demonstrate the advantages of this technique, we investigate existence of proliferating cells on corneal endothelium of Fuchs' dystrophy by detecting Ki67 expression and organization of lateral membrane of normal EC by staining of neural cell adhesion molecule (NCAM). Results showed that temperature strongly influenced immunostaining quality and reliability. In particular, conventional temperature (-20°C for methanol and 4°C for formaldehyde) were mostly inefficient, and room temperature (RT) appears at first-line temperature. The detection of EC in S phase of cell cycle indicates the cell proliferation may be one mechanism of compensation to slow down the EC loss during Fuchs' dystrophy. Hexagonal organization towards apical pole of EC, lateral membrane organization demonstrated an increasing irregularity towards basal pole. This characteristic expression of NCAM helped us to understand better the histology and physiology of EC. We suggest NCAM as a new marker of EC. In conclusion, fixative temperature is critical to optimize the protocol of immunolocalization on EC of whole flat-mounted cornea. An optimal protocol may offer a more complete and reliable information for the studies of corneal endothelium. We believe the presented protocols and their advantages might be also benefited to other tissues like corneal epithelium, lens epithelium and retina.

INTRODUCTION

The monolayer of tightly packed hexagonal flat cells forming the endothelium at the posterior surface of the cornea is crucial for the maintenance of its transparency. By controlling the stromal hydration it ensures the stability of the perfect organization of collagen fibers that explains tissue transparency [1]. Despite their fundamental role in vision, endothelial cells (EC) lose their proliferative capacity after birth [2], which explains the limited possibilities of wound healing in case of pathological processes. Nevertheless, in the healthy cornea, a very slow endothelial renewal by the proliferation

of cells situated at the extreme periphery of the endothelium and their centripetal migration was recently suggested [3] and partially compensate EC losses, resulting in an age-related physiological EC loss of only 0.3 to 0.6% per year [4, 5]. There is consequently no corneal endothelial dysfunction solely caused by physiologic aging. On the contrary, in pathological processes, beyond a certain threshold of EC loss, residual cells cannot achieve their normal functions and cornea become irreversibly edematous causing permanent visual loss, only accessible to a corneal graft. Endothelial dysfunctions constitute therefore one of the first indication for corneal graft [6]. The molecular mechanisms leading to the arrest of EC in the G1 phase of the cell cycle are being stepwise understood [7, 8] but require continuous efforts in order to develop strategies of cell therapy able to trigger and control EC re-proliferation. The possibility to expand EC pool would have considerable therapeutic impact. Expansion could be useful during ex vivo corneal storage by eye banks in order to increase both the number and the quality of cornea available, in vitro with a view of developing bioengineered endothelial allogeneic graft, or even in vivo to cure endothelial dysfunctions. For all these future studies, there is clearly a need for reproducible methods to characterize proteins expression in EC, either for basic research or for quality controls during bioengineering processes.

Because of the limited quantity of EC (300,000 to 500,000 per cornea), protein extraction directly from whole human corneal endothelium in view of performing immunoblots is not the current technique for investigation of protein expression and has only rarely been reported after pooling of EC from several donors[8-11]. Consequently, up to now, immunolocalization techniques are the methods mostly used to detect protein expression in situ in EC. Because of its simplicity, immunohistochemistry (IHC) on cross-sections is currently the main technique used in the literature, despite it allows visualization of only a few EC without a clear subcellular localization due to EC flat shape. Moreover, because of the superficial situation of the endothelium, immunostainings of EC on cross-sections may be subject to staining artifacts frequently encountered at the tissue borders. In a recent study we have systematically developed specific immunolocalization protocols performed directly on the intact endothelium of whole cornea [12]. The en face observation that we use, presents two main advantages: a striking visualization of the whole intact endothelium allowing detection of regional or local difference in staining patterns (going up to the easy detection of isolated rare cells with a specific expression profile, like the detection of rare stem like cells within the endothelium [3]), and a precise subcellular localization. The technique is hybrid between IHC and immunocytochemistry (ICC), because it concerns a cell monolayer on top of an intact tissue. We demonstrated that EC were easily over-fixed when treated with conventional 4% formaldehyde, resulting in poor quality immunostaining. Instead, we showed that 0.5% formaldehyde or pure methanol, each for 30 minutes at room temperature (RT) was first choice fixatives to perform immunolocalization on intact EC of flat-mounted whole corneas. The dilution of primary antibodies 1:200 is available to all tested marketed antibodies. Additional adaptation such as antigen retrieval (AR)

with 0,5% sodium dodecyl sulfate (SDS) in water for 5 minutes at RT was nevertheless necessary after formaldehyde fixation for a few antigens to achieve a better result.

During this previous study, we noticed that temperature during fixation might strongly influence staining quality. For diverse immunolocalization techniques, like IHC and ICC, the recommended fixation temperature is -20°C for methanol and 4°C for formaldehyde, although the influence of the temperature during the fixation on staining quality had not been clearly reported. In order to study the influence of temperature on staining quality and to improve immunolocalization of EC of flat-mounted corneas, we systematically assessed a wide range of temperature during methanol and formaldehyde fixation using four antibodies that had previously proven efficient to reveal characterized proteins located in the different cell compartments. 4°C, 23°C (RT), 37°C or 50°C had been chosen for formaldehyde and -20°C, RT, 37°C or 50°C for methanol. 37°C is the physiological temperature at which the antigen is in their initial conformation. 50°C is the highest temperature on whole corneas without triggering tissue shrinking.

Lastly, in order to demonstrate the two main advantages of this technique, we investigate existence of proliferating cells on corneal endothelium of Fuchs' dystrophy by detecting Ki67 expression and organization of lateral membrane of normal EC by staining expression of neural cell adhesion molecule (NCAM).

METHODS

Human corneas

Ten Organ cultured corneas were used for test of temperature. They were obtained from the Eye Bank of Saint-Etienne and initially stored in 100 mL organ culture medium (CorneaMax, Eurobio, Les Ulis, France) at 31°C without medium renewal for (mean±SEM) 22±10 days (7 to 35, median 21). Endothelial cell density (ECD) was 1976±618 cells/mm^2 (1229 to 2898, median 2004). The corneas were obtained from 7 donors whose age was 75±8 years (54 to 81, median 77), with time from death to retrieval always less than 24 hours. Two fresh corneas were used for test of NCAM. They were obtained from the Department of Anatomy of the Faculty of

Medicine of Saint-Etienne (body donation to science). Donor age was 73 and 68 years, and time from death to procurement was 9 and 23 hours. Two corneal buttons of Fuchs' dystrophy with patients' permission were used for investigation of proliferating cells. They were obtained from operating room within a delay of 30 minutes between their separation from patients and fixation. The age of patients is 61 and 68 years. Handling of the donor tissues adhered to the tenets of the Declaration of Helsinki of 1975 and its 1983 revision in protecting donor confidentiality.

Antibodies

Specific primary antibodies for this study are presented in Table 1. Whenever possible, they were chosen from among antibodies validated for ICC by their manufacturers, which seemed closest to our technique. Non-specific rabbit or/and mouse IgG (Zymed, Carlsbad, CA. Respectively ref 02-6102 and 02-6502) were used as primary antibodies for negative controls (i.e. secondary antibody control [15]). Secondary antibodies were Alexa Fluor 488 goat anti-mouse IgG or/and Alexa Fluor 555 goat anti-rabbit IgG (invitrogen, Eugen, OR).

Immunolocalization on flat-mounted whole corneas

The general processing of corneas followed the protocols previously described by our team [12]. Briefly, corneas were rinsed in PBS, cut into eight pie-shaped wedges to increase the number of experiments while saving rare tissues and fixed immediately after being removed from OC medium. Double staining was chosen, again in order to save human corneas. Fixation was performed for 30 minutes either in formaldehyde 0.5% in PBS pH 7.45 at 4°C, 23°C (RT), 37°C or 50°C, or in methanol at -20°C, RT, 37°C or 50°C. Cell membranes were permeabilized by 1% Triton x-100 in PBS for 5 min at RT after fixation. This step was omitted when SDS was used as AR method or for methanol fixation, as they alter lipids by themselves (it was previously shown that AR with 0.5% SDS in water for 5 min at RT was necessary after formaldehyde fixation, only to reveal histone H3 [12]). The non-specific binding sites were then saturated by incubation with heat-inactivated goat serum for 30 minutes at 37°C. All primary antibodies were diluted 1:200 in PBS containing 2% bovine serum albumin (BSA) and 2% heat-inactivated goat serum. Corneal pieces were totally immersed in 100 µl of this solution in eppendorf microtubes to avoid dehydration of specimens, and incubated at 37°C during 1 hour. Incubation with secondary antibodies diluted 1:500 in PBS containing 2% BSA and 2% goat serum was done for 45 minutes at 37°C. Nuclei were finally counterstained with Hoechst 33342 (Sigma) 10µg/mL in PBS at RT for 2 min. Three rinses in PBS were performed between all steps, except between saturation of non-specific protein binding sites and incubation with primary antibody. The corneal piece was finally placed on a glass slide, covered with PBS and gently flattened using a large glass coverslip retained by adhesive tape. Experiments were done at RT unless otherwise stated. Images were captured by a fluorescence inverted microscope IX81 (Olympus, Tokyo, Japan) equipped with the Cell^P imaging software (Soft Imaging System GmbH, Munster, Germany). This non-confocal microscope was chosen to obtain large-field images able to tolerate the residual 3D aspect of cell layers after flat-mounting. Each assay was repeated at least three times on three different corneas.

Evaluation of immunostaining

Protocols were deemed optimized once labeling exhibited correct localization at light microscopic level, with homogeneous staining in all EC, without zone effect (the first 100 µm near the cutting edges were excluded), and absence of staining in controls.

In case of equivalence between protocols in terms of specificity, the brightest staining was selected. Evaluation of immunostaining was done independently by two

pathologists experienced in immunofluorescence (IF) assessment (MP and JMD), on digital pictures blind to the preparation used. The intensity of staining was rated as null, weak, medium, good and excellent. In case of disagreement, a third judge, also pathologist, (FF) reviewed the pictures.

RESULTS

Four different proteins were known to be consistently expressed in EC with a characteristics pattern. They were either well characterized in human EC or ubiquitous proteins: (1) ZO-1 is a peripheral membrane protein associated with tight junctions [13]; (2) actin is one of the most conserved cytoplasmic proteins in eukaryotes and is distributed in linear circumferential strands that form a hexagonal belt beneath plasmic membrane in EC [14]; (3) heterogeneous ribonucleoprotein L (hnRNP L) is present in the nucleoplasm as part of the hnRNP complexes that play a major role in the formation, packaging, processing, and function of mRNA; (4) bound with DNA, histone H3 is one of the basic nuclear proteins responsible for the nucleosome structure of chromosomal fibres in eukaryotes.

By optimizing the fixative temperature for each of the four proteins, we obtained striking typical staining patterns in EC, in term of signal/noise ratio and precise subcellular localization. One of the main problems that we had met previously during the development of the immunolocalization in EC of falt-mounted whole cornea was the heterogeneous staining of the ubiquitous expressed proteins in endothelium. The right fixation at adapted temperature may solve this problem as you can see in the Figure 1A with small magnification. With large magnification (960x), we observed that the distribution of ZO-1 is not linear, but zigzag between two neighboring cells, and absent at the point where the three neighboring cells join (Figure 1B). The figure 1 showed that this technique with adapted protocol give both an overall view of endothelium and a precise subcellular staining.

Best staining was globally obtained with methanol. During methanol fixation, the conventional temperature of -20°C was optimal only for ZO-1 and totally inefficient for histone H3. RT was optimal for hnRNPL, 37°C for actin and 50°C for histone H3. Other combinations were sub-optimal (Figure 2 and Table 2). SDS was not suitable to combine with methanol fixation because it always triggered partial or complete detachment of EC (Data not shown).

During 0.5% formaldehyde fixation, the conventional temperature of 4°C was optimal only for ZO-1 and totally inefficient for actin and histone H3. RT and 37°C were optimal for hnRNP L and histone H3 but inefficient for actin, and 50°C was never optimal. Formaldehyde did not allow revealing actin at any temperature (Figure 3). AR with SDS induced almost complete detachment of the EC from their basement membrane after 4°C fixation. Increase of the temperature allowed keeping EC attached

during subsequent treatment with SDS but the staining improvement was weak in this condition.

Unsuitable temperatures during fixation might mask completely staining of the expressed proteins in cells (Figure 2, histone H3 at -20°C and figure 3, histone H3 at 50°C); or give heterogeneous staining of ubiquitous proteins (Figure 2, histone at RT or 37°C, and figure 3, hnRNP L at 50°C), or introduce artifact of staining, as you can see in figure 2, hnRNP L, -20°C, a slight cytoplasmic staining for hnRNP L. An optimal temperature during fixation is required for obtaining not only a beautiful picture, but most importantly, the correct information about the expression of the target proteins. There was no unique temperature that gave best results for all antigens and with both fixatives as show in the table 2. Fixation at RT gave nevertheless acceptable staining for all.

Formation of the corneal guttae on Descemet's membrane (DM) is the diagnosis of Fuchs' dystrophy. Ring distribution of nuclei of EC around corneal guttae is characteristic. The staining of nuclei by Hoechst in the picture with magnification 100X showed this characteristic (Figure 4). Few proliferating cells with Ki67 expression were detected in endothelium of corneal buttons of Fuchs' dystrophy. With large magnification 960X, the localization of Ki67 within nucleolus was well demonstrated. The optimal protocol with 0.5% PFA at RT had been previously defined ((12) He et al., Molecular Vision, 2011).

For the purpose of obtaining a more physiological cell structure, we used the fresh corneas with short postmortem and without any conservation in medium of culture. The pictures with magnification 100X and 400X showed all EC expressed NCAM on lateral membrane with irregular distribution (Figure 5). By observing the NCAM staining with large magnification 960X, we demonstrated clearly the increase of irregular organization of lateral membrane from apical to basal pole of EC. Furthermore, lateral cell-cell junctions were not always continuous, and some small spaces were presented between neighboring cells. Epithelial cells of the same corneas did not express NCAM (data not shown). The optimal protocol with methanol at 37°C was defined by the same process described in method.

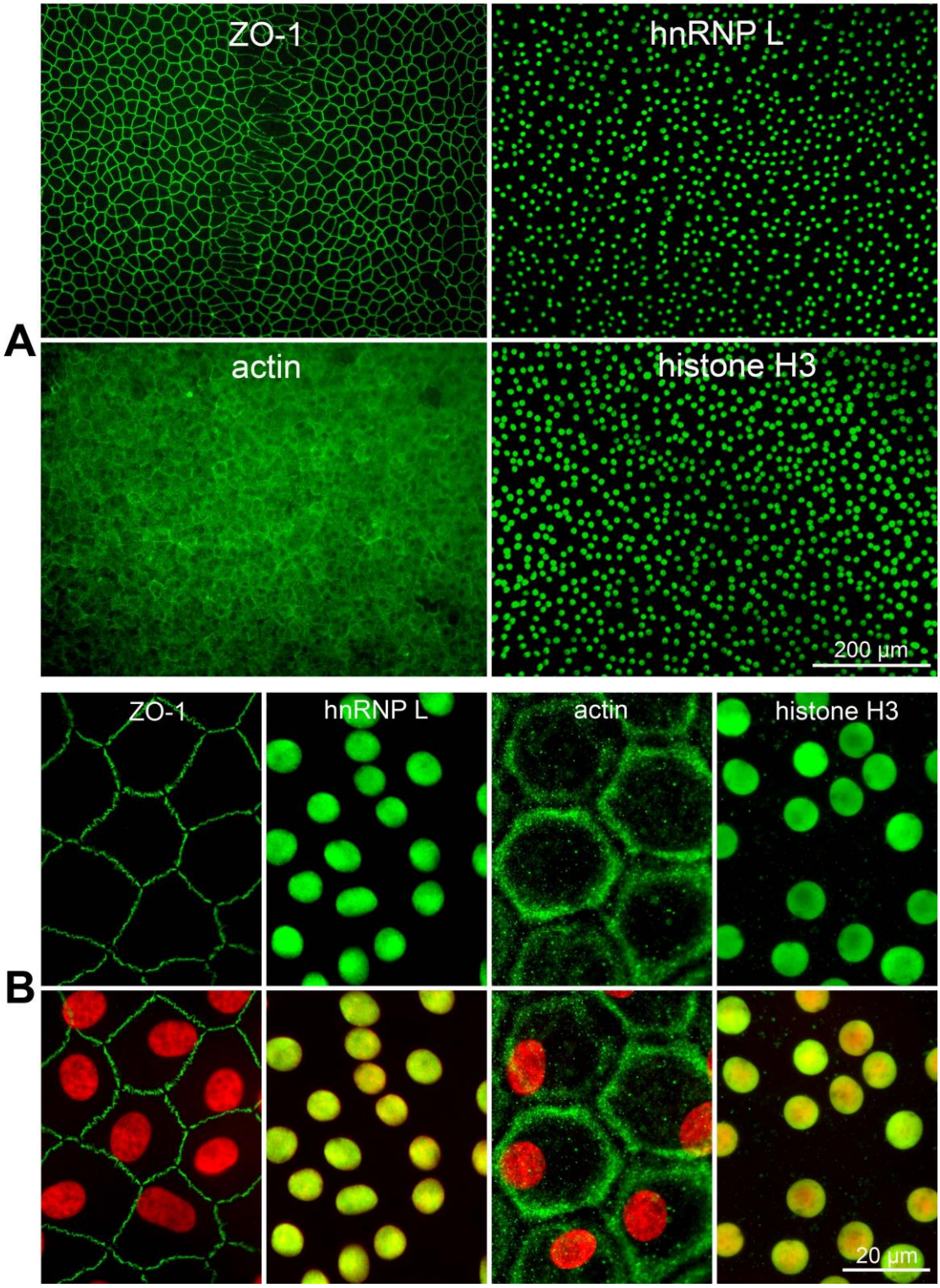


Figure 1. Best results obtained after optimization of fixative temperature for detection in endothelial cells of flat-mounted whole human corneas of: ZO-1 (methanol at -20°C), hnRNP L (formaldehyde at room temperature (RT)), actin (methanol at 37°C), and histone H3 (formaldehyde at RT). A. Low magnification (100X) shows the homogenous staining in all EC. B. High magnification (960X) shows the typical expected staining patterns for each target protein. Upper line: immunostaining alone; lower line: merge with Hoechst 33342.

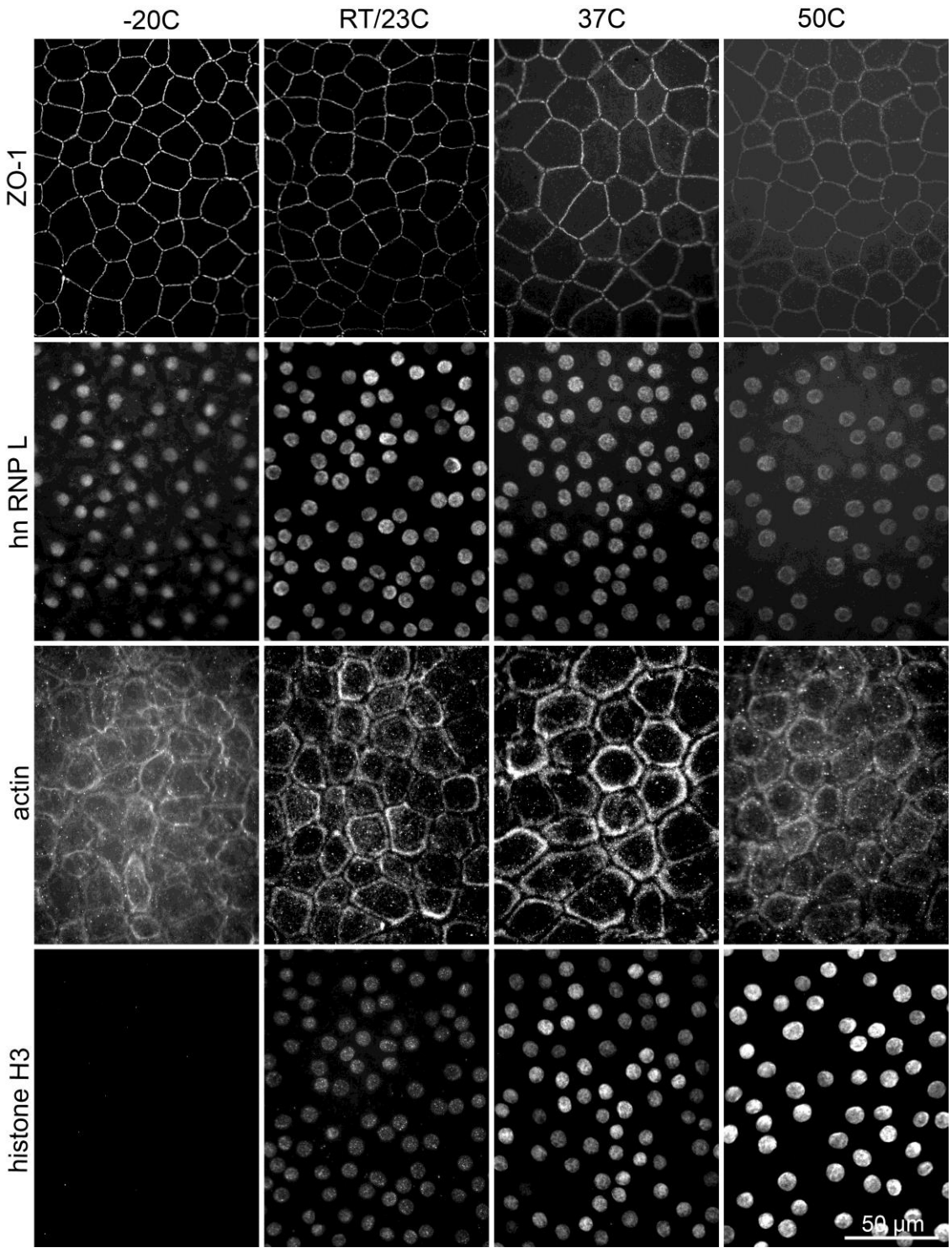


Figure 2. Influence of the temperature during methanol fixation. All corneal pieces were fixed for 30 minutes. No nuclear counterstaining. Magnification 400X.

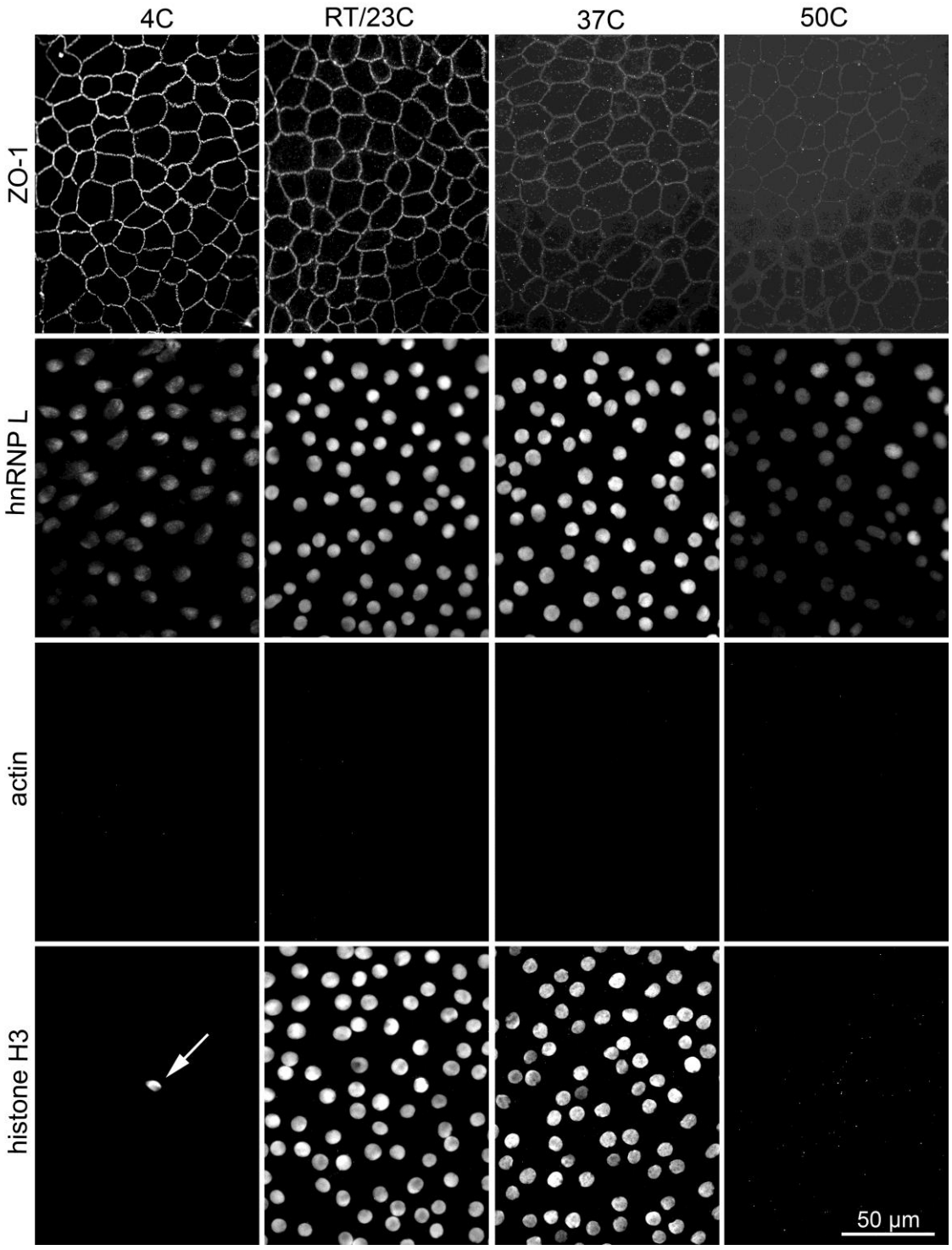


Figure 3. Influence of the temperature during 0.5% formaldehyde fixation. All corneal pieces were fixed for 30 minutes. Fixation alone without antigen retrieval (AR) was used excepted for histone H3 that required AR with SDS; SDS detached almost all endothelial cells from their basement membrane after fixation at 4°C as indicated by the arrow that indicates the single cell still attached. All the EC were present for actin at the four temperatures and for histone H3 at 50°C; the counterstaining with Hoechst is not shown. Magnification 400X.

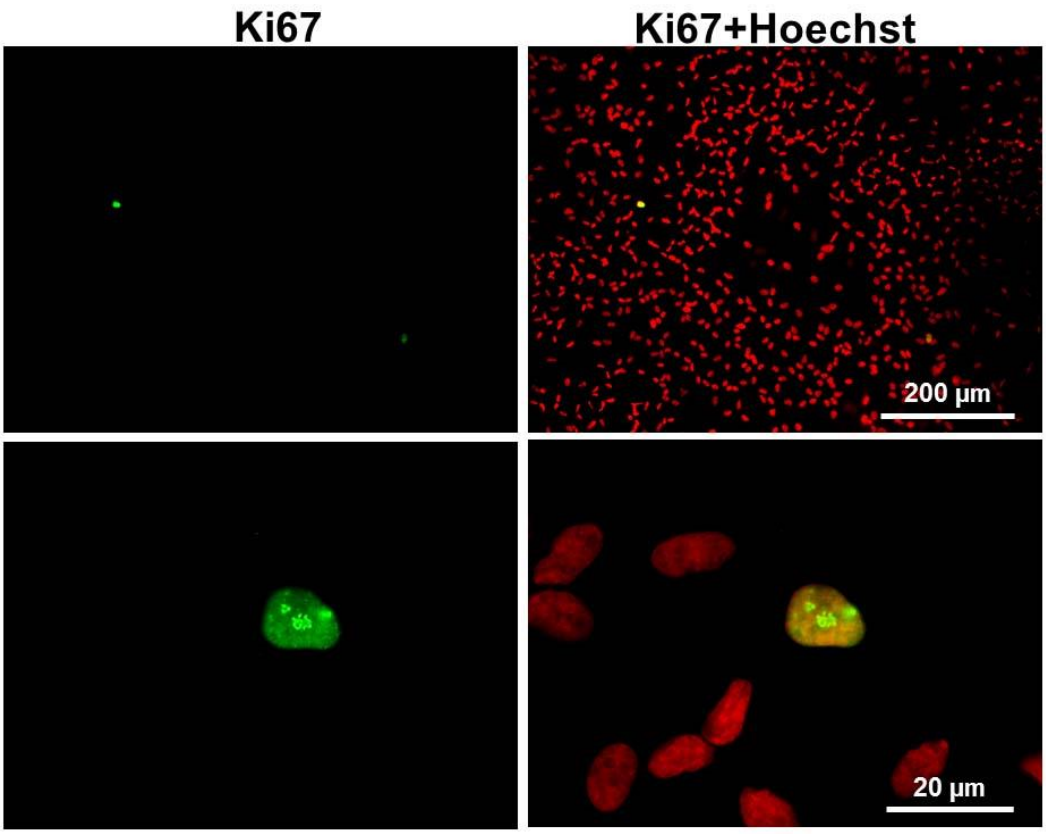


Figure 4. Detection of Ki67 expression in few endothelial cells (EC) on corneal buttons of Fuchs' dystrophy. Low magnification (x100) shows the expression of ki67 in two EC. High magnification shows the localization of Ki67 within nucleolus.

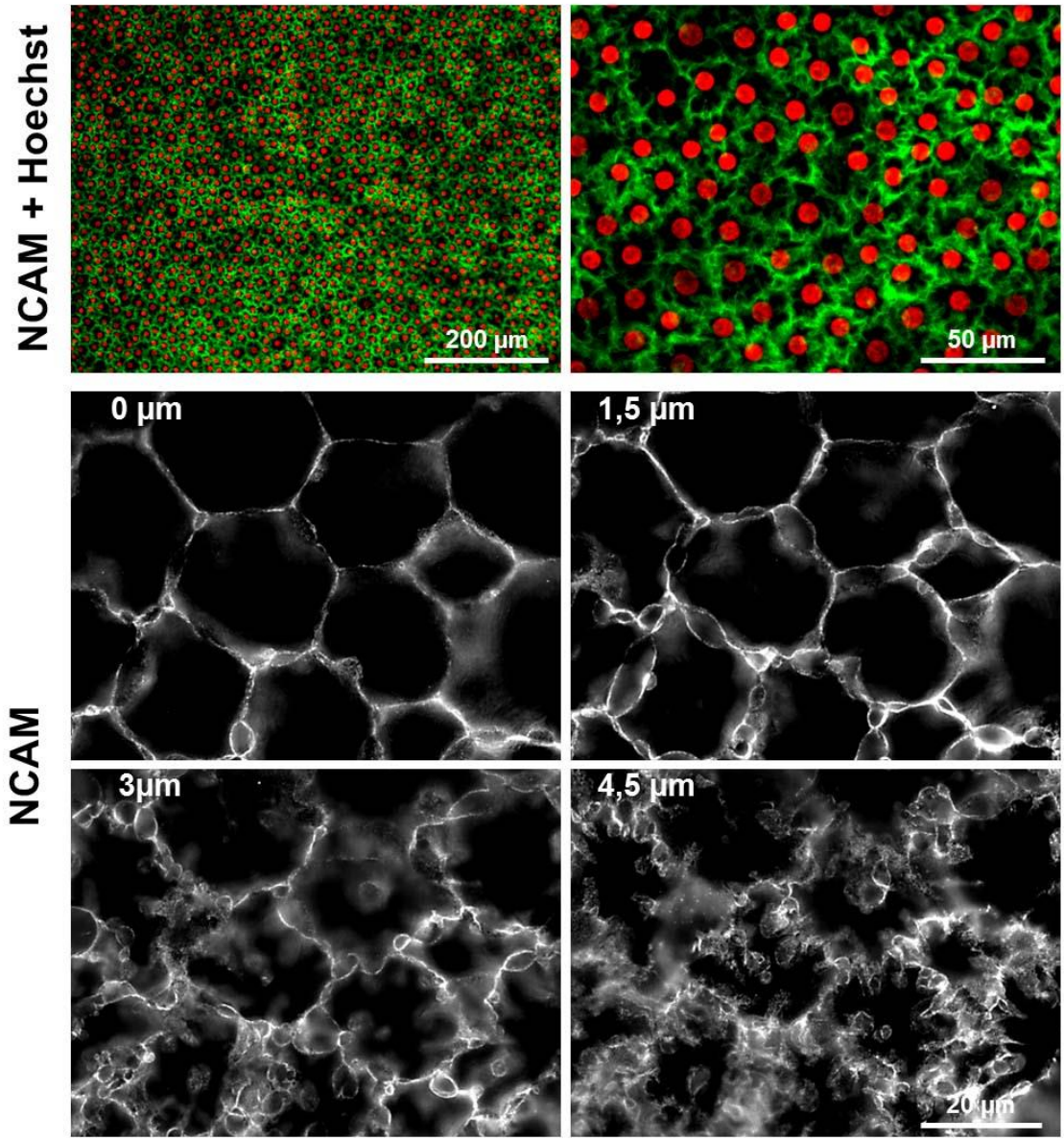


Figure 5. Homogeneous expression of neural cell adhesion molecules (NCAM) in all EC and increasing irregular organization of lateral membrane from apical to basal pole of EC. Upper line: low magnification 100X shows homogeneous expression of NCAM in all EC; medium magnification 400X shows irregular organization of lateral membrane where NCAM was located. Lower lines: high magnification 960X shows expression of NCAM at four different depths from apical pole of EC.

DISCUSSION

In this study, we demonstrated the strong influence of temperature during fixation for immunolocalization in EC of flat-mounted human corneas. For massive tissues, we had observed that prolonged fixation at low temperature ensures a slow regular diffusion within tissue, intended to better preserve tissue and cell morphology. On the contrary, an elevated temperature increases the rapidity of fixation. In case of a superficial cell layer as EC, directly accessible to fixatives, the fixation process is supposed to be extremely rapid whatever the fixative, nevertheless, we found substantial differences between methanol and formaldehyde depending on the temperature.

Results after methanol fixation were particularly dependent on the temperature. The suitable fixation temperature gave a beautiful staining, but most importantly, the correct information of protein expression. As you can see in the figure 2 for the ubiquitous expressed protein histone H3, the unsuitable fixative temperature at -20°C did not show the expression of histone H3, and at 37°C gave a very heterogeneous nuclear staining in the center of endothelium. Only the optimal temperature at 50°C gave the correct information of protein expression: homogeneous nuclear staining.

For methanol fixation, the well-accepted cold fixation at -20°C only reveals ZO-1 located under the cytoplasmic membrane whereas increasing temperatures were required to detect antigens located in the cytoplasm (actin), nucleoplasm (hnRNPL) or bound with DNA (histone H3). The highest temperature tolerable by the cornea was indeed optimal for the deepest antigens, histone H3. Methanol is commonly used during ICC on in vitro-cultured cells and during IHC on tissue frozen cross-sections. Classified as precipitating (or agglutinating) fixatives, it reduces proteins solubility by creating non-covalent bonds between them. Furthermore, its hydrophilic group (-OH) disrupts the hydrogen bonds between amide groups in the secondary protein structure and its hydrophobic group (R-CH2-) disrupts the intramolecular hydrophobic interactions of protein core and thus denatures the proteins by changing their secondary and tertiary structure [16]. The temperature of -20°C, commonly used for tissue fixation during immunolocalization, exploits the precipitating properties of methanol while avoiding protein denaturation. This temperature was efficient only to detect ZO-1. Higher temperature may increase the denaturation of proteins by modifying proteins' tertiary structures, giving access to hidden epitopes. Warm methanol could therefore ensure both fixation and AR. Furthermore, methanol may also lower the denaturation temperature of DNA [17] and consequently facilitate the release of histone H3. Further study with alcohol fixatives at high temperature should be necessary to confirm this effect on other cells and tissues.

Formaldehyde cross-links proteins amino groups with other nearby nitrogen atoms in proteins or DNA through a -CH2- covalent linkage [18] and thus abolishes the biological activities of cells by preserving their intact structure. Four percent formaldehyde is almost a universal concentration for ICC and IHC, but we recently suggested that it results in EC overfixation leading to poor immunostainings, and

therefore recommend using 0.5% formaldehyde instead[12]. In this study, we went one step ahead, by showing that RT and 37°C improve staining results during 0.5% formaldehyde fixation compared with 4°C which is however the recommended temperature for immunolocalization techniques. The absence of improvement with 50°C may be due to accelerated protein cross-linking resulting in over fixation. Lower performance of formaldehyde to reveal actin compared to that of methanol fixation has previously been reported without clear explanation [19].

SDS disrupts the non-covalent bonds in proteins, between proteins and between proteins and other molecules such as DNA, allowing changes in structure conformation of proteins and antigen unmasking [20, 21]. The molecular cross-linking by formaldehyde fixation allows the use of SDS to unmask epitopes while preserving cell and tissue organization, except when fixation is done at 4°C where the protein cross-linking may be not sufficient explaining why EC almost completely detached from their basement membrane. At the opposite, for fixation at 50°C, SDS lost its AR effect, likely because of the overfixation. In between, SDS allows immunostaining of the DNA-binding protein histone H3 on formaldehyde fixed corneas similarly to methanol fixation at 50°C. Note that SDS is however incompatible with methanol fixation that does not create covalent bonds between molecules. In this condition, SDS may completely destruct the cell structure and dissolve the proteins.

The different possible combinations that we assessed, now allows to find the best compromise between preservation of morphology of the fragile corneal endothelial tissue and maintenance of a good antigenicity using chemical AR whenever necessary. If the choice for the type and concentration of fixatives and AR methods are the most crucial steps during the assessment of a new antibody on EC of flat-mounted whole cornea, the temperature during fixation may also be determinant to improve staining quality. RT, but not -20°C for methanol fixation, nor 4°C for formaldehyde 0.5% fixation, may be recommended as first-line fixatives temperature during development of experiments.

Corneal EC are arrested in G1 phase of cell cycle in human adult (7, 8, Joyce). By using immunolocalization on EC of flat-mounted whole corneas, we had never found any proliferating cells expressing ki67 in central endothelium of fresh corneas (3, 12. He). Fuchs' Dystrophy is a degenerative disease of the corneal endothelium whose pathogenesis is still unknown. A slow and progressive decreasing density of EC is due to an increasing apoptosis (PMID:10937560, Borderie et al., IOVS, 2000). The proliferative status of EC in cornea of Fuchs' dystrophy had not been reported. In this study, by investigating corneal buttons of Fuchs dystrophy of diameter 8.25 mm, we found some proliferating cells expressing Ki67. The clear localization of Ki67 within nucleolus indicates these EC entered in S phase of cell cycle (PMID: 8799815, Kill., J Cell Sci, 1996). This observation indicates the cell proliferation may be one mechanism of compensation to slow down the EC loss during Fuchs' dystrophy.

We know the corneal endothelium as a monolayer of hexagonal cells, but it is not exact, hexagonal organization is just at apical pole of EC. By using the

immunolocalization of NCAM on EC of flat-mounted whole cornea, we demonstrated clearly a progressive increase of irregular organization of lateral membrane from apical to basal pole of EC. So EC in physiological condition should be characterized rather a monolayer of cells with hexagonal organization at apical pole (Figure 5, 6).

Interestingly, we observed the lateral cell-cell junctions were discontinuous by forming some inflated pockets between neighboring cells. The water pump is the essential function of endothelium and it had been well studied by team of Bonanno (PMID: 12597924, Bonanno, 2003, Prog Retin Eye Res). But his reported mechanism about regulation of ion transport is not convincing in histology, because it should be difficult to establish a higher concentration of ions in circulating aqueous humor, furthermore, one of the most important active transporter of ion, Na+/K+ ATPase is exclusively localized at lateral membrane of EC. With the new histological observation in this study, we may give another hypothesis: the training of higher concentration of ions outside lateral EC drives water fluid into lateral spaces by forming some inflated pocket of water with higher pressure, and then water is drained into aqueous humor by the small exits where the apical tight junction is absent between the three neighboring cells (Figure 1B, ZO-1 and Figure6).

NCAM distribution exclusively at lateral membrane of EC with hexagonal organization at apical pole and irregular organization at basal pole is characteristic. It was not detected in corneal epithelial cells. NCAM is also known as the cluster of differentiation 56 (CD56), it may be utilized in cell sorting using various methods including flow cytometry. We propose the characteristic expression of NCAM as a marker of corneal EC. It will be very useful in the bioengineering of reconstituted corneal endothelium by using pluripotent stem cells or adult stem cells from other tissues.

By the example of investigation of proliferating cells on endothelium of Fuchs' dystrophy and that of organization of lateral membrane of EC on normal corneas, we showed the two main advantages of the immunolocalization on EC of flat-mounted whole cornea comparing to IHC on cross section of corneas: striking visualization of the whole intact endothelium allowing detection of rare cells with a specific expression profile, and a precise subcellular localization. The mastery of the technique is the precondition. Different from the most of immunolocalization techniques (IHC and ICC) using conventional 4% formaldehyde as fixative that had been demonstrated not suitable for flat-mounted corneal endothelium, 0.5% formaldehyde or pure methanol, each for 30 minutes at RT was first choice fixatives to perform immunolocalization on intact EC of flat-mounted whole corneas and allows the greatest number of antigens to be visualized. In the case of unsatisfactory effect, the temperature during the fixation will be an efficient tool to improve the effect of immunostaining, especially for methanol fixation, 50°C or 37°C is as efficient as RT or -20°C. Such recommendations should be applicable to other cell types localized at the surface of tissue that requires an en face observation, like others ocular tissues: corneal epithelium, les epithelium and retina.

REFERENCES

1. Maurice DM. The structure and transparency of the cornea. J Physiol 1957; 136:263

2. Murphy C, Alvarado J, Juster R, Maglio M. Prenatal and postnatal cellularity of the human corneal endothelium. A quantitative histologic study. Invest Ophthalmol Vis Sci 1984; 25:312-22.6698749

3. He Z, Campolmi N, Gain P, Minh Hathi B, Dumollard JM, Duband S, et al. Revisited Microanatomy of the Corneal Endothelial Periphery: New Evidence for Continuous Centripetal Migration of Endothelial Cells in Humans. Stem Cells 2012; 30:2523-34.22949402

4. Bourne WM, Nelson LR, Hodge DO. Central corneal endothelial cell changes over a ten-year period. Invest Ophthalmol Vis Sci 1997; 38:779-82

5. Moller-Pedersen T. A comparative study of human corneal keratocyte and endothelial cell density during aging. Cornea 1997; 16:333-8.

6. Peh GS, Beuerman RW, Colman A, Tan DT, Mehta JS. Human corneal endothelial cell expansion for corneal endothelium transplantation: an overview. Transplantation 2011; 91:811-9.21358368

7. Joyce NC. Proliferative capacity of the corneal endothelium. Prog Retin Eye Res 2003; 22:359-89.12852491

8. Joyce NC, Harris DL, Zhu CC. Age-related gene response of human corneal endothelium to oxidative stress and DNA damage. Invest Ophthalmol Vis Sci 2011; 52:1641-9.21087955

9. Koh SW, Waschek JA. Corneal endothelial cell survival in organ cultures under acute oxidative stress: effect of VIP. Invest Ophthalmol Vis Sci 2000; 41:4085-92.11095600

10. Koh SW, Chandrasekara K, Abbondandolo CJ, Coll TJ, Rutzen AR. VIP and VIP gene silencing modulation of differentiation marker N-cadherin and cell shape of corneal endothelium in human corneas ex vivo. Invest Ophthalmol Vis Sci 2008; 49:3491-8.18441300

11. Azizi B, Ziaei A, Fuchsluger T, Schmedt T, Chen Y, Jurkunas UV. p53-regulated increase in oxidative-stress--induced apoptosis in Fuchs endothelial corneal dystrophy: a native tissue model. Invest Ophthalmol Vis Sci 2011; 52:9291-7.22064994

12. He Z, Campolmi N, Ha Thi BM, Dumollard JM, Peoc'h M, Garraud O, et al. Optimization of immunolocalization of cell cycle proteins in human corneal endothelial cells. Mol Vis 2011; 17:3494-511.22219645

13. Barry PA, Petroll WM, Andrews PM, Cavanagh HD, Jester JV. The spatial organization of corneal endothelial cytoskeletal proteins and their relationship to the apical junctional complex. Invest Ophthalmol Vis Sci 1995; 36:1115-24.

14. Kim EK, Geroski DH, Holley GP, Urken SI, Edelhauser HF. Corneal endothelial cytoskeletal changes in F-actin with aging, diabetes, and after cytochalasin exposure. Am J Ophthalmol 1992; 114:329-35.1524124

15. Burry RW. Controls for immunocytochemistry: an update. J Histochem Cytochem 2011; 59:6-12.20852036

16. Zellner M, Winkler W, Hayden H, Diestinger M, Eliasen M, Gesslbauer B, et al. Quantitative validation of different protein precipitation methods in proteome analysis of blood platelets. Electrophoresis 2005; 26:2481-9.15895463

17. Herskovits TT, Singer SJ, Geiduschek EP. Nonaqueous solutions of DNA. Denaturation in methanol and ethanol. Arch Biochem Biophys 1961; 94:99-114.13713795

18. Kiernan JA. Formaldehyde, formalin, paraformaldehyde and glutaraldehyde: What they are and what they do. Microscopy Today 2000; 08:8-12

19. Allan VJ. Protein localization by fluorescence microscopy. A practical approach. Oxford: Oxford University Press; 1999.

20. Brown D, Lydon J, McLaughlin M, Stuart-Tilley A, Tyszkowski R, Alper S. Antigen retrieval in cryostat tissue sections and cultured cells by treatment with sodium dodecyl sulfate (SDS). Histochem Cell Biol 1996; 105:261-7.9072183

21. Rajamannan NM, Springett MJ, Pederson LG, Carmichael SW. Localization of caveolin 1 in aortic valve endothelial cells using antigen retrieval. J Histochem Cytochem 2002; 50:617-28.11967273

CONCLUSION

L'absence de capacité proliférative significative de l'endothélium cornéen humain adulte, à l'origine des dystrophies œdémateuses cornéennes in vivo, repose sur des modifications profondes du cycle cellulaire correspondant à une sénescence prématurée. Les mécanismes exacts de cette sénescence, restent à préciser. Ils ne semblent pas liés à une érosion des télomères mais se produiraient en réponse à des dommages oxydatifs de l'ADN qui s'accumulent avec l'âge et sont plus marqués au centre qu'à la périphérie endothéliale. Les voies de signalisation sont peu à peu démembrées et, depuis les travaux initiaux de Nancy Joyce du Schepens Eye Research Institute à Boston dans les années 90, les interrelations des voies impliquant p53, les transcripts des CKIs p21 et p16, CDK4/pRB et la télomérase commencent à être mieux comprises (Sheerin *et al.* 2012). Nous y contribuons dans un premier article en utilisant un microarray spécifique du cycle cellulaire pour l'étude comparative de cellules endothéliales dans différents environnements susceptibles de modifier la stimulation pro-prolifération

Ces mécanismes, encore incomplètement élucidés, limitent également considérablement les possibilités d'expansion in vitro avec un rendement suffisant pour envisager une application de bioingénierie. Après une maturation lente des protocoles de culture primaire, une récente étude du Singapour Eye Institute Research propose, pour la première fois, un protocole capable de produire suffisamment de cellules, et pouvant pratiquement être qualifié de "culture de masse". Cependant l'âge des donneurs utilisés (30 ans et moins), incompatible avec des stratégies de production en Europe, justifie notre second article sur la différenciation, la sénescence et l'optimisation des cultures à partir de donneurs de plus de 50 ans. Il est néanmoins probable que la culture optimisée mais sans modification des CEs elle-mêmes (cycle et/ou sénescence et/ou stress oxydatif) ne permettent pas d'obtenir suffisamment de cellules pour une production semi industrielle. Ces « interventions » feront l'objet des travaux futurs du BiiGC.

Enfin, l'induction de la différenciation de cellules souches en CEs fonctionnelles, encore balbutiante mais dont le BiiGC est déjà partie prenante, devrait bénéficier de la synthèse que nous présentons en première partie sur l'embryologie endothéliale cornéenne humaine, avec en particulier le démembrement récent de nouvelles voies de signalisations (voie Wnt et transition Crête Neurale/mésenchyme

neuronal/endothélium cornéen) déjà appliquées au laboratoire sur des cellules pluripotentes induites.

Comme toute recherche bibliographique, ce travail présente des limites : nous l'avons en effet cantonné à l'exploration des différentes stratégies de production de masse de CEs. Nous n'abordons pas la bioingénierie des supports indispensables à la reconstruction de greffons endothéliaux. Ceci fera l'objet d'une prochaine Thèse du BiiGC.

Les modalités d'introduction de ces CEs dans la chambre antérieure du patient ne sont volontairement pas abordé non plus et devront également faire l'objet de travaux spécifiques. En effet, l'injection de CEs en suspension devra s'accompagner de procédés assurant l'adhérence de la majorité des CEs à la face postérieure de la cornée. Deux preuves de concepts (CEs chargées de billes magnétiques attirées par un aimant et injection de CEs préconditonnées en présence de Rock-inhibiteur pour augmenter leurs capacités d'adhérence et de migration) ont été faites chez l'animal. Elles devront être testées pré-cliniquement sur des cornées humaines présentant un stade précoce des 2 pathologies cibles de cette thérapie cellulaire: la dystrophie endothéliale de Fuchs et la dystrophie bulleuse du pseudophaque. Ces validations précliniques pourraient être effectuées dans un futur proche grâce au bioréacteur cornéen breveté par BiiGC. L'introduction dans la chambre antérieure de greffons endothéliaux bioingénierés devrait pouvoir être réalisée avec les techniques actuelles des greffes endothéliales mais l'adhérence des CEs sur leur support de culture devra alors être aussi puissante que les CEs natives sur leur membrane de Descemet.

Enfin, nous n'abordons pas non plus l'aspect immunologique des futures greffes endothéliales réalisées à partir de greffons bioingénierés. Hormis des CEs qui seraient produites à partir des propres cellules pluripotentes induites de chaque patient ou d'une banque internationale de ces cellules permettant de couvrir la plupart des appariements d'histocompatibilité, la production de masse de CEs de donneurs "tout venant" exposera probablement aux mêmes risques de rejet que les greffes endothéliales actuelles (mais cependant pas plus !). Il conviendra donc de s'interroger sur les modalités de traitement post opératoire pour réduire au minimum l'alloréactivité post greffe de CEs produites par bioingénierie.

Publications et Communications Scientifiques

PUBLICATIONS

Microarray analysis of cell cycle gene expression in adult human corneal endothelium cells with different proliferative status. **Ha Thi BM**, Pipparelli A, Thuret JY, Gain P, Thuret G. (article sousmis à Plos One, 2013)

Corneal endothelial cells from old donors: differentiation, senescence, proliferative capacities and optimized culture conditions. **Ha Thi BM**, He Z, Piselli S, Gain P, Thuret G. (article à sousmettre à Aging Cell, 2013)

Activation of corneal endothelial mistosis by electrical pulse during cornea electroporation. **Ha Thi BM**, He Z, Gain P, Thuret G. (article à sousmettre à Molecular Vision, 2014)

Revisited microanatomy of the corneal endothelial periphery: new evidence for continuous centripetal migration of endothelial cells in humans. He Z, Campolmi N, Gain P, **Ha Thi BM**, Dumollard JM, Peoc'h M, Garraud O, Thuret G. Stem Cells. 2011

Optimization of immunolocalization of cell cycle proteins in human corneal endothelial cells. He Z, Campolmi N, **Ha Thi BM**, Dumollard JM, Peoc'h M, Garraud O, Gain P, Thuret G. Mol Vis. 2011

Effect of fixative temperature on immunolocalization on flat-mounted human corneal endothelium and applications. He Z, Campolmi N, Forest F, **Ha Thi BM**, Dumollard JM, Peoc'h M, Garraud O, Piselli S, Gain P, Thuret G (article en préparation)

COMMUNICATIONS SCIENTIFIQUES ET PRIX

Différenciation de l'endothélium cornéen chez les sujets âgés. **Ha Thi BM**, He Z, Thuret G, Gain P.

- 1er Prix du meilleur poster, Journée IFRESIS, Université Jean Monnet, Saint Etienne, novembre 2013

Bioengineering and stem cells for corneal endothelial cell therapy. Thuret G, He Z, **Ha Thi BM**, Gain P.

- Communication orale, European Association for Vision and Eye Research (EVER), Congrès annuel, Nice, octobre 2013

Label retaining endothelial cells in adult human corneas: new clue for the existence of endothelial stem cells. **Ha Thi BM**, He Z, Gain P, Peoc'h M, Dumollard JM, Garraud O, Thuret G.

- Poster et Communication orale, EVER, Congrès annuel, Nice, octobre 2012
- Communication orale, European Eye Bank Association (EEBA), Congrès annuel, Zagreb, janvier 2013
- Communication orale, Société française d'ophtalmologie (SFO), Congrès annuel, Paris, mai 2013
- 3ème Prix du meilleur poster, Journée de la recherche, Université Jean Monnet, Saint Etienne, juin 2013

Characterization of cell cycle modifications induced by electric pulses in human corneal endothelium. **Ha Thi BM**, He Z, Gain P, Peoc'h M, Dumollard JM, Garraud O, Thuret G.

- Poster, EEBA, Congrès annuel, Zagreb, janvier 2013
- Communication orale, EVER, Congrès annuel, Nice, octobre 2012

Curriculum Vitae

HA THI Binh Minh
née le 25/11/1984 (29 ans)
12, rue Bossuet
42100 SAINT ETIENNE
Tél. +33 (0)6 21 39 19 87
hathibinhminh@gmail.com

INGENIEUR en Biologie et Biotechnologie



Expériences Professionnelles

2011-2014 (3 ans) **Ingénieur de recherche / Doctorant** - *Laboratoire Biologie, Ingénierie et Imagerie de la Greffe de Cornée - St Etienne*
" Différenciation, sénescence et capacité prolifération de l'endothélium cornéen humain "
Microarray & analyse bioinformatique de l'expression de gènes du cycle cellulaire, ***article sousmis à PlosOne***,
Analyse du profil de différenciation, de la capacité prolifération, de la sénescence**,** ***communications aux congrès internationaux, prix du meilleur poster, article sousmis à Aging Cell***,
Bio-ingénierie de l'endothélium par isolement de progéniteurs endothéliaux et réendothélialisation sur biomatériel,
Essais précliniques sur cornées de lapin.

2008-2011 (CDI, 2 ½ ans) **Chef de produit / Ingénieur biochimiste** – *BIOPREDIC INTERNATIONAL - Rennes*
2 gammes de produits prises en charge: les fractions subcellulaires de foie, intestin, épiderme, rein, poumon de différentes espèces, et les produits organotypiques dérivés de la peau et du sang,

- Responsabilités R&D:

Optimisation de processus de fabrication des microsomes, Induction d'activités,
Extraction, caractérisation de vésicule canaliculaire hépatique et de membrane d'érythrocyte.

- Responsabilités Gestion de la production:

Gestion de stock, Approvisionnement, Planification,
Gestion d'équipes de production : formation du personnel, suivi de production, validation qualité,
Management de la qualité: Installation du système documentaire, du flux d'informations interservice.

2008 (6 mois) **Assistant chercheur / Stagiaire** – *Laboratoire de Biochimie, Département Cardiovasculaire, SANOFI AVENTIS - Chilly M*
" Etude des voies de signalisation liées à un GPCR endogène/recombinant par dosage multiplex de phosphoprotéines "
Quantification d'expression du GPCR des modèles cellulaires exprimant le GPCR endogène et recombinant,
Etude d'activation de voies de signalisation MAPK, PI3K par dosage multiplexe Luminex.

2006 (6 mois) **Assistant ingénieur / Stagiaire** – *Laboratoire de MicroBiotechnologie, PIERRE FABRE - Toulouse*
" Production de protéine recombinante en système bactérien en fermenteur "
Mutagenèse, Clonage, Fermentation d'*E.coli* en batch de 5L, Extraction, Purification de protéine,
Optimisation par plan d'expérience et robotisation du dosage d'activité de protéine.

2004 (1 mois) **Ouvrier / Stagiaire** - *BOURJOIS CHANNEL - Compiègne*
Conditionnement de parfums et de produits cosmétiques.

Domaines de compétence

Compétences métier	**Management**	**Langues**
Microbiologie	Gestion du travail en équipe	Anglais: courant
Biologie moléculaire, cellulaire, tissulaire	Gestion de production, calcul de coût	Français: bilingue
Expérimentation animale niveau 1	Gestion du stock, approvisionnement	Espagnol: à réactiver
Biochimie, Bioinformatique	Gestion de la qualité	Vietnamien: langue maternelle
Optimisation des procédés, Criblage	Comptabilité	

Formation

2014 **Doctorat en biologie et biotechnologie** - *Laboratoire Biologie, Imagerie, Ingénieur de la Greffe de Cornée, Université Jean Monnet - St Etienne* - (soutenance en janvier 2014)

2011 **Diplôme universitaire de Médecine Régénératrice** - *Institut de Recherche en Biothérapie, Montpellier*
Spécialité: Thérapie cellulaire et génique

2008 **Double diplôme** - *Université de Technologie de Compiègne*
Diplôme d'ingénieur – Génie Biologique, filière Conception et Innovation de Bioproduits
Master 2 – spécialité Biotechnologie et Mise en œuvre des Fonctions Biologiques

2002 **Baccalauréat Général** - *Lycée Hanoi-Amsterdam, Vietnam* **-** Mention : Très Bien

Centres d'intérêt

Vie associative
Visite des Malades dans des Etablissements Hospitaliers, visiteur bénévole *2010-2013*
Gériatrie Trousseau, CHU de Saint Etienne
Soin palliatif du Centre de cancérologie Eugène Marquis, CHU de Rennes
Association de Coopération Médecins-Etudiants, coordinatrice *2011-2013*
COMUTEC – Forum rencontre Entreprises/Etudiants, accompagnateur d'entreprise *2006-2007*

Loisirs Plongée sous-marine, Voyage, Peinture (école des beaux arts de Compiègne), Théâtre (improvisation), Danse.

ABSTRACT

Corneal endothelial engineering is becoming a more and more realistic solution to restore vision from corneal edema. This method focus to regenerate corneal endothelium by direct injection of corneal endothelial cells (ECs) into patient anterior chamber at the early stage of endothelial dystrophies, or by grafting a transparent biocompatible material covered by a monolayer of ECs. These two techniques require both in vitro isolation and amplification of ECs or endothelial-like cells.

In this thesis, different strategies to obtain a high quantity of functional ECs for clinical application are explored:

1- Due to the limit proliferative capacity of EC, the first strategy consists to analyze mechanisms implicated EC cell cycle arrest and then to optimize protocol for native EC isolation or for cell proliferation activation ex vivo. This is summarized in three publications. **The first publication describes the cell cycle regulation by comparing transcriptional expression of 112 genes in 6 biological models of EC with different proliferative profile**: in vivo, postmortem, organ-culture, confluent primary culture, non confluent primary culture and immortalized cell line. , The key molecular actors identified using the combining microarray analysis and gene ontology methods are consistent with previous findings about oxidative DNA damage mechanism. **The second publication characterizes EC differentiation process and its impact on EC proliferative capacity in old donor corneas**. Analyses of differentiation/progenitor markers and of proliferative capacity underline the differentiation process of EC from the centre to the peripheral corneal endothelium. Thereby, an optimized culture protocol was developed, allowing the formation of high-density monolayer (> 2000 cells/mm^2) with stable endothelial morphology. We proved the possibility to make profit from a majority of old-donor cornea grafts invalidated for penetrating graft In **the third publication, the activation of endothelial cell cycle by electric pulses directly in corneal graft was characterized**. We confirm the activation of endothelial cell cycle at different phases but also the damage of tissue during electroporation.

2- Second strategy consists of the amplification of ECs from potential EC progenitors. Using sphere forming culture and a new method to detect slow-cycling cells, we demonstrate the existence of "young" ECs population with higher proliferative capacity in corneal periphery. The isolation of ECs by sphere formation is one possible step for ECs selection in vitro.

3- The differentiation of embryonic stem cells, mesenchymal stem cells or induced pluripotent stem cells into corneal endothelial cells is the third approach considered by our laboratory. The manipulation of stem cells differentiation would be based on the molecular mechanisms implicated in the formation of corneal endothelium from periocular mesenchymal cells described in the first part of the bibliography.

Finally, in order to validate the quality of endothelial cell mass obtained, we revisited recent methods for the evaluation of corneal endothelial identity (immunolocalisation of specific markers), for the measurement of pump activity of cell monolayer (Ussing chamber, perfusion chamber) or directly in deswelled cornea using the bioreactor patented by the BiiGC laboratory.

RESUME

La bioingénierie de greffons endothéliaux cornéens est une des solutions réalistes en cours de développement dans quelques laboratoires pour palier au grand déséquilibre entre pénurie mondiale de dons de cornée et besoins immenses et croissant des populations. Cette véritable médecine régénérative consistera à injecter des cellules endothéliales (CEs) dans la chambre antérieure aux stades précoces des dystrophies endothéliales et, pour les stades avancées des pathologies endothéliales, à reconstruire in vitro des greffons endothéliaux composés d'un support transparent et biocompatible colonisé par une monocouche des CEs. Dans les 2 cas, la première étape obligatoire est la production de masse de CEs ou de "CE-like".

Dans ce travail, nous avons exploré les différentes possibilités pour obtenir suffisamment des CEs fonctionnelles pour envisager des applications cliniques:

1- L'expansion de CEs natives prélevées sur des cornées de donneurs, ou culture primaire, se heurtent aux capacités prolifératives limitées des CEs in vitro. Un des prérequis étant la compréhension des mécanismes d'arrêt de la prolifération des CEs humaines, nous avons fait la synthèse bibliographique des connaissances sur leur cycle cellulaire et leur sénescence, et présentons **2 articles originaux: le premier utilise un microarray spécifique de 112 gènes de contrôle du cycle cellulaire pour comparer les profils transcriptionnels des CEs** de 6 modèles biologiques comportant théoriquement un stimulus prolifératif croissant: in vivo, post mortem, organoculture, culture primaire confluente, culture primaire non confluente et lignée immortalisée. Nous identifions de nombreux acteurs impliqués dans l'arrêt du cycle, en particulier ceux impliquant une réponse à des dommages oxydatifs de l'ADN. **Le second article explore les capacités prolifératives résiduelles des CEs de donneurs âgés de plus de 50 ans**, qui sont les plus nombreux en Europe et donc les pourvoyeurs habituels de CEs pour la bioingénierie. Nous montrons qu'une optimisation des techniques de culture permet d'obtenir in vitro une mosaïque endothéliale de 2000 cellules/mm2. Enfin, nous montrons, **dans un troisième article qu'un stimulus physique inattendu constitué d'un train d'impulsion électrique permet d'obtenir un très grand nombre de figures mitotiques** mais uniquement dans des zones de faible DCE, démontrant encore une fois l'importance majeur de l'inhibition de contact dans l'arrêt prolifératif.

2- La sélection et l'expansion, par culture en sphère, des progéniteurs endothéliaux de la périphérie endothéliale pourrait être un moyen de contourner la sénescence de la majorité des CEs. La synthèse bibliographique montre que la plupart des travaux publiés émanent d'une seule équipe japonaise. Dans notre second article, nous avons montré, pour la première fois, l'existence de rares "label-retaining cells" dans les cornées de donneurs âgés, qui pourraient correspondre à ces progénieteurs. Nous avons également montré qu'il était possible d'obtenir des sphère avec ces donneurs.

3- La différenciation de cellules souches embryonnaires, mésenchymateuses ou des cellules pluripotentes induites est enfin la troisième voie qui pourrait permettre de produire des CEs en grand nombre. La méthodes d'induction de la différenciation pourrait reproduire le schéma physiologique et désormais bien caractérisé de formation de l'endothélium à partir du mésenchyme périoculaire dérivé de la crête neurale et que nous rappelons au début de notre mémoire bibliographique.

Nous rappelons également les méthodes utilisables pour caractériser les cellules obtenues: vérification de leur identité par immunomarquage d'un panel de protéines caractéristique (en absence de marqueur unique spécifique) et vérification de leur fonctionnalité par msures de leurs capacités de pompage ionique, au minimum de façon indirecte sur chambre d'électrophysiologie de type Ussing, au mieux de façon directe en quantifiant la déturgescence d'une cornée humaine conservée dans le bioréacteur breveté du BiiGC.